

---

**On the biomechanics of ligaments and  
muscles throughout the range of hip motion**

---

by

Richard Jan van Arkel

February 2015

A thesis submitted to Imperial College London  
for the degree of Doctor of Philosophy  
and for the Diploma of Imperial College

Department of Mechanical Engineering  
Imperial College London, SW7 2AZ



### **Originality Declaration**

I hereby declare that all work contained in this thesis has been produced by me and that all else has been appropriately referenced.

### **Copyright Declaration**

The copyright of this thesis rests with the author and is made available under a Creative Commons Attribution Non-Commercial No Derivatives licence. Researchers are free to copy, distribute or transmit the thesis on the condition that they attribute it, that they do not use it for commercial purposes and that they do not alter, transform or build upon it. For any reuse or redistribution, researchers must make clear to others the licence terms of this work





## **Abstract**

At the limits of the range of hip motion, impingement, subluxation and edge loading can cause osteoarthritis in natural hips or early failure hip replacements. The aim of this PhD was to investigate the role of hip joint soft tissues throughout the range of hip motion to better understand their role in preventing (or perhaps even causing) these problematic load cases. A musculoskeletal model was used to investigate the muscular contribution to edge loading and found that in the mid-range of hip motion, the lines of action of hip muscles pointed inward from the acetabular rim and thus would stabilise the hip. However, in deep hip flexion with adduction, nearly half the muscles had unfavourable lines of action which could encourage edge loading. Conversely, in-vitro tests on nine cadaveric hips found that the hip capsular ligaments were slack in the mid-range of hip motion but tightened to restrain excessive hip rotation in positions close to the limits of hip motion. This passive restraint prevented the hip from moving into positions where the muscle lines of action were found to be unfavourable and thus could help protect the hip from edge loading. The ligaments were also found to protect the hip against impingement and dislocation. Out of the labrum, the ligamentum teres and the three capsular ligaments, it was found that the iliofemoral and ischiofemoral ligaments were primary restraints to hip rotation. These two capsular ligaments should be prioritised for protection/repair during hip surgery to maintain normal hip passive restraint. Whilst this can be technically demanding, failing to preserve/restore their function may increase the risk of osteoarthritic degeneration or hip replacement failure.



## **Acknowledgements**

I would like to thank Dr Jonathan Jeffers for providing me with the opportunity to research a topic that I have found so interesting. Your continued guidance, knowledge, support and enthusiasm have been truly invaluable – I have very much enjoyed studying for my PhD under your supervision.

I would also like to thank Prof Andrew Amis for sharing his boundless expertise with me and for creating and leading a research group that has been so stimulating to work in.

It was also a pleasure to work with and learn from my journal paper co-authors: Prof Justin Cobb, Dr Andrew Philips and Dr Luca Modenese. You were all so willing to share your knowledge, ideas and previous work with me and this greatly improved my own research. Thank you.

To all the members of the Biomechanics group, thank you, because undoubtedly you have helped me at some point and I have enjoyed working with you all. In particular: Camilla Halewood, thank you for teaching me how to use all of the lab equipment; Mr Breck Lord, thank you for showing me how to identify the hip ligaments on my first day of testing; Dr Joanna Stephen, thank you for patiently teaching me to analyse my data with appropriate statistical tests; and Philip Wilson, thank you for expertly manufacturing my test rig for me.

To office 362, I have had a lot of fun working with you all – you are all excellent people.

I am truly grateful for the financial support I personally received from the Institute of Mechanical Engineers and the Engineering and Physical Sciences Research Council. I would also like to acknowledge the Wellcome Trust, Arthritis Research UK and the Engineering and Physical Sciences Research Council (again) for providing financial support for the research.

Finally, I would also like to thank mum, dad and the lovely Hannah for everything and more.



# Contents

<b>1 Introduction .....</b>	<b>1</b>
<b>1.1 Motivation.....</b>	<b>1</b>
<b>1.2 Aims and Objectives.....</b>	<b>2</b>
<b>1.3 Structure.....</b>	<b>3</b>
<b>2 Literature Review .....</b>	<b>5</b>
<b>2.1 Coordinate Systems and Basic Definitions .....</b>	<b>6</b>
2.1.1 The hip .....	6
2.1.2 Acetabular Measurements.....	6
2.1.3 Femoral Measurements.....	8
2.1.4 Movements.....	10
2.1.5 Coordinate systems.....	10
2.1.6 Joint stability.....	11
<b>2.2 Normal Hip Joint Kinematics and Loads.....</b>	<b>12</b>
2.2.1 Kinematics measurement techniques .....	13
2.2.2 Normal kinematics.....	14
2.2.3 In-vivo force measurement with instrumented implants .....	15
2.2.4 Force measurement with musculoskeletal models.....	16
2.2.5 Normal hip joint forces.....	17
<b>2.3 Soft Tissue Anatomy and Biomechanics .....</b>	<b>18</b>
2.3.1 Muscles .....	18
2.3.2 The Capsular Ligaments .....	20
2.3.3 The Ligamentum Teres .....	23
2.3.4 The Acetabular Labrum .....	25
2.3.5 Cartilage.....	28
<b>2.4 Causes of hip pain, instability and osteoarthritis in the native hip .....</b>	<b>29</b>
2.4.1 Acetabular labral tears.....	29
2.4.2 Femoroacetabular impingement .....	30
2.4.3 Controversy in the treatment of FAI and Labral Tears .....	32
<b>2.5 Hip arthroplasty clinical results .....</b>	<b>33</b>
2.5.1 Metal-on-metal bearings.....	34
2.5.2 Metal-on-metal hip resurfacing .....	34
2.5.3 Ceramic-on-ceramic bearings.....	36
2.5.4 Hip arthroplasty technique and the effects on soft tissues .....	36
2.5.5 Current practice and future developments .....	37
<b>2.6 Mechanisms of edge loading and dislocation of hip replacements .....</b>	<b>38</b>

## CONTENTS

2.6.1 Mechanisms and consequences of dislocation .....	38
2.6.2 Preventing dislocation .....	39
2.6.3 Mechanisms and consequences of edge loading .....	39
2.6.4 The effect of high inclination on the risk of edge loading.....	41
2.6.5 The effects of prosthesis design on the risk of edge loading.....	41
2.6.6 The effects of soft-tissue balancing on the risk of edge loading .....	43
2.6.7 The effects of impingement and posterior edge loading on the risk of edge loading .....	44
2.6.8 Posterior Edge Loading without Impingement.....	45
2.6.9 Future Research.....	46
<b>2.7 Modelling techniques for studying hip biomechanics with focus on cadaveric testing .....</b>	<b>46</b>
2.7.1 Modelling techniques.....	46
2.7.2 Measurement techniques: resecting/repairing tissues to infer their function	47
2.7.3 Measurement techniques: Kinematics .....	50
2.7.4 Measurement techniques: Contact Stress/Pressure .....	50
2.7.5 Measurement techniques: Strain .....	51
2.7.6 Good practice when cadaveric testing: neutral position and coordinate system.....	53
2.7.7 Good practice when cadaveric testing: physiological loading.....	53
2.7.8 Cadaveric testing limitations .....	53
<b>3 Hip abduction can prevent posterior edge loading of hip replacements .....</b>	<b>55</b>
<b>3.1 Introduction.....</b>	<b>56</b>
3.1.1 Clinical motivation .....	56
3.1.2 Known mechanisms of edge loading and unexplained edge loading wear..	56
3.1.3 Aims and hypothesis .....	56
<b>3.2 Methods.....</b>	<b>57</b>
3.2.1 Muscle contribution to edge loading .....	57
3.2.2 Effects of implant design .....	58
3.2.3 Effects of implant orientation .....	59
3.2.4 Comparison with in-vivo force data.....	59
<b>3.3 Results.....</b>	<b>59</b>
3.3.1 Muscle contribution to edge loading .....	59
3.3.2 Effects of implant design .....	60
3.3.3 Effects of implant orientation .....	61
3.3.4 Comparison with in-vivo force data.....	62

<b>3.4 Discussion .....</b>	<b>63</b>
3.4.1 Most important findings .....	63
3.4.2 Limitations .....	64
3.4.3 Comparison with published research.....	66
3.4.4 Clinical relevance and conclusion.....	68
<b>3.5 Acknowledgements .....</b>	<b>68</b>
<b>4 Design and manufacture of a six-degrees-of-freedom hip joint testing system</b>	<b>69</b>
<b>4.1 Introduction.....</b>	<b>70</b>
4.1.1 Clinical motivation .....	70
4.1.2 The need for a six-degrees-of-freedom testing rig .....	70
4.1.3 Rig Specification.....	72
<b>4.2 Materials and methods .....</b>	<b>72</b>
4.2.1 Rig design tools and existing components.....	72
4.2.2 Material selection .....	72
4.2.3 Rig manufacture .....	73
4.2.4 Testing the rig's capabilities .....	73
4.2.5 Experimental validation .....	74
<b>4.3 Results.....</b>	<b>74</b>
4.3.1 The testing system .....	74
4.3.2 Material choice .....	76
4.3.3 The rig's capabilities.....	77
4.3.4 Experimental validation .....	77
<b>4.4 Discussion .....</b>	<b>79</b>
4.4.1 Most important finding .....	79
4.4.2 Rig limitations.....	79
4.4.3 Testing method limitations.....	80
4.4.4 Comparison to other work .....	81
4.4.5 Conclusion .....	82
<b>4.5 Acknowledgements .....</b>	<b>83</b>
<b>4.6 Assembly Drawings.....</b>	<b>84</b>
<b>5 A low-cost repeatable solution for aligning hip joint specimens in a known coordinate system in-vitro.....</b>	<b>91</b>
<b>5.1 Introduction.....</b>	<b>92</b>
<b>5.2 Materials and Method .....</b>	<b>93</b>
5.2.1 Drilling jigs.....	93
5.2.2 Intact to potted data collection .....	93

## CONTENTS

5.2.3 Intact to potted calculations .....	95
5.2.4 Quantification of additional error from pot to testing rig .....	96
<b>5.3 Results.....</b>	<b>97</b>
<b>5.4 Discussion.....</b>	<b>99</b>
5.4.1 Most important findings .....	99
5.4.2 Limitations .....	99
5.4.3 Comparison to other work.....	100
5.4.4 Conclusion .....	101
<b>5.5 Acknowledgements .....</b>	<b>101</b>
<b>5.6 Assembly Drawings.....</b>	<b>102</b>
<b>6 The envelope of passive motion allowed by the capsular ligaments of the hip</b> .....	<b>105</b>
<b>6.1 Introduction.....</b>	<b>106</b>
6.1.1 Clinical motivation .....	106
6.1.2 Previous range of motion research .....	106
6.1.3 The role of the hip joint capsule .....	106
6.1.4 Aims and hypothesis .....	107
<b>6.2 Materials and Methods .....</b>	<b>107</b>
6.2.1 Specimen preparation .....	107
6.2.2 The testing rig.....	108
6.2.3 Testing protocol.....	108
6.2.4 Data analysis.....	111
6.2.5 Statistical analysis .....	111
<b>6.3 Results.....</b>	<b>112</b>
6.3.1 The passive restraint envelope: the range of un-resisted rotation .....	113
6.3.2 The passive restraint envelope: mid-slack .....	113
6.3.3 Slack-to-taut and torsional stiffness .....	114
<b>6.4 Discussion.....</b>	<b>115</b>
6.4.1 Most important findings .....	115
6.4.2 Limitations .....	116
6.4.3 Comparison with published research.....	118
6.4.4 Clinical relevance and conclusion.....	121
<b>6.5 Acknowledgements .....</b>	<b>121</b>
<b>7 The capsular ligaments provide more hip rotational restraint than the</b> <b>acetabular labrum and the ligamentum teres.....</b>	<b>123</b>
<b>7.1 Introduction.....</b>	<b>124</b>



7.1.1 Clinical motivation .....	124
7.1.2 Previous hip ligament research .....	124
7.1.3 Aims and hypothesis .....	125
<b>7.2 Materials and Methods .....</b>	<b>125</b>
7.2.1 Specimen preparation .....	125
7.2.2 Testing protocol.....	126
7.2.3 Statistical Analysis.....	127
<b>7.3 Results.....</b>	<b>128</b>
7.3.1 Contributions of the capsular ligaments (combined), ligamentum teres and labrum.....	129
7.3.2 Contributions of the individual capsular ligaments .....	129
7.3.3 Subluxation and dislocation.....	130
<b>7.4 Discussion .....</b>	<b>131</b>
7.4.1 Most important findings .....	131
7.4.2 Limitations .....	133
7.4.3 Comparison with published research.....	135
7.4.4 Clinical relevance .....	135
7.4.5 Conclusion .....	136
<b>7.5 Acknowledgements .....</b>	<b>136</b>
<b>8 Discussion .....</b>	<b>137</b>
8.1 Most important findings .....	137
8.2 Limitations .....	137
8.3 Comparison to clinical research.....	138
8.4 Innovative methodology developed .....	139
8.5 Research impact.....	139
8.6 Conclusion .....	140
<b>9 Future Work .....</b>	<b>141</b>
<b>9.1 Muscle contribution to edge loading.....</b>	<b>141</b>
9.1.1 The effect of surgery on the muscle contribution to edge loading .....	141
9.1.2 The protective effect of gluteus medius activity .....	141
<b>9.2 Capsular ligament research .....</b>	<b>143</b>
9.2.1 Improvements to the rig and experimental set-up .....	143
9.2.2 Experimental measurement of ligament length changes and properties ....	143
9.2.3 Investigating the effects of surgical approaches on ligamentous restraint..	144
9.2.4 Investigating the role of capsular ligaments following total hip arthroplasty	144
9.2.5 Investigating the role of the capsular ligaments in hip stability .....	145

## CONTENTS

<b>10 Bibliography .....</b>	<b>147</b>
<b>11 Appendices .....</b>	<b>189</b>
<b>A3 Hip Abduction Prevents Edge Loading Appendices .....</b>	<b>189</b>
<b>A3.1 Muscle wrapping geometries .....</b>	<b>189</b>
<b>A3.2 Plugin overview .....</b>	<b>190</b>
A3.2.1 How it works.....	190
A3.2.2 More information .....	191
<b>A3.3 Modelling a hip replacement in MatLab .....</b>	<b>191</b>
A3.3.1 Initialising the cup.....	191
A3.3.2 Orientating the cup.....	192
A3.3.3 Verification of the cup position .....	193
<b>A3.4 Calculation to determine if muscles edge loads in a given hip position</b>	<b>193</b>
A3.4.1 Method 1: Calculating the angle between the cup-axis and the muscle line of action .....	194
A3.4.2 Method 2: Finding the intersection point between the cup-face and the muscle line of action.....	195
<b>A3.5 Conversion between Bergmann's and the ISB's coordinate systems....</b>	<b>196</b>
<b>A3.6 The effects of internal and external rotation on the number of muscles         that edge load .....</b>	<b>197</b>
<b>A3.7 The effects of grouping muscle fibres together .....</b>	<b>197</b>
<b>A3.8 How cup position effects the risk of edge loading.....</b>	<b>200</b>
<b>A3.9 Further work - how gluteal weakness could increase the risk of edge         loading.....</b>	<b>201</b>
A3.9.1 Materials and methods.....	201
A3.9.2 Results.....	201
A3.9.3 Discussion .....	202
<b>A4 Six-degrees-of-freedom rig design appendices.....</b>	<b>207</b>
<b>A4.1 Component drawings .....</b>	<b>207</b>
<b>A5 Repeatable in-vitro alignment jigs appendices.....</b>	<b>221</b>
<b>A5.1 Component Drawings .....</b>	<b>221</b>
<b>A5.2 Calculating directions of the axes of the ISB and Pot reference frames</b>	<b>226</b>
A5.2.1 ISB Pelvic Reference Frame Axes .....	226
A5.2.2 ISB Femoral Reference Frame Axes.....	226
A5.2.3 Pelvic Pot's and Rig's Reference Frame Axes .....	227
A5.2.4 Femoral Pot's Reference Frame Axes.....	229





## Figures

Figure 2.1 Definitions of Anteversion and Inclination (Murray, 1993). Reproduced with permission and copyright © of the British Editorial Society of Bone and Joint Surgery .	7
Figure 2.2 The abductor moment arm and the femoral offset. ....	9
Figure 2.3 Movements of the hip (van Arkel et al., 2015). Reproduced with permission and copyright © of the British Editorial Society of Bone and Joint Surgery.	10
Figure 2.4 Diagram defining the pelvic XYZ and femoral xyz axes (Wu et al., 2002). Reproduced with permission and copyright © from Elsevier .....	12
Figure 2.5 How ligaments provide stability (van Arkel and Amis, 2013). Reproduced with permission and copyright © from Elsevier. ....	14
Figure 2.6 Kinematics during the gait cycle for a single leg from heel strike to heel strike for a normal subject (Kadaba et al., 1990). Reproduced with permission and copyright © from John Wiley and Sons.....	15
Figure 2.7 The London Lower Limb Model (Modenese et al., 2011) produced in OpenSim (Delp et al., 2007). ....	17
Figure 2.8 Output from HIP98 (Bergmann et al., 2001). ....	18
Figure 2.9 Hip Joint muscles from an anterior view (left), posterior view of the superficial muscles (bottom left) and posterior view of the deep muscles (bottom right) (Ohara, 2006). Reproduced under the creative commons licence CC BY-SA 3.0.....	19
Figure 2.10 The capsular ligaments of the hip (Gray, 1918). Reproduced from 20th U.S. edition of Gray's Anatomy (copyright expired, available in the public domain). ....	22
Figure 2.11 The intra-articular ligamentum teres (Gray, 1918). Reproduced from 20th U.S. edition of Gray's Anatomy (copyright expired, available in the public domain). ....	24
Figure 2.12 Pincer and Cam FAI (Ganz et al., 2008). Reproduced with permission and copyright © from Springer.....	31
Figure 2.13 Increasing 'jump' distance with increasing femoral head size (van Arkel and Amis, 2013). Reproduced with permission and copyright © permission from Elsevier .	40
Figure 2.14 A diagram showing how high inclination can increase the risk of edge loading (van Arkel and Amis, 2013). Reproduced with permission and copyright © from Elsevier. ....	41

## FIGURES

Figure 2.15 A diagram showing how changing the prosthesis design can expose it to superior edge loading (van Arkel and Amis, 2013). Reproduced with permission and copyright © from Elsevier. ....	42
Figure 2.16 A diagram showing how poor soft tissue tensioning can lead to edge loading (van Arkel and Amis, 2013). Reproduced with permission and copyright © from Elsevier .....	43
Figure 2.17 A diagram showing how impingement can lead to secondary edge loading (van Arkel and Amis, 2013). Reproduced with permission and copyright © from Elsevier. ....	44
Figure 2.18 An example anterior/posterior laxity test as two ligaments are cut and a constant force is applied.....	49
Figure 2.19 Application of muscles loads using cables when cadaveric testing (Scifert et al., 2001). Reproduced with permission and copyright © from Elsevier. ....	54
Figure 3.1 A diagram showing how a change in hip position can cause a muscle to contribute to edge loading. ....	58
Figure 3.2 The definitions of $\alpha$ and $\beta$ in the transverse and sagittal planes respectively .....	60
Figure 3.3 List of the muscles included in the study indicating the percentage of positions in the complete range of motion at which each muscle could contribute to an edge loading force vector in a well-positioned cup.....	61
Figure 3.4 The percentage of muscles that can contribute to edge loading as a function of hip flexion with neutral rotation and different ab/adduction in a well-positioned cup	62
Figure 3.5 The effect of reducing the subtended angle of the cup arc on the possible muscle contribution to edge loading for a well-positioned cup with neutral hip abduction and rotation. ....	63
Figure 3.6 The number of muscles that can contribute to edge loading of a well-designed cup at 100° hip flexion and neutral hip rotation with varying hip abduction and cup orientation.....	64
Figure 3.7 The correlation between the direction of the contact vector relative to the pelvis and the position of the hip. ....	65
Figure 3.8 How an aspherical femoral head could invalidate the modelling assumptions.....	66

Figure 4.1 The custom built testing rig with a synthetic right hip joint mounted in flexion, adduction and neutral rotation. ....	75
Figure 4.2 A convergence analysis for the finite element analysis mesh. ....	77
Figure 4.3 The von Mises stresses in the testing rig under 1 kN of compressive load applied at the level of the hip joint centre.....	78
Figure 4.4 The resultant displacement of the rig under 1 kN vertical compressive load. ....	79
Figure 4.5 Experimental measurement of the rig's stiffness.....	81
Figure 5.1 The pelvic (left) and femoral (bottom) drilling jigs to prepare X/x and Z/z axes holes in the pelvis/femur respectively.....	94
Figure 5.2 Box plots of pelvic misalignment after using the drilling jig method to pot the pelvis in the ISB reference frame in terms of hip adduction/abduction (Add), internal/external rotation (IR), and flexion/extension (Flx).....	97
Figure 5.3 Box plots of pelvic misalignment caused when mounting the pelvic pot into the test rig in terms of hip adduction/abduction (Add), internal/external rotation (IR), and flexion/extension (Flx). ....	98
Figure 5.4 Box plots of pelvic misalignment when using the complete system including the drilling jigs and the test rig compared to an intact ISB reference frame in terms of hip adduction/abduction (Add), internal/external rotation (IR), and flexion/extension (Flx).....	98
Figure 5.5 Box plots of femoral misalignment after using the drilling jig method to pot the pelvis in the ISB reference frame in terms of hip adduction/abduction (Add), internal/external rotation (IR), and flexion/extension (Flx).....	99
Figure 5.6 The maximum misalignment caused by falsely identifying the femoral head is low due to the long length of the femur. ....	101
Figure 6.1 Anterolateral view of a hip in the testing rig in flexion, adduction and external rotation.....	109
Figure 6.2 Ten internal/external rotation cycles from one hip joint specimen. ....	110
Figure 6.3 The mean ab/adduction with standard deviation when 5 Nm torque was applied as flexion was varied whilst internal/external rotation was fixed in the neutral position (n=9). ....	113

## FIGURES

Figure 6.4 The rotation passive restraint envelope (with standard deviation), the points of mid-slack and the 5 Nm measurement boundaries across a complete hip range of motion (n=8).	114
Figure 6.5 The mean range of rotational slack as flexion (x-axis) and ab/adduction (different lines) varies with 95 % confidence intervals.	115
Figure 6.6 The position of the mid-slack point as flexion varies.	117
Figure 6.7 Mean angular change between the transition point and 5 Nm of rotational restraint (left) and torsional stiffness (right) with 95 % confidence intervals as flexion (x-axis) and ab/adduction (different lines) varies.	118
Figure 6.8: A comparison between clinical, experimental and computational range of motion measurements and the results from the present study for internal and external rotation at 90° flexion with neutral ab/adduction (top), and for flexion/extension with neutral ab/adduction and internal/external rotation (bottom).	119
Figure 7.1 Anterior view of a left hemipelvis mounted in the custom built testing rig.	126
Figure 7.2 An internal/external rotation cycle showing the change in torque as different ligaments are resected for one specimen positioned at 60° flexion and full adduction.	130
Figure 7.3 Mean percentage internal and external rotation restraint with 95 % confidence intervals provided by the hip capsule, labrum and ligamentum teres for a complete range of motion.	131
Figure 7.4 Mean percentage contributions to internal (top) and external (bottom) rotation restraint with 95 % confidence intervals provided by individual capsular ligaments for a complete range of hip motion.	132
Figure 7.5 Posterolateral views (top) and inferior view (bottom) of a hip in deep flexion with adduction and internal rotation.	133
Figure 9.1 A diagram showing how a robotic actuator can be used to directly measure ligament forces by resecting the acetabulum.	146
Figure 11.1 Wrapping surfaces included in the model in order to improve the muscle geometrical representation	190
Figure 11.2 Defining an acetabular cup in MatLab	191
Figure 11.3 Calculating if a muscle edge loads based on the angle it makes with the cup axis	194



Figure 11.4 Calculating if a muscle edge loads based on its intersection point with the cup face plane.....	196
Figure 11.5 The percentage of muscles that can contribute to edge loading as a function of hip flexion with neutral ab/adduction and different hip rotation for a well-positioned cup.....	197
Figure 11.6 The percentage of muscles that can contribute to edge loading with muscle fibres are grouped as complete muscles (the original analysis, left) and each muscle fibre plotted individually (right). It can be seen that there is little difference between the two analyses. ....	198
Figure 11.7 The percentage of the number of muscles that can contribute to edge loading (the original analysis, left) and the percentage of total force capacity at the hip that could contribute to edge loading (the percentage of physiological cross sectional area, right). It can be seen that there is little difference between the two analyses. ...	198
Figure 11.8 A comparison between the edge loading analysis based on whole muscles and muscle fibres. ....	199
Figure 11.9 The percentage of muscles that can contribute to edge loading as a function of hip flexion with neutral internal/external rotation with varying cup position	200
Figure 11.10 A comparison between the hip joint reaction forces for the unmodified Delp musculoskeletal model (solid lines) and Bergmann's in vivo forces for an average patient walking at their normal speed (dotted lines). ....	203
Figure 11.11 The effect of reducing the available maximum strength of the gluteus medius (solid green line) and minimus (dashed green line) on the forces (top) and abduction moments (bottom) provided by the muscles at the start (left), middle and end (right) of the single leg stance phase of gait. ....	204
Figure 11.12 The angle between the joint reaction force and the edge of the acetabular cup for the same gait cycle as the maximum available strength in the gluteus medius and minimus was reduced in a musculoskeletal model. ....	205
Figure 11.13 Left) a posterior view of a pelvis and the optical tracker. Right) anterior view of a pelvis with the right anterior superior iliac spine being digitised with the optical tacking probe.....	227
Figure 11.14 Calculating the pelvic rig's frame of reference. ....	229
Figure 11.15 Calculating the femoral pot's frame of reference.....	230

## FIGURES

Figure 11.16 Box plots of error estimates for the optical tracking digitising methodology in terms of adduction, internal rotation and flexion (all positive) for the pelvic ISB, pot and rig datasets.....	239
Figure 11.17 Error estimates for the optical tracking digitising methodology in terms of adduction, internal rotation and flexion (all positive) for the femoral ISB and pot datasets. ....	240
Figure 11.18 Box plots of the angle the hip joint reaction force makes in the coronal plane (left) and sagittal plane (right) for different patients (different rows).....	245
Figure 11.19 Mean angular change between the transition point and 5 Nm of rotational restraint (left) and torsional stiffness (right) with 95 % confidence intervals for internal and external rotation. It can be seen that the magnitude of restraint is largely symmetrical for hip rotation.....	247
Figure 11.20 A comparison between the passive restraint envelope and the positions of labral impingement. ....	250
Figure 11.21 The proportion of specimens for which a labral impingement was recorded before the 5 Nm restraint limit for internal rotation (top) and external rotation (bottom) in all hip positions. ....	251
Figure 11.22 A torque-rotation plot for one hip specimen in 60° flexion and neutral ab/adduction. Reducing the cut-off value effectively reduces the slack region as a smaller gradient is required to be considered taut. The opposite is true when increasing the cut-off gradient. ....	252
Figure 11.23 Sensitivity of the passive restraint envelope and slack region to variation in the cut-off gradient for automatic detection of the slack region. ....	252
Figure 11.24 A comparison between clinical, experimental and computational range of motion measurements and the results from the present study for internal and external rotation at neutral ab/adduction and neutral flexion/extension (top), and for flexion/extension with neutral ab/adduction and internal/external rotation (bottom)...	253
Figure 11.25 A comparison between average kinematics (solid black curves) of a hip replacement patient (Bergmann et al., 2001) for gait (left), stair climbing (middle) and rising from a high (50 cm) chair (right), with the range of motion required to develop 5 Nm of passive restraint from the hip ligaments (dashed grey curves). ....	255
Figure 11.26 A comparison between average kinematics (solid black curves) for high-dislocation-risk activities of daily living (Nadzadi et al., 2003) including a deep flexion sit-to-stand (left), tying a shoe-lace whilst sitting (middle) and pivoting whilst standing	

(right), with range of motion required to develop 5 Nm of passive restraint from the hip ligaments (dashed grey curves).....	256
Figure 11.27 Anatomical drawing of the medial and lateral arms of the iliofemoral ligament (left) (Gray, 1918)and corresponding photo of a hip specimen (right) in a neutral hip position .....	258
Figure 11.28 Cutting the medial iliofemoral ligament example .....	259
Figure 11.29 Photos of the ischiofemoral ligament. ....	262
Figure 11.30 Anterolateral view of the lateral iliofemoral ligament taut in mid-flexion, abduction and external rotation. ....	263
Figure 11.31 Lateral views of the medial iliofemoral ligament taut in extension (top left) and slack in flexion (top right) and anterior inferior views of it taut in internal and external rotation in hip extension (bottom left and right respectively). All other ligaments have been resected .....	264
Figure 11.32 Anterior views a hip in neutral flexion. The pubufemoral ligament taut in abduction (left), and slack in adduction (right). ....	265
Figure 11.33 Anteroinferior view a hip in mid-flexion, abduction and distraction so that the intra-articular ligamentum teres can be seen (not its functional position). ....	266
Figure 11.34 Lateral-inferior view of a distracted hip with all ligaments resected showing the labrum at the rim of the acetabulum. The intra-articular portions of the posterior and superior portions of the labrum can be seen. ....	267
Figure 11.35 Small subluxation of the femoral head caused by the ligamentum teres. ....	268
Figure 11.36 Male (X) versus female (O) contributions to internal rotational restraint with standard deviation for all six periarticular soft-tissues in all hip positions tested. It can be seen there is little difference between the genders. ....	269
Figure 11.37 Male (X) versus female (O) contributions to external rotational restraint with standard deviation for all six periarticular soft-tissues in all hip positions tested. It can be seen there is little difference between the genders. ....	270



## Tables

Table 2.1 Direction Definitions (Hogervorst et al., 2009).....	6
Table 2.2 Common definitions of anteversion and inclination (Murray, 1993) .....	7
Table 2.3 Mean ( $\pm$ SD) anteversion and inclination for a normal acetabulum .....	8
Table 2.4 Mean ( $\pm$ SD) anteversion (AV), neck-shaft angle (NS), femoral offset (FO), head diameter ( $\varnothing$ FH) and head-neck offset (HNO) for a normal femur.....	9
Table 2.5 Rotation axes definitions and the sign convention used in this thesis .....	10
Table 2.6 Range of Motion of a Normal Male Hip (Boone and Azen, 1979).....	11
Table 2.7 Definitions of pelvic XYZ and femoral xyz.....	13
Table 2.8 Muscle Groups and their functions.....	20
Table 2.9 Primary limiting functions of the capsular ligaments (Fuss and Bacher, 1991; Martin et al., 2008) .....	23
Table 2.10 Surgical Technique and Soft Tissue Damage .....	37
Table 3.1 The models and dimensions of implant designs studied .....	59
Table 4.1 The aluminium rig's response to different load cases.....	80
Table 5.1 Anatomical locations for screw placement .....	95
Table 6.1 Morphological measurements of the eight hips included in the data analysis. ....	112
Table 6.2 All significant increases/decreases measured for the slack region, slack-to-taut and torsional stiffness. Similarities between increases in the slack region, decreases in slack-to-taut and increases in torsional stiffness are highlighted in red. When no difference was detected for the one-way RMANOVA, the effect size is not given (n.s.). ....	116
Table 7.1 Morphological measurements of the nine hips included in the data analysis. ....	129
Table 11.1 The mean $\pm$ standard deviation percentage contributions of the capsular ligaments (C), the ligamentum teres (LT) and the labrum (L) to internal rotation restraint in all hip positions.....	260
Table 11.2 The mean $\pm$ standard deviation percentage contributions of the capsular ligaments (C), the ligamentum teres (LT) and the labrum (L) to external rotation restraint in all hip positions. ....	261



# 1 Introduction

## 1.1 Motivation

It is estimated that one in four people will suffer from hip osteoarthritis in their lifetime (Murphy et al., 2010). The cause of the disease can vary between people (Dieppe and Lohmander, 2005), however it is believed to be mechanical in origin for many with trauma, unfavourable joint shapes or excessive loading leading to high stresses, cartilage damage and osteoarthritis (Ganz et al., 2003; Wearing et al., 2006). This degenerative condition is currently irreversible and can greatly impact a person's quality of life by causing severe pain and restricting their mobility. The end-stage treatment for patients with severe osteoarthritis requires complete replacement of the articulating surfaces with an engineered alternative – a total hip replacement. The implantation of this technology is considered by some to be the most successful surgical procedure in modern medicine: 95 % of primary hip replacements survive for more than 10 years without the need for revision surgery and it is not uncommon for patients to experience an imperceptible, 'silent', hip replacement. Consequently, it has become a high-volume elective surgical procedure with over 620,000 primary procedures performed in the UK between 2003 and 2013 (NJR, 2014). However, whilst the overall statistics are impressive, following surgery one in ten patients limp, experience severe or moderate pain or struggle with simple activities such as putting on their socks (NZJR, 2014). Over 75,000 procedures are being performed in the UK each year, so addressing these problems could improve quality of life for many individuals. Moreover, there is further opportunity for improvement when treating younger patients who are more active; currently the revision rate for people aged <55 years old is approximately three times that of patients over 75 (NJR, 2014), yet these younger patients have greater need for longevity from their implant due to their young age.

Many of the functional limitations experienced by hip replacement patients involve movements that require a large range of hip motion. It is also at the limits of the range of hip motion where complications such as dislocation and edge loading occur. Edge loading is considered to be one of the main causes of early failures for the hard-bearing hip replacements that have been designed for a younger, more active patient; it has been linked to squeaking in ceramic hips (Walter et al., 2011) and the high failure rate (in some cases >30 % at seven years (NJR, 2014)) of metal-on-metal hip replacements (Kwon et al., 2010). The effects of implant design and component positioning on edge loading risk have been extensively researched, however, there is less information

## CHAPTER 1

regarding the roles of muscles and ligaments and their causative/protective roles for the mechanisms of edge loading. The periarticular muscles and ligaments have a known role in preventing dislocation following hip replacement surgery and one of the main mechanisms for edge loading is a partial subluxation that relocates before complete dislocation occurs; hence, it is likely these soft tissues also have an important preventative role for edge loading as well.

Impingement and edge loading at the limits of the range of hip motion has also been identified as one of the causes of osteoarthritis in a native hip and there is increasing interest in joint preserving hip surgery to remove the source of impingement before the joint degrades to relieve pain and potentially prevent osteoarthritis (Leunig and Ganz, 2014). However, for any intra-articular hip surgery, it is necessary to cut muscles and/or ligaments to gain access to the joint; this is true not only for established open surgical techniques (Ganz et al., 2001), but also for arthroscopic, 'key-hole', joint preserving surgery (Bedi et al., 2013; Domb et al., 2013) as well as minimally invasive hip replacement surgery (Lovell, 2008). Each approach has its pros and cons and damages some tissues, whilst protecting/repairing others. What is more, it is known that the choice of approach can affect outcomes for patients; for example, a posterior approach for hip replacement surgery results in a higher risk of dislocation than a lateral approach unless the posterior ligaments and muscles are repaired (Kwon et al., 2006). Understanding the biomechanical function of these soft-tissues and how they contribute to normal joint function is essential for making educated decisions about which surgical approaches to use, and which tissues to protect/cut/repair depending on an individual patient's functional requirements following surgery.

Developing a deeper understanding of the biomechanical function of muscles and ligaments at the limits of the range of hip motion could help advance both early intervention and hip replacement surgery; particularly when considered in relation to edge loading. This therefore forms an exciting opportunity for clinically relevant biomechanical research.

### **1.2 Aims and Objectives**

The aim of this thesis is to improve the understanding of the biomechanics of hip muscles and ligaments at the limits of hip motion to better understand their influence on the mechanisms of edge loading. This breaks down into two more specific objectives:

- i. To investigate the muscle contribution to edge loading throughout the range of hip motion to better understand if/how surgical approaches/rehabilitation strategies could help prevent edge loading.



- ii. To investigate the role of ligaments in restraining excessive hip rotation and preventing impingements so that the most important ligaments can be preferentially protected/repaired during surgery.

### **1.3 Structure**

Following the literature review, which explores the topics introduced in section 1.1 in more detail, this thesis presents four self-contained papers in a journal format: one has been published in the Journal of Orthopaedic Research, one is in press with the Bone and Joint Journal, one is under consideration at the Journal of Biomechanics and the fourth paper will be submitted after this thesis. In the middle of these research papers is also an additional chapter, which gives an overview of the design of a hip joint testing system that was designed and manufactured for the subsequent experimental tests.

Each paper provides a concise description of the methods and main findings and so is also supported by an extensive set of appendices which describe parts of the method in finer detail, provide supporting sensitivity analyses, describe secondary results which were not included in the paper and provide more extensive verification for some of the key findings. The appendices are numbered to match their accompanying chapter and they are referenced and summarised in the main papers at the most relevant point.



## 2 Literature Review

Some of the text and images in this literature review extracts from my papers detailed below, and have been reprinted with permission. The text and images are cited when used. The two papers used in this chapter are:

van Arkel, R., Amis, A., 2013. (i) Basics of orthopaedic biomechanics. *Orthopaedics and Trauma* 27(2):67-75.

van Arkel, R.J., Amis, A.A., Cobb, J.P., Jeffers, J.R.T., 2015. The capsular ligaments provide more hip rotational restraint than the acetabular labrum and the ligamentum teres: an experimental study. *Bone & Joint Journal* 97-B, 484-491.

## CHAPTER 2

### 2.1 Coordinate Systems and Basic Definitions

The sagittal plane separates left/right, the coronal plane separates front/back and the transverse plane separates top/bottom. Front/back, top/bottom and inside/outside have clinical terms which are always used when describing views of the torso and limbs as detailed in Table 2.1.

#### 2.1.1 The hip

The hip joint approximates a ball and socket joint (Cereatti et al., 2010) that connects the femur to the pelvis, i.e. the lower limb to the torso. The femur provides the ball, which sits inside the acetabular socket in the pelvis. The pelvis is made of three bones, the ilium, ischium and pubis, which fuse during childhood (Gray, 2008). Cranially, the pelvis attaches to the lumbar spine via the sacrum and distally the femur is attached to the tibia at the knee joint (Gray, 2008). For a healthy lower limb, when standing up right it should be possible to draw a vertical line through the hip, knee and ankle joint centres; this mechanical axis of the lower extremity forms a plane (parallel to the sagittal plane) when flexion and extension in three dimensions are considered (Whiteside, 2002).

#### 2.1.2 Acetabular Measurements

The orientation of the acetabulum (or acetabular cup in a hip replacement) is described in terms of anteversion (opposite retroversion) and inclination (also known as abduction). Anteversion is measure of how much the socket faces forwards, and inclination a measure of how much it is tilted upwards. The exact definition of these orientations depends on context with the most common definitions shown in Table 2.2 and Figure 2.1. Measurements for a normal acetabulum are given in Table 2.3.

Clinically, the degree of acetabular anteversion or inclination is important as it

Table 2.1 Direction Definitions (Hogervorst et al., 2009)

Direction Pair	Basic Definition	Finer Detail
Anterior/Posterior	Front/Back	In animals this is Belly/Back-side
Ventral/Dorsal	Front/Back	In animals this is Belly/Back-side
Medial/Lateral	Inside/Outside	Towards/Away From the middle of the body
Superior/Inferior	Top/Bottom	Above/Below
Cranial/Caudal	Top/Bottom	Towards the Head/Tail, useful for describing the spine, pelvis etc.
Proximal/Distal	Top/Bottom	Towards the Beginning/End, useful for describing limbs which start at the torso and end at the hands or feet.

Table 2.2 Common definitions of anteversion and inclination (Murray, 1993)

Orientation	Definition	Notes
Operative Anteversion	The angle between the longitudinal axis of the patient and the acetabular axis as projected on to the sagittal plane.	Akin to flexion of the acetabular axis
Operative Inclination	The angle between the acetabular axis and the sagittal plane.	Akin to abduction of the acetabular axis
Radiographic Anteversion	The angle between the acetabular axis and the coronal plane.	
Radiographic Inclination	The angle between the longitudinal axis and the acetabular axis when this is projected on to the coronal plane.	
Anatomical Anteversion	The angle between the transverse axis and the acetabular axis when this is projected on to the transverse plane.	Similar to internal rotation of the acetabulum about a longitudinal body axis.
Anatomical Inclination	The angle between the acetabular axis and the longitudinal axis.	

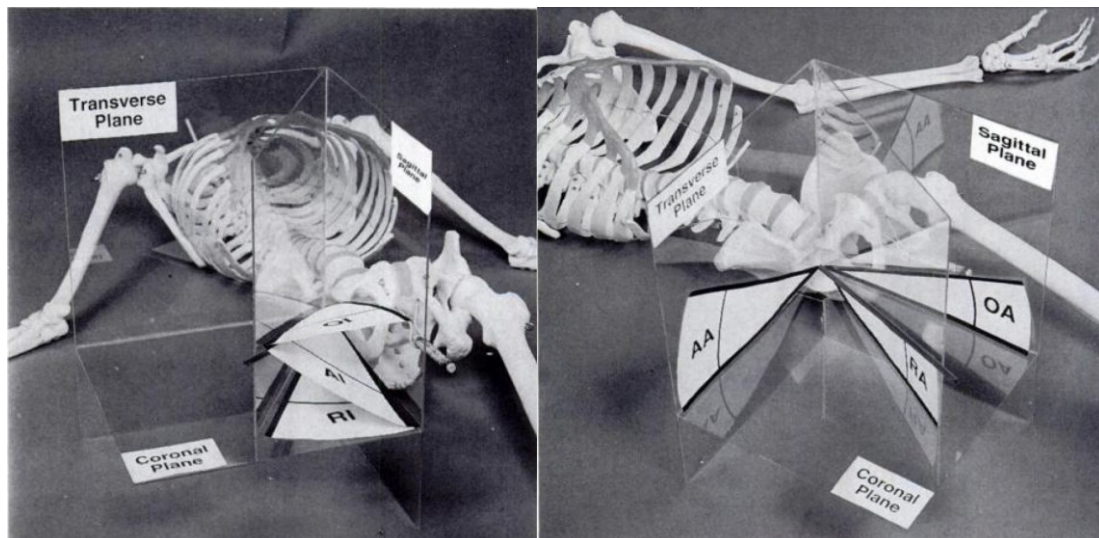


Figure 2.1 Definitions of Anteversion and Inclination (Murray, 1993). Reproduced with permission and copyright © of the British Editorial Society of Bone and Joint Surgery

Preceding letters: O is operative, R is radiographic, and A is anatomical. Following letters: A is anteversion, I is inclination.

influences both the range of motion before impingement in the native (Reynolds et al., 1999) and replaced hip (D'Lima et al., 2000) as well as the severity of component wear in metal-on-metal (De Haan et al., 2008a; Grammatopoulos et al., 2010a) and ceramic on ceramic hip implants (Esposito et al., 2012) (see section 2.6).

Another important measurement for the acetabulum is its subtended angle: a deficient acetabulum (an under-covered hip) is at risk of edge loading and higher wear rates in both the native hip (Chagini et al., 2009), where it is more commonly known as dysplasia and measured as the centre-edge angle (Tönnis et al., 1987; Cooperman, 2013), and the replaced hip (Jeffers et al., 2009; Langton et al., 2009). Conversely, an

## CHAPTER 2

Table 2.3 Mean ( $\pm$  SD) anteversion and inclination for a normal acetabulum

Reference	Study type	#	Gender	Anteversion ( $^{\circ}$ )	Inclination ( $^{\circ}$ )
Gray	-	-	Male	14	45
			Female	19	
Nakahara et al.	CT	36	Male	$17.5 \pm 6.1^{\circ}$	$36.4 \pm 3.2^{\circ}$
		70	Female	$21.3 \pm 6.8^{\circ}$	$39.1 \pm 4.1^{\circ}$
Cobb et al.	CT	12	Male	$22 \pm 6^{\circ}$	$51 \pm 3^{\circ}$
		8	Female	$26 \pm 6^{\circ}$	
Krebs et al.	Cadaveric	100	-	$20.7 \pm 3.8^{\circ}$	$39.8 \pm 7.0^{\circ}$

Gray (Gray, 2008); Nakahara et al. (Nakahara et al., 2011); Cobb et al. (Cobb et al., 2010); Krebs et al. (Krebs et al., 2009).

over-covered hip is at great risk of impingement (Cobb et al., 2010; Leunig and Ganz, 2014).

### 2.1.3 Femoral Measurements

Femoral anteversion represents how far the femoral head is rotated forwards compared to an axis at the knee; it is typically measured as the angle the femoral neck makes with the epicondylar axis.

A varus deformity is one such that a bone or joint is twisted inward, towards the midline of the body; for the hip this means that the neck-shaft angle is decreased and is known as coxa vara. Valgus, the opposite, is an outward twist and an increase in the neck-shaft angle at the hip known as coxa valga.

The amount of femoral anteversion and varus/valgus is clinically important as these angles directly affect the femoral offset and hence the abductors moment arms and strength (McGrory et al., 1995) (Figure 2.2). Weak hip abductors can cause clinical problems such as postoperative limp in hip replacement patients (Masonis and Bourne, 2002) or iliotibial band syndrome in young athletic patients (Fredericson et al., 2000). Femoral anteversion can also influence the range of motion before impingement in both the native (Audenaert et al., 2012) and replaced hip (Burroughs et al., 2005).

Head-neck offset indicates the relative size and position of the femoral head compared to the femoral neck. The offset can be measured as an average around the neck or specified to be the anterior/posterior head-neck offset as appropriate. Head-neck offset is clinically important when considering hip impingement; high head-neck offset increases the range of motion before impingement in both the native (Hogervorst et al., 2009; Audenaert et al., 2012) and replaced hip (Burroughs et al., 2005; Incavo et al., 2011), see sections 2.4.2 and 2.6.7.

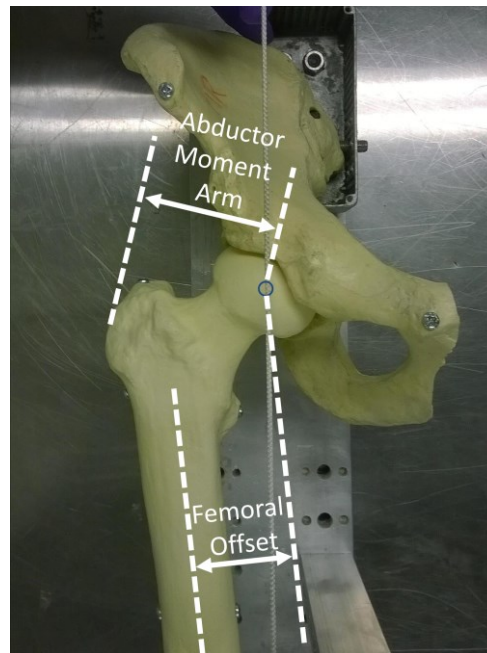


Figure 2.2 The abductor moment arm and the femoral offset.

The piece of white string running superior-inferiorly highlights the mechanical axis of the femur running from the femoral head centre (blue circle) to the mid-point of the femoral epicondyles (not shown).

For an average person, left and right proximal femurs can be considered symmetric with mean variation less than 4 % between sides (Young et al., 2012); measurements for a normal femur are given in Table 2.4.

Table 2.4 Mean ( $\pm$  SD) anteversion (AV), neck-shaft angle (NS), femoral offset (FO), head diameter ( $\varnothing$ FH) and head-neck offset (HNO) for a normal femur

Reference	Study type	#	Gender	AV ( $^{\circ}$ )	NS ( $^{\circ}$ )	FO (mm)	$\varnothing$ FH (mm)	HNO (mm/ $\varnothing$ FH)
Gray	-	-	-	10-15	135	-	-	-
Nakahara et al.	CT	36	Male	$20.3 \pm 9.9$	$125.1 \pm 4.9$	-	$48.5 \pm 2.4$	-
		70	Female	$25.2 \pm 9.8$			$42.9 \pm 2.3$	
Ellis et al.	CT	76	-	$9.3 \pm 6.5$	$124.2 \pm 5.8$	-	$45.9 \pm 4.7$	$0.29 \pm 0.02$
Unnanuntana et al.	Cadaveric	100	Male	$8.9 \pm 8.3$	$133.9 \pm 5.9$	$42.7 \pm 5.7$	$55.5 \pm 3.2$	-
		100	Female	$11.4 \pm 7.5$	$131.5 \pm 5.7$	$39.7 \pm 6.0$	$48.7 \pm 2.5$	
Yoshioka et al.	Cadaveric	16	Male	$7 \pm 6.8$	$129 \pm 7.3$	-	$52 \pm 3.3$	-
		16	Female	$8 \pm 10.0$	$133 \pm 6.6$		$45 \pm 3.0$	

Gray (Gray, 2008); Nakahara et al. (Nakahara et al., 2011); Ellis et al. (Ellis et al., 2011); Unnanuntana et al. (Unnanuntana et al., 2010); Yoshioka et al. (Yoshioka et al., 1987)

## CHAPTER 2

### 2.1.4 Movements

Movements of the hip are described as flexion/extension, ab/adduction, internal/external rotation and these are shown in Figure 2.3 and described in Table 2.5. Flexion, adduction and internal rotation are considered the positive direction throughout this thesis. Normal range of motion values are given in Table 2.6.

### 2.1.5 Coordinate systems

The pelvic coordinate system is typically based on a left-right axis such as between the anterior superior iliac spines (Bartz et al., 2000; Wu et al., 2002; Incavo et al., 2011) or

Table 2.5 Rotation axes definitions and the sign convention used in this thesis

Movement	Equivalents	Sign	Description (Hogervorst et al., 2009)
Flexion		+	Bending, lower limb moves anteriorly
Extension		-	Straightening, lower limb moves posteriorly
Adduction		+	Limb moves towards midline of the body
Abduction		-	Limb moves away from the midline of the body
Internal Rotation	Endorotation, medial rotation.	+	The greater trochanter turns inwards, the anterior femur moves towards the anterior pelvis.
External Rotation	Exorotation, lateral rotation	-	The greater trochanter turns outwards, the posterior femur moves towards the posterior pelvis.

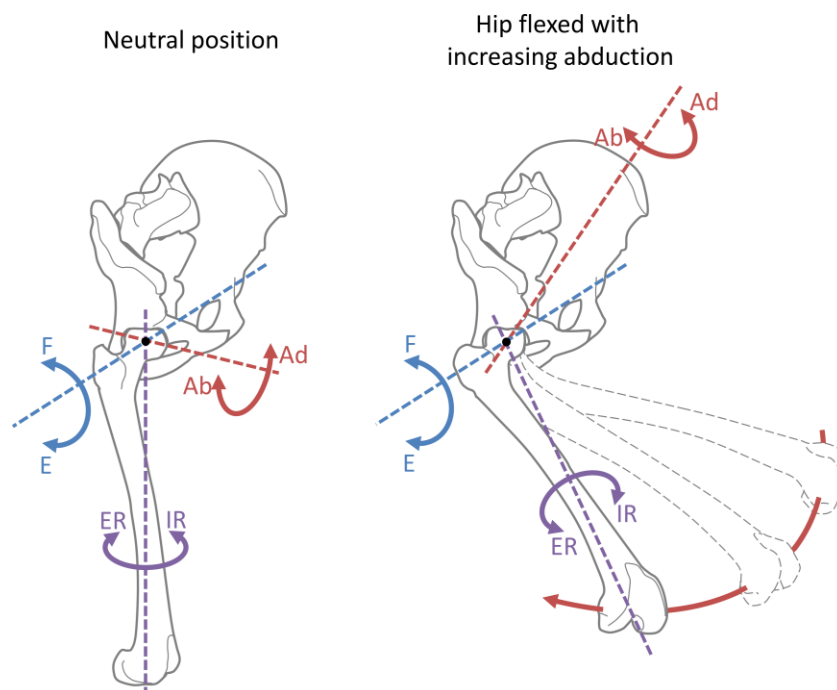


Figure 2.3 Movements of the hip (van Arkel et al., 2015). Reproduced with permission and copyright © of the British Editorial Society of Bone and Joint Surgery.

Flexion/extension, F/E, is a movement about an axis fixed to the pelvis; internal/external rotation, IR/ER, is a movement about an axis fixed to the femur; and ab/adduction, Ab/Ad, is a movement about a floating axis.



Table 2.6 Range of Motion of a Normal Male Hip (Boone and Azen, 1979)

<b>Motion</b>	<b>Maximum <math>\pm</math> SD (<math>^{\circ}</math>)</b>
Flexion	121.3 $\pm$ 6.4
Extension	12.1 $\pm$ 5.4
Abduction	40.5 $\pm$ 6.0
Adduction	25.6 $\pm$ 3.6
Internal Rotation	44.4 $\pm$ 4.3
External Rotation	44.2 $\pm$ 4.8

the hip joint centres (Bergmann et al., 2001) combined with a third point in the sagittal plane such as the midpoint between the posterior-superior iliac spines (Wu et al., 2002), the pubic symphysis (Bartz et al., 2000) or the centre of the L5-S1 vertebral body (Bergmann et al., 2001).

The femoral coordinate system is based on a superior-inferior axis such as a mechanical axis based on the femoral head centre and the midpoint of the epicondyles (Wu et al., 2002) or the insertion point of the posterior cruciate ligament (Yoshioka et al., 1987), or more simply using the femoral shaft (Bergmann et al., 2001) combined with an axis for neutral hip rotation such as the femoral epicondyles (Yoshioka et al., 1987; Wu et al., 2002) or the posterior aspect of the femoral condyles (Bergmann et al., 2001; Incavo et al., 2011).

The origin of the coordinate system is typically the femoral head centre and the movement axis are defined such that flexion/extension occurs about the pelvic left-right axis, internal/external rotation about the superior-inferior long-axis of the femur, and ab/adduction is floating.

In recent years, the ISB established a well-defined coordinate system that is now used for much hip research (Wu et al., 2002) and hence will be used as the coordinate system in this thesis. The definition of the pelvic X, Y and Z (uppercase letters), femoral x, y and z (lowercase letters), and movement  $e_1$ ,  $e_2$  and  $e_3$  axes are detailed in Table 2.7 and Figure 2.4.

#### *2.1.6 Joint stability*

A stable object is one that returns to its original place when it is displaced. For a joint this would mean the joint returns to/maintains its original position upon application of an external load. This stability can be achieved actively or passively; active stability comes from the action of muscles, and passive stability from joint shape, ligaments and fibrocartilage structures. The body makes use of both types of stability as passive

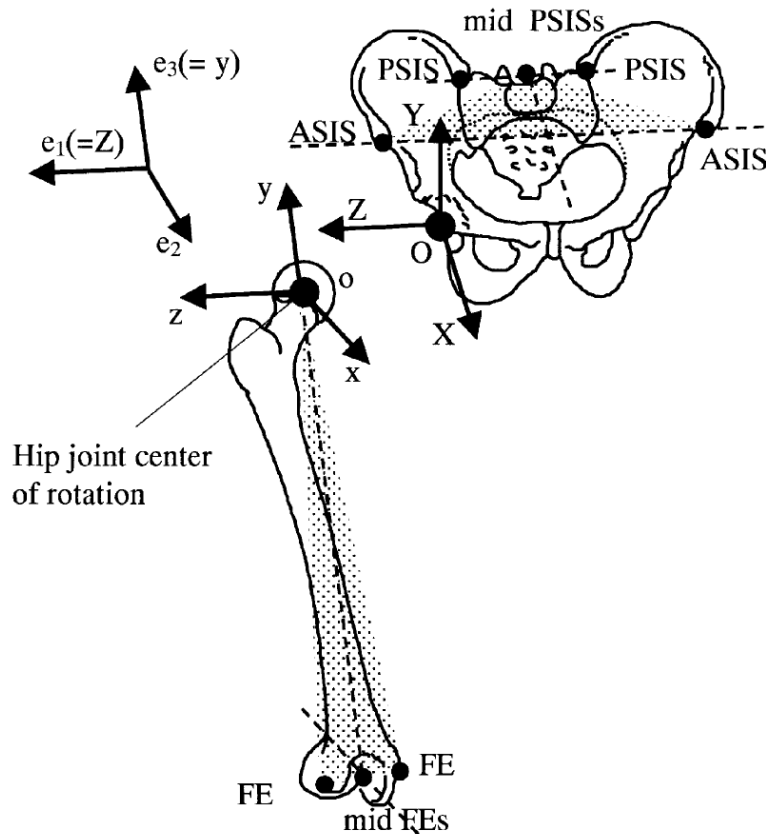


Figure 2.4 Diagram defining the pelvic XYZ and femoral xyz axes (Wu et al., 2002). Reproduced with permission and copyright © from Elsevier

The ASIS/PSIS are the anterior/posterior superior iliac spine respectively; and FE represents the femoral epicondyles.

stability is advantageous in terms of energy expenditure and does not require neuromuscular control whereas active stability allows fine control of limb position over a large range of motion. The amount of restoring force exerted by a ligament, and hence its contribution to stability, is proportional to its increase in length during the movement (van Arkel and Amis, 2013) (Figure 2.5).

Stability can also be referred to as restraint and these two terms can be used interchangeably; however, as a rule of thumb when describing joint biomechanics, stability is used to describe resistance to translations whereas restraint is used to describe resistance to rotation.

## 2.2 Normal Hip Joint Kinematics and Loads

A normal person, or an active hip replacement patient with a good functional outcome, typically walks >1.2 million gait cycles, climbs 100,000 steps and rises from a chair 22,000-28,000 times per annum (Morlock et al., 2001; Dall and Kerr, 2010). Thus, these activities of daily living are frequently studied to determine the success of a treatment program, the effects of a disease, or for pre-clinical testing of implants.

Table 2.7 Definitions of pelvic XYZ and femoral xyz

Axis	System	Definition
O	Pelvic	Origin coincident with the right (or left) hip centre of rotation.
X	Pelvic	The line parallel to a line lying in the plane defined by the two ASISs and the midpoint of the two PSISs, orthogonal to the Z-axis, and pointing anteriorly.
Y	Pelvic	The line perpendicular to both X and Z, pointing cranially.
Z	Pelvic	The line parallel to a line connecting the right and left ASISs, and pointing to the right.
o	Femoral	Origin, coincident with the right (or left) hip centre of rotation.
x	Femoral	The line perpendicular to both y- and z-axis, pointing anteriorly
y	Femoral	The line joining the midpoint between the medial and lateral FEs and the origin, and pointing cranially.
z	Femoral	The line perpendicular to the y-axis, lying in the plane defined by the origin and the two femoral epicondyles, pointing to the right.
$e_1$	Movement	Flexion/extension and medial/lateral translation, coincident with the Z-axis (pelvic).
$e_2$	Movement	Ab/adduction and anterior/posterior translation, floating axis perpendicular to axes $e_1$ and $e_3$ .
$e_3$	Movement	Internal/external rotation and proximal/distal translation, coincident with the y-axis (femoral).
Neutral	All	When the pelvic and femoral coordinate systems (O/o, X/x, Y/y and Z/z) are coincident. (A similar position to standing upright).

### 2.2.1 Kinematics measurement techniques

Range of motion can be measured with a goniometer (Boone and Azen, 1979; Roach and Miles, 1991; Nussbaumer et al., 2010). However, when complex movements are studied, real-time techniques are needed and so kinematics of the hip joint are most commonly found using optical tracking systems (Bergmann et al., 2001; Nadzadi et al., 2003; Yoshioka et al., 2007; Charbonnier et al., 2009; Mellon et al., 2011; Kwon et al., 2012) such as the Vicon system (Vicon, Oxford, UK). For these systems to work, reflective markers are placed on skin adjacent to anatomical landmarks such as the femoral epicondyles and the anterior/posterior iliac spines. The results from this method are widely used as they can be used to explore most possible movements and can be combined with ground reaction force data easily by performing the movement on a force plates.

Key limitations of optical tracking measurements include the errors that are introduced from soft tissue artefacts between the skin-markers and the underlying bony anatomical landmark (Lu and O'Connor, 1999; Murphy et al., 2011) and difficulties in determining the joint centre (Lopomo et al., 2010; Heller et al., 2011) from surface measurements. These limitations can be overcome using low-dose high-frame-rate

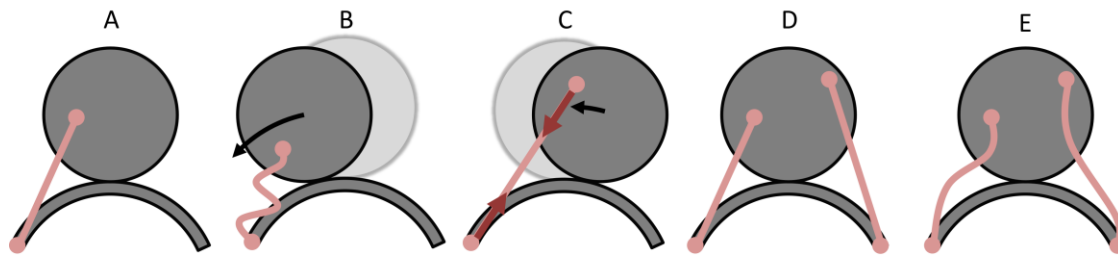


Figure 2.5 How ligaments provide stability (van Arkel and Amis, 2013). Reproduced with permission and copyright © from Elsevier.

A) A partially stable configuration. B) When the ball of the joint is rolled to the left then the joint is unstable and the ball is able to continually roll and would permanently dislocate unless relocated by muscle action. C) If the ball is rolled to the right then the ligament provides a passive restoring force, which is proportional to the amount of rotation, and thus returns the ball to its original position. D) A fully stabilised joint with a limited range of motion. E) A joint protected against dislocation by ligaments, with a larger range of motion than D, however muscular action is needed to enhance joint stability where the ligaments are slack.

fluoroscopy. For example, a known CAD model (usual based on a prior CT scan, or known prosthesis design) can be matched to a series of 2D fluoroscopic in-vivo images to measure hip kinematics (Koyanagi et al., 2011; Dimitriou et al., 2015). However the main disadvantage of these systems is a very small viewing window, which makes measurement of movements with large displacements of the lower limb challenging as the joint can easily move out of the field of view. This is less of a problem for a Vicon system where a large volume can be captured using multiple cameras. Another disadvantage is that fluoroscopic techniques have an inherent radiation exposure associated with them which limits the number of repeats that can be performed for each patient.

### 2.2.2 Normal kinematics

Gait is described in two phases: the stance phase when the foot is in contact with the ground, and the swing phase when it is not. Stance begins with heel strike and ends with toe-off and a typical gait cycle is shown in Figure 2.6. It can be seen that the peak range of motion during gait utilises only a small portion of the available range of hip motion (Table 2.6, page 11), however many hip pathologies affect movements that require a greater range of motion and hence it is important to study a variety of daily activities including gait. During daily activities such as tying a shoe, rising from a low chair, or pivoting on the spot average kinematics can exceed: 100° flexion, 15° extension, 15° adduction, 20° abduction, 20° internal or 45° external rotation (Johnston and Smidt, 1970; Nadzadi et al., 2003). Moreover, an average ballet dancer can exploit extreme hip range of motion during dance moves utilising up to: 110° flexion, 40° extension, 70° abduction or 35° internal rotation during different movements (Charbonnier et al., 2011).

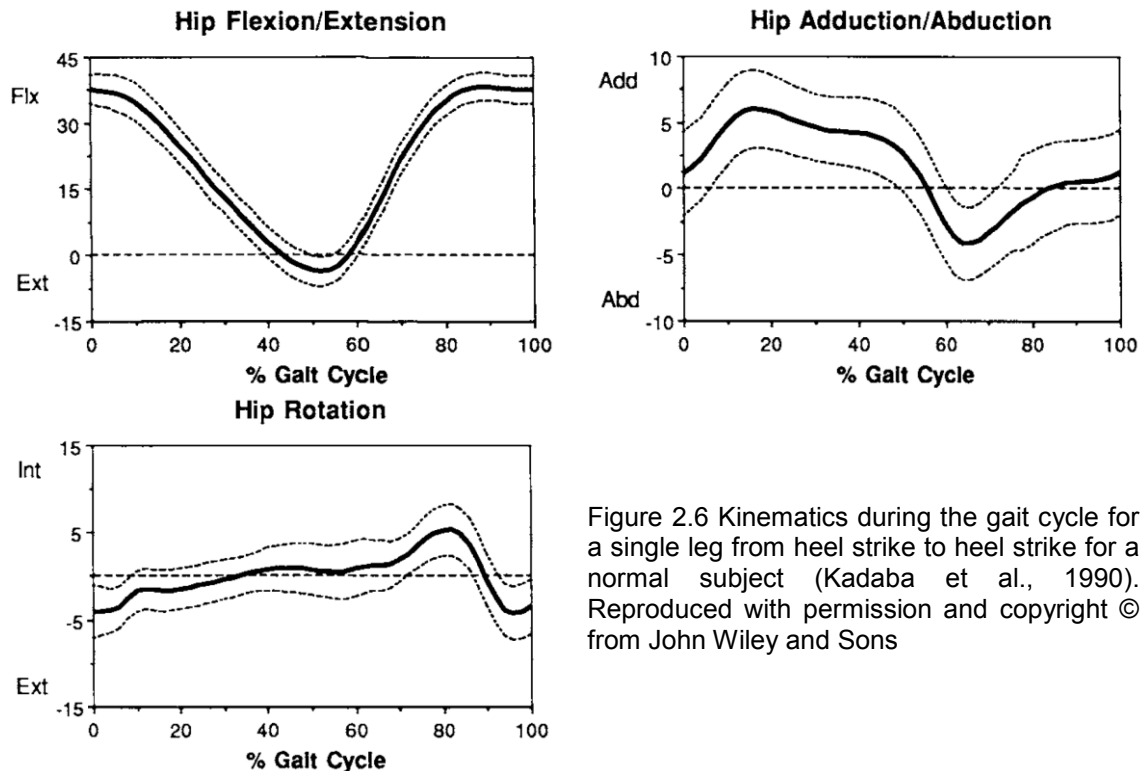


Figure 2.6 Kinematics during the gait cycle for a single leg from heel strike to heel strike for a normal subject (Kadaba et al., 1990). Reproduced with permission and copyright © from John Wiley and Sons

### 2.2.3 *In-vivo* force measurement with instrumented implants

Early work to instrument implants used pressure sensors under the surface of the femoral head to measure *in vivo* contact pressures (Hodge et al., 1986; Hodge et al., 1989); typical peak contact pressures during the gait cycle range from 2.4-5.5 MPa with pressures up to 18 MPa being recorded when rising from a chair. Aside from providing researchers with contact pressure values during daily activities, one of the main findings from these tests was that hip joint muscles frequently co-contract resulting in higher contact forces than that predicted by a Newtonian inverse dynamics analysis using ground reaction forces (Park et al., 1999).

More recently the Bergmann group have produced what is now the gold standard for hip joint (and knee, shoulder and spine) loading using their strain gauge instrumented implants (Bergmann et al., 2001; Bergmann, 2008). The three strain gauges are implanted in the femoral neck to monitor the force components acting on the ceramic ball, with a transmitter to send data telemetrically to computers outside of the patient. The latest design also has a fourth strain gauge in the femoral shaft to provide information on temperature changes experienced by the implant (Bergmann, 2010). This highly regarded work is used frequently by both researchers and industry to produce realistic tests to validate new prosthesis and understand the hip joint. The original data were published (Bergmann et al., 2001) and all the data were made freely available on a cd, 'HIP98'. The HIP98 cd provided both the hip joint contact forces

## CHAPTER 2

during seven daily activities along with kinematics and muscles loads for some trials (Heller et al., 2001). More recently Bergmann's research has been expanded and has resulted in the OrthoLoad database (Bergmann, 2008) where hundreds of trials ranging from gait to stumbling to getting out of a car/bath can be freely downloaded for the hip, spine, shoulder and knee.

The greatest strength of taking measurements with instrumented implants is that it gives true in-vivo measurements; however, the biggest weakness is that they can only be taken in patients who have had joint pathology and required a joint replacement. The surgical procedures for these are invasive, damaging muscles and changing the joint anatomy and hence the loads will not be completely representative of normal subjects, though provide a good baseline.

### *2.2.4 Force measurement with musculoskeletal models*

The key advantage of using musculoskeletal models to estimate joint forces is that they can be used for any person regardless of the presence/lack of hip pathology and do not require invasive insertion of instrumented/implants. Models are typically developed from established cadaveric databases detailing measurements of muscle origins and insertions for a normal limb (Brand et al., 1982; Hoy et al., 1990; Glitsch and Baumann, 1997; Klein Horsman et al., 2007). Two of these datasets (Brand et al., 1982; Klein Horsman et al., 2007) have been used to produce open-source musculoskeletal models which can be used to estimate moment arms and muscles forces during daily activities (Delp et al., 1990; Modenese et al., 2011); an example model is shown in Figure 2.7.

The models estimate forces using ground reaction force and kinematic data typically recorded with a Vicon system or equivalent. The joint kinetics can be calculated directly from this data and knowledge of the subject anthropometric data (mass, estimates of limb moments of inertia, etc.) using inverse dynamics. Calculation of the joint reaction force however requires knowledge of the muscle forces and the system of equations for calculating these forces is frequently indeterminate due to the large number of muscles. The equations can be solved using an optimisation routine such as minimising the sum of muscle forces (Heller et al., 2001), stresses (Modenese et al., 2011; Yoshioka et al., 2012), activations (Yoshioka et al., 2012) or metabolic energy (Correa et al., 2010). Alternatively the number of equations can be reduced by combining muscle actuators until the system is no longer indeterminate (Heller, 2005). Once the muscle forces are known, the contact force can be calculated by summing the force vectors (Modenese et al., 2011).

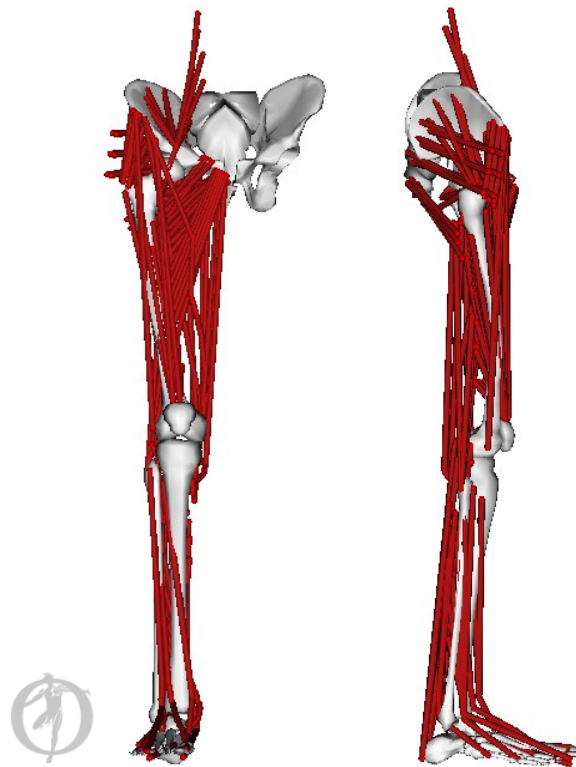


Figure 2.7 The London Lower Limb Model (Modenese et al., 2011) produced in OpenSim (Delp et al., 2007).

Whilst these models are becoming more advanced with muscle wrapping (Delp et al., 1999; Blemker and Delp, 2005) and muscle-tendon length calculations (Arnold et al., 2010), the inherent need for the optimisation routine or equivalent and the difficulty in accounting for muscle co-contraction means that they still cannot be relied upon to determine hip joint contact forces for novel activities without validation against results from instrumented implants and EMG signals (Modenese et al., 2011; Mellon et al., 2013). Indeed a recent study showed that a current state-of-the-art model could be used to calculate the magnitude of the joint reaction force measured in-vivo, however would not be able to recreate the direction of this force (Modenese et al., 2013).

#### *2.2.5 Normal hip joint forces*

Typical hip forces during daily activities exceed 200 % body weight: during gait the peak force equates to 1.8 kN for an average patient and in excess of 3.9 kN for a high-load patient (Bergmann et al., 2010). An example gait cycle is shown in Figure 2.8.

These high hip joint forces occur because the muscles which actively stabilise and move the joint have moment arms which are shorter than a typical moment arm for the subject's centre of mass; thus the muscles forces have to sum to greater than body weight to balance the joint or move the centre of mass. What is more, muscle co-contraction is not uncommon to ensure stability in all 6-degrees-of-freedom resulting in

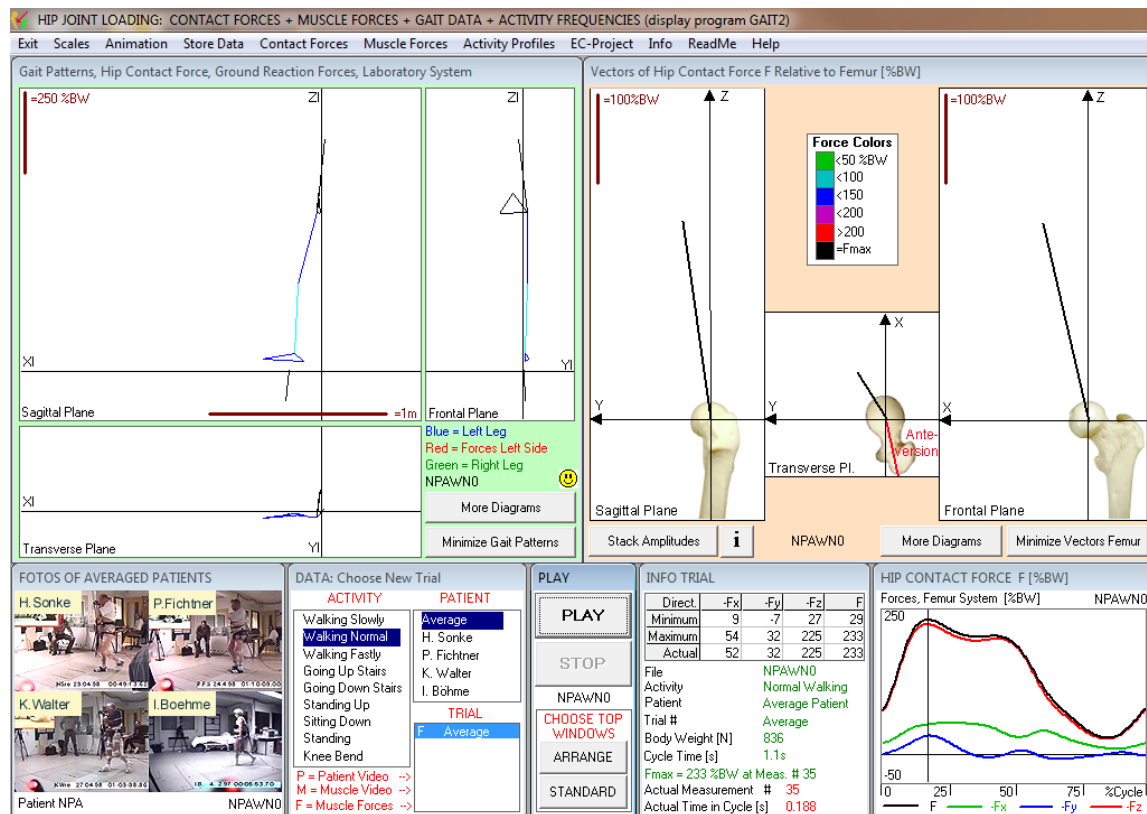


Figure 2.8 Output from HIP98 (Bergmann et al., 2001).

The classic gait contact force cycle can be seen in the bottom right corner. It can be seen that the peak contact force vastly exceeds bodyweight (233 % for the average patient) and occurs during heel strike (representative diagram top left). A second, smaller peak at toe-off can also be seen on the bottom right contact force graph.

even higher loads. During stumbling, when many muscles co-contrast to stiffen and stabilise the joint, the hip joint reaction force can exceed 11 kN (Bergmann et al., 2010).

## 2.3 Soft Tissue Anatomy and Biomechanics

### 2.3.1 Muscles

There are twenty-two muscles that span the hip joint with seven of these muscles (tensor fascia lata, rectus femoris, sartorius, gracilis semimembranosus, semitendinosus and the bicep femoris long head) extending over both the hip and knee (Gray, 2008). Figure 2.9 shows many of the hip joint muscles and Table 2.8 details all the muscles of the hip, their common groupings and their functions. The origins and insertions of these muscles have been quantified in numerous datasets for the production of musculoskeletal models (see 2.2.4).



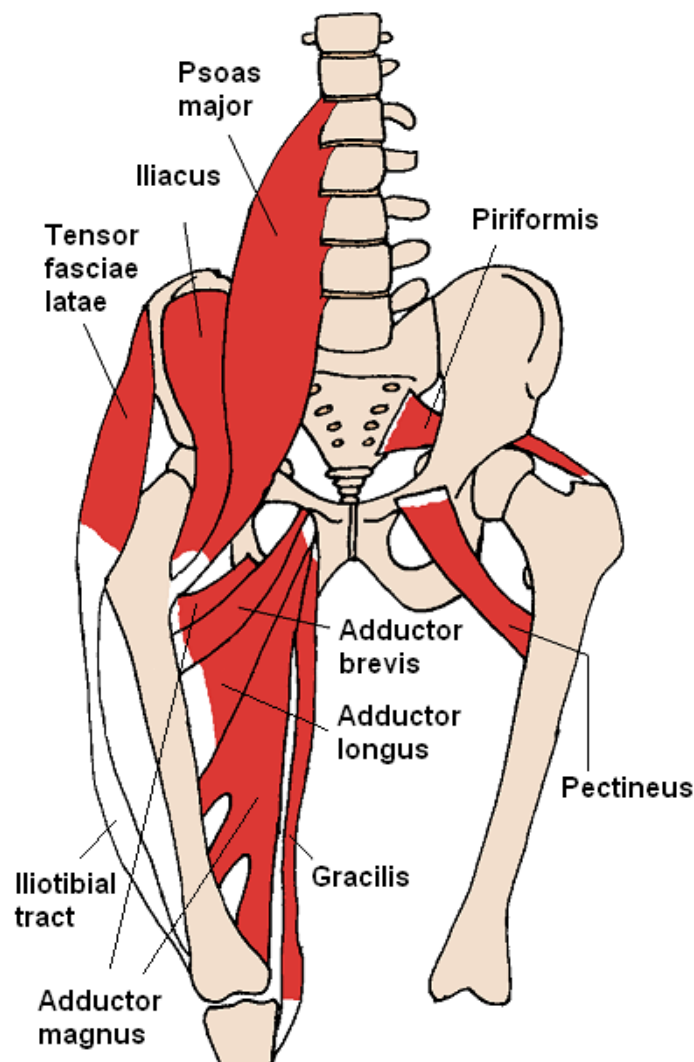
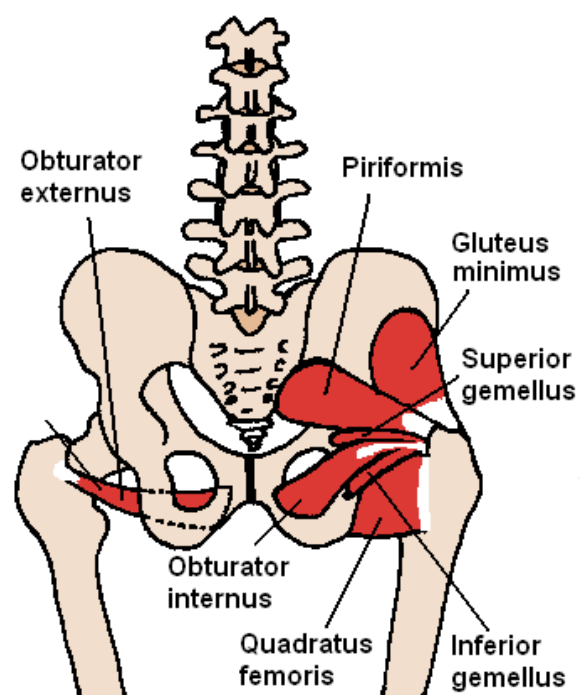
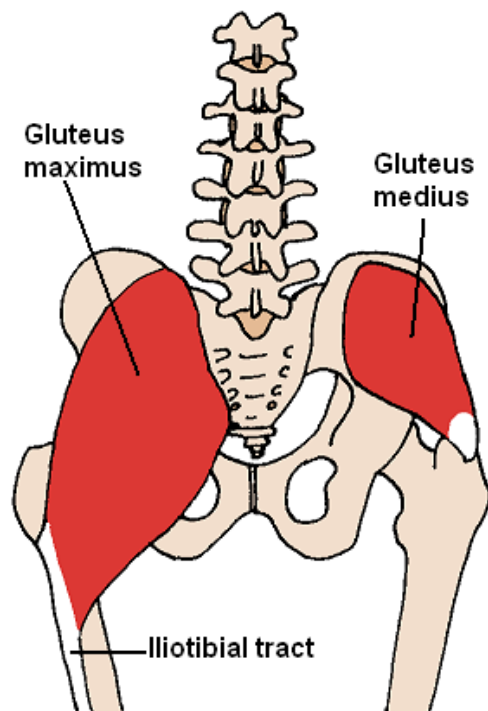


Figure 2.9 Hip Joint muscles from an anterior view (left), posterior view of the superficial muscles (bottom left) and posterior view of the deep muscles (bottom right) (Ohara, 2006). Reproduced under the creative commons licence CC BY-SA 3.0.

The sartorius, rectus femoris and hamstrings are not shown, the rectus femoris and sartorius are positioned anteriorly, the hamstrings posteriorly and they extend down the length of the femur.



## CHAPTER 2

Table 2.8 Muscle Groups and their functions

Group	Muscles	Primary Hip Joint Function	Secondary Hip Joint Function
Gluteal and Abductors	Gluteus Maximus	Extensor <sup>1,2,3,4</sup>	External Rotator, <sup>1,5,6</sup> Adductor <sup>3</sup>
	Gluteus Medius	Abductor <sup>1,2,3</sup>	Internal Rotator <sup>1,2,5</sup>
	Gluteus Minimus	Abductor <sup>1,2,3</sup>	Internal Rotator <sup>2,5</sup>
	Tensor Fascia Lata	Abductor <sup>1,2,3</sup>	Flexor, <sup>2,3</sup> Internal Rotator <sup>1</sup>
Adductors	Adductor Brevis	Adductor <sup>1,2,3</sup>	Extensor <sup>2</sup>
	Adductor Magnus	Adductor <sup>1,2,3</sup>	Extensor <sup>2,3,4</sup>
	Adductor Longus	Adductor <sup>1,2,3</sup>	Extensor, <sup>2</sup> Flexor <sup>1,2,3</sup>
	Pectineus	Adductor <sup>1,2,3</sup>	Flexor <sup>2,3</sup>
	Gracilis	Adductor <sup>1,2,3</sup>	Extensor, <sup>2</sup> Flexor <sup>3</sup>
Hamstrings	Bicep Femoris (long and short head)	Extensor <sup>2,3,4,7</sup>	Adductor <sup>3</sup>
	Semimembranosus	Extensor <sup>2,3,4,7</sup>	Adductor <sup>3</sup>
	Semitendinosus	Extensor <sup>2,3,4,7</sup>	Adductor <sup>3</sup>
Short External Rotators	Obturator Externus	External Rotator <sup>1,2,5</sup>	Adduction <sup>2</sup>
	Obturator Internus	External Rotator <sup>1,2,5</sup>	Abduction <sup>2</sup>
	Piriformis	Abductor <sup>1,2</sup>	External Rotator <sup>2</sup>
	Superior Gemellus	External Rotator <sup>1,2</sup>	Abductor <sup>2</sup>
	Inferior Gemellus	External Rotator <sup>1,2</sup>	-
	Quadratus Femoris	External Rotator <sup>2,5</sup>	Extensor <sup>2</sup>
Iliopsoas and Flexors	Iliacus	Flexor <sup>1,2,3,6</sup>	-
	Psoas Major	Flexor <sup>1,2,3,6</sup>	-
	Psoas Minor (often absent <sup>1</sup> )	Flexor <sup>1,2,6</sup>	-
	Sartorius	Flexor <sup>1,2,3</sup>	Abductor, <sup>2</sup> External Rotator <sup>1</sup>
	Rectus Femoris	Flexor <sup>1,2,3</sup>	Abductor <sup>2</sup>

1 – (Gray, 2008), 2 – (Dostal et al., 1986), 3 – (Colgan et al., 1994), 4 – (Németh and Ohlsén, 1985), 5 – (Delp et al., 1999), 6 – (Blemker and Delp, 2005), and 7 – (Basmajian and De Luca, 1985).

### 2.3.2 The Capsular Ligaments

#### Anatomy

The hip joint is surrounded by an encasing, strong ligamentous structure known as the hip joint capsule. Aside from the native bony stability afforded by the ball and socket joint shape, this is one of the main structures that provide stability to the hip. The hip

capsule is made up of iliofemoral, pubofemoral and ischiofemoral ligaments (Gray, 2008).

The iliofemoral ligament arises superior to the acetabulum and inferior to the anterior inferior iliac spine (the origin of the rectus femoris muscle tendon). It inserts along the entire length of the intertrochanteric line (Fuss and Bacher, 1991; Gray, 2008) however the ligament is frequently described as two separate regions which contain the bulk of the collagen fibres: the lateral arm, which inserts into the anterior-superior greater trochanter, and the medial arm which inserts anterior to the lesser trochanter (Figure 2.10) (Martin et al., 2008; Wagner et al., 2012). The iliofemoral ligament is the thickest (Stewart et al., 2002) and the strongest of the three capsular ligaments (Hewitt et al., 2001; Hewitt et al., 2002).

The ischiofemoral ligament arises at the ischial portion of the acetabulum and spirals around the posterior femoral head to insert anterosuperiorly at the base of the greater trochanter and the superior tip of the intertrochanteric line (Figure 2.10), posterior to and merging with fibres of the lateral arm of the iliofemoral ligament (Gray, 2008; Martin et al., 2008). Some authors also describe an additional inferior bundle of fibres that inserts alongside the medial arm of the iliofemoral ligament and pubofemoral ligament in the proximity of the lesser trochanter (Fuss and Bacher, 1991; Wagner et al., 2012).

The pubofemoral ligament arises at the pubic portion of the acetabular rim at the obturator crest and the superior ramus of the pubis. Its fibres form a sling around the inferior femoral head and blend with and insert alongside the medial iliofemoral ligament, slightly anterior to the lesser trochanter (Gray, 2008; Martin et al., 2008; Wagner et al., 2012) (Figure 2.10). Martin et al. also describe a second arm of this ligament which inserts posteriorly on the intertrochanteric crest (Martin et al., 2008), however, no other authors identify this fibre bundle but instead identify an O-ring like band of fibres that surround the posterior femoral neck, but have no distinct insertion into the intertrochanteric crest. This band of fibres is called the femoral arcuate ligament (Fuss and Bacher, 1991; Hewitt et al., 2002), or the zona orbicularis (Ito et al., 2009; Wagner et al., 2012).

Fuss and Bacher provide the most detailed description of the capsular ligaments and provide paired illustrations and photos. They describe additional small fibres bundles to the main ligaments described above such that the entire circumference of the capsule is defined in terms of ligament fibre bundles (Fuss and Bacher, 1991). They also describe the merging of ligament fibres in greater detail, using the term pilema to

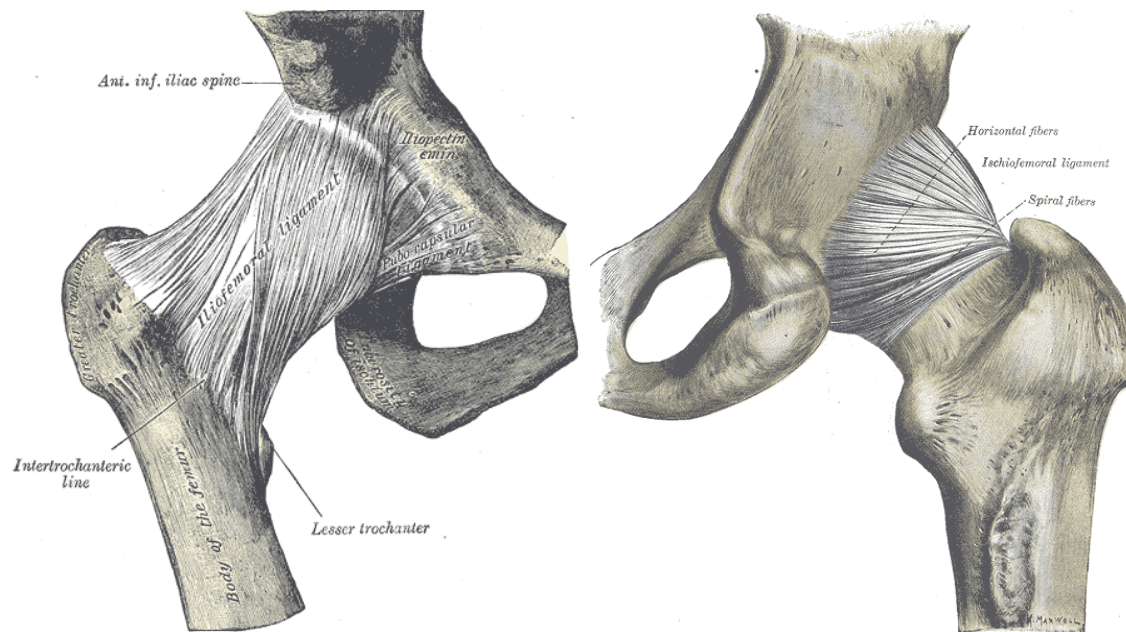


Figure 2.10 The capsular ligaments of the hip (Gray, 1918). Reproduced from 20th U.S. edition of Gray's Anatomy (copyright expired, available in the public domain).

Left) anterior view of a right hip showing the medial and lateral arms of the iliofemoral ligament traversing across the anterior portion of the hip. The pubofemoral ligament can be seen to arise from the pubic portion of the acetabulum (its insertion, posterior to the medial arm of the iliofemoral ligament, cannot be seen). Right) Posterior view of a right hip showing the ischiofemoral ligament spiralling round the posterior femoral neck (Gray, 1918). Images

describe these regions: the lateral pilema consists of the lateral iliofemoral and superior ischiofemoral ligaments at their femoral insertion at the superior intertrochanteric line, the medial pilema the medial iliofemoral, pubofemoral and inferior ischiofemoral ligaments at their shared femoral insertion adjacent to the lesser trochanter, and the posterior pilema between the ischiofemoral ligaments' superior and inferior fibres bundles and the femoral arcuate ligament.

The capsular ligaments are homogeneously innervated with both proprioceptive and nociceptive nerve endings suggesting a role in sensing both spatial orientation and pain (Haversath et al., 2013).

### Biomechanics

Each of the capsular ligaments has a role in restraining hip joint movements and the main functions of each ligament is summarised in Table 2.1. Fuss and Bacher provide a more detailed qualitative description of where within the range of hip motion ligament fibres tauten and they assess both primary and secondary functions of the ligaments (Fuss and Bacher, 1991). Recent quantitative work shows that ligaments have a role in restraining hip rotations: cutting the iliofemoral ligament results in increased external rotation range of motion (Martin et al., 2008; Myers et al., 2011; Safran et al., 2013) which supports the description provided by Fuss and Bacher. Martin et al also report

Table 2.9 Primary limiting functions of the capsular ligaments (Fuss and Bacher, 1991; Martin et al., 2008)

<b>Movement</b>	<b>Main limiting ligament</b>
Flexion	Ischiofemoral (inferior portion)
Extension	Iliofemoral (medial arm)
Abduction	Pubofemoral
Adduction	Ischiofemoral (superior portion)
Internal Rotation	Ischiofemoral (superior portion)
External Rotation	Iliofemoral (lateral arm)

that the ischiofemoral ligament limits internal rotation in low flexion/extension and that the pubofemoral ligament limits external rotation in extension (Martin et al., 2008).

The ligaments also have a role in stabilising the hip: cutting the iliofemoral ligament results in a significant increase in anterior displacement when rotating the hip in low flexion/extension (Myers et al., 2011) and in a neutral hip position the capsule stabilises the hip against medial, lateral and inferior displacements (Ito et al., 2009; Smith et al., 2014). A significant stabilising role against lateral, inferior and anterior displacements at the extremes of the range of hip motion has also been measured after a partial capsulotomy (Safran et al., 2013). Research into the role of soft tissues in stabilising hip replacements has suggested that the capsular ligament helps cradle the femoral head, resisting subluxation and dislocation in deep hip flexion (Elkins et al., 2011b; Colbrunn et al., 2013).

### 2.3.3 The Ligamentum Teres

#### Anatomy

The femoral head is directly attached to the acetabular socket via the Ligamentum Teres, the ligament of the femoral head (Gray, 2008). The ligament is described as a strong, triangular structure that arises predominantly from the transverse acetabular ligament (Rao et al., 2001; Cerezal et al., 2010) and also from the posteroinferior portion of the cotyloid fossa (Gray and Villar, 1997) and inserts into the inferolateral femoral head (Figure 2.11). It is made of three bundles: posterior, anterior and medial, of which the posterior bundle is longest, and the medial bundle thinnest (Demange, 2007). It also has free nerve ends in the ligament which suggests that it has a proprioceptive role similar to that of the anterior cruciate ligament (Leunig et al., 2000).

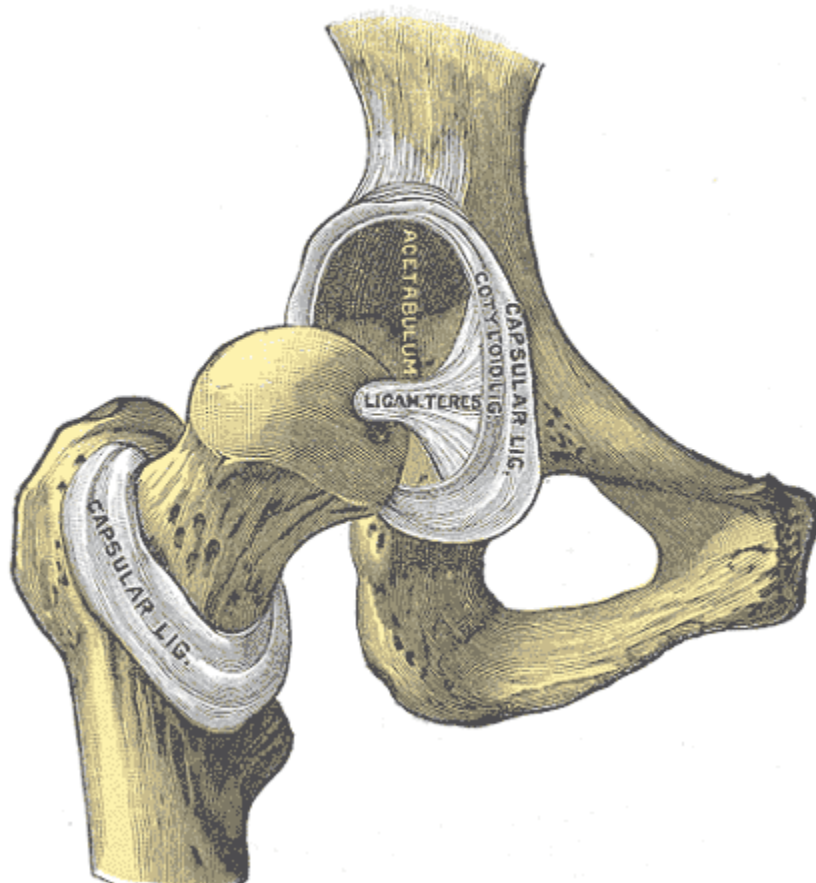


Figure 2.11 The intra-articular ligamentum teres (Gray, 1918). Reproduced from 20th U.S. edition of Gray's Anatomy (copyright expired, available in the public domain).

### Biomechanics

It has been suggested that the Ligamentum Teres Femoris, the ligament of the femoral head, is a vestigial structure (Kapandji, 1978), that still has some function in juveniles as a blood supply to the femoral head (Wertheimer and Sd, 1971; Gray and Villar, 1997). Some authors believe that it has no mechanical function (Erb, 2001). Given that tissues remodel in response to presence/lack of mechanical stimulus then it might be expected that a tissue that has no mechanical function would have a low mass and strength (Woo et al., 1982); however the ligament is described as 'strong' in more than 70 % of cadavers aged over 60 (Tan and Wong, 1990) suggesting that the ligament could have a mechanical role in some hips.

Early work suggests that it is taut when the hip is semi-flexed and adducted, and relaxed in abduction (Gray, 2008) and this is supported by more recent arthroscopic observations (Gray and Villar, 1997; Rao et al., 2001; Kelly et al., 2003; Bardakos and Villar, 2009); research using MRI scans of cadaveric tissue that found ligament to be slack in abduction and internal rotation (Cerezal et al., 2010). A string model suggested that the ligament is taut during external rotation and flexion (90-120°), or internal

rotation and extension (Martin et al., 2012). Earlier work by this group showed that the capsular ligaments are lax during 30° flexion (Martin et al., 2008) (semi flexed) but taut during extension, and hence they hypothesize that the Ligamentum Teres acts as a secondary stabiliser in extension, but a primary stabiliser in flexion (Martin et al., 2012). These string model results were supported by recent cadaveric tests (Martin et al., 2013) which also showed that the ligamentum teres could help prevent hip joint subluxations by wrapping around the femoral head (Kivlan et al., 2013). However, none of these tests consider the ligamentum teres' relative importance compared to the capsule. Research with an intact hip capsule showed that cutting the ligamentum teres (using arthroscopy) produced a small (1.3°) significant increase in the range of hip adduction in neutral hip flexion; however this is unlikely to be clinically significant and there were no other significant differences detected during flexion, extension or abduction movements (Demange, 2007). Therefore more research is needed to clarify the function of this tissue relative to the capsular ligaments.

#### *2.3.4 The Acetabular Labrum*

##### Anatomy

The triangular shaped acetabular labrum is a fibrocartilage structure that surrounds the rim of the acetabulum directly connecting to the articular cartilage and bone. At the articular surface the labrum is covered by a meshwork of thin fibrils and the main substance of the labrum consists of a matrix with circumferential collagen fibres (Petersen et al., 2003). These fibres blend with the transverse acetabular ligament at the inferior portion of the acetabulum forming a complete circle comprising of these two tissues around the acetabulum (Ferguson et al., 2000a). The average labrum is 4 mm to 7.4 mm high, is largest in the anterior portion of the acetabulum (Won et al., 2003) and deepens the acetabular socket by increasing its surface area by 22-28 % and its volume by 31-33 % (Seldes et al., 2001; Tan et al., 2001).

Labral attachment varies around the acetabulum: the anterior labrum has predominantly a flat insertion with the cartilage and the bone, whereas the posterior labrum typically inserts below the bony rim (Won et al., 2003). Moreover, the anterior labrum had a sudden transition to articular cartilage and solely circumferential fibres parallel to the bony rim, whereas the posterior labrum had a gradual transition between cartilage and fibrocartilage, with both circumferential and radial collagen fibre bundles (Cashin et al., 2008).

## CHAPTER 2

The labrum is innervated with both proprioceptive and nociceptive nerve endings in high numbers near its acetabular insertion suggesting it could have a role in spatial orientation or be the cause of pain for hip disorders (Haversath et al., 2013).

### Biomechanics

Early work showed that the labrum (and the knee meniscus) helped maintain joint space between articular cartilage surfaces under a static load (Terayama et al., 1980) and found that the labrum could act like an O-ring and seal a higher pressure within the joint which could aid joint stability (Takechi et al., 1982). Further investigation has shown that through sealing synovial fluid in the central compartment, the labrum encourages more uniform pressure distribution within the hip helping prevent contact between the articulating surfaces and thus protecting the solid cartilage matrix from high strain (Ferguson et al., 2000a, 2003). This labral seal strengthens with external rotation but weakens with flexion and internal rotation (Dwyer et al., 2014), which is likely due to the changing congruency of the femoroacetabular joint with different hip positions. The seal is also significantly impacted by labral tears/resection which allows fluid to escape the joint space preventing formation of the protective pressurised fluid layer (Cadet et al., 2012). The labrum can help prevent cartilage consolidation by augmenting fluid retention within the cartilage layers (Ferguson et al., 2000b, 2003; Haemer et al., 2012).

The labral seal not only protects the cartilage from increased contact stresses by allowing a pressurised fluid layer to develop, but also promotes greater joint stability: cadaveric models have shown that venting the labral seal, or tearing the labrum results in a decrease in the amount of force needed to distract the hip as well as increasing the amount of femoral head displacement during extension, abduction and external rotation movements under hip joint compression (Crawford et al., 2007). Another study showed that, in a neutral hip position, a 2 cm labrectomy in the absence of the hip joint capsule significantly reduced the stability ratio (peak anterior force required for dislocation divided by the joint compression force). However, this study also found a 3 cm circumferential tear, or a radial tear did not affect it suggesting that only severe labral tears or labrectomy effects hip stability (Smith et al., 2011). This is supported by Myers et al. who showed that the labrum only provides secondary stability with the iliofemoral ligaments providing greater external rotation restraint, and more stability against anterior femoral head displacement (Myers et al., 2011). This is further corroborated by results from Ito et al. who found that the proximal capsular provides primary stability against hip joint distraction (Ito et al., 2009).



Another possible advantage of this labral seal is that it could promote better lubrication of the articular surface by encouraging fluid-film lubrication. A theoretical model showed that an intact, tight fitting labrum can maintain a squeezed fluid-film (Hlavacek, 2002) and recent experimental work supports this hypothesis (Song et al., 2012); however this cadaveric model utilised a loading cycle that is an order of magnitude longer than a gait cycle (13 seconds versus 1 second) and it is known that lubrication regimes change with the velocity of the articulating surfaces (Accardi et al., 2011; Myant et al., 2012) so further evidence is needed to support a conclusion that the labral seal promotes better joint lubrication.

Whilst the labral seal aids load support through maintaining fluid within the joint helping to prevent contact between the articulating surfaces, there are contrasting reports regarding the labrum's ability to increase contact area and hence further reduce contact stresses in cases where solid contact does occur between the articulating surfaces. Whilst some research suggests that the labrum has little/no role in load support in a normal hip (Konrath et al., 1998; Henak et al., 2011), other studies suggest that labral tears/resection result in decreased contact areas, increased contact stresses (Lee et al., 2015) and increased strain in the cartilage (Greaves et al., 2010) implying it does have a role in load support. The differences could be due to the wide variation in testing methodology including computational modelling (Henak et al., 2011) and cadaveric modelling using single use pressure films (Konrath et al., 1998), real-time digital pressure measurement (Lee et al., 2015) and MRI scans (Greaves et al., 2010). The differences could also be caused by variation in the hip kinematics and load cases; those used include gait (Henak et al., 2011; Lee et al., 2015), stair climbing/descent (Henak et al., 2011; Lee et al., 2015) and single leg stance (Konrath et al., 1998; Greaves et al., 2010). Indeed the labrum is most likely to contribute to load support in a load case where the contact force is close to the edge of the acetabulum. A study looking at extreme movements in extension measured considerable labral strains with the hip placed under joint compression (Dy et al., 2008). This suggests that the labrum may participate more in load support during movements that require the extremes of the range of motion. The labrum's anatomy also suggests a role in load support through increasing the weight-bearing surface of the acetabulum. This is confirmed by the anatomy where a tidemark like attachment between the labrum and bone is typically observed adjacent to weight-bearing articular cartilage (Seldes et al., 2001).

A final function that the labrum may pose is as a soft buffer against bony impingement as a study which measured labral strains through the range of hip motion measured the

## CHAPTER 2

greatest labral strains in positions of impingement (Safran et al., 2011). However this study did not apply any controlled loads which could have affected their results.

Thus it can be concluded that the labrum has a role as a fluid seal both within the joint space and articular cartilage and that it also has a secondary role as a hip stabiliser. It may also have a role in helping reduce friction between the articulating surfaces, in load support and as a buffer against bony impingements.

### *2.3.5 Cartilage*

#### Anatomy

The femoral head is covered in hyaline cartilage which makes contact with the horseshoe shaped cartilage in the acetabulum. The cartilage is thickest at the anterolaterally on the femoral head and anterosuperiorly in the acetabulum, the main load bearing regions (Gray, 2008) and whilst the surfaces are reciprocally curved, they are not completely congruent (Rushfeld, 1979; Anderson et al., 2010).

Articular cartilage has little regenerative capacity, yet in many people it can provide a low friction articulating surface capable of transmitting the high in vivo contact stresses through the joint for their whole lives (Rushfeld, 1979). Cartilage is able to do this due to its biphasic properties: it has both a solid and a liquid phase. Its strength is due to collagen fibres, which anchor into subchondral bone, pass through the thickness of the cartilage and are tangential to the articulating surface. This arrangement traps hydrophilic proteoglycan molecules, which attract water by osmosis, creating a tense 'swollen' hydrated structure (van Arkel and Amis, 2013).

#### Biomechanics

A basic description of the function of articular cartilage is that the solid cartilage matrix is protected against high contact stresses by movement of the fluid between its pores. This movement creates large drag forces, which result in pressure gradients that can support the applied load (Katta et al., 2008). In other words, provided the cartilage is well hydrated, the load is supported by the fluid and not the solid matrix, and hence it is protected from damage. Furthermore, articular cartilage provides a low friction surface as solid-on-solid contact between two adjacent articulating surfaces is prevented by a lubricating fluid layer (van Arkel and Amis, 2013). The lubrication mechanism is such that the coefficient of friction decreases as the joint moves more quickly: at a low speed, the joint exhibits boundary lubrication with synovial fluid molecules forming a low friction brush-like layer, however when the joint moves quickly, hydrodynamic lubrication can occur providing an even lower coefficient of friction (Accardi et al.,

2011). Unfortunately, surface damage leads to fibrillation, when the proteoglycans escape and the cartilage loses its tensed, hydrated stiffness, and that allows degenerative changes to cascade. For the hip, the lifetime risk of osteoarthritis is one in four (Murphy et al., 2010) with a lifetime risk of needing a total hip replacement, the leading treatment for end-stage hip osteoarthritis, between 7 and 12 % for men and women respectively (Culliford et al., 2012).

## **2.4 Causes of hip pain, instability and osteoarthritis in the native hip**

### *2.4.1 Acetabular labral tears*

Labral tears cause hip pain and have been associated with early signs of degenerative changes in adjacent articular cartilage (McCarthy et al., 2001a). Labral tears occur most frequently anteriorly/anterosuperiorly (Fitzgerald, 1995; Seldes et al., 2001; McCarthy et al., 2003) and whilst they are a cause of hip pain (Haversath et al., 2013), they are also commonly observed in pain-free asymptomatic hips (Register et al., 2012). The most common type of labral tear is a separation at the labral-cartilage junction, which has been coined a watershed lesion (McCarthy et al., 2001b).

### Causes

There are three theories for the causes of labral repairs: the first is that they are caused predominately by abnormal hip morphology; research by Ganz and colleagues showed that femoroacetabular impingement, FAI, (see 2.4.2) can cause labral tears (Ganz et al., 2003; Beck et al., 2005). A detailed finite element simulation of stresses in the labrum and adjacent articular cartilage with varying hip morphology showed that stress in the labrum increases significantly for stand-to-sit activity for cam and pincer hips confirming the mechanism of FAI for labral injury (Chegini et al., 2009). Moreover, a decreasing centre-edge angle, which creates a dysplastic hip, led to much higher stresses in the lateral edge of the acetabulum and the labrum (Chegini et al., 2009; Henak et al., 2011) in a similar mechanism to that of superior edge loading of hip replacements (2.6.4). Thus abnormal bony morphology, whether dysplastic, cam or pincer, leads to greater stresses in the acetabular labrum and hence explains why young patients with these conditions frequently experience labral injuries.

The second is that extreme range of motion manoeuvres can generate significant strains in the labrum (Dy et al., 2008; Safran et al., 2011) suggesting that labral tears could occur in young patients during sporting activity. Indeed, a motion-capture/computational modelling (Charbonnier et al., 2009) study and MRI research (Duthon et al., 2013) into extreme movements in ballet dancers showed that these

## CHAPTER 2

movements can cause impingements, subluxation and high contact pressures in the labrum for a patient with normal bony morphology and thus could be a cause of labral lesions (Charbonnier et al., 2009).

Finally, there are anatomical differences in the labrum that could expose the anterosuperior quadrant to injury: it has significantly lower compressive stiffness compared to the posterior quadrant, and significantly lower tensile properties compared to the anteroinferior quadrant (Smith et al., 2009). Moreover, the anterior labrum's fibres are orientated parallel to the labral-chondral junction which could further expose it to a common watershed type tear (Cashin et al., 2008).

### Treatment

Treatment of labral tears can involve resection, debridement or reattachment (Kelly et al., 2005) and early clinical results show that patients have improved outcomes when the labrum was re-fixated/repared for both open (Espinosa et al., 2006) and arthroscopic (Larson and Givens, 2009; Schilders et al., 2011) treatment for femoroacetabular impingement. However, not all labral tears can be treated or repaired, for example posterior tears are less likely to be repaired due to ossification of the rim (Larson and Givens, 2009).

#### *2.4.2 Femoroacetabular impingement*

Femoroacetabular impingement, FAI, in natural hips can occur as results of extreme range of motion requirements (Charbonnier et al., 2011), or more commonly due to abnormal bony morphology (Leunig and Ganz, 2014). A decade ago, a clear link between FAI, hip pain and previously idiopathic osteoarthritis was established (Ganz et al., 2003) alongside surgical interventions to treat these anomalies early in a bid to treat pain and delay the onset, or even prevent hip osteoarthritis (Lavigne et al., 2004). Surgery to treat symptomatic FAI is becoming increasingly popular and has promising short term results (Beck et al., 2004; Leunig et al., 2009; Clohisy et al., 2010; Ng et al., 2010; Impellizzeri et al., 2012; Papalia et al., 2012). There are two main mechanisms described for FAI: cam and pincer (Figure 2.12).

### Cam Hips

Cam FAI results from an increased prominence on the femoral neck which abuts onto the articular cartilage during flexion and internal rotation (Ganz et al., 2003). The non-spherical femoral head effectively has an increased neck radius which is described on radiographs through measuring the alpha angle (Tannast et al., 2007b) and triangular index (Gosvig et al., 2007). Cam deformity is more common in male subjects (Gosvig

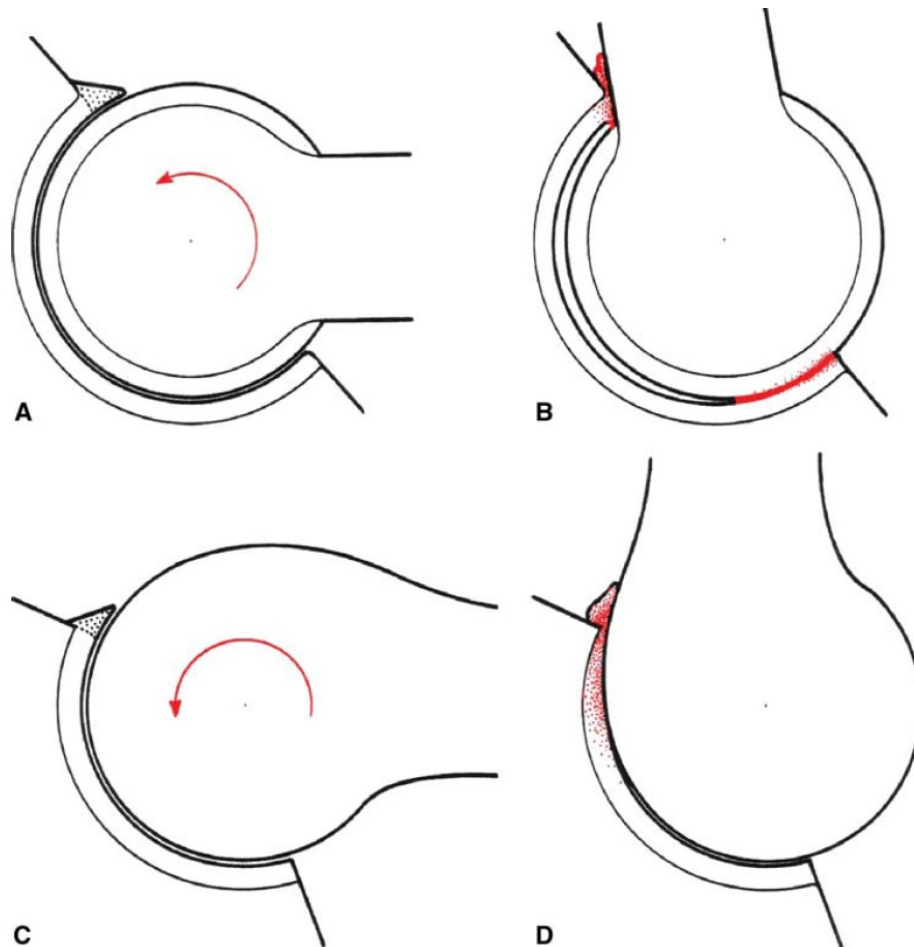


Figure 2.12 Pincer and Cam FAI (Ganz et al., 2008). Reproduced with permission and copyright © from Springer.

A) A pincer acetabulum provides over coverage of the femoral head which during flexion of the hip leads to B) impingement and direct anterosuperior labral stress with a contrecoup lesion on the posterior labrum and cartilage in a similar mechanism to edge loading of hip replacements (see section 2.6). C) A cam hip has a non-spherical femoral head which during flexion and internal rotation leads to D) impingement between the femoral neck and the anterosuperior articular cartilage and labrum.

et al., 2008) and is thought to develop in response to high quantities of athletic activity during adolescence (Siebenrock et al., 2011). The cam deformity causes direct chondral damage and results in separation of the labrum from the anterosuperior region of the acetabulum (Beck et al., 2005). In this mechanism, the cartilage is damaged first whilst the labrum remains principally uninvolved (Peters and Erickson, 2006; Ganz et al., 2008). Treatment of cam FAI involves removal of the osseous bump through open (Ganz et al., 2003; Lavigne et al., 2004) or arthroscopic surgery (Philippon et al., 2007b); whilst there is a lack of conclusive evidence as to whether arthroscopic surgery provides improved results over open surgery (Papalia et al., 2012) arthroscopy is more favourable for athletes where a quick return to sport is desired (Philippon et al., 2007a).

### Pincer Hips

Pincer FAI is caused by a defect of the acetabulum which leads to over coverage of the femoral head (Ganz et al., 2003). This can be caused by a general deformity where the hip socket being too deep, coxa profunda or more extreme protrusio acetabuli, or by a local deformity such as acetabular retroversion which results in a prominent anterior wall (Reynolds et al., 1999; Ganz et al., 2003; Tannast et al., 2007b). Pincer deformities are more prominent in middle aged women (Tannast et al., 2007b) with the first structure to fail being the anterosuperior part of the acetabular labrum at the point where the impingement happens (Ganz et al., 2008; Leunig and Ganz, 2014). Repeated abutment of the femoral neck into the anterior wall during flexion of the hip can lead to a 'contrecoup' lesion of the articular cartilage posteriorly through subluxation of the femoral head (Beck et al., 2005; Wassilew et al., 2013) through a similar mechanism to that of edge loading following total hip replacement (De Haan et al., 2008a; Matar et al., 2010) (see section 2.6.7). Treatment of pincer FAI can involve acetabular rim trimming (Lavigne et al., 2004) or reorientation of the acetabulum (Ganz et al., 2003) through a reverse periacetabular osteotomy (Ganz et al., 1988; Siebenrock et al., 2003).

#### *2.4.3 Controversy in the treatment of FAI and Labral Tears*

Like cam deformity, pincer hips are often diagnosed from radiographs (Tannast et al., 2007b) which has led to the diagnosis of cam-pincer deformity where both mechanisms are present (Beck et al., 2005). However, recent research using CT scans found that cam and pincer morphology are distinct variations and not mixed (Cobb et al., 2010; Masjedi et al., 2013): pincer hips had deeper acetabula when compared to normal hips whereas cam deformities are coupled with acetabula that are normal or even marginally shallower. The implication of this is that false diagnosis followed by surgical rim trimming of a 'cam-pincer' hip could leave the acetabulum deficient by making a shallow cam hip even less deep and hence expose the hip to an increased prevalence of edge loading, similar to that of superior edge loading of hip replacements (see section 2.6.4).

As with all hip surgery, both arthroscopic and open early interventions techniques require incisions to gain access to the joint and necessarily cut the hip joint capsule and its intertwined ligaments, which completely surround the hip, frequently leaving the incision unrepaired (Ganz et al., 2001; Bedi et al., 2011b). Whilst many patients seemingly tolerate this in the short-term, recent data has suggested that those with capsular repair have superior clinical results to those without (Frank et al., 2014).

Worryingly, long-term data is not available, capsular defects are common in patients requiring revision hip arthroscopy (Philippon et al., 2007d; McCormick et al., 2014) and there are cases of extreme post-operative instability leading to dislocation (Matsuda, 2009; Ranawat et al., 2009; Sansone et al., 2013; Austin et al., 2014). Consequentially, there are concerns that non-dislocating separations of the articular surfaces are underreported yet may have long-term consequences (Domb et al., 2013); a small femoral head subluxation out of the acetabulum would concentrate all the joint reaction force onto a small area of cartilage and over time this 'edge loading' mechanism causes osteoarthritis (Mei Dan et al., 2012) in a similar way to that caused by abnormal bony morphology (Leunig and Ganz, 2014). Moreover, subluxation and edge loading are known causes of high wear following metal-on-metal hip replacement (De Haan et al., 2008a) (sections 2.5.1 and 2.6.7), or stripe wear and squeaking following ceramic-on-ceramic total hip replacement (Walter et al., 2011; Esposito et al., 2012) (sections 2.5.3 and 2.6.7). Similarly, all types of hip replacements are at risk of dislocation if the capsule is left unrepaired (Kwon et al., 2006) (see section 2.6.1).

The mean age for early intervention is 34 (Harris et al., 2013), many years lower than life expectancy, and hence there is a long time over which adverse effects from capsular incision could develop. What is more, if the index surgery does not prevent osteoarthritis, any capsular defects from early intervention procedures will only increase the likelihood of complications should total hip replacement be required (Ng et al., 2010; Harris et al., 2013). Hence, more research is needed to determine if unrepaired capsular incisions could inadvertently cause long term harm; it was not long ago that meniscectomy (McDermott and Amis, 2006) and labrectomy were common (Konrath et al., 1998) whereas now advanced arthroscopy surgery is performed solely to repair these tissues.

## **2.5 Hip arthroplasty clinical results**

Hip replacement surgery is the end stage treatment for severe hip osteoarthritis as well as providing options for femoral neck fractures, avascular femoral head necrosis and chronic hip dysplasia. Consequently, it has become a common surgical procedure with 620,400 procedures performed between 2003 and 2013 in the UK alone. The overall survivorship of hip replacements is very good with only a 5.75 % cumulative risk of revision hip surgery at ten years (NJR, 2014).

A hip replacement typically consists of two components, a femoral and acetabular component. A variety of bearing combinations are used for the articulating surfaces with the first reliably successful hip replacement system being a metal-on-polyethylene

## CHAPTER 2

bearing (Charnley, 1970; Charnley, 1972). The biggest problem for these devices was high wear requiring revision surgery to replace the liner, or to stabilise a socket/stem if the component has become loose due to the body's reaction to the polyethylene wear debris (Murray and O'Connor, 1998; McKellop et al., 1999; Archibeck et al., 2000). Indeed, aseptic loosening is still the most common failure mechanism for hip replacements (NJR, 2014). Consequently, new devices that are more wear resistant or avoid polyethylene have been developed and implanted in a bid to reduce rates of loosening including metal-on-highly-cross-linked-polyethylene, metal-on-metal, ceramic-on-ceramic, ceramic-on-polyethylene and ceramic-on-metal (NJR, 2014).

### *2.5.1 Metal-on-metal bearings*

Large diameter bearings are more resistant to dislocation (Bartz et al., 2000; Burroughs et al., 2005; Kluess et al., 2007) which led to their a drive to increase bearing sizes; however, when combined with a polythene liner the wear rates of large diameter bearings are too high (Amstutz and Le Duff, 2006). However, advanced metal manufacturing techniques allowed metal-on-metal articulations to be made which in ideal laboratory conditions produced exceptionally low wear rates (Udofia and Jin, 2003; Isaac et al., 2009; Fisher, 2011) as well as offering a lower dislocation rate due to an increased jump distance (see section 2.6.1). Therefore metal-on-metal hip replacement looked like an attractive option to counter two of the main failure mechanisms for hip replacements: aseptic loosening and dislocation. As a result large diameter metal-on-metal arthroplasty gained popularity in the last decade though some designs experienced bad clinical results (Langton et al., 2009; Langton et al., 2011a) which culminated in the recall of the implant (Underwood et al., 2011; Underwood et al., 2012) only after it had been implanted tens of thousands of patients (MHRA, 2010; Cohen, 2011).

Subsequent research has shown that these large diameter metal bearings were more adversely affected by edge loading (see section 2.6). The result was a steep decline in the popularity of metal-on-metal hip replacements and an increase in the risk of revision for hip implanted after 2003 and before 2010 (NJR, 2014). However, with in excess of 100,000 patients having been implanted with failure prone devices there is still a need for research into metal-on-metal devices to understand how failures can be identified, treated or even prevented.

### *2.5.2 Metal-on-metal hip resurfacing*

Despite the failure of large diameter metal-on-metal total hip replacements, many surgeons still consider metal-on-metal hip resurfacing as the best treatment option for a



young male patient (McMinn et al., 2011; Treacy et al., 2011; Holland et al., 2012). This treatment option spares the femoral neck and so potentially offers more natural hip anatomy, restoration of the femoral head centre and abductor moment arm, resistance to dislocation due to the large head and easier revision for the femur where more bone stock has been preserved. High survivorship results in this demanding patient cohort with the Birmingham Hip Resurfacing have been reported by the surgeons involved with designing the implant: 98 % at thirteen-years (McMinn et al., 2011) and 98 % at ten-years (Treacy et al., 2011). Whereas others surgeons report ten-year survivorship results comparable to those for a total hip replacement for males, 95 %, but worse for females 74-85 % (Holland et al., 2012; Murray et al., 2012). This worse performance in women could be due to increased metal sensitivity in women, and/or because smaller components have higher failure rates (Langton et al., 2011b; Murray et al., 2012) (female hips are typically smaller in diameter than male hips, see Table 2.4, page 9).

The biggest problem with metal-on-metal resurfacing is that there is a risk that high volumes of metal ions can be released into the body (Langton et al., 2011b) which can lead to the muscle decay and formation of pseudotumours (Pandit et al., 2008; Kwon et al., 2010; Kwon et al., 2012). This is both painful for the patient and requires complication revision surgery which is costly to the NHS (Vanhegan et al., 2012) and consequentially many surgeons no longer consider it a viable treatment option, particular for women.

Poorly positioned acetabular cups are considered to be one of the main causes for increased prevalence of edge loading (see section 2.6) and metal ions release (De Haan et al., 2008a; Isaac et al., 2009; Fisher, 2011; Hart et al., 2011a) and indeed a different safe-zone has been identified for hip resurfacing (Gross and Liu, 2012) versus total hip arthroplasty (Lewinnek et al., 1978). However, consistent accurate placement of the acetabular component is difficult for a number of reasons generally when performing a hip replacement: firstly the position of the pelvis on the operating table is poorly defined (Jeffers, 2012), secondly most cups are placed by eye by the surgeon (De Haan et al., 2008b) and thirdly the pelvis in the operation table looks different to that seen on radiographs and there are differences between the two coordinate systems (Murray, 1993). Moreover, hip resurfacing is considered a more technically demanding operation which adds further difficulty to the procedures. The steep learning curve associated with resurfacing arthroplasty can be reduced by incorporating navigation in the operating theatre (Cobb et al., 2007) and this helps with the positioning of the critical acetabular component, though this technology has not been widely adopted (Jeffers, 2012).

## CHAPTER 2

For an experienced surgeon, operating on an appropriate patient (large, young, male), resurfacing continues to provide an excellent treatment option; indeed in this population 10 year survival rates as high as 99 % have been reported by non-implant-designer surgeons (Murray et al., 2012). However, given the high incidence of failures of metal-on-metal total hip replacements, and the poor performance of resurfacings in females, it is unlikely to become a high volume procedure with many surgeons opting to use ceramic-on-ceramic total hip replacement instead (NJR, 2014).

### *2.5.3 Ceramic-on-ceramic bearings*

Ceramic-on-ceramic devices experience extremely low wear rates of 0.2 mm<sup>3</sup>/year (Lusty et al., 2007a; Esposito et al., 2012) and their particulate wear debris is biologically inert (Jazrawi et al., 1999; Jeffers and Walter, 2012). The survival rate of ceramic bearings is impressive with authors reporting ten-year survival of third generation bearings of 97 % or better (Lee et al., 2010; Mesko et al., 2011). Revision can occur due to common factors such as hip dislocation and infection, but more specifically to ceramic bearing couples liner canting and dislocation, chipping on insertion, squeaking secondary to edge loading (see section 2.6) and fracture can cause problems (Jeffers and Walter, 2012). Ensuring the components are clean, using pre-assembled acetabular components and zirconia toughened alumina ceramic materials may help reduce these problems making this an ideal technology for a younger and more active patient (Jeffers and Walter, 2012). There are some concerns that the zirconia phase in these toughened ceramics could become unstable in the body, however there are currently no adverse reports of this in the literature (Jeffers and Walter, 2012).

Recent material advances have allowed manufacturers develop thin walled ceramic-on-ceramic resurfacing devices (Dickinson et al., 2011a) which are in the early stages of clinical trials (McDonnell et al., 2013). This design evolution has the potential to offer the benefits promised by metal-on-metal resurfacing without the risks of adverse reactions to metal debris. Ceramic articulations are likely to continue to be used in hip arthroplasty and provide promising options for younger patients, though the high cost of these devices will always be of concern (Gioe et al., 2011).

### *2.5.4 Hip arthroplasty technique and the effects on soft tissues*

The hip joint is entirely surrounded by muscles and the capsule so it is impossible to perform a hip replacement or resurfacing without cutting soft-tissues. Table 2.10 details the main surgical approaches and which soft tissues are cut/damaged as well as common postoperative complications. Whilst this thesis considers principally the

biomechanical effect of soft-tissue trauma, it should be noted that surgeons also have to consider blood supply to the lower extremity and preservation of the sciatic nerve, the communication pathway for the lower limb.

### 2.5.5 Current practice and future developments

Cementless total hip arthroplasty is the most common procedure with metal-on-plastic the most common bearing combination; however for cementless fixation the use of ceramic-on-ceramic bearings (38 % of procedures) has nearly caught up with metal-on-polyethylene (42 %) (NJR, 2014). The posterior approach has become the most popular surgical technique as it can preserve the abductor muscles and reduces operative time (Masonis and Bourne, 2002; NJR, 2011).

With a continual drive to design a hip replacement with superior longevity for younger, more active patients (50-60 years of age) (NJR, 2014), or even as to provide a

Table 2.10 Surgical Technique and Soft Tissue Damage

Incision	Usage (NJR, 2011)	Muscular Damage	Main Advantages	Complications
Posterior (Gibson, 1950; Masonis and Bourne, 2002)	57 %	Gluteus maximus split, piriformis, superior and inferior gemelli, obturator internus, quadratus femoris cut. Piriformis can be cut to improve exposure. Gluteus medius can be damaged.	Abductors not damaged, reduced operative time	Posterior dislocation, though this can be reduced with posterior repair techniques (Chiu et al., 2000; Sioen et al., 2002; Mihalko and Whiteside, 2004).
Lateral (transgluteal and direct) (Bauer et al., 1979; Hardinge, 1982; Masonis and Bourne, 2002)	37 %	Gluteus medius and minimus damaged (though damage varies according to exact approach take)	Low dislocation rate	Abductor dysfunction and postoperative limp
Transtrochanteric (Charnley, 1970; Masonis and Bourne, 2002)	<1 %	No direct cuts. Gluteus medius and minimus, vastus lateralis moved out the way through trochanteric osteotomy and are effectively damaged is trochanter reattached poorly.	Great visibility of the acetabulum and femur	Non-union of the greater trochanter leads to instability, abductor dysfunction and a limp
Direct Anterior (Matta et al., 2005; Lovell, 2008)	<1 %	Fascia lata cut though no direct muscular cuts in modern technics. The old technique involved rectus femoris, piriformis and tensor fascia lata cuts.	Does not affect dislocation rate, abductor function spared.	Poor visibility makes surgical complications harder to deal with. Transient nerve palsy can occur.

## CHAPTER 2

treatment options for very young patients with complex hip disease (Amstutz et al., 2007; Nizard et al., 2008), there is increasing emphasis on using harder, lower wearing bearing couples, as reflected by first the increased use of metal-on-metal, and now ceramic-on-ceramic articulations. Research into failure mechanisms that affect these hard bearing couples, such as edge loading, could be beneficial, helping to improve hip replacement technology further.

Moreover, whilst >90 % of hip replacement implants survive >10 years (NZJR, 2014), less than half of total hip replacement patients rate their implanted hip function as excellent and 5 % report no improvement or worse problems (NJR, 2013); indeed, since 2013 the UK registry has included patient reports outcomes measures (PROMs) in its database in response to an increased emphasis on outcome and not just survivorship of implants (NJR, 2013). Registry data from New Zealand, which also includes PROMs, suggests that one in ten patients limp, struggle to put on socks or continue to experience moderate/severe hip pain following total hip replacement affecting their quality of life despite the impressive survivorship data for the implants (NZJR, 2014). It is clear that prevention would be far superior to end-stage treatment and hence research that contributes to advancing early intervention surgeries, such as those detailed in section 2.4, or could improve functional outcomes following total hip replacement would also be beneficial.

### **2.6 Mechanisms of edge loading and dislocation of hip replacements**

Subluxation of the femoral head out of the acetabular cup can cause severe clinical problems for hip replacement patients. Small subluxations can lead to edge loading and high wear and large subluxations can lead to complete dislocation of the hip.

#### *2.6.1 Mechanisms and consequences of dislocation*

Dislocation has been a concern throughout the history of total hip arthroplasty (Charnley, 1972; Amstutz et al., 1975; Brown and Callaghan, 2008; Kumar et al., 2014); a single dislocation event is traumatic for the patient but can be treated with closed reduction, however recurrent dislocation is the third most common reason for revision hip surgery (following aseptic loosening and pain) (NJR, 2014).

The most common mechanism for dislocation is following an impingement event where the femoral neck or surrounding bone impinges on the acetabular cup/pelvis causing the femoral head to lever-out of the acetabulum and dislocate. It can occur anteriorly following a posterior impingement in hip extension with excessive external rotation (Charnley, 1970; Charnley, 1972; Nadzadi et al., 2003), or more commonly, in a ratio of

1.6:1 (Pedersen et al., 2005), it occurs posteriorly following an anterior/anterosuperior impingement in deep hip flexion with internal rotation (Bartz et al., 2000; Nadzadi et al., 2003; Brown and Callaghan, 2008).

### *2.6.2 Preventing dislocation*

Three strategies exist to reduce the risk of dislocation. The first is careful cup positioning (Charnley, 1970; Charnley, 1972); the first recommended safe-zone for acetabular orientation was based on dislocation risk (Lewinnek et al., 1978) and subsequently many authors have explored the effects of component positioning on impingement and dislocation risk (Yuan and Shih, 1999; D'Lima et al., 2000; Burroughs et al., 2005; Pedersen et al., 2005): too little inclination or anteversion increases the risk of anterior impingement and posterior impingement in flexion and internal rotation, however, too much inclination or anteversion increases the risk of posterior impingement in extension and external rotation.

The second strategy to prevent dislocation is appropriate soft-tissue preservation, tensioning and repair (Charnley, 1970). This is particularly important for a posterior approach where the posterior capsule and adjacent muscles are resected (see Table 2.10, page 37) which exposes the hip to subluxation and dislocation; many clinical (Chiu et al., 2000; White et al., 2001; Masonis and Bourne, 2002; Kwon et al., 2006; Kumar et al., 2014) and research papers (Sioen et al., 2002; Mihalko and Whiteside, 2004; Elkins et al., 2011b; Bunn et al., 2014) have shown how appropriate repair of these soft tissues reduces the risk of dislocation by providing passive resistance to dislocation regardless of the cup orientation.

The third strategy for preventing dislocation is to increase the size of the femoral head (or more specifically the head-neck ratio) which increases the range of motion before impingement (Bartz et al., 2000; Burroughs et al., 2005; Kluess et al., 2007; Kluess et al., 2008; Incavo et al., 2011; Bunn et al., 2014) and also increases the 'jump' distance between subluxation and eventual dislocation (Figure 2.13). Indeed, this is particularly relevant when considering hip resurfacing which has an unfavourable head-neck ratio yet a high dislocation resistance as the large jump tautens the soft tissues which prevent the femoral head from dislocating (Colbrunn et al., 2013).

### *2.6.3 Mechanisms and consequences of edge loading*

Edge loading has caused clinical problems for hard on hard bearings: in metal-on-metal hips it has led to early failure of implants (Kwon et al., 2010; Langton et al., 2011b; Underwood et al., 2011), and in ceramic-on-ceramic bearings it has caused

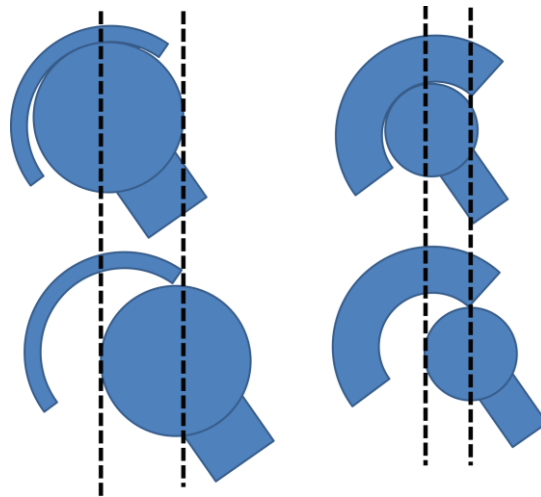


Figure 2.13 Increasing 'jump' distance with increasing femoral head size (van Arkel and Amis, 2013). Reproduced with permission and copyright © permission from Elsevier

A large diameter femoral head (left) needs to sublux further than a small head (right) before dislocation can occur.

higher wear rates and hip squeaking (Walter et al., 2008; Jarrett et al., 2009; Hannouche et al., 2011) (see sections 2.5.1, 2.5.2 and 2.5.3). The problem can be particularly severe for patients with metal-on-metal prosthesis as the high volume of metal ions released by this wear mechanism (De Haan et al., 2008b; Langton et al., 2008; Yoon et al., 2012) can lead to an adverse reaction to metal debris and the formation of pseudotumours (Kwon et al., 2010) and in some cases muscle atrophy (Toms et al., 2008).

Edge loading occurs when the contact vector approaches the edge of the joint resulting in an uneven stress distribution in the material and lubricant starvation (Jalali Vahid et al., 2001); as the available contact area is reduced at the edge of the acetabular component, the contact pressure increases causing a reduction in the lubricating film's thickness (Myant et al., 2012). This leads to increased friction (Sariali et al., 2010) and higher wear of the bearing surfaces (Kwon et al., 2010). Moreover, if the joint is completely starved of lubricant then the contact stresses caused by daily activities can exceed the yield strength of the bearing material which also contributes higher wear rates (Elkins et al., 2011a). It is important to note that the effects of edge loading begin as the contact patch extends past the cup rim and hence edge loading can occur when the contact vector is inbound from the cup edge (i.e. without the hip dislocating) (Underwood et al., 2011; Underwood et al., 2012). The range of possible contact patch semi-angles (describing the angle between the contact centre point and edge) for ceramic-on-ceramic (Mak and Jin, 2002) and metal-on-metal bearings (Dowson et al., 2007; Kwon et al., 2012) has been estimated to be between 5 and 30°. In other words,

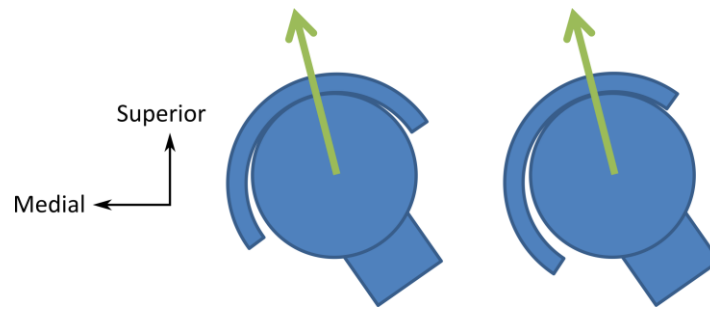


Figure 2.14 A diagram showing how high inclination can increase the risk of edge loading (van Arkel and Amis, 2013). Reproduced with permission and copyright © from Elsevier.

The superior edge of a well-positioned (left) is more lateral than a highly inclined cup (right, the cup has been inclined  $20^\circ$ ). The green arrow shows a typical gait contact vector which passes is much closer to the superior edge of the highly inclined cup and is therefore at a much greater risk of edge loading.

the outer diameter of the contact patch is between 5 and  $30^\circ$  closer to the cup edge than the joint reaction force vector).

#### *2.6.4 The effect of high inclination on the risk of edge loading*

Superior edge loading occurs more commonly in acetabular components with high inclination (Jeffers et al., 2009) and results in high wear of metal-on-metal devices (De Haan et al., 2008b; Langton et al., 2008; Grammatopoulos et al., 2010a). This is because for a highly inclined cup the superior edge of the cup is more medial which means that there is a greater chance the contact vector comes close to the edge of the cup (Figure 2.14). The big problem with superior edge loading is that it can occur during single-leg weight bearing activities such as gait (Mellon et al., 2013). This means that there is the possibility of frequent, repetitive edge loading during daily activities where the joint reaction force exceeds 200 %BW (Bergmann et al., 2010) (see 2.2.5, page 17) resulting in the release of high volumes of metal ions. Indeed, a new safe-zone, with low inclination, has recently been recommended for metal-on-metal resurfacings to reduce the risk of edge loading and associated complications (Gross and Liu, 2012).

Component mal-positioning is considered by some to be the main factor exposing the joint to edge loading and early failures of metal-on-metal prostheses (Isaac et al., 2009; Fisher, 2011). However, other evidence suggests that pseudotumours can form in patients with well-positioned cups suggesting that patient susceptibility is also important (Matthies et al., 2012).

#### *2.6.5 The effects of prosthesis design on the risk of edge loading*

Initially metal-on-metal acetabular cups were designed to be less than a hemisphere to reduce the risk of impingement (Wiadrowski et al., 1991). This was thought to be

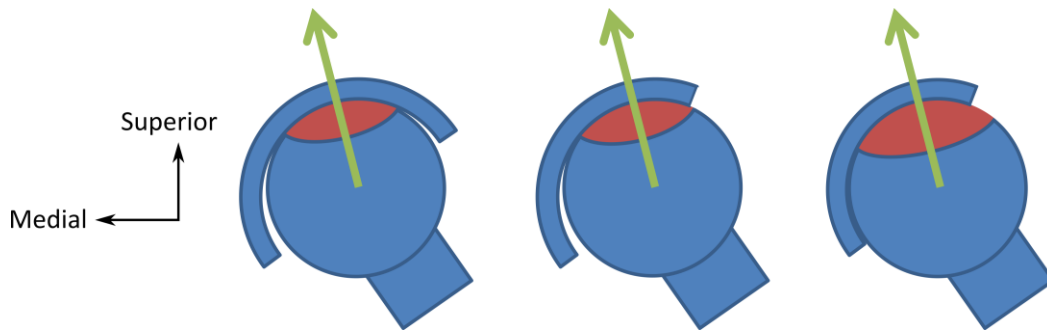


Figure 2.15 A diagram showing how changing the prosthesis design can expose it to superior edge loading (van Arkel and Amis, 2013). Reproduced with permission and copyright © from Elsevier.

A bearing with a large coverage arc (left) is at low risk of edge loading as the contact patch (red area) during activities such as gait (green arrow contact vector) is well centred within the acetabulum. Reducing the articular arc angle too far to prevent impingement provides less femoral coverage and thus is at a greater risk of edge loading (middle). When combined with low clearance, which increases the contact patch size, the bearing is at an extremely high risk of edge loading (right).

advantageous for resurfacing hip arthroplasty as the loosening moment when a large head impinges is much greater than that for a small head due to the increased lever arm of the impinging force (Charnley, 1970) and hip resurfacing devices have unfavourable head-neck ratios (Klues et al., 2008). However, cups with low articular arc angles have subsequently been found to be more prone to edge loading as the acetabular cup provides less femoral head coverage (Jeffers et al., 2009; Langton et al., 2009; Underwood et al., 2011) (Figure 2.15A&B). The problem is exacerbated when the cup is implanted with high inclination as both factors increase the risk of superior edge loading (De Haan et al., 2008b; Griffin et al., 2010).

Similarly, low clearance between the components was introduced to large diameter bearings as it was thought to enable fluid film lubrication and hence reduces friction and wear between the bearing surfaces (Udofia and Jin, 2003). However, lubricant starvation occurs at the edge of the cup (Jalali Vahid et al., 2001) and now it is believed that low clearance is actually a risk factor for an increased prevalence of edge loading as it leads to an increased contact patch size between the bearings (Underwood et al., 2012) (Figure 2.15B&C). This increased contact patch means that edge loading occurs with the contact vector direction further from the edge of the cup and thus can occur during many activities, including gait (Kwon et al., 2012; Mellon et al., 2013).

Designs such as the articular surface replacement, ASR, which have low articular arc angles and low clearances, are particularly prone to edge loading (Underwood et al., 2011; Underwood et al., 2012) and this may explain why some designs have performed better than others (Langton et al., 2009; NJR, 2011); the ASR was to be recalled due its exceptionally high failure rates (MHRA, 2010; Langton et al., 2011a; NJR, 2011).



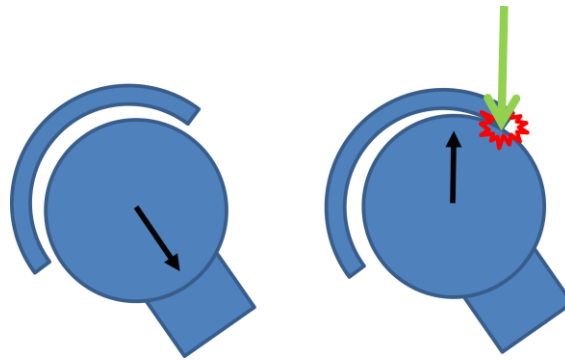


Figure 2.16 A diagram showing how poor soft tissue tensioning can lead to edge loading (van Arkel and Amis, 2013). Reproduced with permission and copyright © from Elsevier

Without appropriate soft-tissue tension, the femoral head can sublux from the acetabulum during gait (left) and when it relocates it can impact on the hard-edge of the acetabulum leading to edge loading wear (right).

Recent research has suggested that softening the edge with a radius or chamfer could act to reduce the contact stress under edge loading conditions (Mak et al., 2011). However, there is an inherent trade-off between increasing the edge radius and reducing the cup articular arc angle and hence a complex relationship exists between cup edge radius, cup positioning and peak contact stresses which means even small changes in design can have large differences (Elkins et al., 2012). Furthermore, increasing the cup radius also reduces the dislocation safe zone and hence avoiding high edge loading stresses and dislocation are opposing goals which prohibit simple design change solutions to the edge loading problem (Elkins et al., 2012).

#### 2.6.6 The effects of soft-tissue balancing on the risk of edge loading

Superior edge loading of implants can be caused by microseparation of the hip joint centres caused by soft tissue laxity during the swing phase of gait as when the hip relocates femoral head can impact on the sharp edge of the acetabular cup during heel strike leading to wear of the bearing surfaces (Nevelos et al., 2000) (Figure 2.16). Wear simulator studies have shown that this produces this mechanism can produce the higher wear rates and the characteristic wear stripes that are seen on ceramic bearings (Stewart et al., 2003; Affatato et al., 2011). This wear mechanism is believed to affect both metal-on-metal (Leslie et al., 2009) and ceramic-on-ceramic articulations (Al Hajjar et al., 2010).

Gait and side leg lift fluoroscopy measurements have shown that microseparation can happen *in vivo*, though it does not affect all patients during gait (Lombardi et al., 2000). Moreover, a detailed look at the orientation of wear scars in ceramic retrievals shows that the majority of wear stripes must have been caused by posterior edge loading during deep flexion and not superior edge loading during gait (Walter et al., 2004).

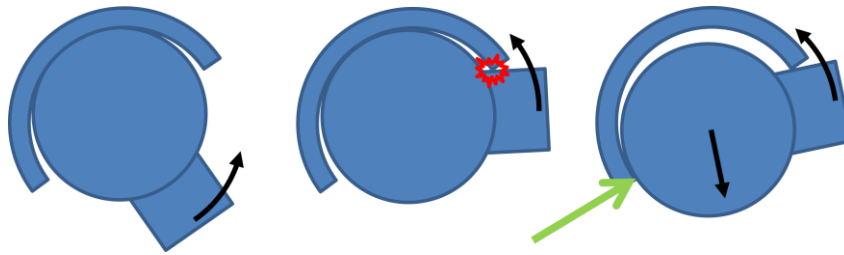


Figure 2.17 A diagram showing how impingement can lead to secondary edge loading (van Arkel and Amis, 2013). Reproduced with permission and copyright © from Elsevier.

Under most conditions the femoral neck is far away from the acetabular rim (A). However as the hip flexes deeply, anterior/anterosuperior impingement can occur (B) and any further rotation results in a lever out subluxation of the femoral head in the socket exposing it to posterior edge loading (C).

### 2.6.7 The effects of impingement and posterior edge loading on the risk of edge loading

When the femoral neck impinges anteriorly/anterosuperiorly on the acetabular rim or periacetabular bone during deep flexion it causes a lever-out subluxation of the femoral head leading to posterior edge loading (De Haan et al., 2008a) (Figure 2.17). This subluxation mechanism for posterior edge loading is identical to that which ultimately leads to posterior dislocation (Scifert et al., 1999; Bartz et al., 2000; Pedersen et al., 2005; Brown and Callaghan, 2008; De Haan et al., 2008a; Elkins et al., 2011a; Elkins et al., 2012) (see section 2.6.1).

Impingement is known to occur following total hip arthroplasty with reports of over half of all hip replacements showing signs of impingement (Wiadrowski et al., 1991; Shon et al., 2005; Marchetti et al., 2011); however these studies are inherently biased as retrievals only give evidence from failed hip replacements. Impingement followed by posterior edge loading is particularly concerning in hard-on-hard bearings where it exposes the femoral head to a sharp, hard edge on the posterior rim (Jeffers and Walter, 2012; Sanders et al., 2012). Consequentially there has been much research exploring how to avoid impingement.

Implant designs with large head/neck ratio have greater pre-impingement range of motion (Bartz et al., 2000; D'Lima et al., 2000; Kluess et al., 2008; Marchetti et al., 2011) as does a less than hemispherical cup (Wiadrowski et al., 1991). Surgeons can also help prevent impingement and edge loading through careful positioning of the acetabular component (De Haan et al., 2008b; Langton et al., 2009; Marchetti et al., 2011). For example, component anteversion affects how much the cup face opens anteriorly and ceramic retrievals have shown that cups with low anteversion increase the prevalence of posterior edge loading (Lusty et al., 2007b) and a similar conclusion was found from metal-on-metal follow up studies (De Haan et al., 2008a; Langton et

al., 2009; Hart et al., 2011a). This is likely because low anteversion provides less femoral head coverage in deep hip flexion and results in the anterior/anterosuperior edge being positioned more anterolaterally increasing the risk of impingement. Conversely, high anteversion can increase the risk of impingement and lever-out in hip extension with external rotation (Charnley, 1970). Results in the literature report excessive anteversion as a risk factor for high metal ion concentrations from edge loaded bearings (De Haan et al., 2008a; Langton et al., 2009). However, there are unknown factors associated with cup anteversion as another contrasting study showed that cobalt and chromium ion levels from edge loading were negatively correlated with anteversion (Hart et al., 2011a; Hart et al., 2011b).

Fortunately, whilst more common, posterior edge loading generally causes lower wear rates than superior edge loading (Esposito et al., 2012); this is likely due to the relative infrequency of deep hip flexion activities such as rising from a chair, when posterior edge loading is a risk, compared to the occurrences of a gait cycle, when superior edge loading is a risk (Morlock et al., 2001; Kwon et al., 2012) (see section 2.2.2).

#### *2.6.8 Posterior Edge Loading without Impingement*

Ceramic clinical retrievals show evidence that edge loading occurs in the majority of all hip replacements (Nevelos et al., 1999; Lusty et al., 2007b; Walter et al., 2011; Esposito et al., 2012) and whilst some clinical retrievals with posterior edge loading wear show evidence of anterosuperior impingement (Walter et al., 2004; Matar et al., 2010), most do not (Walter et al., 2004; Walter et al., 2011; Esposito et al., 2012). Some authors believe that posterior edge loading is a part of normal hip function of the replaced hip, particularly during flexion of the hip (Esposito et al., 2012; Jeffers and Walter, 2012). A recent *in vivo* metal-on-metal showed that edge loading occurred in all hips (30/30) in all patients (19/19) during sit-to-stand activity following hip resurfacing (Kwon et al., 2012); other work by these authors demonstrates that patient specific activity patterns can pre-dispose certain patients to edge loading (Mellon et al., 2011; Mellon et al., 2013).

There are no direct studies examining the influence of surgical approach on edge loading prevalence. However, if analogies with dislocation are drawn then posterior capsular repair and transosseous muscular repair could potentially help reduce posterior edge loading rates as clinical (Chiu et al., 2000; Kwon et al., 2006) and cadaveric data (Sioen et al., 2002; Mihalko and Whiteside, 2004) suggests these techniques reduce dislocation rates.

## CHAPTER 2

### *2.6.9 Future Research*

Edge loading has attracted a lot of attention in the literature recently due to early failure of large diameter metal-on-metal bearings and ceramic hip squeaking. The mechanisms for superior edge loading are well explained. Similarly, the squeaking phenomenon from ceramic hips is becoming well understood and is often not a serious condition requiring revision. However, there are some contrasting clinical observations when it comes to impingement, such as the effects of high anteversion on metal ion concentrations and there is a lack of a complete explanation for the high prevalence of posterior edge loading in the absence of any evidence of impingement which warrants further work. Moreover, any research that provides further detail on how to prevent subluxation and edge loading will have the additional benefit of helping prevent dislocation as well. These results could also be important for the native hip where impingement also causes problems.

## **2.7 Modelling techniques for studying hip biomechanics with focus on cadaveric testing**

### *2.7.1 Modelling techniques*

Computational modelling strategies vary according to the desired outcome measure: finite element techniques are principally used to measure stresses and strains (Ferguson et al., 2000b, a; Pedersen et al., 2005; Anderson et al., 2008; Chegini et al., 2009; Anderson et al., 2010; Dickinson et al., 2011b; Henak et al., 2011; Mak et al., 2011; Harris et al., 2012; Zou et al., 2013; Liechti et al., 2014) and musculoskeletal rigid-body models are used to investigate dynamic movements (Delp et al., 1990; Delp et al., 2007; Arnold et al., 2010; Modenese, 2012; Modenese and Phillips, 2012; Mellon et al., 2013; Mellon et al., 2015) (see section 2.2.4). Discrete element analyses can also be used when a rigid body assumption is appropriate providing a faster solution than the finite element equivalent (Abraham et al., 2013). The greatest strength of computational models is that many iterations and changes can be made to variables to gain a quantitative understanding of the relative effects of each change. For example Chegini et al. investigated the effects of changing the centre-edge angle and alpha angles on hip impingement stresses (Chegini et al., 2009), Elkins et al. investigated how changing the acetabular cup-lip radii affects edge loading severity and dislocation risk (Elkins et al., 2012), Mellon et al. investigated how different gait and chair rising motion patterns affects the risk of edge loading (Mellon et al., 2013) and Liechti et al. evaluated how different acetabular morphology and surgical treatment options effected stress distributions in the hip during walking and sitting down (Liechti et al., 2014).

However, computational models are only as accurate as their inputs and thus can be limited by inaccurate material properties (Ferguson et al., 2000b, a; Henak et al., 2011), errors in input kinematics due to skin artefacts (see 2.2.1, page 13) or the need to simplify the model to reduce the computational expense of the calculation to enable clinically useful computational research. Examples of these simplifications include: neglecting soft tissues (Heller, 2005; Anderson et al., 2008), assuming unidirectional, homogeneous fibre distribution within the tissue (Elkins et al., 2011b), rigid body dynamics (Bunn et al., 2014), geometry simplification (Anderson et al., 2010) or using optimisation routines to solve equations (Modenese et al., 2013).

Cadaveric testing overcomes many of the limitations of computational simulations as the samples have natural bony and soft tissue anatomy and mechanical properties which are inherently important for researching natural joint function (McDermott and Amis, 2006; Masouros et al., 2008). This makes it particularly useful for researching soft-tissues/procedures which are unreliable to model computationally due to a lack on input data or validation techniques. What is more, cadaveric testing is frequently used to generate input data for computational models. This testing method is explored further in the following sections.

#### *2.7.2 Measurement techniques: resecting/repairing tissues to infer their function*

The most common way to determine a tissues function is to cut it away and see the joint biomechanics are affected. For example a hip ligament can be cut and the change in rotational joint laxity can be measured; if the joint rotates further after the ligament has been cut, provided that no others testing conditions have been changed, then it can be assumed that the ligament was controlling hip rotation (Martin et al., 2008).

Similarly, the efficacy of a surgical repair can be assessed by first cutting a tissue, the repairing it and calculating the different between the intact, cut and repaired state. For example cutting iliofemoral ligament alone, or both the iliofemoral and labrum, resulted in increased anterior translation at the hip when the hip is externally rotated; however cutting the labrum alone did not. Similarly repairing the iliofemoral ligament alone, or both the labrum and iliofemoral ligament, restored intact hip anterior translation; however, whilst repairing the labrum alone did reduce the amount of anterior laxity, it did not restore intact hip kinematics. This implies that the iliofemoral ligament is a primary stabiliser and should be prioritised for repair and that labrum is a secondary stabiliser which can offer functional benefits in the absence of the iliofemoral ligament (Myers et al., 2011).

## CHAPTER 2

These techniques have been used extensively for many years to study knee joint mechanics (Furman et al., 1976; Butler et al., 1980; Amis and Dawkins, 1991; Xerogeanes et al., 1995; Amis et al., 2003; Gupte et al., 2003; Kondo et al., 2010; Amis, 2012; Stephen et al., 2013; Hunt et al., 2014; Stephen et al., 2014), however, these techniques have only been adapted to the hip in recent years with the focus on the labrum (Konrath et al., 1998; Ferguson et al., 2003; Crawford et al., 2007; Ito et al., 2009; Myers et al., 2011; Smith et al., 2011; Song et al., 2012), and more recently the capsular ligaments (Martin et al., 2008; Ito et al., 2009; Myers et al., 2011; Safran et al., 2013; Smith et al., 2014). These techniques have also been applied to study hip mechanics before/after hip replacement/resurfacing (Bartz et al., 2000; Wik et al., 2010; Colbrunn et al., 2013) or before/after soft tissues repairs during a hip replacement procedure (Sioen et al., 2002; Mihalko and Whiteside, 2004).

Some authors measure changes by hand (Furman et al., 1976; Martin et al., 2008; Kivlan et al., 2013; Martin et al., 2013; Safran et al., 2013) however it is preferable to use a rig that allows repeatable and controlled application of loads/torques/kinematics (Butler et al., 1980; Amis and Dawkins, 1991; Crawford et al., 2007; Smith et al., 2011). Indeed, in recent years many research groups have invested in robotic actuators which allow controlled applications of loads/torques and kinematics in all six-degrees-of-freedom providing excellent test-retest repeatability which is essential for these techniques (Colbrunn et al., 2013; Martínez et al., 2013; Athwal et al., 2014; Smith et al., 2014).

When a rig/robotic actuator is used, two measurement techniques can be applied for studying the role of soft tissues: either constant loads/torques are applied and the changes in kinematics is measured (Mihalko and Whiteside, 2004), or constant kinematics are applied and the change in load/torque measured (Amis and Dawkins, 1991; Xerogeanes et al., 1995). The first relates more closely to clinical practise; for the clinical tests for anterior cruciate ligament deficiency measured a change in anterior drawer laxity, however, the second technique, which is known as superposition is advantageous as it allows measurements to be recorded independent of the tissue cutting order (Butler et al., 1980; Amis and Dawkins, 1991); this is because a spring always produces the same force for the same displacement (assuming no viscoelastic effects) and hence it can be assumed that the ligaments function the same provided there length change patterns (and hence the joint kinematics) are not altered. This second technique would be useful in the context of hip research as where cutting order is a key limitation of current experiments (Martin et al., 2008). However, the method only works if the kinematics are exactly repeated; deviations in any degrees of freedom

could affect the amount of strain a ligament experiences and hence the amount of resistive force/torque it generates. Conveniently, both measurements can be recorded in the same experiment assuming that subsequent tests do not surpass the yield strength of the remaining ligaments (secondary stabilisers may not be able to provide sufficient force to stabilise the joint and hence could rupture when they experience increased strain in a more lax joint).

Figure 2.18 gives an example to demonstrate the differences between the two techniques. It can be seen that cutting ligament 1 resulted in a large increase in posterior displacement ( $d_{p1}$ ) and a small increase in anterior displacement ( $d_{a1}$ ) whereas cutting ligament 2 resulted in a large increase in anterior displacement only ( $d_{a2}$ ). Thus it might be concluded that ligament 1 provided primary stability against posterior translations and secondary stability against anterior displacements whilst ligament 2 provided primary stability against anterior displacement only. This would be useful to infer what could be causing laxity in a clinical setting. However, the cutting order bias limits the functional implication of the results for an intact and normal joint: ligament 2 was tested after ligament 1 and hence was not compared to the intact case, but to a weakened joint. What is more, comparing ligament 2 directly to the intact case ( $d_{a2'}$  and  $d_{p2'}$ ) would be misleading as it would include the effect of cutting both ligaments and would lead to a false conclusion that cutting ligament 2 results in increased posterior displacement ( $d_{p2'}$ ). Therefore, to assess the function of the

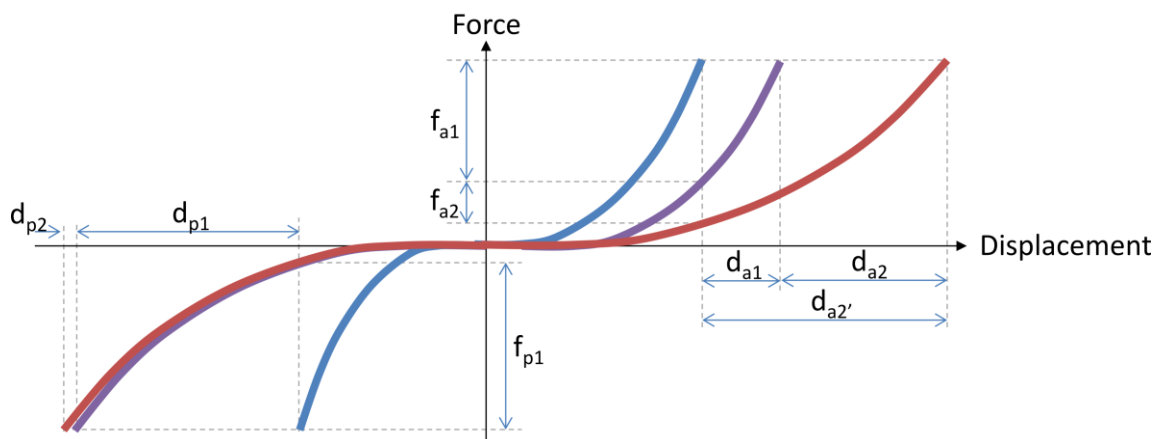


Figure 2.18 An example anterior/posterior laxity test as two ligaments are cut and a constant force is applied.

The blue line represents an intact joint, the purple line represents the repeated measurements after cutting ligament 1, and the red line after cutting ligament 2.  $d_{a1}$  and  $d_{a2}$  are the increases in anterior displacement for the same anterior drawer force after cutting ligaments 1 and 2 respectively.  $d_{p1}$  and  $d_{p2}$  are the equivalent displacements in the posterior direction.  $d_{a2'}$  and  $d_{p2'}$  are the total increases in displacement for the same drawer force after cutting both ligaments 1 and 2.  $f_{a1}$  and  $f_{a2}$  are the reductions in anterior force for the same displacement kinematics after cutting ligaments 1 and 2 respectively.  $f_{p1}$  and  $f_{p2}$  are the equivalents in a posterior direction; however  $f_{p2}$  is effectively zero so is not shown.

## CHAPTER 2

ligaments in a normal joint a repeated kinematics procedure is needed (measuring the decrease in force). Doing so would show for this example that ligament 1 was actually the primary stabiliser for both anterior and posterior translation, having contributed more than half the native joint stability ( $f_{a1}$  and  $f_{p2}$  are both greater than half the applied load). Ligament 2 only had a small secondary role in resisting anterior displacements. It is important to note how these different methods can influence the conclusions.

### *2.7.3 Measurement techniques: Kinematics*

As for clinical measurements, *in-vitro* kinematics of cadaveric joints can be simply measured using a goniometer (Burroughs et al., 2005). When greater accuracy is required: rotational transducers can be mounted to the testing rig to track rotations (Bartz et al., 2000; Southgate et al., 2009), linear variable differential transformers, LVDTs, can be used to track displacements (Southgate et al., 2009; Smith et al., 2011), or infrared reflective markers and an optical motion analysis system can be used to measure both displacements and rotations (Crawford et al., 2007; Lopomo et al., 2010; Safran et al., 2013; Signorelli et al., 2013; Dwyer et al., 2014; Dwyer et al., 2015).

### *2.7.4 Measurement techniques: Contact Stress/Pressure*

The purpose of the cadaveric testing is to understand the biomechanics of the joint and this frequently means understanding the effects of various soft tissue injuries or surgical procedures on the cartilage contact pressures because abnormal contact pressures can lead to cartilage damage and osteoarthritis. The testing procedure usually involves comparing the contact pressure before injury/surgical procedure to that after and thus provides information on the function and importance of the soft tissue/how well the treatment restores natural function (Konrath et al., 1998). A common way to measure contact pressure is using single use pressure sensitive films (Afoke et al., 1987; Eckstein et al., 1997; Konrath et al., 1998; Sparks et al., 2005; Anderson et al., 2008); these films are typically cut into rosettes to prevent crinkle artefacts from affecting the results when the flat sheets are wrapped around the femoral head. For real time pressure information, Tekscan pressure sensors can be used (Stephen et al., 2014; Lee et al., 2015). These sensors still suffer from crinkle artefacts and can also be affected by liquid exposure (Jansson et al., 2013); it is recommended to soak the sensors in saline solution for 48hrs prior to testing to counter the latter limitation (Jansson et al., 2013).

Contact pressures can also be measured through a casting technique: a quick curing polyether casting material, or bone cement, can be inserted into a hip prior to loading. The hip is then functionally loaded and the casting material is squeezed out of the joint



in location of high pressure. Once cured, the resulting cast can be used to infer the contact area in the hip and with knowledge of the applied load can be used to estimate the contact pressures within the joint (Afoke et al., 1980, 1984; von Eisenhart-Rothe et al., 1997).

A recent method to measure intra-articular contact pressure is to use an in-fibre Bragg grating sensor. The Bragg grating reflects light inside a single mode optical fibre and the wavelength of the reflected light changes in response to the load strains on the Bragg grating. Whilst the technology is not widely adopted yet, early results are promising and importantly the sensor can be used without excising the hip joint capsule (Dennison et al., 2010).

The final pressure measurement in hip joints is of hydrostatic pressure (not to be confused with the contact pressure on the articular surfaces). A pressure transducer can be inserted into the fat pad of the acetabular fossa, which is unable to develop significant amounts of solid stress in the tissue itself, to determine the pressurisation within the joint (Ferguson et al., 2003; Dennison et al., 2010).

#### *2.7.5 Measurement techniques: Strain*

Another technique to determine the function and importance of tissues is to measure the strains within them or within surrounding tissues to determine when the tissue is taking load. In bones, this is frequently used in a before and after test to determine if a procedure such as arthroplasty significantly changes the strains in the tissue. The conventional method for measuring strains in bone is by mounting strain gauges directly on it giving strain values at specific points of interest (Kroeber et al., 2002; Anderson et al., 2005; Taddei et al., 2006). However strain gauges cannot be used to measure soft-tissue strains as the gauge cannot be mounted to the wet-tissue surface, and even if it could, the modulus of the gauge is much higher than that of the tissue and therefore would not measure any strain.

More recently, digital image correlation, an optical strain measuring technique that tracks deformations of a painted speckle pattern, has been used to produce full-field surface strain measurements similar to those produced in a finite element model (Dickinson et al., 2011b; Dickinson et al., 2012). These full-field 3D measurements are advantageous when compared to strain gauges as: they can theoretically be taken in high strain gradient regions, it is not necessary to identify a point region of interest prior to testing and it can be used on different scale levels provided an appropriate speckle pattern can be applied. What is more, digital image correlation has also been used to measure strains in soft tissues including mouse arteries (Genovese et al., 2011b, a)

## CHAPTER 2

and intervertebral discs (Spera et al., 2011). However, the measurement noise affects the results and consequently special and time filtering is can be used to reduce the noise, and for biomechanical applications small strains (such as transverse/shear strains in a compressive/tensile test) may have to be neglected due to their poor signal-to-noise ratio, thus preventing calculation of the principal strains (Sztefek et al., 2010). Another disadvantage of digital image correlation technique limits its application for soft tissue mechanics: it requires careful calibration when using a stereo system to acquire 3D strain fields (Sutton et al., 2009) which can take significant amounts of time, which is not ideal for cadaveric testing of soft tissues that could dry out and start to decompose. The technique also requires direct line of sight and that the region of interest remains in the camera focus; this limits the range of motion over which soft-tissue could be tested with a digital image correlation system and also all superficial soft-tissue would have to be necessarily excised to measure strains in deep tissues limiting the accuracy of the cadaveric model.

An alternative method for measuring soft-tissue strains is to use linear variable differential transformers, LVDTs: a suture is anchored to a ligament origin, guided along the length of the fibres to the insertion point and then attached to a LVDT which can measure length changes in the ligament as the joint is moved (Stephen et al., 2012). Differential variable reluctance transducers, DVRTs, can be used as an alternative to LVDTs. These devices are similar to strain gauges but can be mounted to soft tissues using small barbs (Safran et al., 2011; Smith et al., 2011); however, the capsule needs to be removed or requires open windows so that the device can be mounted deep soft tissues such as the labrum. Whilst the quoted accuracy for these devices is low, 1.5  $\mu\text{m}$  (Safran et al., 2011; Smith et al., 2011), it has not been verified for biomechanical applications where movements of the sensor could cause measurement noise.

The final popular method for measuring soft tissue strains is Roentgen Stereophotogrammetric Analysis, RSA (Selvik, 1989). This technique involves inserting small radio opaque beads into a soft tissue or bone and then imaging the tissue with bi-planar fluoroscopy/radiographs. The position of the ball relative to each other before and after an event can then be calculating using a calibration cages and displacements as low as 50  $\mu\text{m}$  can be measured (Selvik, 1989). The technique has been used effectively to measure strains in soft tissues such as the labrum (Dy et al., 2008) as well as measuring graft migrations *in-vivo* (Khan et al., 2006). Both of these studies demonstrated a key advantage of the technique in that it does not require line-of-sight and soft tissue damage made to access the area of interest can be repaired before

testing. Advances in RSA have meant that researchers no longer even have to use tantalum metal beads with carefully inserted radiopaque sutures (Cashman et al., 2010) and model based RSA for implant migration both proving successful (Valstar et al., 2001; Kaptein et al., 2003; Kaptein et al., 2007). The key limiting factor for RSA is the high equipment cost associated with the necessary imaging equipment, and for *in-vivo* studies, the necessity of radiation exposure.

#### *2.7.6 Good practice when cadaveric testing: neutral position and coordinate system*

Any inaccuracies in the starting position will affect all subsequent results so a well-defined neutral position is essential for cadaveric testing. It is also essential for ensuring that the study method can be repeated by other authors to validate the results – a key component of the scientific method. Coordinate systems are discussed in more detail in section 2.1 (page 10)

#### *2.7.7 Good practice when cadaveric testing: physiological loading*

The main advantage of cadaveric testing is that the specimens provide a close match to the *in-vivo* case. To ensure that any testing is realistic, it is important to apply physiological loading to any test rigs to mimic forces the joint experiences *in-vivo* further improving the fidelity of the cadaveric model. The simplest case is to apply axial loads to the femur, so that there is hip joint compression, along with a fixed-value joint torque to rotate the limb, (Crawford et al., 2007; Dy et al., 2008; Elkins et al., 2011b; Smith et al., 2011) (Figure 2.19). A slightly more realistic simulation is achieved by applying the load medially (Ferguson et al., 2003; Dennison et al., 2010) or simulating an abductor mechanism (Cristofolini, 1997; Konrath et al., 1998) to reflect the direction of the force during many routine activities (Bergmann et al., 2001). An alternative is to simulate individual muscle forces using cable-pulley systems (Bartz et al., 2000; Scifert et al., 2001; Wik et al., 2010) (Figure 2.19). However, since results from instrumented implants provided *in vivo* contact forces, using these forces exactly during testing has become the most accurate way to apply physiological loads (Anderson et al., 2008; Anderson et al., 2010; Greaves et al., 2010). Recent six-axis robotic test systems allow theoretically allow the application of realistic kinematics and forces for any daily activity and recently have been used to study the hip joint capsule (Smith et al., 2014).

#### *2.7.8 Cadaveric testing limitations*

Cadaveric testing is limited to measurements at a fixed point in time as there are no living cells; for measuring time dependent changes such as joint morphogenesis, development, healing or decay then imaging/follow-up studies with patients

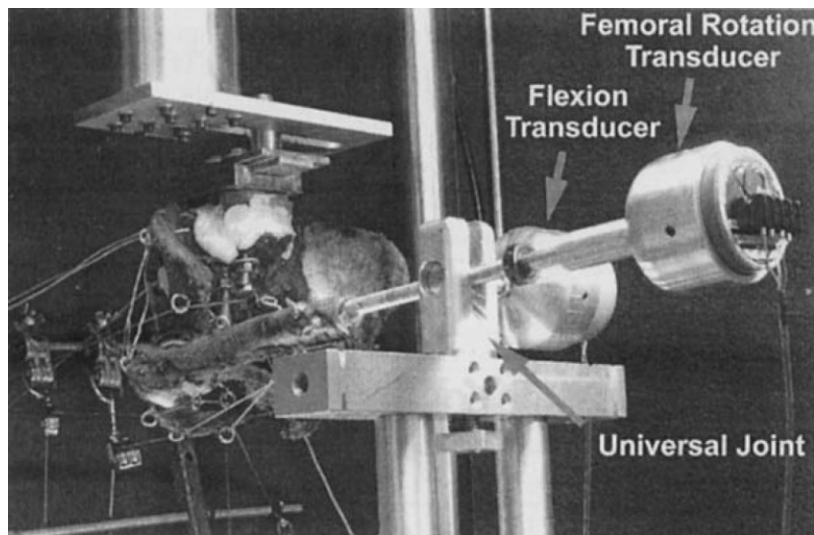


Figure 2.19 Application of muscles loads using cables when cadaveric testing (Scifert et al., 2001). Reproduced with permission and copyright © from Elsevier.

(Lohmander et al., 2007; Siebenrock et al., 2011), animal models (Philippon et al., 2007c; Siebenrock et al., 2013; Nowlan et al., 2014) and computational models (Giorgi et al., 2014) offer more scope. Similarly, cadaveric testing only allows for the measurement of passive effects (soft tissue restraint, bone strains, etc.) and not active contributions from muscles (all though this can be simulated with hanging weights). Another limitation is that there is a lot of variability between individuals so repeats on many different specimens is needed, however human tissue is not readily available and this can lead to problems when the sample sizes are low (Smith et al., 2009). Power analyses can be used to determine an appropriate sample size prior to commencing the research to prevent this limitation (Myers et al., 2011).

Other limitations include age of the donor, static representations of a dynamic situation, accuracy of the measuring equipment, material properties changing as tissue decays, temperature and hydration of tissues, measuring results in fixed locations and not over the whole tissue and having to dissect away tissue to inset measuring equipment (Bartz et al., 2000; Crawford et al., 2007; Anderson et al., 2008; Dy et al., 2008; Smith et al., 2008; Wik et al., 2010). The decay of tissues can be minimised through freezing specimens whilst storing them prior to use; this has been shown to cause minimal effect on the viscoelastic behaviour of ligaments (Moon et al., 2006), muscles (Van Ee et al., 2000), tendons with less than 4 freeze-thaw cycles (Lee et al., 2009; Huang et al., 2011; Ren et al., 2012), bone (Shaw et al., 2012) and entire tissues such as the spine (Panjabi et al., 1985). Furthermore, testing for two days once the specimens have been defrosted has little effect on the test-retest reliability of cadaveric tests (Stephen et al., 2012).

### **3 Hip abduction can prevent posterior edge loading of hip replacements**

Edge loading causes clinical problems for hard-on-hard hip replacements, and edge loading wear scars are present on the majority of retrieved components. We asked the question: are the lines of action of hip joint muscles such that edge loading can occur in a well-designed, well-positioned acetabular cup? A musculoskeletal model, based on cadaveric lower limb geometry, was used to calculate for each muscle, in every position within the complete range of motion, whether its contraction would safely pull the femoral head into the cup or contribute to edge loading. The results show that all the muscles that insert into the distal femur, patella, or tibia could cause edge loading of a well-positioned cup when the hip is in deep flexion. Patients frequently use distally inserting muscles for movements requiring deep hip flexion, such as sit-to-stand. Importantly, the results, which are supported by in vivo data and clinical findings, also show that risk of edge loading is dramatically reduced by combining deep hip flexion with hip abduction. Patients, including those with sub-optimally positioned cups, may be able to reduce the prevalence of edge loading by rising from chairs or stooping with the hip abducted.

The material presented in this chapter has been published in the Journal of Orthopaedic research and is reproduced in full with permission and copyright © from John Wiley and Sons.

van Arkel, R.J., Modenese, L., Phillips, A.T.M., Jeffers, J.R.T., 2013. Hip abduction can prevent posterior edge loading of hip replacements. Journal of Orthopaedic Research 31(8):1172-1179.

### 3.1 Introduction

#### 3.1.1 *Clinical motivation*

Edge loading damages hard-on-hard hip replacements and causes clinical problems: for metal-on-metal (MoM) implants, excessive edge loading wear can lead to pseudotumours and early revision (Kwon et al., 2010) and for ceramic-on-ceramic (CoC) bearings, edge loading has been related to higher wear rates and audible hip joint squeaking (Walter et al., 2008).

#### 3.1.2 *Known mechanisms of edge loading and unexplained edge loading wear*

Edge loading describes the increased contact stress resulting from a decreased contact area between the acetabular cup and femoral head at the rim of the cup. It occurs when the cup provides insufficient coverage of the head preventing a full circular contact area from developing around the hip joint contact force vector (Underwood et al., 2011). This mechanism particularly affects MoM implants with reduced cup subtended angles (Underwood et al., 2011) and/or poor cup positioning (De Haan et al., 2008a), as these factors bring the rim closer to the path of the contact vector and expose the hip to edge loading (Kwon et al., 2012). However, clinical evidence also exists of unexplained edge loading wear on retrievals from well-designed, well-positioned MoM components (Underwood et al., 2011) and a recent in vivo MoM resurfacing study showed that posterior edge loading occurs in all hips in all patients when extending from deep hip flexion when rising from a chair (Kwon et al., 2012).

Edge loading can also occur as a consequence of near-dislocation events: anterior impingement in deep hip flexion and internal rotation, the most common mechanism, causes small subluxations of the head that exposes it to posterior edge loading on the hard edge of the cup, leading to extreme contact stresses and wear (Elkins et al., 2011a). However CoC implant retrievals showed that posterior edge loading wear scars are present on the majority of bearings and occur most commonly in the absence of impingement (Walter et al., 2004; Esposito et al., 2012).

#### 3.1.3 *Aims and hypothesis*

Given the high incidence of posterior edge loading reported in the absence of impingement and the strong influence of muscles on the hip joint contact force (Bergmann et al., 2001), we hypothesised that the lines of action of muscles are such that edge loading can occur in all hips when they are deeply flexed during routine activities, and so we addressed two research questions: are the lines of action of hip

joint muscles such that they could cause edge loading of a well-designed, well-positioned acetabular cup?; and, how sensitive are the results to geometrical variation of the cup through changes to the implant design or orientation?

## 3.2 Methods

### 3.2.1 Muscle contribution to edge loading

A lower limb model was developed (Modenese et al., 2011) based on a digitized cadaveric right leg specimen that detailed muscle origin and insertion points (Klein Horsman et al., 2007). More detailed information about the model can be found in a previous study that compared computed hip joint contact force magnitudes with those measured in vivo (Modenese et al., 2011). The model's muscle geometry included an anatomical wrap for the iliopsoas muscle fibres around the pelvis to ensure it pulled the femur in the correct direction. To keep representative muscle geometry throughout a complete range of motion, additional muscle wrapping surfaces were applied to the gluteus maximus superior fibres, gluteus maximus inferior fibres, the gemelli, and obturator internus; images of these wraps and the rationale behind them is explained in depth in appendix A3.1 (page 189).

The full hip range of motion for an adult male (Boone and Azen, 1979) was discretized into 5° positions of flexion (−10° to 120°), abduction (−25° to 40°), and rotation (−40° to 40°) totalling 6,426 hip orientations. Angles were referenced in accordance with the ISB recommendations for joint coordinate systems (Wu et al., 2002). OpenSim version 2.4.0 (Delp et al., 2007) was used to place the model in each of these static positions, and the direction of the force vector exerted by each muscle onto the pelvis was calculated using an OpenSim plugin, which is available for free download together with detailed documentation (Modenese et al., 2012). An overview of how the plugin works is included in appendix A3.2 (page 190).

The hip was modelled in MatLab (version 2011b, The MathWorks, Inc., Texas, USA) as a typical Ø28 mm bearing with an acetabular subtended arc angle of 168° (e.g., the Biolox Forte cup) well-positioned at 20° anteversion and 45° inclination using the radiographic definition (Murray, 1993). Appendix A3.3 (page 191) gives a detailed description of how this hip replacement was modelled and orientated according to the definition published by Murray. A conservative edge loading risk-zone, which allows for the circular contact patch surrounding the force vector, was defined within 5° of the cup edge. The unit force vectors acting on the pelvis calculated by the plugin were applied at the centre of rotation as equal and opposite unit reaction forces. For each muscle, we calculated if its contraction would safely pull the head into the cup (Figure 3.1A) or

contribute towards creating an edge loading force vector (Figure 3.1B). Appendix A3.4 (page 193) details the calculation steps used to determine if a muscle would contribute to edge loading and also describes how two different methods were used and cross-validated to ensure this critical calculation was correct.

### 3.2.2 Effects of implant design

The muscle contribution to edge loading was then re-calculated for a well-positioned cup for the implant designs in Table 3.1. The effect of varying the edge load risk-zone was studied by varying the angle in the range 5–30°, which represents the range of possible contact patch semi-angles for CoC (Mak and Jin, 2002) and MoM bearings (Dowson et al., 2007; Kwon et al., 2012).

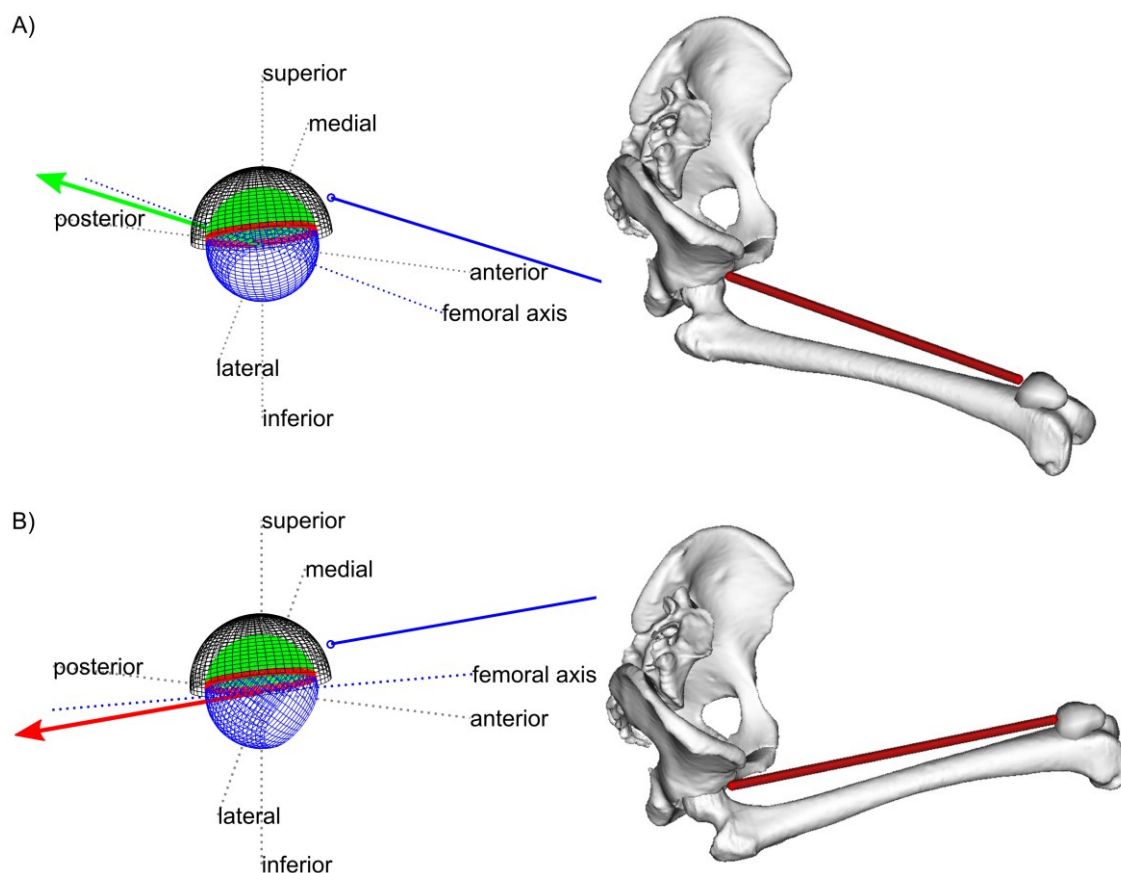


Figure 3.1 A diagram showing how a change in hip position can cause a muscle to contribute to edge loading.

(A and B) Diagrams of the line of action of the rectus femoris (blue line) and its unit reaction force at the hip joint (red/green arrow) at 90° flexion and neutral rotation. The cup liner is divided into a green safe zone and a red edge load risk-zone. (A) The hip is abducted 20° and the rectus femoris pulls the head (blue sphere) into the cup safe zone. (B) The hip is adducted 20°, now the line of action of the rectus femoris pulls the head out of the cup and thus it could contribute to an edge loading contact vector. Representative images from the musculoskeletal model are shown.



Table 3.1 The models and dimensions of implant designs studied

Material Couple	Implant	Head diameter (mm)	Subtended Angle (°)
CoC	Bilox Forte	28	168
CoC	Delta Motion	36	168
MoM	Adept	38	161
MoM	Adept	58	161
MoM	ASR	59	152
MoM	ASR	39	144

### 3.2.3 Effects of implant orientation

For the original cup design, the effects of different acetabular orientations were investigated by varying the angles for all nine possible combinations of 5°, 20°, and 35° (low, medium, and high) anteversion with 30°, 45°, and 60° (low, medium, and high) inclination.

### 3.2.4 Comparison with in-vivo force data

Bergmann's in vivo tests (Bergmann et al., 2001) provide kinematic and force data for 16 trials of sit-to-stand. The data were retrieved from HIP98 (Bergmann et al., 2001) and used to test the correlation between hip flexion angle, abduction and rotation at the point of maximum hip joint contact force, and two angles that define how much the force points into the cup:  $\alpha$  in the transverse plane, and  $\beta$  in the sagittal plane (Figure 3.2). For 15 of the trials, the maximum hip contact force occurs at, or shortly after the point of seat off and maximum hip flexion; however, the trial HSRCU3 has unique dynamics and is less suitable to study forces in deep flexion because the maximum load occurs much later than the point of seat off. Thus, the data were tested both with and without trial HSRCU3. A 5° shaft-mechanical axis angle which is equivalent in direction to knee valgus, which does not affect correlation statistics, was used to convert from Bergmann's z-axis to the ISB's y-axis (Wu et al., 2002). The rationale for this correction is described in appendix 0 (page 196).

## 3.3 Results

### 3.3.1 Muscle contribution to edge loading

All the muscles that inserted into the distal femur, patella, or tibia can contribute to edge loading of a well-positioned cup within a normal range of motion, whereas other large muscles, such as the gluteus medius, cannot. Figure 3.3 lists the included muscles and the percentage of positions in the range of motion where the line of action of that muscle could contribute to an edge loading hip contact force.

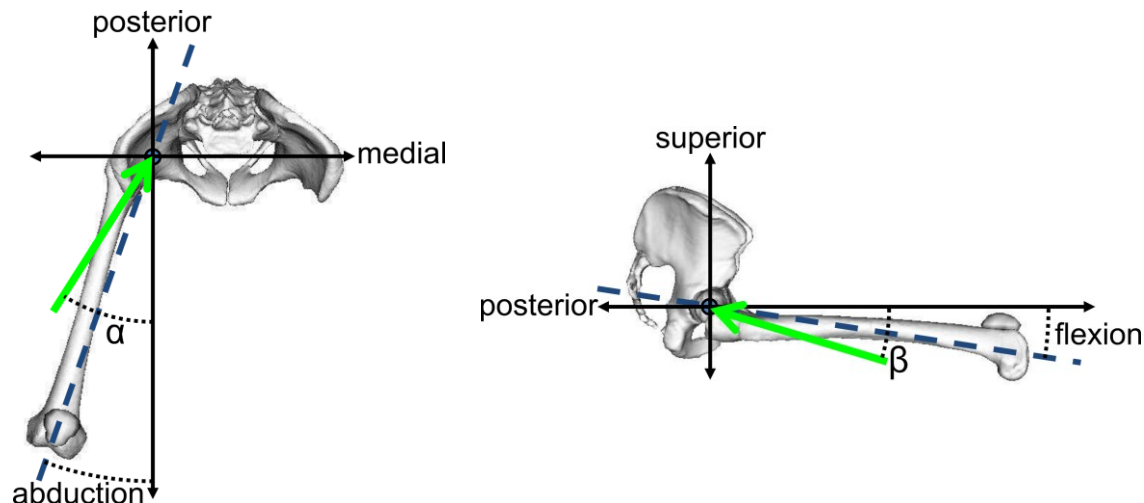


Figure 3.2 The definitions of  $\alpha$  and  $\beta$  in the transverse and sagittal planes respectively

The green arrows are projections of the resultant force at the pelvis into these planes, and the blue dashed lines highlight the femoral axis.

The risk of edge loading was particularly prevalent during deep flexion (Figure 3.4). For a well-positioned cup, the percentage of muscles that could contribute to edge loading increased from 0 % to 39 % (9/23) as flexion increased from 80° to 100° with neutral abduction and rotation.

Hip abduction dramatically reduced the muscular contribution to edge loading in deep flexion (Figure 3.4); at  $\geq 20^\circ$  abduction, no muscles contributed to edge loading up to 95° of flexion. Hip flexion with adduction had the opposite effect; when the hip was in 20° adduction, muscles could cause edge loading above 50° flexion. Internal or external rotation of the hip made little difference to the risk of edge loading (appendix A3.6, page 197). For ease of communication, these results group all muscle fibres together to form individual muscles with the exception of the gluteus maximus where its distinct insertions are modelled as separate muscles; this grouping of muscle fibres did not affect the results as shown in appendix A3.7 (page 197). This appendix also shows that the results are unaffected when re-plotting the results as a percentage of total muscle force capacity.

### 3.3.2 Effects of implant design

Decreasing the subtended angle of the cup arc increased the maximum possible muscle contribution to edge loading and decreased the flexion angle at which muscle contribution to edge loading was possible (Figure 3.5). However, changing the size of the bearing in isolation did not affect the possible muscular contribution to edge loading. Changing the edge load risk-zone had the same effect as decreasing the subtended angle as both changes reduced the safe coverage of the head. For

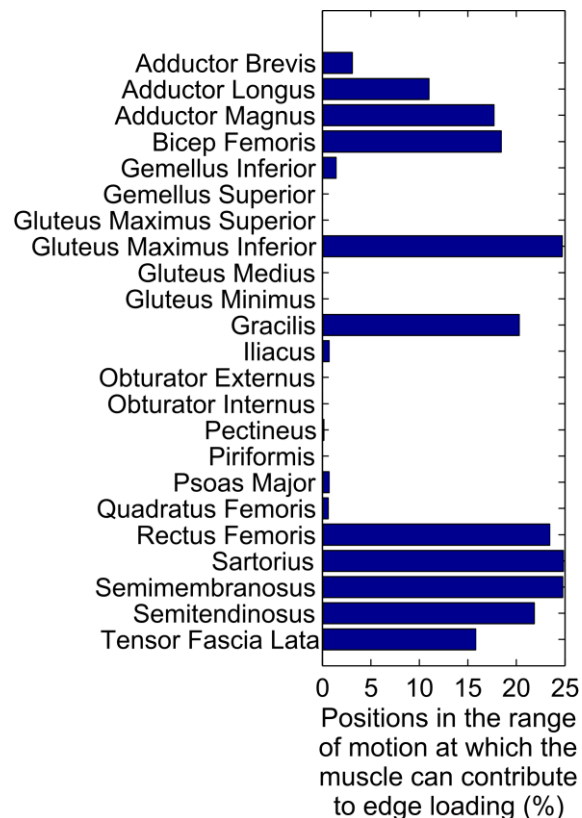


Figure 3.3 List of the muscles included in the study indicating the percentage of positions in the complete range of motion at which each muscle could contribute to an edge loading force vector in a well-positioned cup.

example, two bearings with subtended angles of  $168^\circ$  and  $152^\circ$  and edge load risk-zones of  $13^\circ$  and  $5^\circ$ , respectively, were equivalent (safe coverage arcs of  $142^\circ$ ).

### 3.3.3 Effects of implant orientation

For all cup positions, the general trend was the same as shown in Figure 3.4; the percentage of muscles that can contribute to edge loading increased rapidly at a given flexion angle, was highest in deep flexion, and abducting the hip had a protective function. Internal and external rotation had a larger effect in some cup positions in comparison to a well-positioned cup; however, the dominant effect was still driven by hip flexion, then ab/adduction.

The following trends are based on data from the complete range of motion which is shown in full in appendix A3.8 (page 200); however, many of the trends can be seen in Figure 3.6. Low anteversion decreased the flexion angle at which edge loading could occur but had little effect on the maximum number of muscles that could edge load a hip; it effectively shifted the lines in Figure 3.4 to the left. High anteversion had the opposite effect; it allowed higher flexion angles before large numbers of distal muscles could contribute to edge loading.

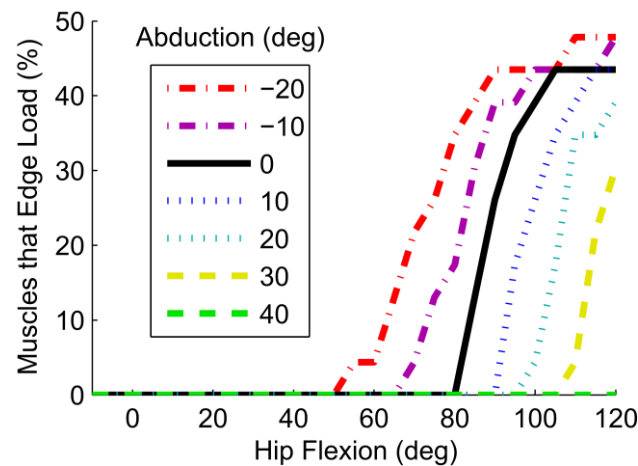


Figure 3.4 The percentage of muscles that can contribute to edge loading as a function of hip flexion with neutral rotation and different ab/adduction in a well-positioned cup

Low inclination had two effects: it increased the maximum number of muscles that can cause edge loading forces over all flexion angles, because some of the short external rotators and obturator muscles had contact vectors that were in the inferior portion of the risk-zone. It also reduced, but did not eliminate, the effect of abducting the hip in deep flexion on the number of muscles that can contribute edge loading force components.

High inclination had three effects. First, it decreased the number of distally inserting muscles that can contribute to edge loading in flexion. Second, it increased the effect of abducting the hip during flexion. Third, it allowed the iliopsoas muscles to contribute to edge loading forces in low flexion or extension angles, and also the distally inserting muscles when the hip was adducted in low flexion or extension.

Combining high/low anteversion with high/low inclination provided a combination of the above effects. For example low inclination and low anteversion resulted in high muscle contribution to edge loading at lower flexion angles.

### 3.3.4 Comparison with in-vivo force data

At maximum load, strong, significant correlations existed between the abduction angle and  $\alpha$  (Figure 3.7A,  $r = -0.85$ ,  $p\text{-value} < 0.001$ ), and the flexion angle and  $\beta$  (Figure 3.7B,  $r = -0.91$ ,  $p\text{-value} < 0.001$ ). Excluding the abnormal trial HSRCU3 resulted in an even stronger correlation between abduction and  $\alpha$  (Figure 3.7A,  $r = -0.94$ ,  $p\text{-value} < 0.001$ ).

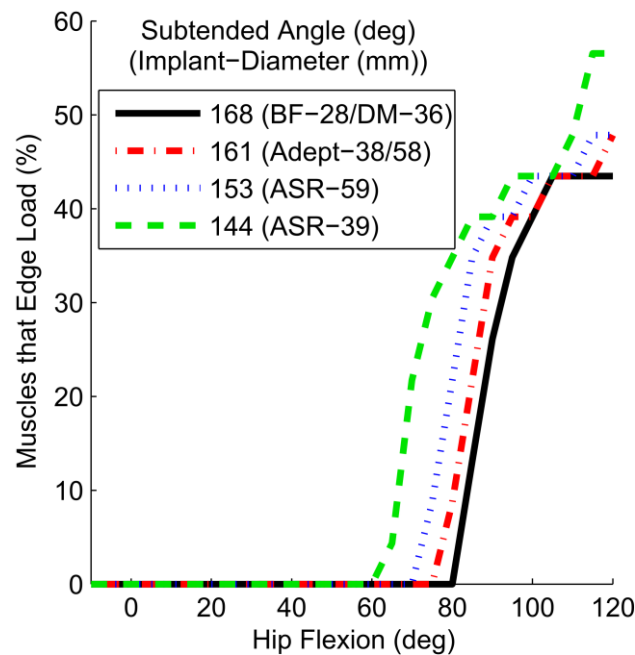


Figure 3.5 The effect of reducing the subtended angle of the cup arc on the possible muscle contribution to edge loading for a well-positioned cup with neutral hip abduction and rotation.

### 3.4 Discussion

#### 3.4.1 Most important findings

This study showed that the lines of action of distally inserting muscles can contribute to edge loading of a well-positioned acetabular cup when the hip is in deep flexion, and abducting the flexed hip moves the lines of action of these muscles away from the edge and into a safe-zone inside the cup. This is because the lines of action of the distally inserting muscles are tied to the position of the femur (Figure 3.1). The positive benefit of abduction is true for all cup designs (Table 3.1) and orientations tested (Figure 3.6). Incorporating abduction into activities in deep flexion, like sit-to-stand, may be a useful rehabilitation exercise for patients to avoid edge loading wear, and this may be particularly beneficial to patients with the ASR implant. Moreover, combining high flexion angles with abduction could also prevent shear dislocation (without impingement) (Bartz et al., 2000; Nadzadi et al., 2003) by bringing the lines of action of all the muscles to within the cup (Figure 3.4). Abduction of a flexed hip also moves the femoral neck and surrounding bone away from the anterior portion of the acetabulum and pelvis, the most common deep flexion impingement site (Bartz et al., 2000; Kessler et al., 2008), adding further weight to the finding that hip abduction in deep hip flexion is of benefit to patients.

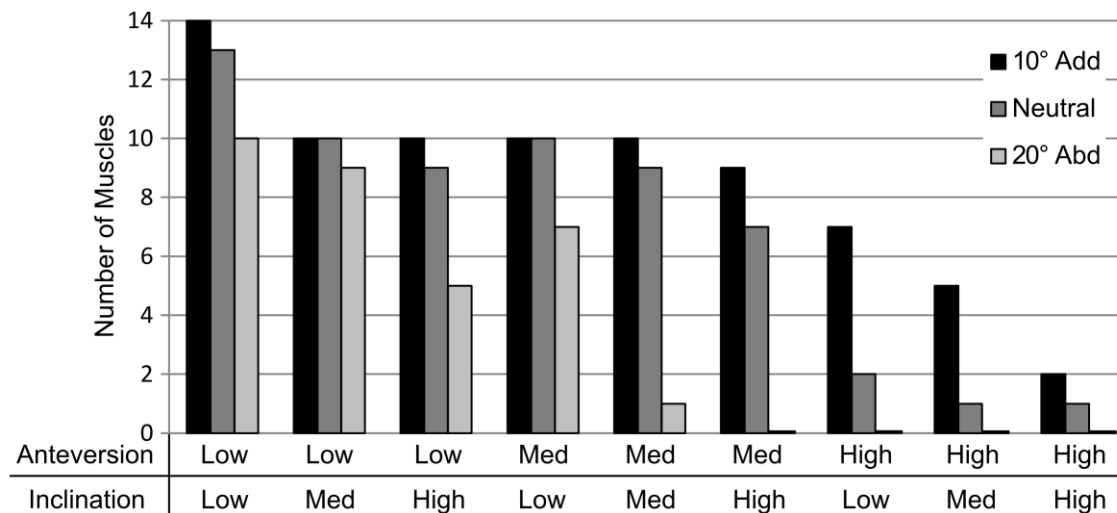


Figure 3.6 The number of muscles that can contribute to edge loading of a well-designed cup at 100° hip flexion and neutral hip rotation with varying hip abduction and cup orientation.

### 3.4.2 Limitations

The adopted methodology is purely geometrical and does not include explicit calculation of the hip contact force vector because the individual muscle contributions are assessed only with respect to their direction. Despite this limitation, the data showed strong equivalence to the resultant load vector measured in instrumented implants. Also, while our study cannot find specific hip positions or movements that cause edge loading, it does show that the lines of action of muscles are such that edge loading of a well-positioned cup in the absence of subluxation is only possible in deep flexion, and abducting the hip can prevent this. Indeed, the approach avoids some of the limitations associated with determining force magnitudes through modelling: first, it does not require an optimization routine. A recent study showed that a musculoskeletal model based on the same anatomic dataset used here could potentially reproduce the hip contact force direction measured in vivo, but the optimization techniques currently employed for estimating muscle forces are unable to yield muscle recruitment adequate to accurately estimate that vector (Modenese et al., 2013). Second, it allows the full range of motion to be explored, and so the results encompass all the activities that a hip replacement patient could do.

This model assumes that the line of action of the hip joint reaction force passes through hip's centre of rotation. This is valid when the femoral head and acetabular cup are spherical and concentric (or marginally off concentric due to the small difference in diameter of the femoral head and acetabular cup), as shown in Figure 3.8. This is a reasonable assumption for a total hip replacement, which has engineered components, and in some cases for a native hip with normal anatomy which approximates well to a

## HIP ABDUCTION PREVENTS EDGE LOADING

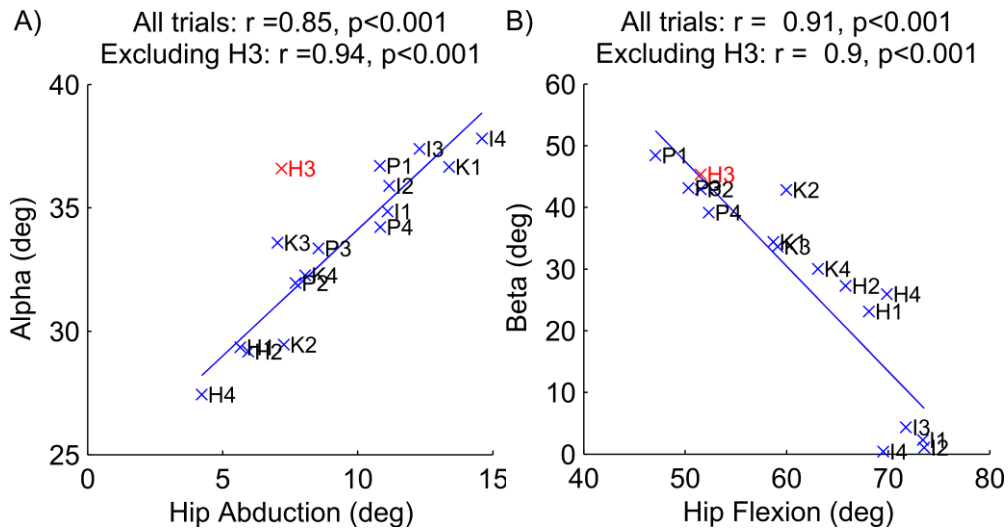


Figure 3.7 The correlation between the direction of the contact vector relative to the pelvis and the position of the hip.

Points are labelled with the first letter of the trial name and trial number according to the sit-to-stand trial in HIP98 (e.g., H1 = HSRCU1 in HIP98), and lines of best fit are shown. The trial with abnormal dynamics (HSRCU3) is highlighted in red.

spherical ball-and-socket joint (Cereatti et al., 2010). However, this assumption is not valid when the native or replaced hip subluxes due to either impingement or acetabular insufficiency; the former can affect a pincer hip or a mal-positioned total hip replacement whilst the latter can affect dysplastic hips. It is also not valid when the femoral head is not spherical such as a cam deformity. This is because impingement, asphericity and/or subluxation can result in multiple points of contact between the head and cup. The reaction force at each point of contact must be locally normal to the joint surface and so the resulting forces may not only act closer to the edge of the acetabulum and increase the risk of edge loading, but also could have a very high magnitude (Figure 3.8) increasing the risk of damaging the joint surfaces.

A final limitation of the model is that muscles are modelled as straight lines and not as a volume which can contract as the muscle generates force. Other authors have developed more realistic models of muscles that consider their entire shape and volume using finite-element modelling (Blemker and Delp, 2005); however these techniques are computationally heavy and would be impractical when studying all the muscles of the hip in all hip positions. This limitation could particularly have affected the gluteus maximus because it has a large volume and so could undergo large changes in shape as it contracts. It also wraps around many deep muscles (which may also change shape) which could further affect its line of action. It would also be an interesting extension to the model to consider if contraction of the gluteus maximus in deep flexion could act to stabilise the hip against posterior dislocation by generating compressive forces in the deep muscles which it wraps around. Importantly, for the

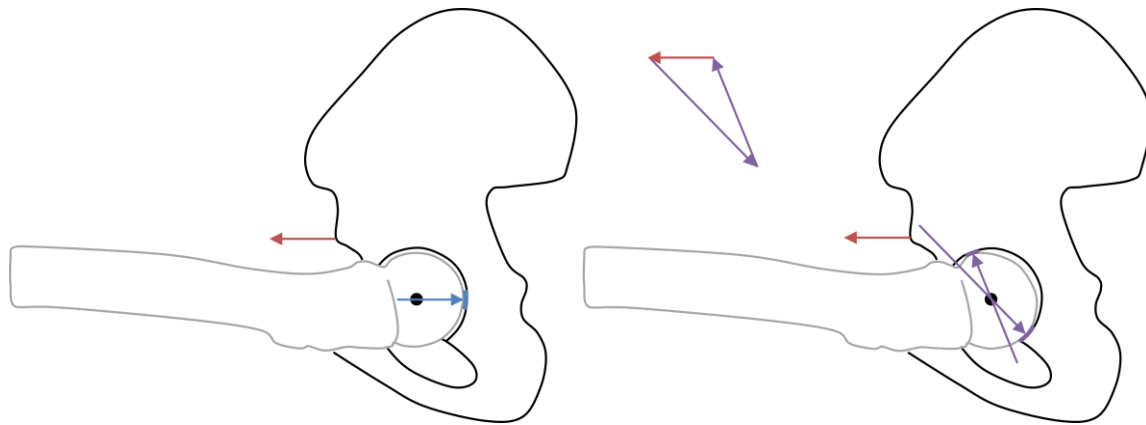


Figure 3.8 How an aspherical femoral head could invalidate the modelling assumptions.

The rectus femoris (red arrow) is acting on the pelvis and is resisted by an equal and opposite reaction from the femoral head acting on the acetabulum (blue/purple arrows). Left) the model used in this chapter assumes that there is a single component to the reaction force that passes through the centre of rotation (blue arrow). Right) this assumption is not valid for an aspherical, impinged and/or subluxed hip as there can be multiple points of contact (purple arrows). It can be seen that both the risk of edge loading and the magnitude of force could be increased by the presence of an aspherical femoral head.

majority of muscles, their changing shape when contracting is unlikely to influence the main conclusions of this study for a similar reason that internal/external rotation has less of effect than flexion/ab/adduction – it is the long distally inserting muscles that experience the greatest change in their lines of action and this variation is predominantly driven by the large movements of the lower limb. The musculoskeletal model was based on anatomical data from a male specimen however for the same reason (movements of the lower limb cause larger variation in the lines of action of distally inserting muscles than variations in anatomical origin/insertion) it is likely that the conclusions would also apply to female specimens. Indeed, the *in vivo* data analysed (Figure 3.7) included both male and female subjects and corroborates the main conclusion that hip abduction could prevent edge loading of hip replacements.

### 3.4.3 Comparison with published research

*In vivo* resultant joint reaction force measurements from instrumented implants (Bergmann et al., 2001) corroborate the findings by showing that the direction of the maximum resultant joint force relative to the pelvis is highly correlated with the position of the femur during sit-to-stand activity (Figure 3.7). The *in vivo* data show that posterior edge loading is possible in deep flexion as flexion is correlated with a more posteriorly pointing load vector (Figure 3.7B). It also supports the result that activity modification can reduce the risk of edge loading: higher abduction at the point of seat off was strongly correlated with a more medially angled force relative to the pelvis, and hence a force that points more inbound, further away from the posterior edge of the acetabulum (Figure 3.7B).



Rising from a chair can require  $>100^\circ$  of hip flexion, with abduction varying from  $-10^\circ$  to  $20^\circ$  (Bergmann et al., 2001; Nadzadi et al., 2003). This movement relies on considerable muscle force from the distally inserting hamstrings, rectus femoris, and gluteus maximus, and little contribution from the gluteus medius and short external rotators (Doorenbosch et al., 1994; Bartz et al., 2000; Yoshioka et al., 2012). Hence, the muscles that can contribute to creating an edge loading force (Figure 3.3) during deep flexion (Figure 3.4) are known to be highly active during sit-to-stand, while muscles that provide a protective function are not. This may explain the high incidence of edge loading wear reported clinically, (De Haan et al., 2008a; Kwon et al., 2010; Underwood et al., 2011; Esposito et al., 2012) and why edge loading occurred in all MoM resurfacing patients when rising from a chair (Kwon et al., 2012).

The implant sensitivity study showed that decreasing the subtended cup angle increased the possibility of muscle contribution to edge loading (Figure 3.5). This supports results from explanted MoM bearings that show that cups with reduced subtended angles edge loaded significantly more and suffered significantly higher wear rates (Underwood et al., 2011) and emphasizes the need to mitigate the risks of edge loading for new cup designs that have reduced subtended arcs.

Our results support findings from ceramic retrievals where the majority of edge loading wear occurred posteriorly during high flexion (Walter et al., 2004; Esposito et al., 2012) with low cup anteversion increasing the risk (Lusty et al., 2007b). Interestingly, we also showed that high inclination can help protect against posterior edge loading by moving the inferior edge of the cup more laterally and thus in an anteverted cup it provides more posterior coverage of the head. However, high inclination should be avoided as it can expose the joint to superior edge loading in low flexion or extension angles, and edge loading during gait can have severe consequences (De Haan et al., 2008a; Esposito et al., 2012; Kwon et al., 2012). Indeed recent MoM resurfacing research using AP X-rays suggests that low inclination is beneficial, particularly for small bearings (Gross and Liu, 2012). However, in both established (Esposito et al., 2012) and contemporary (McDonnell et al., 2013) CoC bearings, a combination of low inclination and low anteversion led to high incidences of posterior edge loading wear and squeaking. This is the cup orientation at greatest risk of posterior edge loading from muscle action (Figure 3.6), and so low inclination should be combined with higher anteversion to provide better coverage of the head throughout the range of motion.

Muscles damaged in the most common surgical approaches (lateral: gluteus medius and minimus, posterior: short external rotators) (Masonis and Bourne, 2002) never cause edge loading of well-positioned cups (Figure 3.3). Intraoperative repair and

## CHAPTER 3

rehabilitative strengthening of these muscles may reduce the risk of edge loading as weakened muscles may lead to the patient substituting their function for a distally inserting alternative (Dostal et al., 1986) that could contribute to an edge loading force. Appendix A3.9 (starting page 201) describes some pilot work designed to investigate this hypothesis further; it was found that reducing the strength of the gluteus medius and minimus resulted in increased dependence on the tensor fascia lata and joint reaction force that passed to the edge of the cup. This forms the basis for an interesting avenue for further work (see chapter 0).

Edge loading can be caused by soft tissue laxity leading to microseparation during gait (Nevelos et al., 2000), by impingement in deep flexion with internal rotation (Elkins et al., 2011a), or by low subtended angles and/or high inclination providing insufficient superior coverage of the head (De Haan et al., 2008a; Kwon et al., 2012). We do not discount these phenomena but provide an additional mechanism by which edge loading could occur in all hip replacement patients: posteriorly in deep flexion due to muscle forces alone.

### *3.4.4 Clinical relevance and conclusion*

In answer to our research questions, we showed that all the distally inserting muscles could cause edge loading of well-designed, well-positioned acetabular cups when the hip is deeply flexed. Low subtended arc angles and suboptimal cup orientation can increase the risk of edge loading through muscle action, but does not alter the general trend observed for a well-designed, well-positioned cup. However, our most important finding is that all patients, regardless of how their prosthesis was designed or implanted, can reduce the prevalence of posterior edge loading, and perhaps dislocation, by introducing abduction to activities that require deep flexion; this can easily be implemented for activities such as rising from a chair and stooping by separating the knees before performing the movement.

## **3.5 Acknowledgements**

The OpenSim model and plug-in used were developed by Luca Modenese (a co-author on the paper). My only role in the development of the London Lower Limb model was to improve the wrapping surfaces of the gluteus maximus such that it gave realistic moment arms throughout the range of hip motion.

This study was funded, in part, by the Engineering and Physical Sciences Research Council and the Institution of Mechanical Engineers.

## **4 Design and manufacture of a six-degrees-of-freedom hip joint testing system**

The capsular ligaments, labrum and ligamentum teres could have an important role of preventing impingement, subluxation, edge loading and dislocation in the native hip; however research is needed to better understand the scope of this passive protection and if it could be preserved during joint preserving surgery, or replicated following a total hip replacement. Therefore, the aim of this study was to design and manufacture a six-degrees-of-freedom testing rig to investigate the hip's passive restraint envelope using a cadaveric model. A rig was designed to fit into the working volume of a dual-axis materials-testing-machine whilst allowing application of torque/angular positions in all three rotary degrees of freedom using the ISB coordinate system. The rig was designed such that it could apply physiological loads and be used by an operator working alone. The rig was manufactured and its capabilities were tested using finite element modelling with an experimental validation. When the rig was loaded with 1,100 N angled 20° medially/superiorly with 25 Nm internal/external rotation torque, the finite element model predicted peak stresses that were a third of the proof stress of the aluminium alloy used. When applying 110 N hip joint compression angled 20° medially/superiorly with 5 Nm internal/external rotation torque the model predicted a maximum hip joint centre displacement of 0.4 mm. The finite element model over-predicted the displacement of the hip joint centre: it predicted a stiffness of 270 N/mm whereas the measured rig stiffness was 300 N/mm. It was concluded that the rig is suitable for testing the passive restraint envelope of the hip. Engineering drawings are provided.

### 4.1 Introduction

#### 4.1.1 *Clinical motivation*

Chapter 3 found that the hip could be exposed to unfavourable muscles lines of action in deep flexion and adduction thus increasing the risk of edge loading and dislocation. These lines of action are the same for both a native and replaced hip yet dislocation of the native hip is extremely rare and typically only occurs following extreme trauma or with an underlying deformity (Tönnis et al., 1987; Matsuda, 2009; Ranawat et al., 2009; Cross et al., 2010; Sansone et al., 2013; Austin et al., 2014). This could be due to better coverage provided by the native acetabulum and indeed dysplastic hips are at a greater risk of dislocation (Tönnis et al., 1987); however, retroverted hips have poor coverage of the femoral head in deep flexion and are known to impinge and sublux in deep flexion yet do not dislocate (Reynolds et al., 1999; Wassilew et al., 2013; Leunig and Ganz, 2014). This suggests that the protection against dislocation could also be due to another factor.

The passive soft-tissues (capsular ligament, ligamentum teres and labrum) could offer protection in two ways: firstly, by restricting hip range of motion and thus protecting the hip from moving into at-risk positions, or secondly through contributing a force that resists dislocation directly. Understanding the mechanisms of this passive soft-tissue restraint would be clinically useful for two reasons: firstly, it could lead to better optimised soft-tissue repair techniques following a total hip replacement to further reduce dislocation rates (Kumar et al., 2014) and perhaps help prevent edge loading, and secondly because it could help protect patients from iatrogenic dislocation (Matsuda, 2009; Ranawat et al., 2009; Domb et al., 2013; Sansone et al., 2013; Austin et al., 2014) or more subtle micro-instability (Mei Dan et al., 2012; Domb et al., 2013; Frank et al., 2014) following joint preserving surgery.

#### 4.1.2 *The need for a six-degrees-of-freedom testing rig*

Computational models provide an excellent method for quantifying relative changes (see section 2.7.1, page 46); indeed two authors have used models to this effect to examine the effects of passive soft-tissue restraint on total hip replacement dislocation (Elkins et al., 2011b; Bunn et al., 2014). However, without appropriate validation, computational models can be unreliable for defining absolute values. For understanding the role of passive ligamentous and labral restraint in the native hip, there is a need for baseline quantitative data with absolute values and hence it would be more appropriate to test cadaveric specimens. This data has existed for many years for the knee (Blankevoort et al., 1988; Wilson et al., 2000), yet has only loosely been

defined for the hip ligaments by tests performed by hand (Martin et al., 2008; Safran et al., 2013). To ensure accuracy in these baseline values however, a repeatable testing rig is needed.

Few authors have established testing rigs that allow application of a flexion/extension torque (Elkins et al., 2011b; Smith et al., 2014) or an ab/adduction torque (Crawford et al., 2007; Dy et al., 2008; Smith et al., 2014) with most applying only internal/external rotation movements at fixed intervals of flexion/abduction (Delp et al., 1999; Sioen et al., 2002; Mihalko and Whiteside, 2004; Burroughs et al., 2005; Martin et al., 2008; Myers et al., 2011; Ng et al., 2011). This may be in part due to the aims of the tests: many of them examine impingement/dislocation and the at-risk positions require applying an internal rotation torque with the hip positioned in deep flexion, or external rotation torque with the hip in extension. However, it could also be due to the difficulty in applying flexion/extension torques, and even more so in applying ab/adduction torques, due to nature of a hip's movement axes: internal/external rotation acts about the femur which provides a natural shaft which can be connected easily to a pulley or a materials testing machine. Although flexion/extension movements are fixed to the pelvis, they are a little more complex to model in a cadaveric test as there is not natural shaft to clamp onto and thus require the design of a pelvic fixture. However, ab/adduction torques are difficult to apply as the movement axis is floating (perpendicular to the flexion and rotation axis) and thus depends on both the position of the pelvis and the femur and hence requires a complex testing rig.

Unfortunately, total hip replacement research suggests flexion angle and the degree of ab/adduction greatly affect the risk of dislocation (Bartz et al., 2000). Similarly, the results in chapter 3 suggest that variations in flexion/extension and ab/adduction are important to consider as these movements change the lines of action of distally inserting muscles and this could lead to edge loading conditions. Therefore, the objective of this chapter is to design a hip joint testing rig that allows application of torque in all three rotational degrees of freedom but also allowing the rig to be fixed in positions of interest for internal/external rotation tests. This would allow tests to both replicate and build on previous dislocation and edge loading research methods, whilst also providing the flexibility to test over a complete range of hip motion to determine the effects of varying hip flexion and ab/adduction. So that the tests are clinically meaningful, the rig should ideally mimic the ISB coordinate system and also allow application of physiological loads (see sections 2.7.6 and 2.7.7, page 53).

## CHAPTER 4

### *4.1.3 Rig Specification*

- i. Mimic the ISB coordinate system
- ii. Allow torques/rotation to be applied in all three rotational degrees of freedom over a full range of (in-vivo) hip motion (Boone and Azen, 1979).
- iii. Allow application force in a physiological direction.
- iv. To accommodate any pelvis/femur sized within three standard deviations of the mean size (Yoshioka et al., 1987; Seidel et al., 1995).
- v. To require only a single user as an operator.
- vi. To be able to be manufactured from as fewer raw material extrusions as possible to keep cost low.
- vii. To be able to be manufactured in Imperial College London's mechanical engineering department (CNC milling/turning, laser cutting, as well as various manual machines (lathe, mill, surface grinder, pillar drill, etc.).

## **4.2 Materials and methods**

### *4.2.1 Rig design tools and existing components*

The hip joint testing rig and mounting system were designed in a computer aided drawing package (SolidWorks version 2011 x64, Dassault Systèmes S.A., Vélizy, France) to fit inside the working volume of a commercially available dual-axis servo-hydraulic materials-testing-machine (model 8874, software MAX v9.3, Instron Ltd, High Wycombe, UK). This actuator was capable of applying torques/loads and rotations/displacements about a vertical axis and has in-built position transducers and a load-cell to accurately record displacements, forces and torques. The load cell could measure up to 1 kN of force and 25 Nm of torque and so these are the maximum loads/torques the rig needs to be able to resist. An existing x-z bearing table that fitted in the servo-hydraulic machine's working volume was also available for use; this table consists of two platforms mounted on ball bearings that allow free movement in the horizontal plane. Models for a typical pelvis/femur were downloaded from the BEL repository (Biomechanics-European-Laboratory, 2009).

### *4.2.2 Material selection*

Two alloys were identified as possible material choices: aluminium alloy EN 6082 T6 and stainless steel 303. Both are non-rusting alloys with high yield stresses and excellent machinability (compared to other aluminium and stainless alloys). 303 is

stiffer than 6082T6 however it is also more difficult to machine (higher tool wear), heavier (which would make the components more difficult to handle for a single user when testing) and more expensive. Thus, where possible, 6082T6 was considered preferable.

To evaluate components could be manufactured from aluminium alloy, the design iterations were tested using SolidWorks' inbuilt finite element package to determine the safety factor for the rig compared to the maximum testing load. It was also used to measure the deflection at the level of the hip joint. These tests were conducted using simplified rig models which considered only components directly on the load path (from the base to the hip centre). For the same reason, no fasteners were modelled and parts were assumed to be perfectly mated so that the rig could be modelled as one component, thus eliminating any contact problems. The pelvis was modelled as a large metal extrusion with a raised Ø46 mm circular bosses onto which the load/torques could be applied (the size of an average femoral head, see Table 2.4, page 9). This pseudo-pelvis was sufficiently deep that it had negligible deflection under the applied load thus allowing the load to be applied at the level of the hip joint but without affecting any displacement measurements. The rig was positioned in the worst case position with all components positioned at the extreme slot locations to maximise the moments of the joint reaction force. A fixed boundary condition was applied to the base of the rig and a mesh convergence study was performed for the most complex load case (medial and vertical loading with an internal rotation torque).

The minimum expected material properties were applied in accordance with the relevant standard (Aalco-Metals-Ltd, 2013, 2014b). The rig was automatically meshed using the computer aided design software. The top of the x-z bearing table was fixed in space and a vertical compressive load of 1 kN was applied at the level of the hip joint centre.

#### *4.2.3 Rig manufacture*

An Imperial College London technician manufactured the rig. *Whilst I was responsible for the rig's design, engineering drawings, assembly and testing, all components were expertly manufactured by Philip Wilson.*

#### *4.2.4 Testing the rig's capabilities*

The capabilities of the final design were tested further by applying the following additional load cases to the finite element model: 25 Nm internal/external rotation torque (applied about the materials testing machine's vertical axis) with no load, 1 kN

## CHAPTER 4

superior load with 364 N medial load (resultant force direction 20° superior-medial) with no torque, 1 kN superior load with 364 N medial load with 25 Nm internal/external rotation torque and finally 100 N superior load with 36 N medial load and 5 Nm internal/external rotation torque. Whilst the latter load case was comparatively low, it was included because it was the load case used for the experiments detailed in chapters 6 and 7.

### *4.2.5 Experimental validation*

To validate the finite element predictions of the rig's load capabilities. The stiffness of the manufactured rig was measured directly in the materials-testing-machine. A vertical load was applied through the femoral pot, directly on to a steel pseudo-pelvis which was sufficiently deep to have negligible deflection compared to that of the rig. The rig was preloaded at 300 N for one minute and then was loaded up to 600 N before being unloaded for the start of the tests which consisted of three 0-600 N load cycles with a period of 10 s.

## **4.3 Results**

### *4.3.1 The testing system*

A six-degrees-of-freedom testing system was designed such that all components could be made from a single 5m long extrusion of  $\frac{3}{4}$ " aluminium flat bar except for: the rotating flexion and adduction axes' shafts which were made from stainless steel for increased stiffness (see 4.3.2) and the femoral/pelvic pots which were made from aluminium alloy billets/castings. Cut away features and complex shapes were avoided where possible to facilitate manufacture; they were only used to reduce the weight to allow operation by a single user, or to prevent impingement of the rig on the materials-testing-machines sides during movements with a large range of motion. Assembly drawings for this rig are presented at the end of this chapter, and individual component drawings included in appendix A4. The alignment system used to mount specimens into this rig in the ISB system is described and validated in the next chapter (page 91).

The materials-testing-machine was used to apply superior/inferior loads and translations as well as internal/external rotation torques and angular positions (Figure 2.19). The actuator head was fixed to the femur allowing internal/external rotation about the femoral y-axis as defined by the ISB. Whilst these movements about the materials-testing-machine's axes, the load-cell and displacement transducers could continually record the passive resistance and position of the hip. This allowed for high



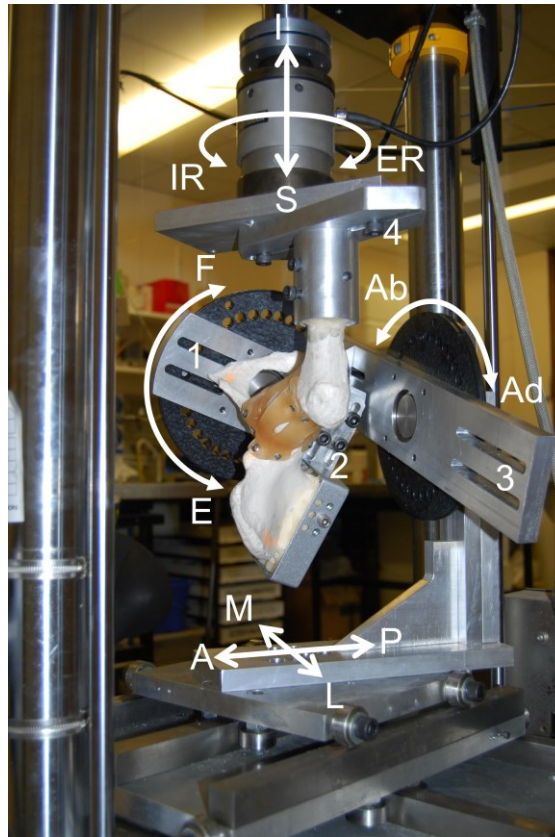


Figure 4.1 The custom built testing rig with a synthetic right hip joint mounted in flexion, adduction and neutral rotation.

Ab/adduction (Ab/Ad), internal/external rotation (IR/ER), flexion/extension (F/E), anterior/posterior translation (A/P), superior/inferior translation (S/I) and medial/lateral translation (M/L) directions are shown. If the rig was in the neutral position, then the slots could be used to align the pelvic hip centre in the A/P (1), S/I (2), and M/L (3) directions. Slot 4 could also be used to adjust the femoral head centre location relative to the servo-hydraulic machine's vertical axis.

accuracy when performing clinically relevant internal/external rotation tests at fixed positions of flexion/extension and ab/adduction.

For testing about the flexion/extension or ab/adduction axes, two pulleys were used to apply torques using two hanging-weights couples. The flexion axis was tied to the pelvis, and the entire flexion unit moved as the hip was ab/adducted such that ab/adduction remained mutually perpendicular to hip flexion and rotation throughout testing. Printed goniometers were laminated on the reverse of these pulleys and bolts holes allowed fixed angular positions to be specified at  $10^\circ$  intervals; a g-clamp could also be used to achieve a finer resolution. A two-degrees-of-freedom horizontal bearing table allowed anterior/posterior/medial/lateral translation to occur freely. A hanging weight looped through an external pulley and attached to this bearing table could be used to apply a medial/lateral or anterior/posterior loads.

Slots in the flexion, adduction and rotation axes allowed for the hip joint centre to be identified iteratively when setting up the rig. This was achieved by adjusting the

## CHAPTER 4

pelvis/femoral position using these slots until no translations occur when a rotation was made about any of the three axes. The slots were sized such that they can accommodate any hip sized within three standard deviations of the mean. These slots on the flexion and adduction axis could additionally be used to attach a weight that balanced the mass of the rig and pelvis so that when flexion/extension/ab/adduction torque was applied, all of it was used to rotate the hip (i.e. the weight of the rig/pelvis did not act to increase/decrease the applied torque).

The flexion axis's anterior-posterior set-up translation arm, and hence the pelvis, could easily be attached to or removed from the test rig using M8 bolts. However the arm maintained the specimen's alignment when removing and reattaching as it mounted directly onto the flexion axis bearing using a tight-tolerance clearance fit; the maximum possible displacement for this fit was less than 50  $\mu\text{m}$  displacement. The rig was cantilevered to enable this action to be performed by a single user. This shape had two further advantages: it allowed for direct access to the periarticular hip tissues without having to remove the specimen from the testing rig, and also allowed for better photos as the view of the hip was not obstructed. A disadvantage of the cantilever design could have been a decreased stiffness; however, this was countered by doubling the thickness of the main supports and adding a triangular stress support.

### 4.3.2 *Material choice*

Five iterations of the rig design were needed to achieve a final design which had a safety factor of 2 when built from 6082T6. The mesh convergence analysis of the final designed showed at least 45,000 elements were needed for the finite element analysis (Figure 4.2). This analysis predicted a maximum von Mises stress of 105 MPa under 1 kN load for this design (Figure 4.3); this peak stress occurred adjacent to the bolt holes in the superior-inferior set-up translation arm. The maximum displacement of the hip joint centre was less than 4 mm under the 1 kN load (Figure 4.4). As the rig was modelled as a single material, the peak strain occurred in the same position as the peak stress; however, there were also relatively high strains (0.55  $\mu\epsilon$ ) recorded in the aluminium shaft axes (see the stresses in Figure 4.3). These strains would have had a big effect on the displacement at the level of the hip joint due to the large distance between shafts and the joint centre. Hence, manufacturing the shafts out of stiffer stainless steel was considered an excellent way to reduce the displacement of the hip centre under load, whilst maximising the use of cheaper and lighter aluminium alloy throughout the rest of the rig.

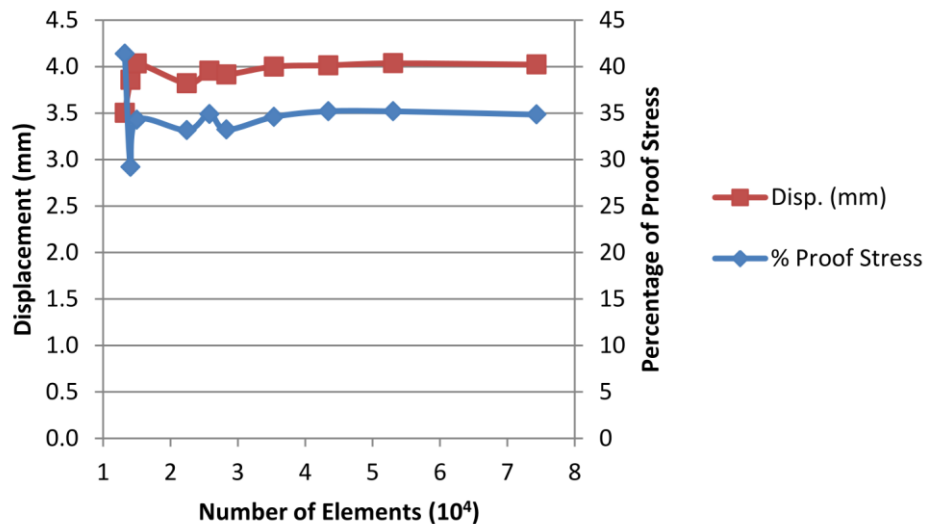


Figure 4.2 A convergence analysis for the finite element analysis mesh.

The load case examined was 1 kN with 364 N medial load and 25 Nm internal rotation torque. It can be seen that the mesh converged when the number of elements exceeded 45,000.

#### 4.3.3 The rig's capabilities

For loading in the absence of torque, it was found that the 1 kN load in isolation resulted in the highest von Mises stresses in the rig despite an increase in the total applied load when a medial component was included (Table 4.1). This was because the medial component of load provided a bending moment in the opposite direction to that of the 1 kN superior load on the superior-inferior set-up translation arm (which was the component that experienced the peak stresses).

In the absence of load, the stresses caused by internal and external rotation torques were identical (as expected for a linear elastic model), however internal rotation acted to increase stresses when a medial component of load was present, whereas external rotation decreased the maximum stress. This was because the internal rotation torques acted to increase the bending moment caused by the medial load whereas the external rotation torque acted to oppose it. Thus, only the internal rotation (worst case) results have been reported in Table 4.1.

For the load case used in chapters 6 and 7 the worst case peak stress was only 4 % of the yield and the resultant displacement of the hip joint centre only 0.4 mm (Table 4.1).

#### 4.3.4 Experimental validation

The mean ( $\pm$  S.D.) stiffness of the rig recorded during the three load cycles was  $300 \pm 5$  N/mm; a typical load-displacement graph is shown in Figure 4.5. Under 1 kN superior loading, the finite element model predicted a displacement in the y-direction of 3.7 mm and hence a superior-inferior stiffness of 270 N/mm.

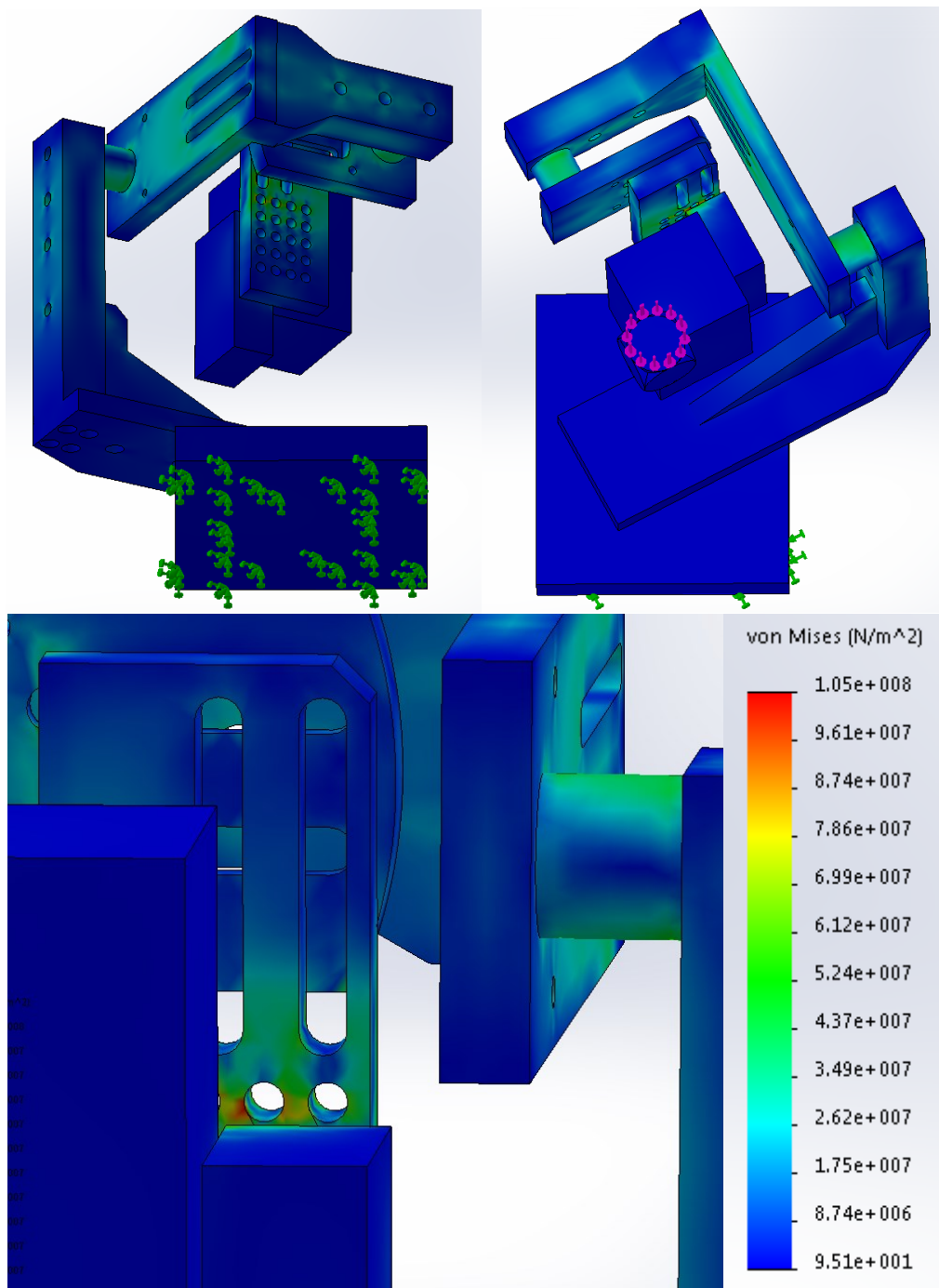


Figure 4.3 The von Mises stresses in the testing rig under 1 kN of compressive load applied at the level of the hip joint centre.

Top) different views showing the simplified rig. The stresses in the shafts were relatively high and were positioned far from the point of applied load and hence the strain in this region could cause large deflections at the hip joint centre. Bottom) a zoomed view of the superior-inferior set-up translation arm showing the peak stresses concentrated around the 8.5 mm holes. The peak stress was less than half that of the proof stress for 6082 T6 Aluminium Alloy bar (250 MPa) (Aalco-Metals-Ltd, 2013).

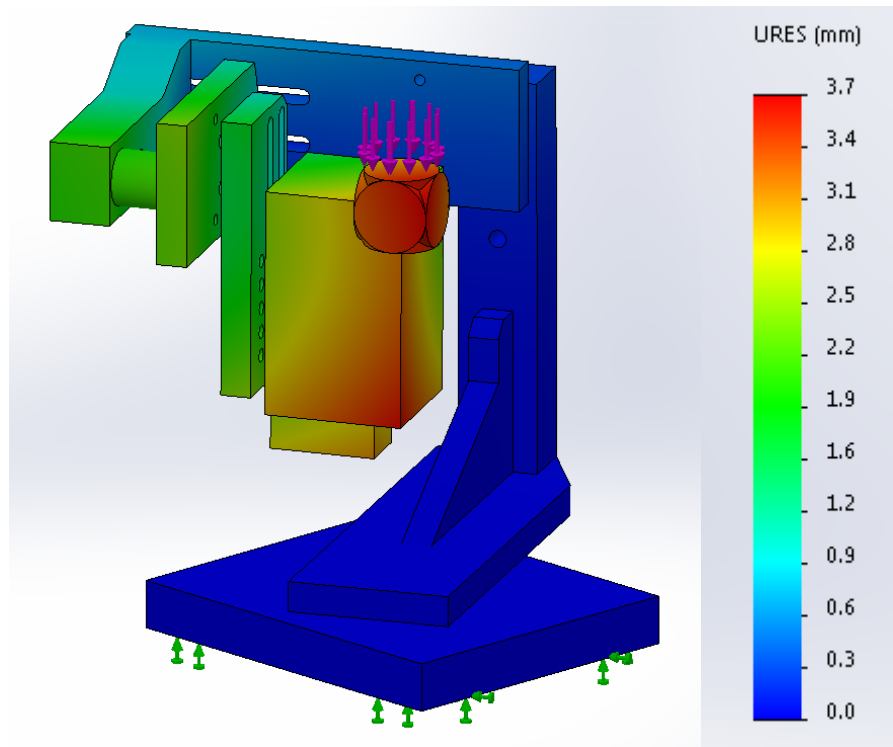


Figure 4.4 The resultant displacement of the rig under 1 kN vertical compressive load.

The rig has been deformed according to these displacements at a scale of 1:1. It can be seen the displacement at the hip joint was 3.7 mm.

#### 4.4 Discussion

##### 4.4.1 Most important finding

The most important result from this chapter was the development of a testing system that allows for clinically relevant testing of hip joint soft-tissues over a complete range of hip motion using the ISB system. The rig was capable of handling simultaneous application 1,000 N of superior load, 360 N medial load and 25 Nm of internal/external rotation torque with a safety factor of 2 and a maximum displacement of 4 mm. For the load case used in subsequent cadaveric tests, the maximum displacement was only 0.4 mm.

##### 4.4.2 Rig limitations

Whilst free to occur in response to an applied load, the rig was limited in that it could not control translations in the anterior/posterior/medial/lateral directions. What is more, loads applied by a hanging weight in the medial/lateral direction were only medial/lateral in the ISB system when in the neutral ab/adduction; as the hip ab/adducts, the Z-axis moves and hence the direction of the applied load was no longer in the ISB system. Finally the rig was limited in that there was a two-axes load-cell/position sensor for the ISB y-axis, however loads/translations/rotations/torques

Table 4.1 The aluminium rig's response to different load cases

<b>Superior Force (N)</b>	<b>Medial Force (N)</b>	<b>Internal Rotation Torque (Nm)</b>	<b>Max Stress (MPa)</b>	<b>% Proof Stress</b>	<b>Max Displacement (mm)</b>
0	0	25	19	7	0.6
1000	0	0	105	42	3.7
1000	364	0	79	32	3.8
1000	364	25	87	35	4.0
100*	36*	5*	10	4	0.4

\* this is the load case used for subsequent cadaveric testing

were not recorded by the rig and require manual reading. An optical tracking system could be combined with the system to record kinematics if needed.

#### 4.4.3 Testing method limitations

For both the finite analyses, and the in-vitro stiffness testing a pseudo-pelvis was used to isolate the rig's deflection from that of any specimens. It was assumed that these components had zero-deflection (and hence all deflection was due to the rig), however in reality these components will have had small deflections. The finite element analysis also relied on a number of assumptions to enable quick testing of multiple rig design iterations including using one material, excluding fasteners and assuming perfect mates between components. This latter assumption was reasonable given that a typical M8 bolt (the smallest size used) torqued to 12.5 Nm (the standard tightening torque) provides a minimum of 6.0 kN of axial clamping force (Tohnichi, 2012). A typical coefficient of friction between aluminium components (Mindivan et al., 2008), and aluminium and steel components (Panagopoulos et al., 2009) is  $>0.4$ , and hence this clamping force provides sufficient ( $>2.4$  kN) friction force to prevent any movement between components under the maximum load of 1 kN. However, if any movement did occur, then it would increase the displacement at the level of the hip joint.

Despite the simplifications used, the finite element model provided a good match for the experimental data, slightly under-predicting the stiffness in the superior-inferior direction. This means that the results from the finite element analysis provided an overestimate of displacements presented in Table 4.1 and thus represented a worst case. The discrepancy between the experimental and finite element results could be for three reasons: firstly, the manufacture rig had stainless steel shafts to stiffen it (a recommendation from the finite element results, see 4.3.2), but these steel shafts were not included in the finite element model which was modelled as a single component. Secondly, the experimental test did not include the superior-inferior set-up translation

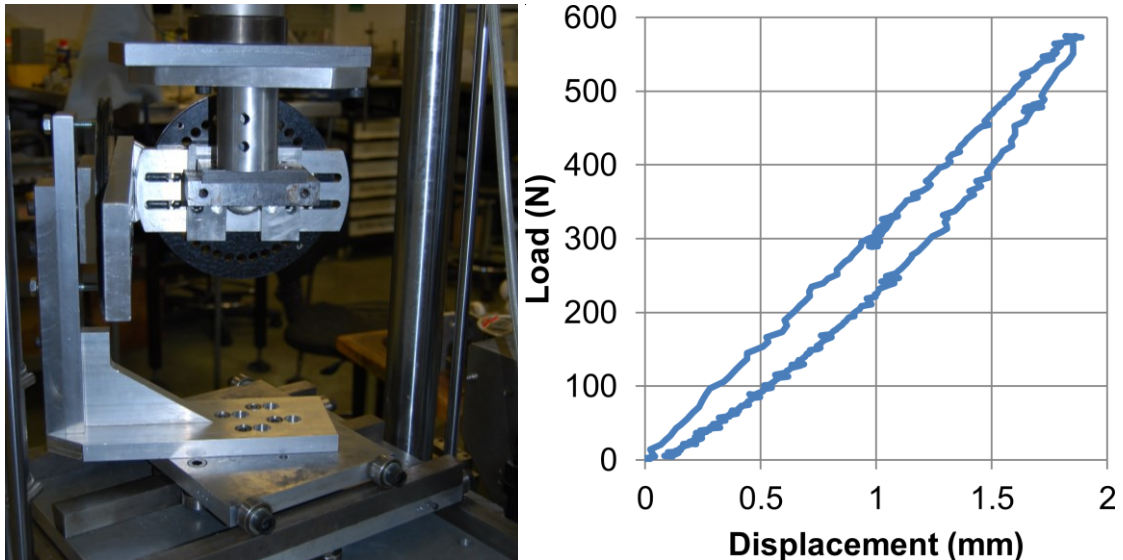


Figure 4.5 Experimental measurement of the rig's stiffness.

Left) A thick, steel, pseudo-pelvis mounted in the testing rig to measure the load-deflection curve of the testing rig. Right) a typical load deflection curve from the test (raw un-filtered data).

arm so that the load could be applied at the level of the hip joint centre; however, this component was found to have the highest strains. The effect of these strains is likely less than that of the shafts as the component is considerably closer to the hip joint centre. Finally, no screws/bolts/nuts/pins were used in the finite element model, instead modelling the holes as empty. This can only act to decrease the performance of the rig as the fasteners would add material and hence stiffen the rig.

#### 4.4.4 Comparison to other work

Hip joint testing rigs designs from other institutions have varied considerably: at one extreme authors have simply clamped the pelvis to a work bench and moved the femur by hand (Safran et al., 2011); this technique was similar to a clinical evaluation of a hip joint. Repeatability of manual tests such as this have been improved with use of a goniometer (Martin et al., 2008) to measure joint angles, an optical tracking system to record angles and translations (Lopomo et al., 2010; Ng et al., 2011; Safran et al., 2013; Signorelli et al., 2013) and a force/torque sensor to record applied loads/torques (Incavo et al., 2011). At the other extreme, robot testing facilities have been used which apply loads/torques, or fix displacements/rotations in all six degrees-of-freedom (Colbrunn et al., 2013; Smith et al., 2014). The rig system developed in this chapter was designed in preference to using a robotic system for two reasons: firstly, robotic testing can be slow typically taking 5-10mins per test (Athwal et al., 2014), however, a single test in the servo-hydraulic machine using this rig system took as little as 10 s. This speed advantage was considered useful for the planned cadaveric tests (chapters 6 and 7) because a short cycle time would allow for more measurements to be taken



## CHAPTER 4

before the specimen decomposes (after approximately 48hrs). Secondly, the development and validation of control protocols for a six-degrees-of-freedom robotic system would have taken a long time and required comparison against known data. Thus, a rig system as developed in this chapter would be needed to collect baseline data which could then be used to validate the robotic system; however appropriate data for the hip did not exist.

A number of other test rigs have also been designed with varying complexity levels between simple manual tests and robotic systems. These rigs have allowed for specification of fixed angles of rotation/torques in two (Sioen et al., 2002; Myers et al., 2011) or three (Delp et al., 1999; Clyburn et al., 2003; Crawford et al., 2007; Dy et al., 2008; Elkins et al., 2011b) rotary degrees-of-freedom without application of loads or torques. They have also been designed to apply specific rotations angles/torques in three degrees of freedom with axial loading (Crawford et al., 2007; Dy et al., 2008; Elkins et al., 2011b; Dwyer et al., 2014; Dwyer et al., 2015; Lee et al., 2015), or with a representative hip joint reaction force (Burroughs et al., 2005; Anderson et al., 2008; Smith et al., 2011), or even with individual muscle loads (Bartz et al., 2000). The rig designed in this experiment offers more functionality than most of the rigs described in this paragraph except perhaps for a comparable infra-red/material-testing-machine system used by Prof Noble's research group (Crawford et al., 2007; Dy et al., 2008; Incavo et al., 2011; Dwyer et al., 2014; Dwyer et al., 2015). This system allowed for the joint movements to be reconstructed in a 3D model retrospectively and consequently allowed for greater analysis of joint translations and movements. However, the testing rig in this chapter was designed to have a larger working volume to allow for investigation throughout the range of hip motion. The rotary axes were also designed to allow application of pure moments through use of the servo-hydraulic machine's rotating axis or a pulley with a hanging-weights couple. These design features were considered advantageous because the magnitude of the applied torque would be constant throughout testing and independent of the reference point: rig rotation would not change the lever arm of the applied torque and the hip would also be free to rotate about its natural centre without affecting the magnitude of the applied torque.

### *4.4.5 Conclusion*

The custom built six-degrees-of-freedom testing system designed in this chapter provides an appropriate testing rig for hip joints in the ISB system. For a load case of 110 N force angled 20°medially/superiorly the rig deflected a maximum of 0.4 mm when an internal/external rotation torque of 5 Nm was applied. This makes it an

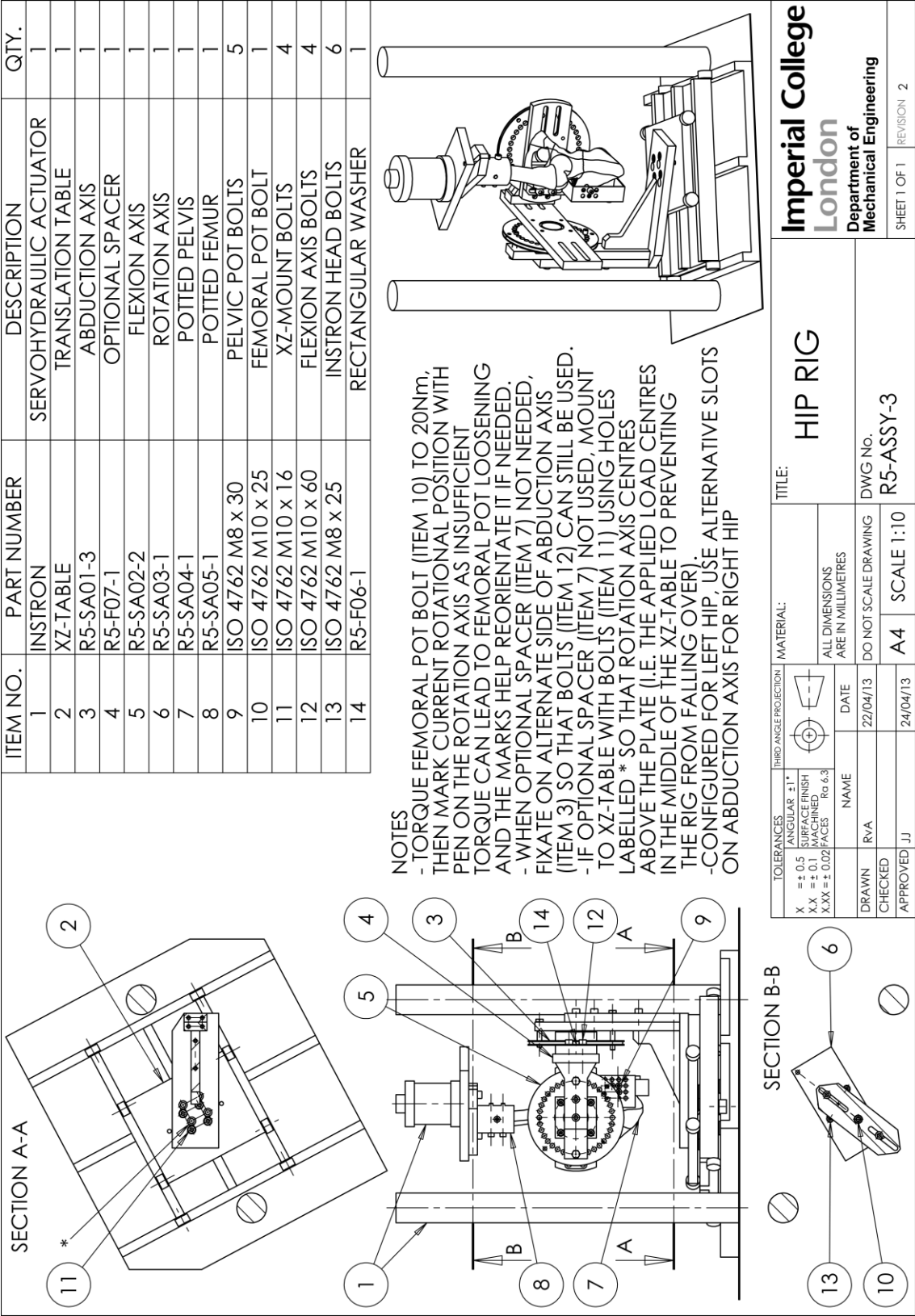


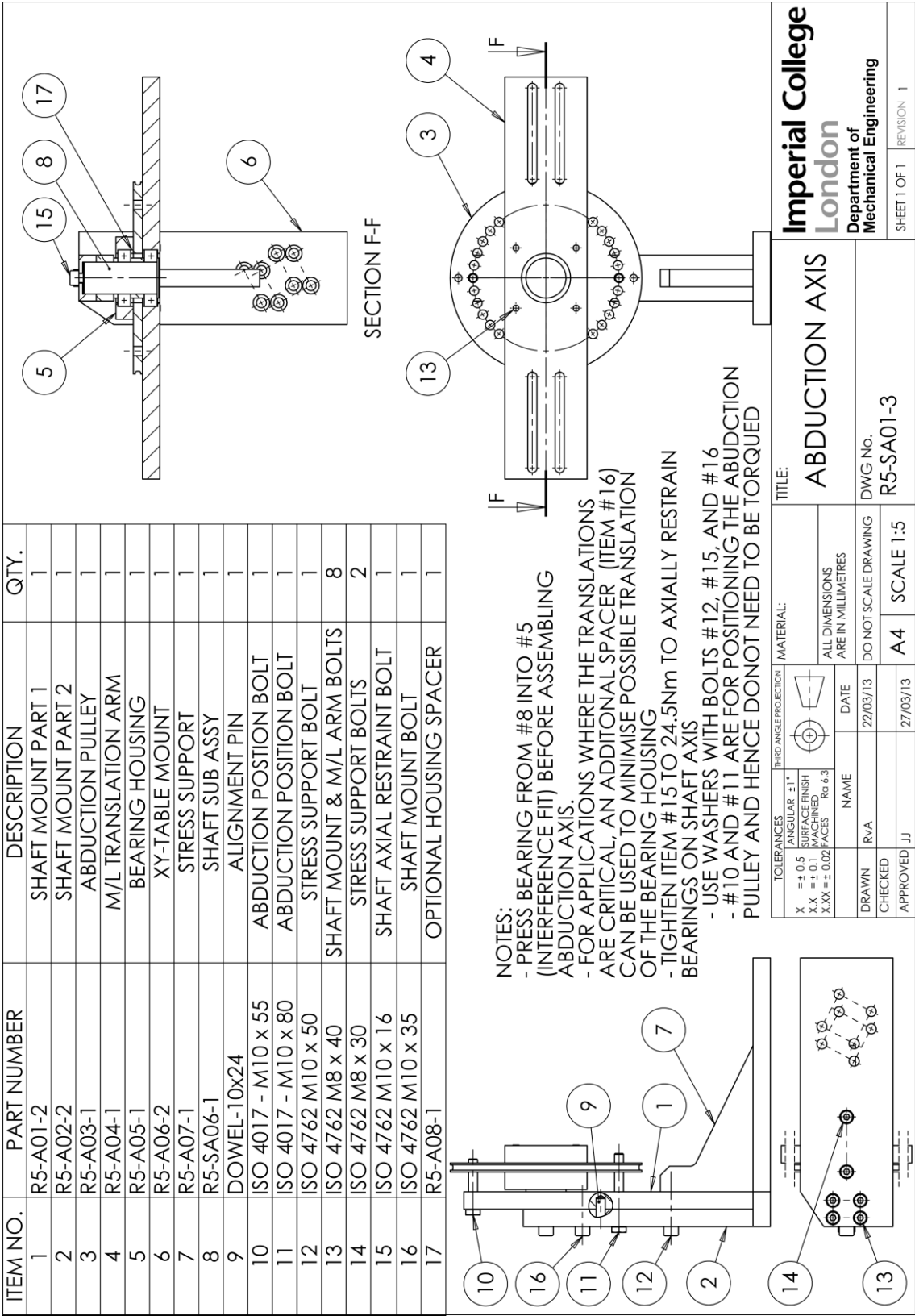
appropriate rig for testing the contributions of soft-tissue under physiological loading. The testing system is further validated in the next chapter, and is used extensively to test the capsular ligaments in chapters 5 and 6.

### **4.5 Acknowledgements**

Thank you to Philip Wilson for manufacturing the rig.

4.6 Assembly Drawings





SECTION B-B

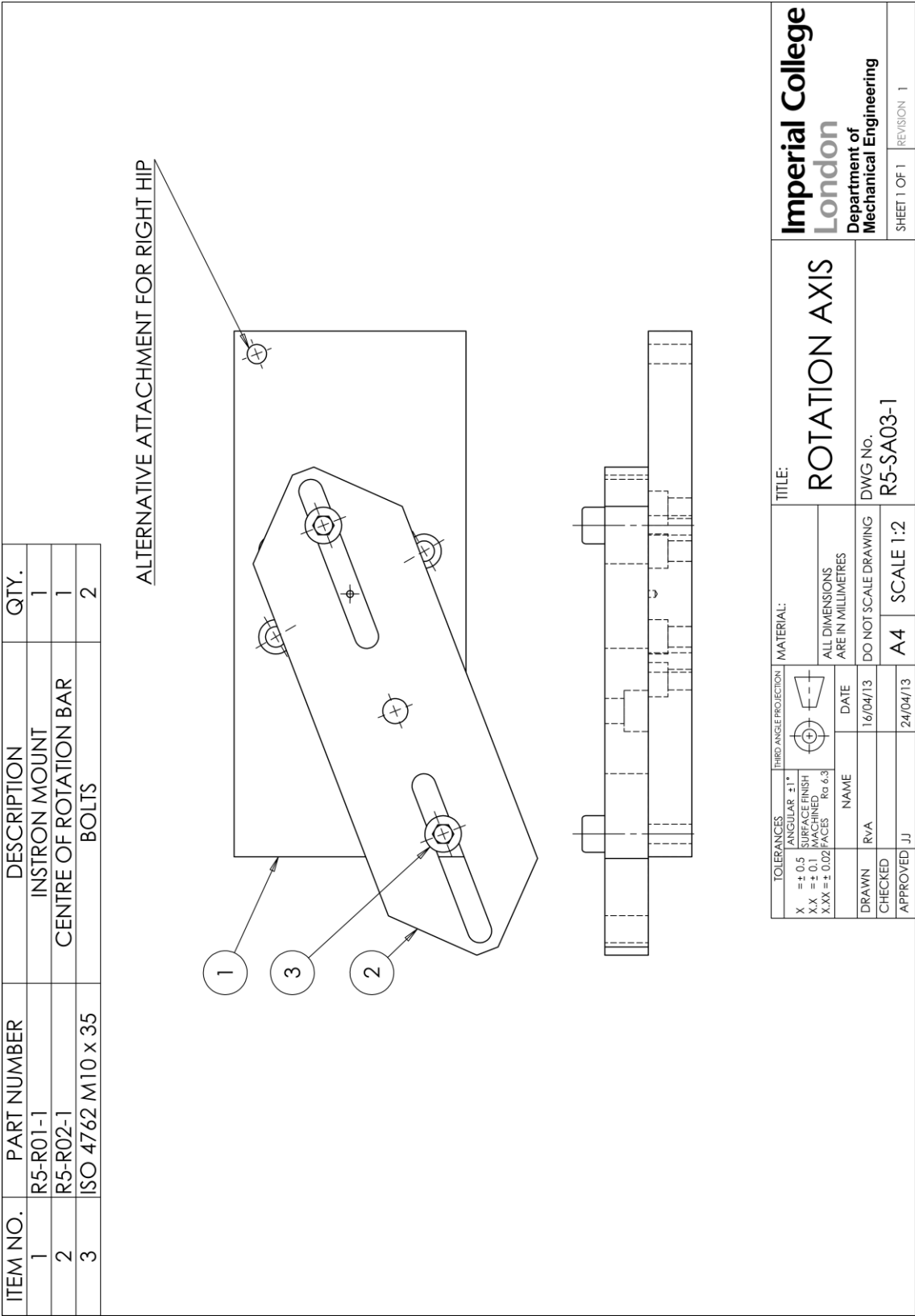
ITEM NO.	PART NUMBER	DESCRIPTION	QTY.
1	R5-F01-1	SHAFT MOUNT PART 1	1
2	R5-F02-1	SHAFT MOUNT PART 2	1
3	R5-F03-1	FLEXION PULLEY	1
4	R5-F04-1	A/P TRANSLATION ARM	1
5	R5-F06-1	RECTANGULAR WASHER	2
6	DOWEL-10x24	ALIGNMENT PIN	1
7	R5-SA06-1	SHAFT SUB ASSY	1
8	R5-A05-1	BEARING HOUSING	1
9	ISO 4762 M10 x 35	SHAFT MOUNT & S/I ARM BOLTS	5
10	ISO 4762 M8 x 40	A/P ARM BOLTS	4
11	ISO 4762 M10 x 16	SHAFT AXIAL RESTRAINT BOLT	1
12	ISO - 4034 - M10	S/I ARM POSITIONING NUT	4
13	ISO 4017 - M10 x 55	FLEXION POSITION BOLT	1
14	ISO 4017 - M10 x 70	FLEXION POSITION BOLT	1
15	R5-F05-1	S/I ARM	1
16	R5-A08-1	OPTIONAL HOUSING SPACER	1

NOTES:

- \* THIS ANGLE DIRECTLY AFFECTS HOW WELL THE RIG IMPLEMENTS THE ISB COORDINATE SYSTEM - CAN BE SET USING SET SQUARE TO ENSURE SUPERIOR-INFERIOR IS PERPENDICULAR TO ANTERIOR-POSTERIOR
- PRESS BEARING FROM #7 INTO #5 (INTERFERENCEFIT) BEFORE ASSEMBLING FLEXION AXIS.
- FOR APPLICATIONS WHERE THE TRANSLATIONS ARE CRITICAL, AN ADDITIONAL SPACER (ITEM #16) CAN BE USED TO MINIMISE POSSIBLE TRANSLATION OF THE BEARING HOUSING
- TIGHTEN 11 TO AXIALLY RESTRAIN BEARINGS ON SHAFT AXIS
- USE WASHERS WITH BOLTS #9 AND #11
- #13 AND #14 ARE FOR POSITIONING THE FLEXION PULLEY AND HENCE DO NOT NEED TO BE TORQUED
- CURRENT CONFIGURATION FOR LEFT HIP, USE ALTERNATIVE SLOTS ON A/P ARM (ITEM #4) FOR RIGHT HIP ENSURING THAT THE CUT AWAY CORNER ON THE S/I ARM(WHERE ARROW #15 POINTS) IS POSTERIOR.

TOLERANCES		THIRD ANGLE PROJECTION	MATERIAL:	TITLE:	
X	± 0.5	ANGULAR ±1°	ALL DIMENSIONS ARE IN MILLIMETRES	FLEXION AXIS	
XX	± 0.1	SURFACE FINISH			
XXX	± 0.02	MACHINED FACES			
DRAWN	RVA	NAME	DATE	DWG No.	
CHECKED			07/12/12	R5-SA02-2	
APPROVED	JJ		12/12/12	DO NOT SCALE DRAWING	REVISION 1
A4			SCALE 1:3		

Imperial College  
London  
Department of  
Mechanical Engineering



ITEM NO.	PART NUMBER	DESCRIPTION	QTY.
1	PELVIS		1
2	R5-P02-1	PELVIC POT	1
3	ISO 4762 M8 x 40	X-AXIS BOLTS	2
4	ISO 4762 M8 x 70	Z-AXIS BOLT	1
5	ISO 4762 M8 x 12	TEMP BOLTS	5
6	ISO - 4036 - M8	THIN NUT	5
7	PMMA	BONE CEMENT	1
8	ISO 4762 M8 x 16	TEMP BOLTS	2
9	ISO - 4034 - M8	NUT	4

SECTION A-A

SECTION B-B

- USE PELVIS MOUNTING JIG TO PREPARE HEMI-PELVIS

- ALL PARTS THAT CONTACT CEMENT SHOULD BE COVERED IN A LIGHT LAYER OF GREASE SO THAT THE PARTS CAN BE REUSED BY DISASSEMBLING THE CEMENTED UNIT (NOTE THAT BOLTS WILL AUTOMATICALLY CREATE A MATING THREAD IN THE BONE CEMENT)

- TIGHTEN ALL NUTS AND FILL UNUSED HOLES WITH TISSUE PAPER OR EQUIVALENT BEFORE FILLING ENTIRE PELVIS POT WITH BONE CEMENT

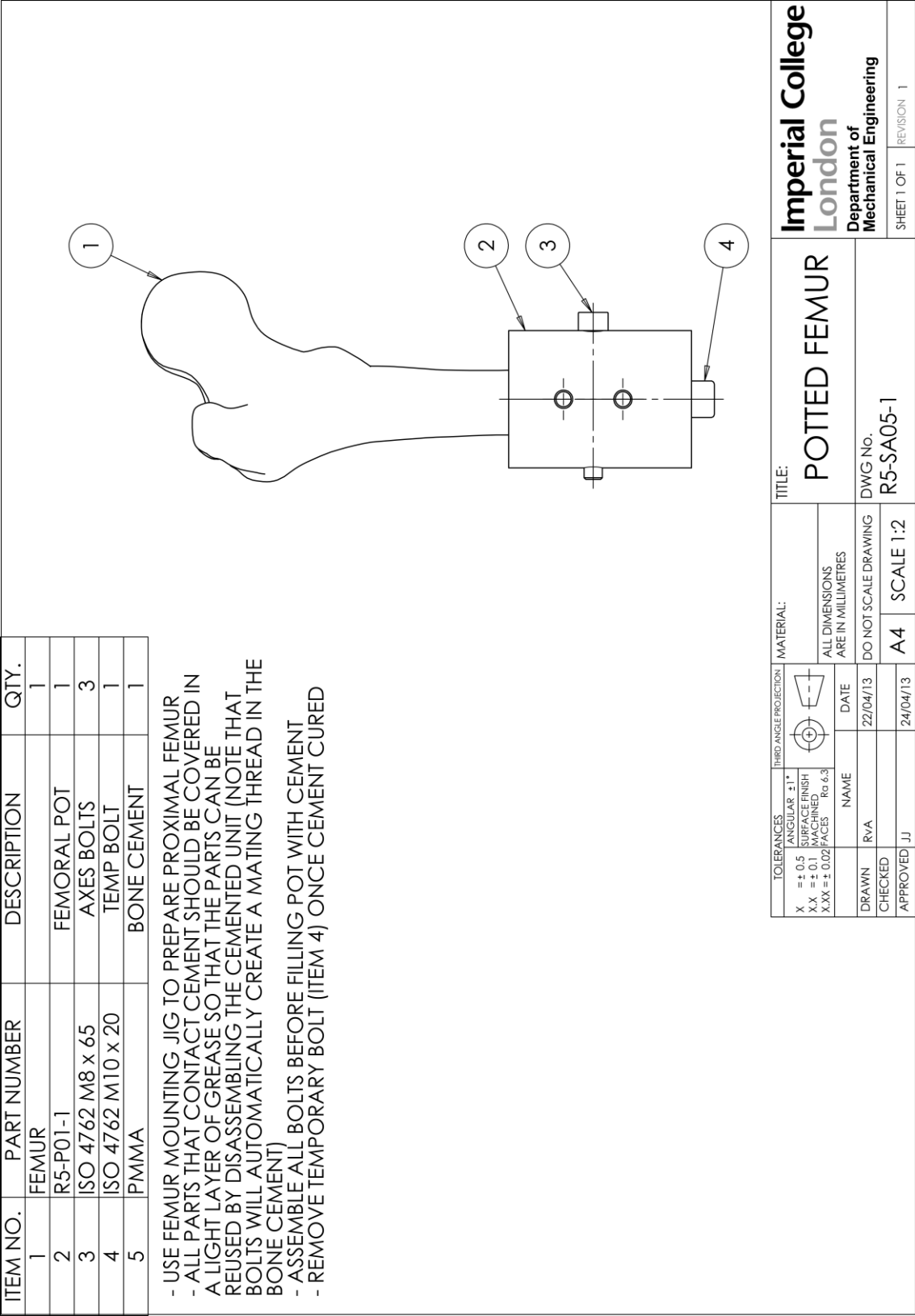
- THICK AND THIN NUTS (ITEMS 6&7) ARE INTERCHANGEABLE - FOR ITEM NUMBERS 5, 6 AND 7: IF EITHER NUT, OR BOLT CANNOT BE TIGHTENED DUE TO CLASH WITH BONE, EITHER MAKE A SMALL BONE RESECTION OR USE A SMALLER NUT/BOLT, OR IN WORST CASE OMIT THE NUT/BOLT ENTIRELY.

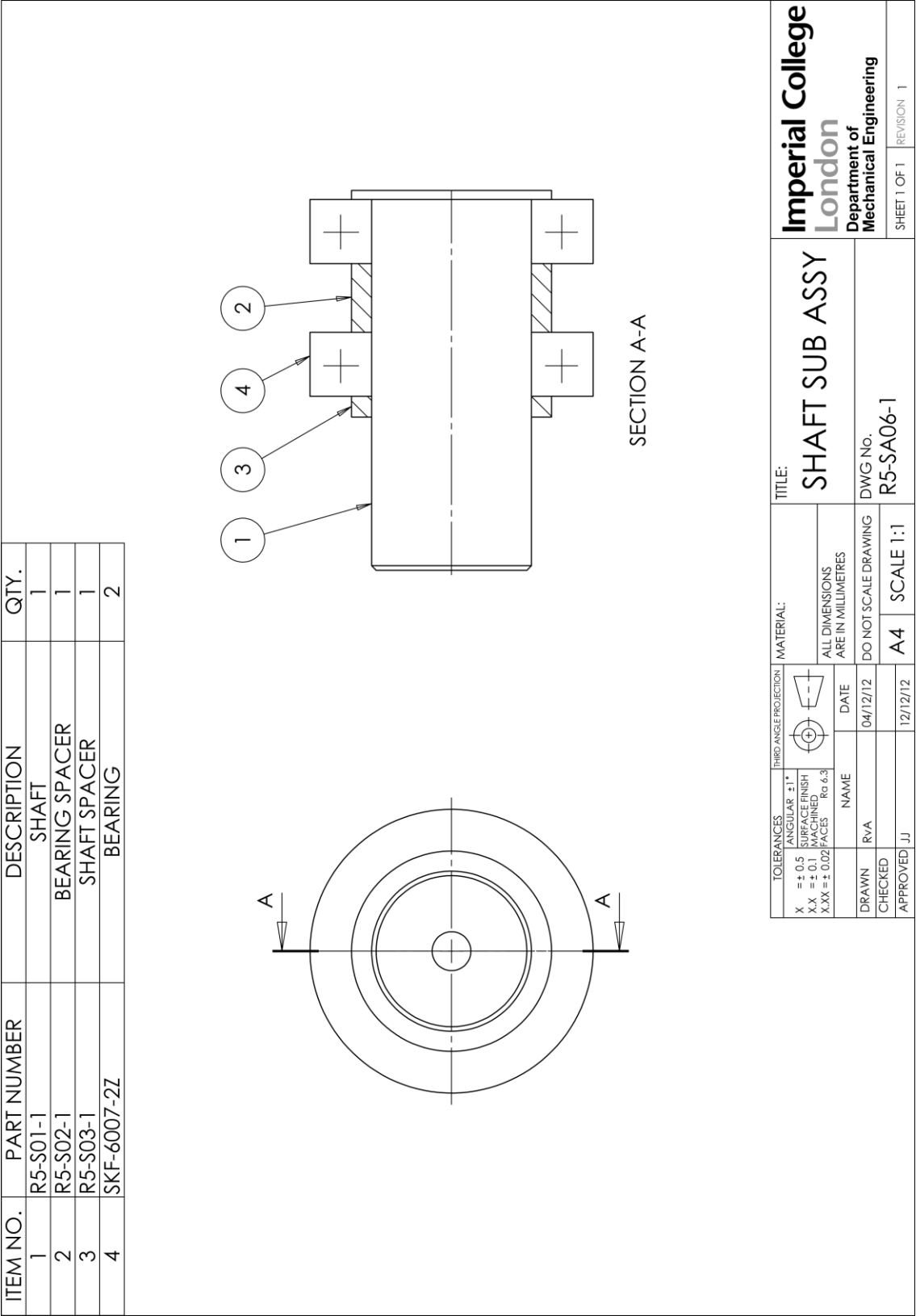
- REMOVE TEMPORARY BOLTS (ITEM 5 & 8) ONCE CEMENT CURED. THE RESULTING HOLES ARE FOR RIG ATTACHMENT.

TOLERANCES	THIRD ANGLE PROJECTION	MATERIAL:	TITLE:
X: $\pm 0.5$	ANGULAR $\pm 1^\circ$	ALL DIMENSIONS ARE IN MILLIMETRES	POTTED PELVIS
X.X: $\pm 0.1$	SURFACE FINISH		
X.XX: $\pm 0.02$	MACHINED FACES Rg 6.3		
DRAWN R/vA	NAME	DO NOT SCALE DRAWING	DWG No. R5-SA04-1
CHECKED	DATE	A4	SCALE 1:2
APPROVED JJ	22/04/13	24/04/13	

**Imperial College**  
**London**  
**Department of**  
**Mechanical Engineering**

SHEET 1 OF 1    REVISION 2







## **5 A low-cost repeatable solution for aligning hip joint specimens in a known coordinate system in-vitro**

In recent years, large numbers of hip biomechanics studies have been published using a variety of innovative in-vitro techniques and the success of these studies is driving the field of orthopaedics forwards. However many do not fully define a coordinate system which makes the quantification of absolute values unreliable, makes comparisons between studies difficult and means that the methods cannot be repeated. The aim of this study was to develop a quick, low-cost solution for repeatable alignment of hemi-pelves with proximal femora in the established ISB coordinate system to encourage use of a properly defined, clinically meaningful coordinate system, when testing in-vitro. Two drilling jigs were designed, manufactured and tested with 4 synthetic full-pelves paired with 8 full-length femora. Seven anatomical landmarks were digitised in the ISB coordinate system before specimens were prepared using the drilling jigs. The resulting 8 hemi-pelves and proximal femora were mounted in bone pots using the drilled features and the anatomical landmarks were re-digitised relative to mechanical features of the pots. The misalignment of the potted specimens compared to the original ISB reference system was calculated using singular value decomposition. The mean misalignment was found to be less than  $1.5^{\circ}$  in all rotation directions (flexion/extension, ab/adduction and internal/external rotation) for both the pelves and femora; this equates to less than 2.5 % of a normal range of hip motion. Engineering drawings are provided to allow users to replicate/modify these jigs for use in other laboratories.

### 5.1 Introduction

There has been a surge in development of innovative in-vitro testing methods to answer challenging research questions about hip joint biomechanics. These methods include: digital image correlation (Dickinson et al., 2011b; Dickinson et al., 2012), roentgen stereophotogrammetric analysis (Dy et al., 2008; Myers et al., 2011), digital variable resistance transducers (Safran et al., 2011; Smith et al., 2011), real-time contact-pressure measurement (Lee et al., 2015), fluid infusion devices (Cadet et al., 2012; Dwyer et al., 2014), accurate optical tracking motion analysis (Lopomo et al., 2010; Safran et al., 2013; Signorelli et al., 2013), 3D digital reconstructions combining CT scans and motion tracking (Crawford et al., 2007; Incavo et al., 2011; Dwyer et al., 2014), combined use of in-vitro and finite element modelling (Anderson et al., 2008; Dickinson et al., 2011b; Elkins et al., 2011b), custom built rigs in servo-hydraulic actuators/materials testing machines (Ito et al., 2009; Elkins et al., 2011b; Dickinson et al., 2012; Song et al., 2012) and six-degrees-of-freedom robotic load/torque actuators (Colbrunn et al., 2013; Smith et al., 2014). Such variation in testing methodology should be encouraged as it not only allows new hypotheses to be tested thus providing insight into the efficacy of different surgical interventions, but also importantly it prevents systematic bias that could result from using the same methodology with the same limitations. However, so that these diverse experimental methods can be comprehensively reviewed and compared between experiments, it is essential that results are published in a repeatable and well-defined coordinate system. This also helps give the in-vitro model contextual meaning to a clinical scenario.

A repeatable hip coordinate system requires definition of a pelvic and femoral body reference frame, the axes of movement for these reference frames, and a neutral starting point. However, many research studies fail to report or reference a full coordinate system (including more than half of the studies described in the opening paragraph). This is not a recent problem: two decades ago, an extensive critical review of in-vitro testing methods for studying hip prosthesis found that 95 % of studies did not fully define a reference frame for the femur (Cristofolini, 1997).

The ISB have published a well-defined coordinate system that reflects a clinical understanding of hip joint movements and relies on landmarks which are easy to identify non-invasively (Wu et al., 2002). Consequently it has been widely adopted in gait analysis and related musculoskeletal modelling research, however, implementation of it in an in-vitro setting can be impractical: identifying the femoral head centre is challenging and additionally a full-pelvis/full-length femur can be too large for the available working volume of test rigs/materials-testing-machines/robotic actuators.

Indeed, most authors prepare specimens such that they test with hemi-pelves or proximal femora only mounted into bone pots using a curing putty/cement, bolt/screws or both (Crawford et al., 2007; Anderson et al., 2008; Dy et al., 2008; Ito et al., 2009; Dickinson et al., 2011b; Elkins et al., 2011b; Myers et al., 2011; Smith et al., 2011; Dickinson et al., 2012; Song et al., 2012; Colbrunn et al., 2013; Dwyer et al., 2014; Smith et al., 2014; Lee et al., 2015). Thus, the aim of this study is to quantify the accuracy of using low-cost drilling jigs to align hemipelves with proximal femora in bone pots whilst preserving the ISB reference frame so that a repeatable, clinically meaningful coordinate system can be more widely adopted for in-vitro hip research.

## 5.2 Materials and Method

### 5.2.1 Drilling jigs

Two drilling jigs (Figure 5.1) were designed such that they could be manufactured using basic workshop machinery (milling machine/lathe) from a single extrusion of aluminium alloy (low cost). They are sized such that any pelvis/femur within three standard deviations of the mean size (Yoshioka et al., 1987; Seidel et al., 1995) will fit in the jig and that they only need one pair of hands to operate. Aside from the jigs, the only equipment needed to use them is some g-clamps to fixate them rigidly to a workbench and a hand power drill with Ø8 mm drill-bits.

Assembly drawings are included at the end of the chapter (from page 102) and individual component drawings can be found in appendix A5.1 (from page 221). The bone potting process was detailed in the assembly drawings from the previous chapter (assembly - section 4.6 from page 84, and components - appendix A4, from page 207); an additional bone pot designs is also included in appendix A5.1 (from page 221). These bone pots attach at the posterior iliac crest/femoral shaft to mimic normal pelvic/knee boundary conditions to encourage normal load transfer within the bone (from the hip to the sacroiliac/knee joint). These pots have machined features that allow rigid attachment to a test rig in a known orientation. Therefore, the objective for the drilling jigs is to orientate the specimens into the bone pots such that the pot features can be related directly to the ISB reference frame.

### 5.2.2 Intact to potted data collection

8 solid foam femora and 4 solid foam pelvises, 2 each of male/female left/right hemipelvis/femora (Sawbone AB, Sweden, model numbers: #1120, #1120-20, #1129, #1129-21, #1301, #1302) were used to test the accuracy of using the drilling jigs. For each bone model, Ø3.5x10 mm screws were inserted into anatomical landmarks as

detailed in Table 5.1. The crossheads of these screws provide a repeatable point for a Polaris optical tracking system's (Northern Digital Inc., Ontario, Canada) digital probe. The screws were positioned such that they could be used to construct the ISB reference frames for the intact pelvis and femora, as well as providing seven repeatable landmarks that cover the extremes of the surface of the bones and would be available for re-calculating the pose of the bones after potting them; this configuration was used as gait analysis research showed that pose estimation was greatly improve by using more than 4 markers with the largest possible spatial distribution (Challis, 1995).

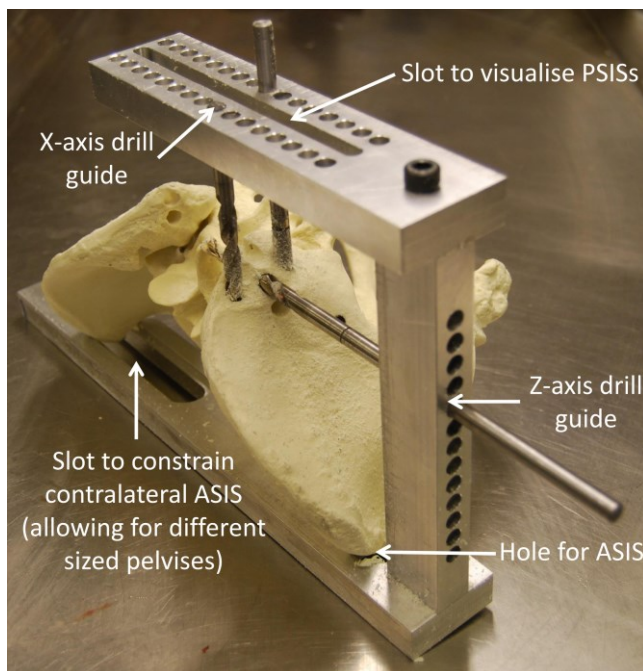


Figure 5.1 The pelvic (left) and femoral (bottom) drilling jigs to prepare X/x and Z/z axes holes in the pelvis/femur respectively.

For the pelvic drilling guide, the anterior superior iliac spines (ASISs) are constrained in a hole whilst the pelvis is rotated until the posterior superior iliac spines (PSISs) can be visualised through the slot positioned directly above the ASISs. For the femoral drilling guide the epicondyles are clamped and aligned with the femoral head centre. The femur can be supported by rigidly clamping the pelvis (shown) or in the absence of the pelvis by supporting the femoral head directly.

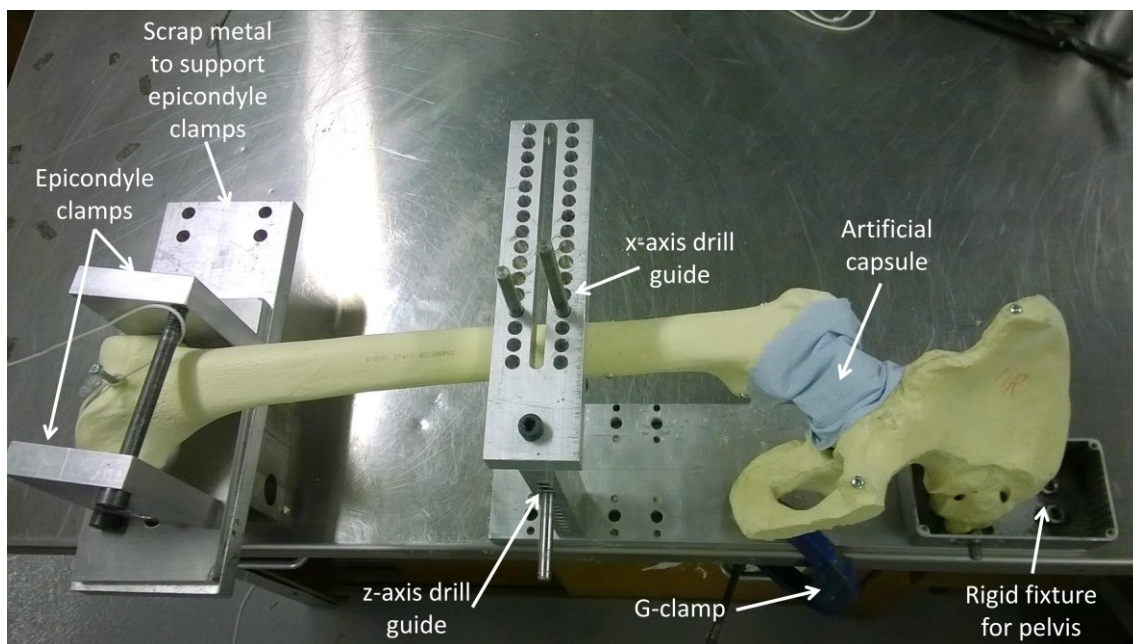


Table 5.1 Anatomical locations for screw placement

Body	For ISB Reference Frame	Repeatable landmarks (for comparing intact and potted)
Pelvis		anterior superior iliac spine
		anterior inferior iliac spine
	left anterior superior iliac spine	pubic tubercle
	right anterior superior iliac spine	ischial tuberosity
	left posterior superior iliac spine	posterior acetabular rim
	right posterior superior iliac spine	superior iliac spine
		acetabulum centre*
Femur		insertion of ligamentum teres
		superior tip of greater trochanter
	medial femoral epicondyle	lateral base of greater trochanter
	lateral femoral epicondyle	lesser trochanter
		medial mid-shaft
	femoral head centre*	lateral mid-shaft
		femoral head centre*

\*these centre points were not pinpointed with screws but were found from a least-squares sphere-fit of >100 digitised points on the surface of the acetabulum/femoral head

All screws for the intact bones were then digitised using the optical tracking system three times. Between repeats the bones were re-orientated in the field of view of the optical tracking system to prevent systematic measurement errors of the digitised points. The synthetic bones were paired to make a hip joint and covered with an artificial hip capsule to prevent direct visualisation of the femoral head (Figure 5.1). The hips were prepared with the drilling jigs before the bisecting the pelves and transecting the femora at the mid-shaft. The artificial capsule was removed and the prepared hemi-pelves and proximal femora were then inserted into the bone pots. For each potted bone, the pot's faces as well as six anterior/posterior, medial/lateral and superior/inferior reference points were then digitised before the seven repeatable landmarks were re-digitised. Again this was repeated three times rotating the potted specimen in the optical tracker's field of view between repeats.

### 5.2.3 Intact to potted calculations

For each repeat within each specimen, the axes of the ISB/pot's reference frame was calculated in MatLab (version 2011b, The MathWorks, Inc., Texas, USA) based on either the intact specimen's/pot's digitised features. Then the repeatable landmarks on the synthetic bones were transformed into the ISB/pot's reference frame before being averaged across the three intact/potted repeats respectively. Appendix A5.2 (page 226) describe the procedure used to digitise the intact and potted bones with images and details the calculations used to define the coordinate system axes. Appendix A5.3

(page 231) then details how these coordinate system axes were used to transform the data into the relevant reference frame.

The misalignment of each body was then quantified as the hip joint rotation away from the ISB-neutral position that would result in the bones new orientation relative to the pot's metal features; if perfectly mounted in the pot, these angles would be zero and hence the pot's reference frame would be equivalent to the ISB body reference frame. The hip joint rotation matrix was calculated from the repeatable landmarks using a well-established singular value decomposition technique (Arun et al., 1987; Challis, 1995) and this was decomposed into angles of flexion/adduction/rotation using established gait analysis equations (Cappozzo et al., 2005). For femoral misalignment calculations, the pelvic body reference frame was treated as constant, and vice-versa. Appendix A5.4 (from page 232) details how this calculation was performed including: a clear definition of the misalignment problem (A5.4.1), a brief literature review for solving an attitude determine problem (A5.4.2), the singular value decomposition calculation (A5.4.3), how to interpret a joint rotation matrix as Euler angles (A5.4.4) and a guide for the practical implementation of the solution (A5.4.5).

### *5.2.4 Quantification of additional error from pot to testing rig*

For the pelvic fixture presented in chapter 4, there are 12/13 connections between components (depending on whether an optional spacer is used) from the pelvic pot to the base of the rig which attaches to the servo-hydraulic machine's x-z table. Therefore to quantify the additional error caused when mounting the pelvis pot into the rig (and thus the error from intact to rig) the optical tracking system was again used to digitise the rig's rotating axis as well as the seven repeatable landmarks on the pelvis after mounting the pot onto the rig. Again this was repeated three times rotating the rig in the optical tracker's field of view between repeats.

For the femoral fixture however, there are only two components between the pot and the mounting bracket for the servo-hydraulic materials-testing-machine and both are manufactured from EN 6082 aluminium alloy 4 x 3/4" (width x thickness) flat bar (A4.1, page 207). Thus, only the flatness tolerance of the flat bar could cause further misalignment of the femoral reference frame and so the maximum possible additional misalignment created when attaching the pot to the servo-hydraulic machine was calculated from this tolerance.

### 5.3 Results

For the pelvis, the mean  $\pm$  standard deviation misalignment after using the drilling jig to mount the specimens into a bone pot in the ISB pelvic reference frame was:  $1.5 \pm 1.6^\circ$  adduction,  $0.5 \pm 1.1^\circ$  internal rotation and  $-0.6 \pm 1.7^\circ$  flexion. The misalignment between the pot's and the rig's pelvis reference frame was:  $0.5 \pm 0.7^\circ$  adduction,  $1.1 \pm 1.3^\circ$  internal rotation and  $-0.1 \pm 1.8^\circ$  flexion. The total misalignment from an intact pelvis, to the rig's representation of the pelvic reference frame including rig tolerances and the pelvic potting process was:  $1.0 \pm 1.6^\circ$  adduction,  $1.5 \pm 1.2^\circ$  internal rotation and  $-0.7 \pm 3.0^\circ$  flexion. The range of misalignment and the absolute misalignment as a percentage of a normal adult range of hip motion for these different stages of mounting the pelvis are shown in Figure 5.2-Figure 5.4.

For the femoral reference frame, the misalignment was  $-0.7 \pm 1.1^\circ$  adduction,  $-0.4 \pm 1.0^\circ$  internal rotation, and  $0.4 \pm 1.5^\circ$  flexion (Figure 5.5). The engineering standard for aluminium alloy flat bar, BS EN 755-2:2013, states that the thickness tolerance of the flat bar used for the test rig components is  $\pm 0.45$  mm. (ThyssenKrupp-Materials, 2013; Aalco-Metals-Ltd, 2014a). This equates to a maximum angular deviation per component of  $0.51^\circ$ . Therefore, assuming the absolute worst case (that the bar is at the tolerance limit and the misalignment for both bars is compounded rather than cancelled out) then a total of  $1.0^\circ$  further misalignment could occur when mounting the femoral pot to the servo-hydraulic machine using the two components.

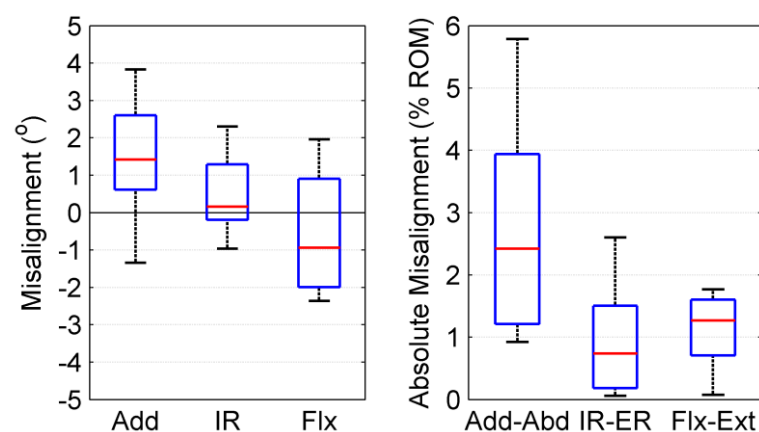


Figure 5.2 Box plots of pelvic misalignment after using the drilling jig method to pot the pelvis in the ISB reference frame in terms of hip adduction/abduction (Add), internal/external rotation (IR), and flexion/extension (Flx)

The whiskers are equal to the range of the data. A) misalignment of the potted pelvis (adduction, internal rotation and flexion are treated as the positive direction) B) the absolute misalignment of the potted pelvis as a percentage of the normal range of hip motion for an adult male (Boone and Azen, 1979).

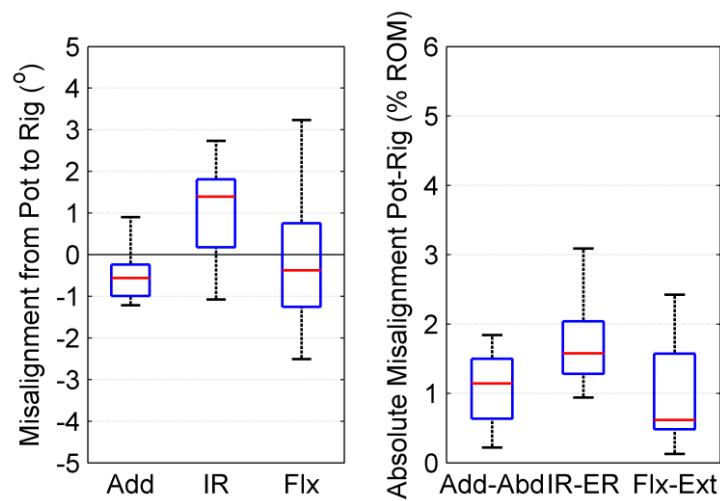


Figure 5.3 Box plots of pelvic misalignment caused when mounting the pelvic pot into the test rig in terms of hip adduction/abduction (Add), internal/external rotation (IR), and flexion/extension (Flx).

The whiskers indicate range of the data. A) misalignment of the pelvis (adduction, internal rotation and flexion are treated as the positive direction) B) the absolute misalignment as a percentage of the normal range of hip motion for an adult male (Boone and Azen, 1979).

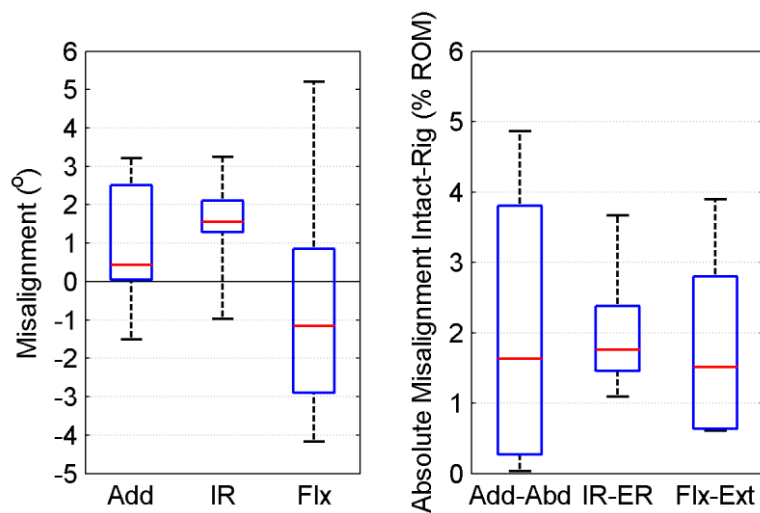


Figure 5.4 Box plots of pelvic misalignment when using the complete system including the drilling jigs and the test rig compared to an intact ISB reference frame in terms of hip adduction/abduction (Add), internal/external rotation (IR), and flexion/extension (Flx)

The whiskers indicate range of the data. A) misalignment of the hemipelvis (adduction, internal rotation and flexion are treated as the positive direction) B) the absolute misalignment of the hemipelvis as a percentage of the normal range of hip motion for an adult male (Boone and Azen, 1979).



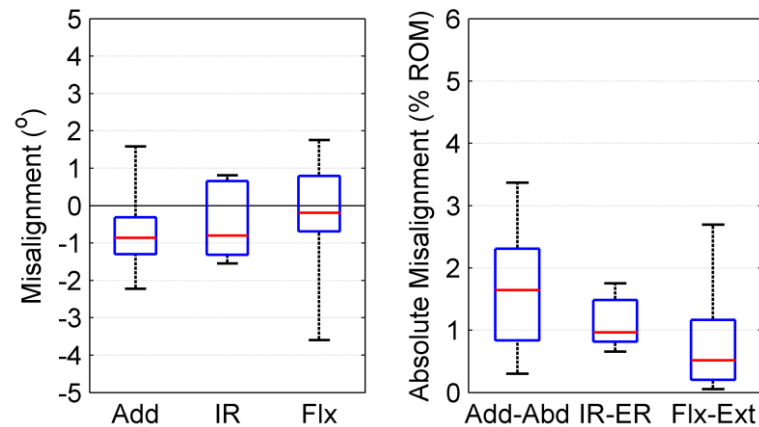


Figure 5.5 Box plots of femoral misalignment after using the drilling jig method to pot the pelves in the ISB reference frame in terms of hip adduction/abduction (Add), internal/external rotation (IR), and flexion/extension (Flx)

The whiskers are equal to the range of the data. A) misalignment of the potted femur (adduction, internal rotation and flexion are treated as the positive direction) B) the absolute misalignment of the potted femur as a percentage of the normal range of hip motion for an adult male (Boone and Azen, 1979).

## 5.4 Discussion

### 5.4.1 Most important findings

The most important finding of this study is that low-cost drilling jigs can be used to align hip joint specimens into bone-pots to mimic the ISB coordinate system when performing in-vitro tests with an average misalignment error of 1° for both the pelvic and femoral bodies (Figure 5.2 and Figure 5.5 respectively). Adopting the methodology presented in this study, or an equivalent system, would help improve the quality of biomechanical research through the results being presented in a known, repeatable and clinically relevant coordinate system.

### 5.4.2 Limitations

Synthetic bones and not cadaveric tissue were used which could have introduced three sources of error: firstly, although we tested 8 hips, the samples were limited to the anatomy of only one male, and one female with each hip side tested twice; however, anatomical variations are unlikely to affect the applicability of the method which relies on easily identified landmarks as recommended by the ISB. Secondly, drilled holes in cadaveric tissue with low bone quality will have a worse tolerance and could feasibly enlarge during testing, especially when high loads are applied, which will increase the misalignment; consequently when testing cadaveric specimens, we only use the drilled holes to align the bones initially, and prefer to securely fixate the bones into the pots using bone cement (see pelvis pot and femoral rig drawing in section 5.6). Finally,

when testing cadaveric specimens that have not been skeletonised, soft-tissue artefacts could affect the implementation of the coordinate system and make determining the femoral head centre more challenging; as is the case when using the ISB system for gait analysis (Lu and O'Connor, 1999; Lopomo et al., 2010). This limitation was partly addressed in the present study by covering the femoral head with artificial hip capsule whilst using the drilling jigs. Moreover, through relying on the long-axis of the femur the drilling jig is relatively insensitive to exact locating of the femoral head centre – see Figure 5.6.

There were also limitations associated with the optical tracking methodology used; appendix A5.5 (page 239) finds the measurement error to equate to a median of  $0.5^\circ$  misalignment. Interesting, this error would have been a lot more severe had multiple repeats in the optical tracker field of view not been used (in some cases it could have been as high as  $6^\circ$ ). This emphasizes the importance of taking repeats when using optical tracking systems in-vitro.

### *5.4.3 Comparison to other work*

The drilling jigs and methodology presented are designed to replicate the widely adopted ISB coordinate system which closely aligns with a clinical understanding of hip movements and has been widely adopted in computational, gait analysis and imaging studies. This allows for easy comparison between testing methodologies. However for cadaveric testing, some authors recommend different coordinate systems based on anatomical landmarks that have a small inter-specimen variance (Yoshioka et al., 1987; Cristofolini, 1997). The drilling jigs methodology present here could easily be adapted to replicate these coordinate systems through designing clamps/features to restrain different anatomical landmarks.

Custom alignment fixtures/jigs have been mentioned in numerous studies and are likely based on similar concepts to that presented here (Crawford et al., 2007; Dy et al., 2008; Song et al., 2012; Smith et al., 2014) though are frequently not described in detail or accompanied by a quantitative validation of their repeatability. Anderson et al. used an optical tracking method to iteratively align specimens to within  $\pm 1^\circ$  of the desired orientation (Anderson et al., 2008) which is similar to the accuracy found using these drilling jigs. Other authors have also developed solutions for aligning hip joint specimens in a known coordinate system using motion tracking systems including: programming digitised points into robotic systems (Colbrunn et al., 2013), directly using optical tracking systems during experiments (Lopomo et al., 2010; Safran et al., 2013; Signorelli et al., 2013), or co-registering CT scans with in-vitro infra-red tracking data

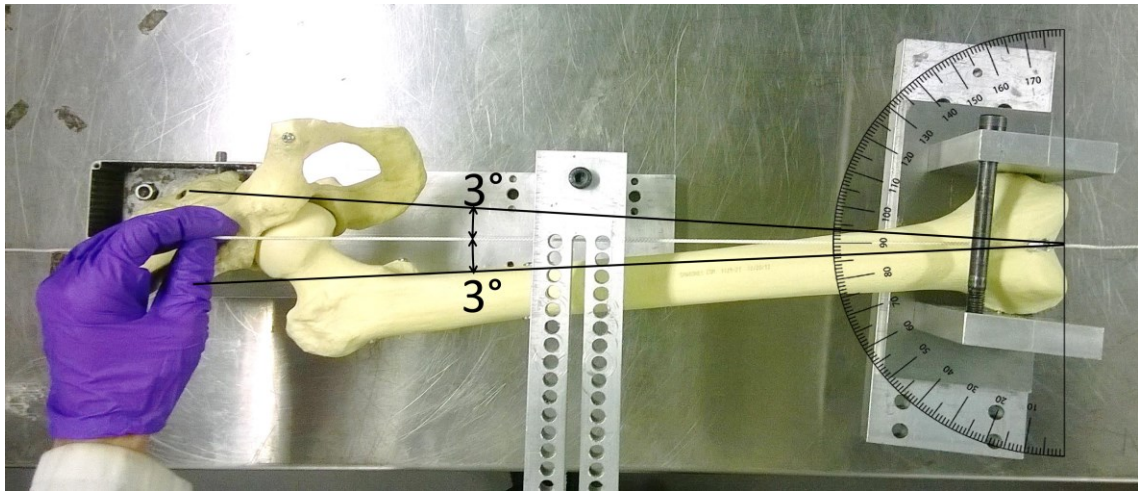


Figure 5.6 The maximum misalignment caused by falsely identifying the femoral head is low due to the long length of the femur.

For the example shown, the white string highlights the mechanical axis of the femur and the black lines demonstrate the extreme medial/lateral boundaries of the femoral head (black lines). Provided the user can correctly identify the femoral head then the misalignment caused by falsely identifying the head centre is limited to a maximum of  $3^\circ$ .

(Crawford et al., 2007; Incavo et al., 2011; Dwyer et al., 2014). In some respects, the drilling jig methodology presented in this paper is inferior to these high-tech techniques; however it is advantageous in that it offers a simple, low-cost, repeatable solution. Moreover, once the specimen has been potted then the method has no further effects on the tests and adds no work to the data analysis.

#### 5.4.4 Conclusion

The method presented could easily be adapted to fit existing set-ups in other laboratories and incorporated into most in-vitro hip joint tests. It could even be for other joints such as the shoulder given the similarities between the humeral and femoral ISB reference frames (Wu et al., 2005). Use of these alignment jigs, or an equivalent, to perform in-vitro tests on hip joints in the ISB coordinate system would be a great improvement over the current norm of not using a fully-defined and repeatable coordinate system. Combining this system with the testing rig presented in chapter 4 would only result in an average misalignment error of less than 2 % of a typical hip's range of motion.

#### 5.5 Acknowledgements

The authors would like to thank Philip Wilson for manufacturing the drilling jigs used in this paper.

5.6 Assembly Drawings

ITEM NO.	PART NUMBER	DESCRIPTION	QTY.
1	JIG03	PELVIC JIG BASE	1
2	JIG01	Z-AXIS GUIDE	1
3	FULL-PELVIS		1
4	JIG02	X-AXIS GUIDE	1
5	ISO 8734 - 6 x 30 - B	PARALLEL PIN (GROUND TO m6)	4
6	ISO 4762 M8 x 20	BOTTOM BOLT	1
7	ISO 4762 M8 x 30	TOP BOLT	1

#1 PUT PRESSURE ON PELVIS TO CONSTRAIN ANTERIOR SUPERIOR ILLIAC SPINE IN SLOT

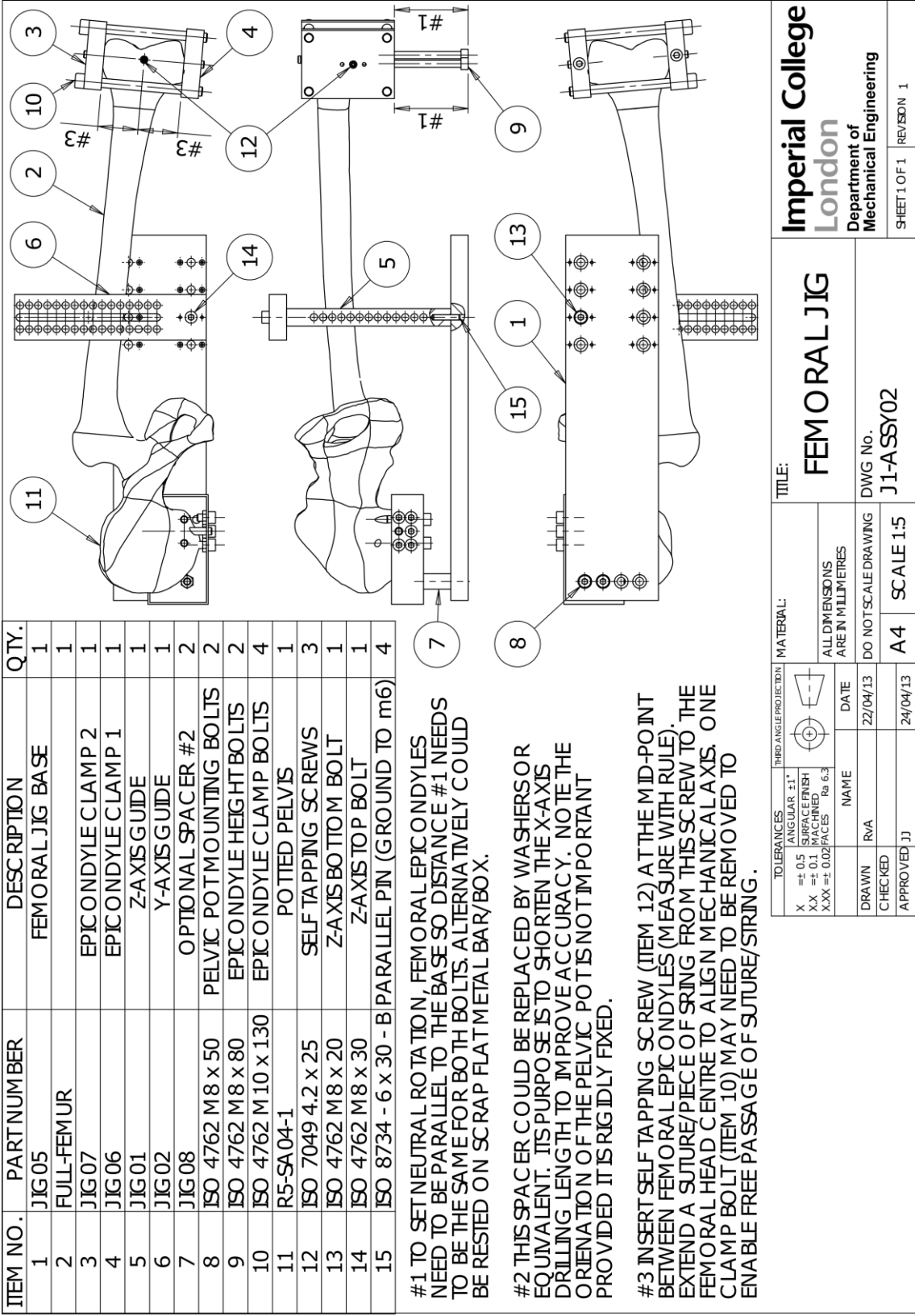
#2 ROTATE PELVIS (MOVEMENT A KIN TO FLEXION) UNTIL POSTERIOR SUPERIOR ILLIAC SPINE BECOMES VISIBLE IN SLOT

#3 JIG CAN BE USED WITH FULL LENGTH FEMURS ATTACHED WHICH CAN EXTEND DISTALLY IN THIS DIRECTION, NOTE THAT FEMORAL POSITIONING DOES NOT AFFECT THE REFERENCE FRAME OF THE PELVIS.

TOLERANCES		THIRD ANGLE PROJECTION	MATERIAL:
X	± 0.5	ANGULAR ±1°	ALL DIMENSIONS ARE IN MILLIMETRES
XX	± 0.1	SURFACE FINISH	
XXX	± 0.02	MACHINED	
NAME		DATE	DO NOT SCALE DRAWING
DRAWN	RVA	22/04/13	A4 SCALE 1:5
CHECKED			
APPROVED JJ		24/04/13	

**Imperial College**  
**London**  
Department of  
Mechanical Engineering

SHEET 1 OF 1    REVISION 1





## **6 The envelope of passive motion allowed by the capsular ligaments of the hip**

Excessive hip rotation can lead to impingements which cause clinical problems for both young adults and hip replacement patients. This study aimed to quantify the passive restraint envelope of the capsular ligaments to clarify their role in restraining hip rotation. Nine cadaveric left hips were skeletonised except for the hip joint capsule and mounted in a six-degrees-of-freedom testing rig. A 5 Nm torque was applied to all rotational degrees of freedom separately to quantify the passive restraint envelope. It was found that the hip was free to internally/externally rotate with a large range of un-resisted rotation (up to  $50\pm 10^\circ$ ) in mid-flexion and mid-ab/adduction, however, the capsular ligaments significantly reduced ( $p<0.014$ ) the available range of rotation in deep flexion/extension and high levels of ab/adduction such that there was a near-zero slack region in some positions. The range of un-resisted rotation was not symmetrical; the mid-slack point was found in an internally rotated position in extension and an externally rotated position in flexion ( $p<0.001$ ). The torsional stiffness of the capsular ligamentous restraint averaged  $0.8\pm 0.3 \text{ Nm/}^\circ$  and was greater in positions where there were large slack regions. The results allow researchers to make informed decisions about the inclusion/exclusion of the capsular ligaments in hip models. When considered alongside clinical measurements, the results also suggest that the capsular ligaments play an important role in hip rotational restraint and that capsular repair is important for achieving normal hip biomechanics post-surgery in patients with large range of motion requirements.

This chapter has been submitted to the Journal of Biomechanics where it is under review. I have presented the work at the following conference:

van Arkel RJ, Cobb JP, Amis AA, Jeffers JRT. The hip joint capsule passively stabilises the hip during normal activities. 11th European Hip Society Congress, 2014, Stockholm, Sweden

### 6.1 Introduction

#### 6.1.1 *Clinical motivation*

Anatomical limits to the range of motion (ROM) of the hip joint are important to prevent impingements, which can lead to serious clinical problems. For young adults, femoroacetabular impingement (FAI) in the native hip causes pain and trauma to the acetabular labrum or articular cartilage and can, in the long-term, lead to osteoarthritis (Leunig and Ganz, 2014). For total hip arthroplasty (THA) patients, impingements cause subluxations and subsequent edge loading and high wear (De Haan et al., 2008a; Esposito et al., 2012) or dislocation (Bartz et al., 2000). Consequently, there is much benefit to be gained from understanding hip ROM and the factors that affect impingement.

#### 6.1.2 *Previous range of motion research*

The majority of hip ROM research considers how impingement is influenced by bony hip morphology and the effects that surgery can have on this (D'Lima et al., 2000; Burroughs et al., 2005; Kubiak-Langer et al., 2007; Tannast et al., 2007a; Kessler et al., 2008; Audenaert et al., 2011; Bedi et al., 2011a; Nakahara et al., 2011; Audenaert et al., 2012; Tannast et al., 2012). Many of these studies, which have used experimental/computational models of the joint, show that both the native and replaced hip are at greatest risk of intra-articular impingement in extension and external rotation, and deep flexion and internal rotation such that there is a non-symmetrical range of hip rotation; the morphology of the hip allows more internal rotation in extension and external rotation in deep flexion (Burroughs et al., 2005; Kessler et al., 2008; Incavo et al., 2011; Nakahara et al., 2011). However, clinical measurements of hip rotation suggest ROM is more symmetrical than these models indicate (Boone and Azen, 1979; Roach and Miles, 1991) and indeed recent research has described how the soft tissues also limit hip ROM (Incavo et al., 2011; Safran et al., 2013). Including these tissues in ROM models has demonstrated that variations in hip geometry within the soft-tissue passive restraint envelope are more important than variations outside it (Incavo et al., 2011).

#### 6.1.3 *The role of the hip joint capsule*

Of the hip soft-tissues, the influence of the hip joint capsule and its intertwined ligaments on ROM restraint is particularly important to consider because any intra-articular hip surgery necessarily involves cuts to these tissues to gain access to the hip, whether open (Leunig and Ganz, 2014) or arthroscopic (Domb et al., 2013) joint



preserving surgery, or THA (Masonis and Bourne, 2002). Recent modelling research shows how the resistive moment developed by these tissues can help prevent hip joint dislocations following THA (Elkins et al., 2011b; Bunn et al., 2014) and recent experimental research shows how cutting the capsular ligaments increases the range of hip motion in the native hip (Myers et al., 2011; Safran et al., 2013). However there is a lack of baseline experimental data describing how the capsular ligaments restrain rotation of the native hip when it is functionally loaded; this is the case for the majority of daily activities (Bergmann et al., 2001). This data would be useful for both assessing the importance of the capsular repair for a patient (Domb et al., 2013) as well as for making informed decision over if the tissue needs to be included in musculoskeletal models (chapter 3). It is also unclear where the hip is passively restrained by soft-tissue and where the joint is free to rotate under the action of hip muscles and external forces. There is also evidence to suggest that increasing hip adduction in high flexion creates unfavourable muscle lines of action (chapter 3) which could reduce hip stability after THA (Bartz et al., 2000), but most hip ligament research focuses on a neutral ab/adduction swing path (Martin et al., 2008; Myers et al., 2011) and so it remains unclear how passive soft-tissue restraints contribute to limiting ROM as hip ab/adduction varies.

## *6.1.4 Aims and hypothesis*

The aims of this study were to quantify the periarticular passive restraint envelope for the hip when it is functionally loaded, and to quantify the amount of rotational stiffness provided by the capsular ligaments once taut. This would define a benchmark to assess soft-tissue repair strategies following early intervention surgery and for making decisions about if/how the capsular ligaments should be included in research models. The null hypothesis is that the passive rotation restraint envelope does not vary throughout hip ROM.

## **6.2 Materials and Methods**

### *6.2.1 Specimen preparation*

Following approval from the local Research Ethics Committee (A6.1, page 241), ten fresh-frozen cadaveric pelvises (six male) with full length femurs were selected based on the patients' medical records. Any patients who had undergone previous hip surgery, or had diagnosed hip disease (such as osteoarthritis) were excluded. Specimens were then defrosted and skeletonised, carefully preserving the hip joint capsule. Guide holes were drilled into the left posterior superior iliac spines and

## CHAPTER 6

femoral shaft before bisecting the pelvis and transecting the femoral mid-shaft. The guide holes based on the contra-lateral pelvis and femoral epicondyles were then used to mount the left hemi-pelvises into a 6 degrees-of-freedom testing rig (Figure 1) according to the International Society of Biomechanics (ISB) coordinate system (Wu et al., 2002) as outlined in chapter 5. Neutral flexion, rotation and ab/adduction equated to a standing upright position (when the ISB pelvic X-Y-Z axes aligned with the femoral x-y-z axes).

### 6.2.2 *The testing rig*

The rig comprised of a femoral-fixture that was attached to a dual-axis servo-hydraulic materials-testing-machine equipped with a two-degree-of-freedom load cell (model 8874, software MAX v9.3, Instron Ltd, High Wycombe, UK) and a pelvic-fixture that could constrain, release or load the other four-degrees-of-freedom (figure 1). Torques (pure moments) could be applied in all three physiological directions: internal/external rotation torque through the rotating axis of the servo-hydraulic machine and flexion/extension or ab/adduction torques with a pulley and hanging-weights couple. This meant that any hip could freely to rotate about its natural centre without affecting the magnitude of applied torque. Fixed angular positions could be applied using position control on the servo-hydraulic machine or with screw clamps on the pulleys. Femoral proximo-distal loads (along the femoral y-axis) were applied by operating the vertical axis of the servo-hydraulic machine in load control whilst an x-z bearing table and a hanging weight applied joint reaction force components in the transverse plane; translations were free to occur in response to the applied load and ligament tension.

### 6.2.3 *Testing protocol*

For each specimen, all tests were performed at room temperature on the same day without removing the specimen from the testing rig. The specimens were kept moist using regular water spray. With the femur in the neutral position, a fixed compressive load of 110 N angled 20° medially/proximally relative to the mechanical axis of the femur was applied. This loading vector represented the average direction of the hip joint contact force and was held constant relative to the femur as the pelvis was flexed/extended and ab/adducted. This value was determined from *in-vivo* force data (Bergmann et al., 2001) by calculating the average angle the joint reaction force makes with the femur for four hip replacement patients performing eight activities of daily living each (Appendix A6.2 page 244). The deflection of the testing rig under this loading condition is negligible (Table 4.1, page 80). To minimise the effect of this load on the rotation torques, the hip's approximate centre of rotation was aligned to that of the

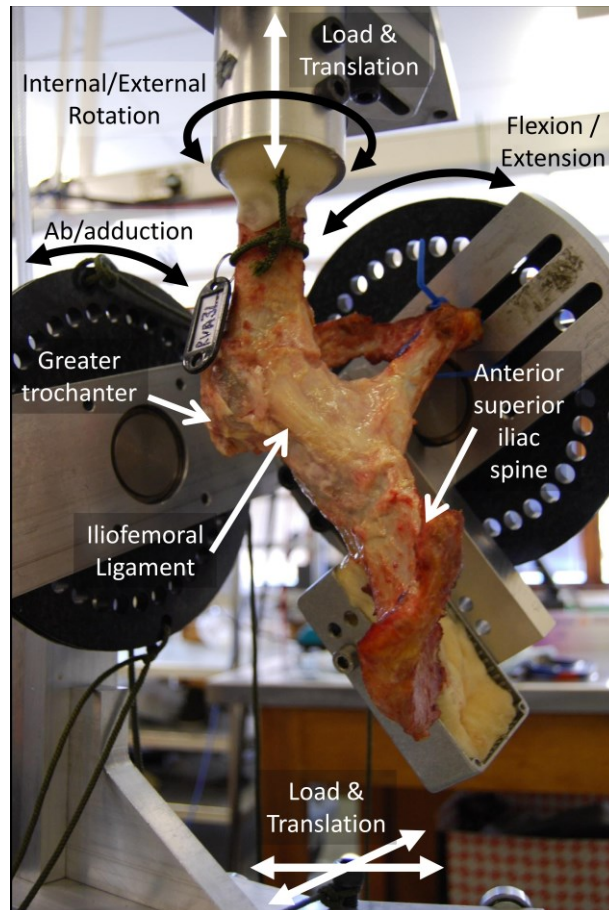


Figure 6.1 Anterolateral view of a hip in the testing rig in flexion, adduction and external rotation.

In this photo, the iliofemoral capsular ligament can be seen to be taut and resisting a 5 Nm external rotation torque being applied by the servo-hydraulic machine. Internal/external rotation and vertical loads are controlled by a dual-axis servo-hydraulic machine (not shown) and horizontal loads and translations are applied using dead weights and a low-friction x-y table (not shown).

testing rig by manually rotating the hip in all three-degrees-of-freedom and iteratively repositioning it until the resulting translations were <2 mm. This limited the maximum possible effect of the 110 N joint reaction force on the applied torque to 0.2 Nm.

Specimens were preconditioned by applying ten internal/external rotation cycles to  $\pm 5$  Nm torque in a neutral flexion/adduction hip position. For each specimen, the ROM with the joint capsule intact was established by applying 5 Nm extension/flexion torques with the hip joint in neutral rotation and ab/adduction to define a value of extension (EXT) and deep flexion (FLX) for the hip. Then, with the joint still in neutral rotation, 5 Nm ab/adduction torques were applied to measure values of high abduction (ABD) and high adduction (ADD) at six different flexion angles (EXT, F0°, F30°, F60°, F90° and FLX). Finally, 5 Nm torques were applied in internal/external rotation at 30 different hip positions; all possible combinations of ABD, AB20° (abducted to 20°), A0° AD20° (adducted to 20°) and ADD at all six flexion/extension angles. At each hip position, these rotation movements were applied by the servo-hydraulic machine using

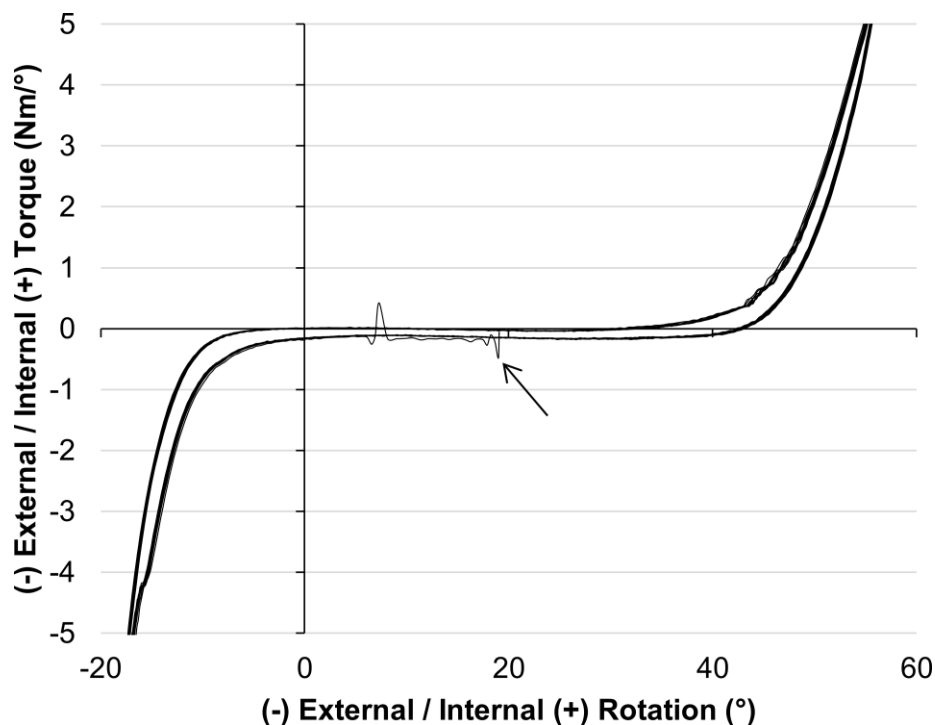


Figure 6.2 Ten internal/external rotation cycles from one hip joint specimen.

The plotted data is as exported by the machine – i.e. it has not been smoothed or filtered. The arrow highlights a start-up 'judder' which affected the first external-internal rotation cycle. The ten lines overlap considerably (the graph lines in the linear region appear much thicker than that for the start-up 'judder' as the ten lines are so concentrated) showing high repeatability with little viscoelastic effect.

a sinusoidal waveform (neutral → external → neutral → internal → neutral) with a 10 s period whilst continuously recording the angle of rotation and passive rotation resistance. Each movement was performed twice and data were analysed from the second iteration so that any servo-hydraulic machine start-up effects did not affect the data analysis (Figure 6.2). The control strategy for the machine is described in greater detail in appendix A6.3 (page 245).

Following testing, specimens were dissected free of all soft-tissues and photographs were taken to assess the bony morphology. A view equivalent to an AP-radiograph was used to measure femoral head diameter, neck-shaft angle, offset and head-neck ratio (Doherty et al., 2008; Grammatopoulos et al., 2010b) as well as acetabular centre edge angle and depth/width ratio (Cooperman et al., 1983; Jacobsen, 2006). To aid identification of the bony anatomy in these photos, two photos with the hip held at the same height were taken, one with the femoral head compressed into the acetabulum, and one with the femur distracted directly laterally so that the entire femoral head and posterior acetabular cartilage were visible. The radiographic teardrop was identified visually on the hemipelvises using the description provided by Goodman et al. (Goodman et al., 1988). The  $\alpha$  and  $\beta$  angles, and the anterior neck offset ratio were assessed in a photo that replicated a 90° Dunn radiograph (Meyer et al., 2006; Clohisy et

al., 2008). Specimens with  $\alpha > 55^\circ$  or centre-edge angle  $< 25^\circ$  were considered abnormal and were excluded from the data analyses (Jacobsen, 2006; Ellis et al., 2011).

#### 6.2.4 Data analysis

Internal/external torque-rotation curves for each specimen in each hip position were plotted using MatLab (version 2011b, The MathWorks, Inc., Texas, USA). The angular positions where the hip joint motion transitioned from slack to stiff was identified by finding the first points where the torque-rotation gradient exceeded  $0.03 \text{ Nm}/^\circ$  for both internal and external rotation. This value of  $0.03 \text{ Nm}/^\circ$  was determined from pilot data by visually inspecting plots of the torque-rotation data alongside the calculated gradient values.

The slack/stiff transition points were then used to calculate three parameters for further analysis: the range of un-resisted rotation (slack region), the location of the mid-slack point and the change in rotation from the transition point to 5 Nm of passive rotation restraint (slack-to-taut). In cases where there was continually passive restraint with no slack region, the mid-slack angle was defined at 0 Nm passive resistance torque (the x-intercept). Finally, the gradient values were additionally used to quantify the aggregate torsional stiffness provided by the soft-tissues at the point of 5 Nm total passive resistance.

#### 6.2.5 Statistical analysis

The values recorded at AD20° and AB20° could not be included in the repeated measures analyses because not all hips could reach these positions in extension or deep flexion. Data were analysed in SPSS (version 22, SPSS Inc, Chicago, Illinois). A Shapiro-Wilk's test of normality was performed on the data's Studentized residuals. The data were then analysed with two- or three-way repeated measured analyses of variance (RMANOVA). The independent variables were the angles of hip flexion (EXT, F0°, F30°, F60°, F90° and FLX) and hip ab/adduction (ABD, A0° and ADD) for the two-way analyses, with an additional factor of direction of rotation (ER and IR) for the three-way analyses. Four dependent variables were analysed: the range of un-resisted rotation (two-way analysis), the angle of mid-slack (two-way analysis), the angular change from the transition point to 5 Nm passive restraint (three-way analysis) and finally the torsional stiffness of the hip at the point of 5 Nm restraint (three-way analysis). Post-hoc one-way RMANOVA and paired t-tests with Bonferroni correction were applied when differences across tests were found. The significance level was set at  $p < 0.05$ . The number of post-hoc comparisons at a given level of flexion was different

from that at a given level of ab/adduction. Therefore adjusted p-values, multiplied by the appropriate Bonferroni correction factor in SPSS, have been reported rather than adjusting the significance level.

### 6.3 Results

One male hip had a visibly aspherical head ( $\alpha=64^\circ$ ) and was excluded from the data analysis. External rotation data for one female specimen was lost due to the capsule rupturing from the bone when 5 Nm torque was applied in external rotation meaning that subsequent hip rotation results are presented for only eight specimens. Morphological measurements of these specimens are presented in Table 6.1. Under 5 Nm torque the mean ( $\pm$  standard deviation) hip joint flexion was  $112\pm10^\circ$  and extension was  $-12\pm7^\circ$ . The range of hip joint ab/adduction varied with the angle of hip flexion; it was largest in  $60\text{--}90^\circ$  of flexion and smallest in hip extension (Figure 6.3). The preconditioning cycles, and the repeated movements in internal/external rotation showed that the subsequent results for internal/external rotation were highly repeatable and that 5 Nm was sufficient torque to generate a linear force-displacement curve (Figure 6.2).

Table 6.1 Morphological measurements of the eight hips included in the data analysis.

Measurement	Mean $\pm$ S.D.	Range
Age	$76 \pm 9$	61 to 89
Femoral head diameter (mm)	$50 \pm 5$	43 to 57
Femoral anteversion ( $^\circ$ )	$9 \pm 11$	-6 to 23
Femoral neck-shaft angle ( $^\circ$ )	$130 \pm 4$	126 to 137
Femoral offset (mm)	$36 \pm 9$	24 to 46
Femoral head/neck ratio	$1.40 \pm 0.07$	1.29 to 1.49
Femoral anterior neck offset ratio	$0.18 \pm 0.02$	0.15 to 0.22
Femoral alpha angle ( $^\circ$ )	$48 \pm 6$	38 to 54
Femoral beta angle ( $^\circ$ )	$45 \pm 5$	36 to 50
Acetabular centre edge angle ( $^\circ$ )	$41 \pm 9$	32 to 54
Acetabular depth/width ratio	$274 \pm 22$	254 to 320
Osteophytes	Two hips had a small osteophyte on the anterior neck that did not impinge on the labrum.	
Osteoarthritis	Despite the medical record exclusion criteria, two hips had visibly thin cartilage and one hip had small isolated defects. There was no severe osteoarthritis that affected the results through increased friction in the joint or notable remodelling of the femoral head or acetabulum.	

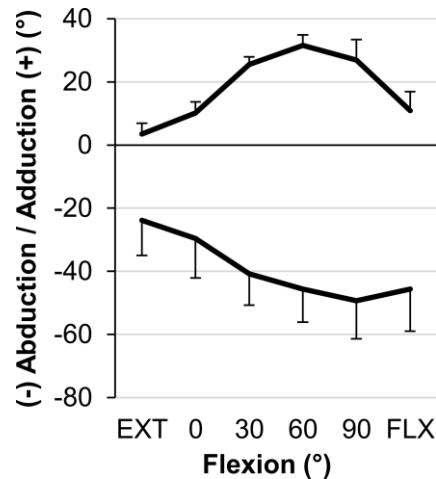


Figure 6.3 The mean ab/adduction with standard deviation when 5 Nm torque was applied as flexion was varied whilst internal/external rotation was fixed in the neutral position (n=9).

### 6.3.1 The passive restraint envelope: the range of un-resisted rotation

The range of un-resisted rotation (slack region) varied with both the angle of hip flexion and ab/adduction (Figure 6.4) and the effect of flexion on the slack region was found to be dependent by the level of ab/adduction and vice-versa ( $p < 0.001$ ). The post-hoc analysis showed that the slack region in neutral ab/adduction was greater than that in high ab/adduction (all  $p < 0.014$ , Table 6.2 and Figure 6.5). The largest difference was at F60° where the mean slack region was  $41 \pm 13^\circ$  larger in neutral ab/adduction than when the hip was highly adducted ( $p < 0.001$ ). Similarly, when the hip was neutrally ab/adducted the hip had a reduced slack region in extension and deep flexion compared to mid-flexion (all  $p < 0.006$ , Table 6.2 and Figure 6.5). The largest mean difference was  $44 \pm 15^\circ$  between F60° and EXT when the hip was in neutral ab/adduction ( $p = 0.001$ ).

### 6.3.2 The passive restraint envelope: mid-slack

The position of the mid-slack point also varied with the angle of hip flexion and abduction (Figure 6.4) with an interaction effect between flexion and ab/adduction ( $p < 0.001$ ). Post-hoc analyses showed that, for both neutral and high adduction, the mid-slack point was found with the hip internally rotated in extension, externally rotated in deep hip flexion ( $p < 0.001$ , Figure 6.6a&b). However, when the hip was highly abducted, no difference was detected between the position of the mid-slack point in deep flexion and extension. Instead, the mid-slack point was found with the hip externally rotated in mid flexion, resulting in a parabolic-like shift in the location of the mid-slack point ( $p < 0.028$  for both F30° and F60° compared to extension, Figure 6.6c).

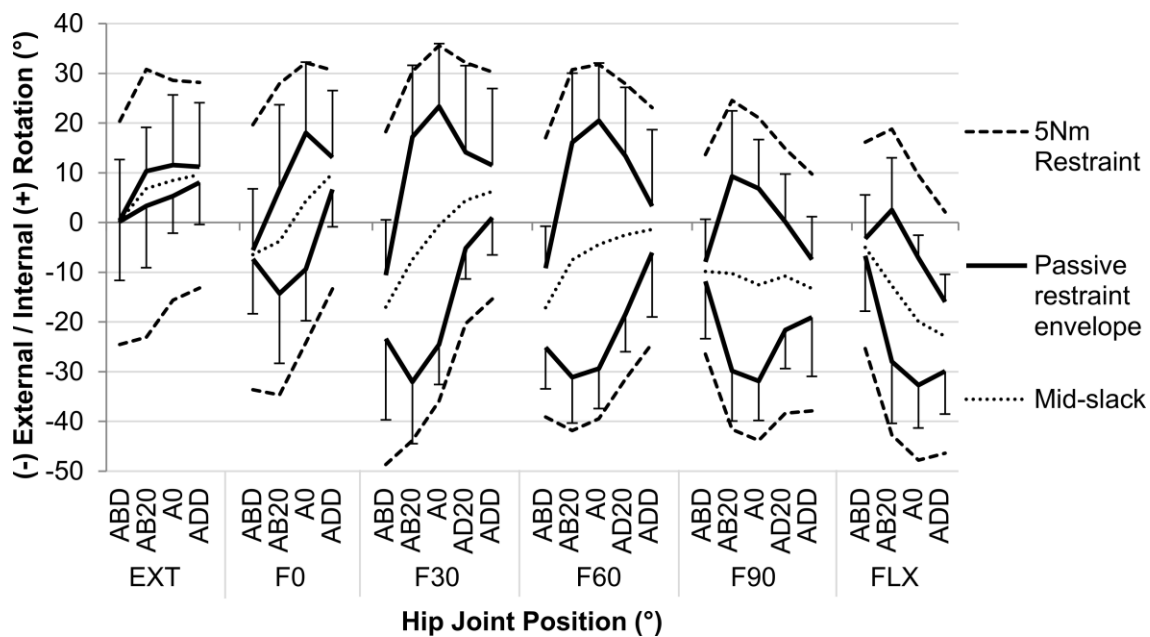


Figure 6.4 The rotation passive restraint envelope (with standard deviation), the points of mid-slack and the 5 Nm measurement boundaries across a complete hip range of motion ( $n=8$ ).

It can be seen that there was a greater range of un-resisted rotation (space between the solid black lines) in mid-flexion and mid-ab/adduction than when the hip was deeply flexed/extended, or highly ab/adducted. It can also be seen that the hip was more open to internal rotation in extension, and external rotation in flexion as the mid-slack points (grey dots) shifted to external rotation as hip flexion was increased. However once the ligaments had started to restrain hip rotation, the internal/external rotation restraint is more symmetrical (equal spacing between solid black lines and dashed grey lines at each position).

### 6.3.3 Slack-to-taut and torsional stiffness

Neither the angular change from the transition point to 5 Nm passive restraint (slack-to-taut) nor the torsional stiffness at 5 Nm restraint were affected by a three-way interaction between flexion, ab/adduction and rotation direction. However, both dependent variables did vary with hip position with a two-way interaction detected between flexion and ab/adduction across both directions of rotation (for slack-to-taut  $p=0.006$ , and for torsional stiffness  $p=0.036$ ). Post-hoc analysis detected differences in similar positions to those found for the slack region (in mid-flexion and mid-ab/adduction, Figure 6.4). Generally, when the slack region increased, torsional stiffness increased and slack-to-taut decreased (Table 6.2 and Figure 6.7). For slack-to-taut, the largest mean difference between levels of ab/adduction was  $15\pm6^\circ$  neutral and high abduction at  $F30^\circ$ , and between levels of flexion was  $8\pm3^\circ$  between  $F60^\circ$  and EXT at neutral ab/adduction (both  $p<0.004$ ). For torsional stiffness, the largest mean significant differences between levels of ab/adduction was  $0.40\pm0.25 \text{ Nm}/^\circ$  between



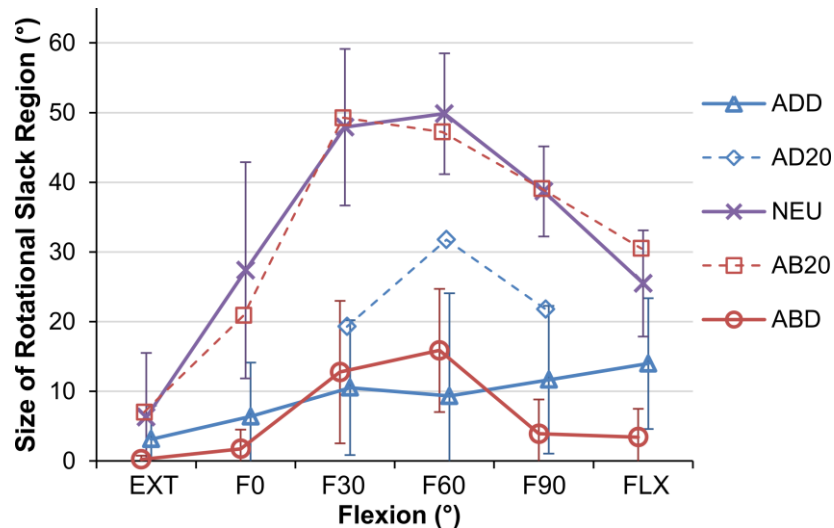


Figure 6.5 The mean range of rotational slack as flexion (x-axis) and ab/adduction (different lines) varies with 95 % confidence intervals.

It can be seen that the hip tightens in deep flexion and extension, and high abduction/adduction whilst the greatest range of slack occurs when the hip is neutrally or partially abducted and mid-flexed.

neutral and high adduction when at F60°, and between levels of flexion was  $0.45 \pm 0.19$  Nm/° between F60° and EXT when in neutral ab/adduction (both  $p < 0.008$ ). The analysis also indicated significant two-way interactions between rotation and flexion across all abduction angles, and rotation and abduction across all flexion angles for slack-to-taut and torsional stiffness respectively (A6.4, page 247).

## 6.4 Discussion

### 6.4.1 Most important findings

The most important finding of this study was that the hip rotation passive restraint envelope varied with the angle of flexion/extension and ab/adduction (Figure 6.4). In a position of mid-flexion and mid-ab/adduction there were large slack regions where the soft tissues provided no rotational restraint (Figure 6.5), which indicate a large in-vivo ROM that allows the hip to move freely under the action of hip muscles during many daily activities. Conversely, towards the extremes of hip ROM (in positions of deep flexion/extension or high levels of ab/adduction) there was a minimal/non-existent slack region, thus limiting the available range of rotation in positions where the hip is vulnerable to impingement and/or subluxation. The results also showed that internal/external rotation restraint is not symmetrical; the mid-slack point displayed a shift from an internally rotated position in extension to an externally rotated position in hip flexion (Figure 6.6). Finally, it shows that once the periarticular soft-tissues began to tauten, the hip tended to require less angular change from slack-to-taut and was stiffer in positions where there was a large slack region (Figure 6.7 and Table 6.2), though

mean changes in slack-to-taut (up to 15°) were considerably less than changes in slack ROM and mid-slack (up to 44° and 33° respectively).

#### 6.4.2 Limitations

The findings of the present study are associated with several limitations; firstly in that it does not distinguish between capsular rotational restraint and that from labral impingement but provides an aggregate rotational restraint from the periarticular tissues. However, within the 5 Nm restraint boundaries examined, the next chapter details research that found that the mean labral contribution to rotational restraint only exceeded 20 % in 6/36 hip positions and was significantly less than the capsular contribution to rotational restraint in all hip positions. Indeed, by combining the analysis techniques from this chapter, with the data from the next, an analysis detailed in appendix A6.5 (pages 248-253) suggests that the capsular ligaments tautened significantly before the labrum began to impinge for most hip positions. Labral impingements were observed most frequently when the hip was in high abduction, which may be the cause of the parabolic shift of the mid-slack point in high abduction (Figure 6.6), and also the few hip positions in low flexion and high abduction where slack-to-taut and torsional stiffness seemingly both increase (Figure 6.7).

Table 6.2 All significant increases/decreases measured for the slack region, slack-to-taut and torsional stiffness. Similarities between increases in the slack region, decreases in slack-to-taut and increases in torsional stiffness are highlighted in red. When no difference was detected for the one-way RMANOVA, the effect size is not given (n.s.).

Hip position	Slack region			Slack-to-taut			Torsional Stiffness		
	Effect Size ( $\eta_p^2$ )	Pairwise t-tests	p-value	Effect Size ( $\eta_p^2$ )	Pairwise t-tests	p-value	Effect Size ( $\eta_p^2$ )	Pairwise t-tests	p-value
ABD	0.489	none	-	0.454	none	-	0.349	F30>EXT F60>F90	0.022 0.018
A0	0.743	F30>EXT F60>EXT F90>EXT F60>F90 F60>FLX F90>FLX	0.002 0.001 0.005 0.006 0.008 0.022	0.629	F30<EXT F60<EXT F90<EXT F60<F90	0.044 0.003 0.040 0.046	0.650	F30>EXT F60>EXT F90>EXT	<0.001 0.004 0.012
ADD	n.s.	none	-	n.s.	none	-	0.462	F90>F0 F90>F30	0.001 0.033
EXT	n.s.	none	-	0.478	A0<ABD	0.050	0.505	A0>ABD	0.043
F0	0.682	A0>ABD A0>ADD	0.013 0.012	0.682	A0<ABD ADD<ABD	0.010 0.035	0.363	A0>ADD	0.048
F30	0.788	A0>ABD A0>ADD	0.001 <0.001	0.785	A0<ABD A0<ADD ADD<ABD	0.001 0.023 0.022	0.786	ABD>ADD A0>ADD	0.031 <0.001
F60	0.871	A0>ABD A0>ADD	<0.001 <0.001	0.878	A0<ABD A0<ADD	<0.001 <0.001	0.596	A0>ABD A0>ADD	0.008 0.028
F90	0.896	A0>ABD A0>ADD	<0.001 0.001	0.433	A0<ADD	0.006	0.678	A0>ABD	0.003
FLX	0.747	A0>ABD A0>ADD	0.001 0.008	n.s.	none	-	n.s.	none	-

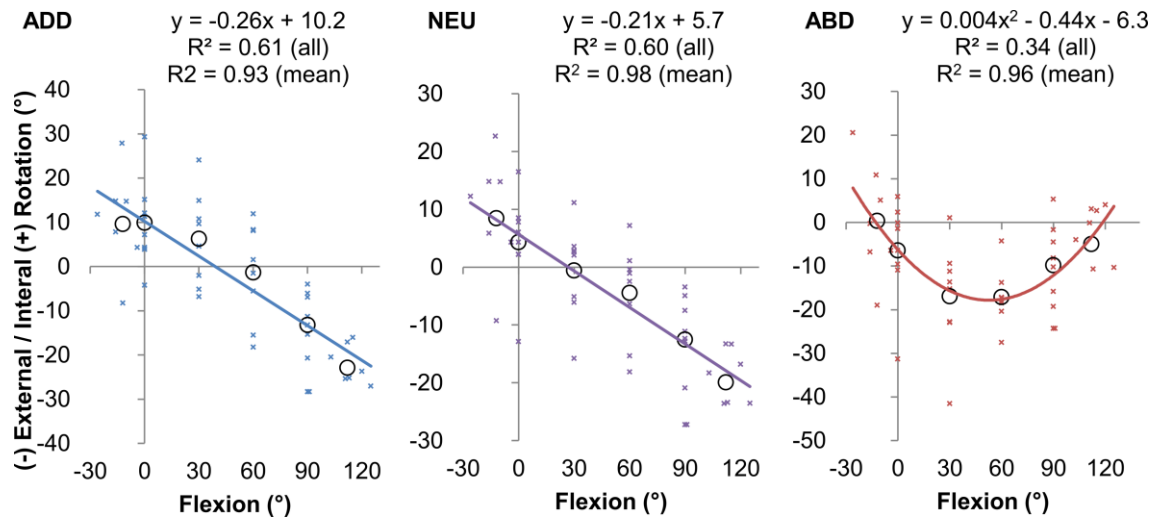


Figure 6.6 The position of the mid-slack point as flexion varies.

When the hip is highly adducted (left) or neutrally ab/adducted (middle) then the range of un-resisted hip rotation is biased to internal rotation in extension and external rotation in flexion as demonstrated by the linear transition of the mid-slack point with increasing hip flexion. When the hip is highly abducted (right) then the mid-slack point positioned most in external rotation in mid-flexion and is better described by a second order polynomial. The equations provided represent a good model for the raw data from all specimens (small crosses, all  $R^2 \geq 0.34$ ) and an excellent model for an average hip as demonstrated by the mean data at each flexion angle (black circles, all  $R^2 \geq 0.93$ ).

The high volume of data meant that the slack to taut transition points had to be calculated by an algorithm and this relied on a value of torsional stiffness ( $0.03 \text{ Nm/}^\circ$ ) determined by pilot testing. A sensitivity study which recalculated the results using values of  $0.01 \text{ Nm/}^\circ$  and  $0.05 \text{ Nm/}^\circ$  found that this choice of value had little effect on the results, and no effect on the conclusions drawn (appendix A6.6, page 250).

This study also modelled compressive loading as an average load with fixed direction. Whilst the load is representative of peak load at toe-off during gait and stair climbing, or when sitting into a chair, the direction of the joint reaction force can vary by up to  $\pm 20^\circ$  compared to this average load (Bergmann et al., 2001). Changes to the joint reaction force could cause translations within the joint which could affect the ligamentous loading and hence the passive restraint envelope. However, the compressive loading applied ensured contact between the femur and acetabulum and previous research suggests that the hip joint can be considered a spherical ball-and-socket ( $<1 \text{ mm}$  of translation within the hip) (Cereatti et al., 2010). Indeed, other authors have previously used similar loading approximations to study hip joint mechanics in-vitro (Dwyer et al., 2015), or even failed to applied loading at all (Martin et al., 2008; Safran et al., 2013).

Another limitation was the high mean age of the cadaveric specimens; they are better matched to patients undergoing THA than those receiving early intervention surgery. This study also did not consider the effects of osteoarthritis on capsular stiffness, or how a smaller head size for a THA may affect the ability of the capsule to wrap around

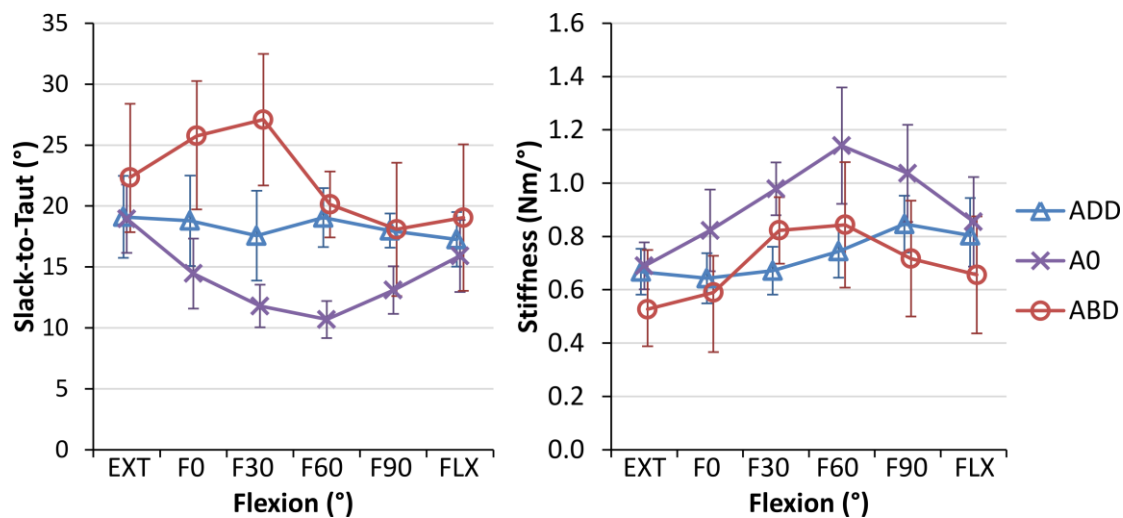


Figure 6.7 Mean angular change between the transition point and 5 Nm of rotational restraint (left) and torsional stiffness (right) with 95 % confidence intervals as flexion (x-axis) and ab/adduction (different lines) varies.

It can be seen that for neutral and high adduction, as slack-to-taut decreases, stiffness increases and vice-versa.

the head and tauten (Colbrunn et al., 2013) or whether hips suffering from FAI have normal capsular anatomy/function. However, regarding the latter, data studies have suggested similarities between hip capsule dimensions in pathological hips (Weidner et al., 2012) and normal hips (Stewart et al., 2002).

#### 6.4.3 Comparison with published research

In Figure 6.8, the passive restraint envelope measured in this study is compared against data taken from 18 studies with a total of more than 2400 subjects, which include clinical goniometer readings, *in-vitro* experiments including skin and muscles and computational impingement models. It can be seen that the passive restraint envelope measured in this study is typically less than clinical measurements for flexion/extension and internal/external rotation at 90° flexion and neutral ab/adduction (other hip positions are examined in A6.7, page 253). This is to be expected as the end-point for hip ROM is likely beyond the 5 Nm restraint end-point in this study and caused by a mix of capsular rotation restraint, passive restraint from muscle stretching and soft/hard tissue impingement. However, in showing that the capsular restraint envelope is less than clinical measurements, these results demonstrates that the periarticular tissues influence the ultimate limits of hip ROM, and may be recruited before these limits to protect the hip from impingement and/or subluxation. This comparison should be treated with caution as clinical measurement of hip motion may inadvertently include the effects of pelvic-tilt and rotation and thus may overestimate hip ROM. Nevertheless, the finding is corroborated when one considers the hard limits measured in computational studies of exclusively bony morphology (Figure 6.8): in all

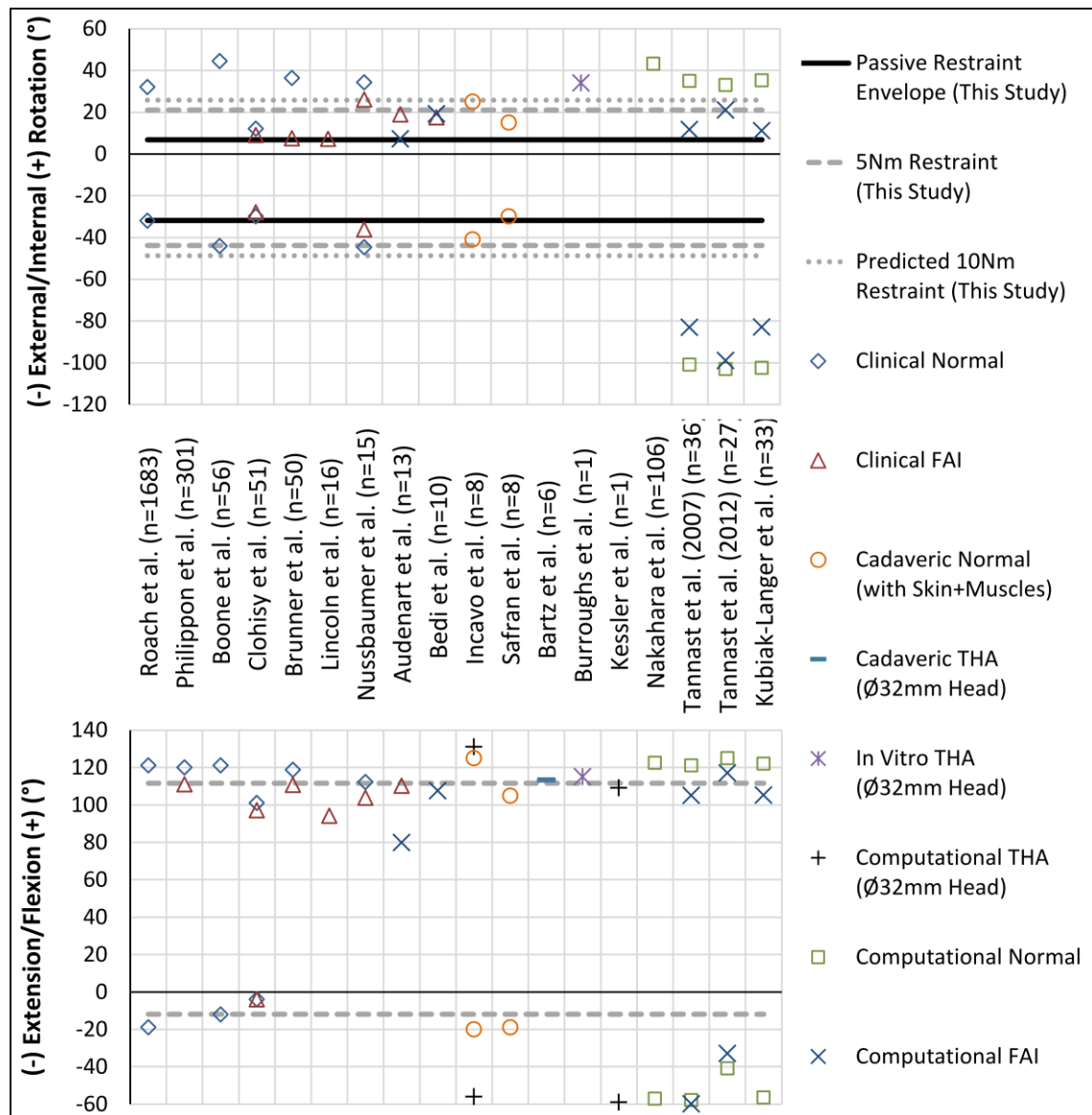


Figure 6.8: A comparison between clinical, experimental and computational range of motion measurements and the results from the present study for internal and external rotation at 90° flexion with neutral ab/adduction (top), and for flexion/extension with neutral ab/adduction and internal/external rotation (bottom).

It can be seen that the passive restraint envelope (for un-resisted rotation) measured in this study are within clinical measurements for normal subjects, compare well to previous cadaveric work and are always less than results from studies which only consider bony impingement as a limit to hip rotation (computational studies). The predicted 10 Nm restraint values are calculated using the mean torsional stiffness measured at 5 Nm restraint.

cases, the mean range of free rotation was less than those bone-bone impingement measurements. The impingement-free range of rotation measured in bone-bone impingement studies is biased towards internal rotation in extension (Kessler et al., 2008; Tannast et al., 2012), and external rotation in flexion (Kubiak-Langer et al., 2007; Tannast et al., 2012); capsular rotation restraint is seemingly able to guide the available range of rotation towards these impingement-free positions as a 30° shift from an internally rotated position in extension to a more externally rotated position in deep flexion, was observed in the mid-slack point (Figure 6.6).

Several authors have reported the total resistance to hip joint distraction/dislocation (Ito et al., 2009; Elkins et al., 2011b), the stiffness of individual ligaments (Hewitt et al., 2002), their contribution to hip rotation restraint (Myers et al., 2011; Smith et al., 2014), or their influence on hip ROM (Safran et al., 2013). However to our knowledge there are no studies measuring the slack region, or the angular change required to tauten the ligaments or torsional stiffness provided by an intact capsule once the ligaments are taut. This study quantifies these variables and the findings correlate well with the understanding of the anatomy of the capsular ligaments. The four capsular ligaments available for limiting hip rotation (medial and lateral arms of the iliofemoral, ischiofemoral and pubofemoral) are the same ligaments which can generate resistive moments against deep flexion/extension or high ab/adduction (Fuss and Bacher, 1991; Martin et al., 2008). This explains the reduced hip rotation slack region observed in the more extreme hip positions (Figure 6.4 and Figure 6.5) as the ligaments are recruited to limit both large movements of the lower limb (flexion/extension or ab/adduction) and hip rotation. It also explains the reduced rotational stiffness (Figure 6.7) in these hip positions as the ligament fibres do not align to purely resist hip rotation but also the other movements. Conversely in mid-flexion and mid-ab/adduction, there is a large slack region available as the ligaments are not resisting movements in any direction. When the hip is excessively rotated in these mid-ROM positions such that the ligaments start to tauten, then the ligaments develop high levels of torsional stiffness in small angular changes (Figure 6.7) as the fibres are orientated more perpendicularly to the axis of hip rotation, directly opposing the movement.

Whilst there were too few specimens to detect significant differences, there was a trend that female hips had a greater range of hip rotation. This is likely due to their smaller head diameters for two reasons: firstly, more hip rotation is also required to generate the same force within the ligament as the change in length of a ligament wrapping around the femoral head's circumference is less due to the decreased radius of the head. Secondly, for the same restraining force, a ligament wrapping around a smaller head generates a smaller torque because the moment arm of the force is less. This is interesting in the context of head-neck ratio and impingement free range of motion as previous hip resurfacing research found that female hips had greater pre-operative head-neck ratios, but frequently had their head-neck ratio reduced during surgery as it was perceived to be advantageous to preserve acetabular bone stock by using the smallest possible head diameter. However, this reduction in head neck ratio is now believed to be one of the main causes of edge loading and pseudotumour formation in a resurfaced hip as decreasing the head neck ratio by 0.1 decreases the impingement-

free range of motion by around  $10^\circ$  (Grammatopoulos et al., 2010b). The present study shows that this reduction in head size may have also increased the risk of impingement and edge loading for a second reason: it would allow for a greater range of un-resisted hip rotation before any ligaments preserved/repaired during surgery could engage and passively protect the hip against impingement. Considering the two research findings in parallel, it could also be hypothesized that for a native hip the increased range of free-rotation caused by a small head is naturally compensated for by increased head-neck ratio and consequently greater impingement free range of motion. Therefore further investigation into relationship between head size, head-neck ratio, impingement free range of motion and the passive restraint envelop is an important area for future research if ceramic-on-ceramic resurfacing devices that are currently in development (Dickinson et al., 2011a) are introduced to the market.

### *6.4.4 Clinical relevance and conclusion*

This study quantified the hip positions where the periarticular soft-tissues restrain hip rotation and those where the joint is slack, how much rotation is required to tighten these tissues, and how much rotational stiffness is provided by them once taut. These results are useful for understanding the role of these tissues in normal hip function when it is loaded during daily activities. Capsular repair adds to operational time and hence these results could help surgeons to make informed decision over whether their biomechanical function is worth preserving during early intervention surgery or restoring following a THA. For example patients whose daily activities and functional expectations only require a ROM within the identified slack region may benefit less from capsular repairs than those with larger ROM requirements. In surgery for young athletic patients who typically have high ROM demands, those with full capsular repairs experienced greater improvement than those with only a partial repair (Frank et al., 2014). The results of the present study may also allow researchers to make informed decisions about the inclusion/exclusion of these soft tissues in hip models; for examples, models which examine movements within the identified slack region could exclude the capsular structures with little loss of fidelity whereas research into movements with a high ROM would be improved by including the passive restraint from these tissues.

### **6.5 Acknowledgements**

This study was funded by the Wellcome Trust and EPSRC [088844/Z/09/Z] and the Institution of Mechanical Engineers. The dual-axis Instron materials-testing-machine was provided by an equipment grant from Arthritis Research UK.





## **7 The capsular ligaments provide more hip rotational restraint than the acetabular labrum and the ligamentum teres**

This in-vitro study of the hip joint examined which soft tissues act as primary and secondary passive rotational restraints when functionally loaded. Nine cadaveric left hips were mounted in a testing rig that allowed application of forces, torques and rotations in all six-degrees-of-freedom. The hip was rotated throughout a complete range of motion and the contribution of the iliofemoral (medial and lateral arms), pubofemoral, ischiofemoral and ligamentum teres ligaments to rotational restraint was determined by resecting a ligament and measuring the reduced torque required to achieve the same angular position as before resection. The contribution from the acetabular labrum was also measured. Each of the capsular ligaments acted as the primary hip rotation restraint somewhere within the complete range of motion, and the ligamentum teres acted as a secondary restraint in high flexion, adduction and external rotation. The iliofemoral lateral arm and ischiofemoral ligaments were primary restraints in two-thirds of the positions tested. Appreciation of the importance of these structures in preventing excessive hip rotation and subsequent impingement/instability may be relevant for surgeons undertaking both joint preserving surgery and arthroplasty.

I presented this work, and was awarded the student biomechanics award (\$1000 cash prize) at the 27<sup>th</sup> Congress of the International Society for Technology in Arthroplasty in Kyoto, Japan.

The work has also been accepted for publication in the Bone and Joint Journal and has been reproduced with permission and copyright © of the British Editorial Society of Bone and Joint Surgery:

van Arkel, R.J., Amis, A.A., Cobb, J.P., Jeffers, J.R.T., 2015. The capsular ligaments provide more hip rotational restraint than the acetabular labrum and the ligamentum teres: an experimental study. Bone & Joint Journal 97-B, 484-491.

### 7.1 Introduction

#### 7.1.1 *Clinical motivation*

There is increasing interest in early intervention hip surgery to treat conditions from instability to femoroacetabular impingement (FAI) in young adults (Bedi et al., 2011b; Domb et al., 2013). However, concerns exist regarding postoperative instability following resection of hip joint ligaments during open (Phillips et al., 2012) or arthroscopic surgery (Martin et al., 2012). Case reports describe instances of rapid joint degeneration to a point requiring total hip arthroplasty (THA) caused by joint subluxation (Benali and Katthagen, 2009; Mei Dan et al., 2012) as well as complete joint dislocation (Matsuda, 2009; Ranawat et al., 2009; Sansone et al., 2013), raising questions about the role of soft tissues in maintaining hip stability.

Instability also affects THA patients, because excessive hip rotation can lead to impingements which destabilise the hip by forcing the femoral head to lever out of the acetabulum, causing edge loading and high wear (De Haan et al., 2008a; Esposito et al., 2012), or even dislocation (Nadzadi et al., 2003). Repairing the capsule and neighbouring muscles can reduce the post-operative dislocation rate (Kwon et al., 2006). However, the importance of the capsule in restraining excessive rotation and preventing impingement in the native hip is little understood and hence it is unclear whether these repair strategies could be optimised to further improve outcomes.

#### 7.1.2 *Previous hip ligament research*

Cutting capsular ligaments results in large increases in rotational joint laxity (Martin et al., 2008; Myers et al., 2011; Safran et al., 2013), however few research studies include the hip joint reaction force which is common to all functional tasks (Bergmann et al., 2001) and is essential to gaining stability from the osseous anatomy; it forces the ball into the socket. There is also some evidence that the ligamentum teres could restrain hip rotation and stabilise the hip (Kivlan et al., 2013; Martin et al., 2013), however its relative importance compared to the capsular ligaments is unknown. For informed decisions to be made about which soft tissues should be preserved or repaired during hip surgery, a complete picture of the relative contributions does not yet exist. The preservation or repair of the primary restraints varies with both open and arthroscopic approaches, so an appreciation of relative importance will contribute to the debate about surgical approaches and repairs.

### 7.1.3 Aims and hypothesis

The present study therefore aimed to quantify the relative contributions of each ligament to restraining hip rotation throughout a complete range of motion under joint compression. Our null hypothesis was that the capsular ligaments, labrum and ligamentum teres contribute equally to hip joint rotational restraint.

## 7.2 Materials and Methods

### 7.2.1 Specimen preparation

Specimens were prepared according to the protocol established in the chapters 5 and 6 following approval from the local Research Ethics Committee (A6.1, page 241). Ten fresh-frozen cadaveric pelves (6 male) with full length femurs were defrosted and skeletonised, carefully preserving the hip joint capsule (the same specimens as for chapter 6). Specimens were bisected into hemi-pelves and the left hip was mounted into a six-degrees-of-freedom testing rig (Figure 7.1) according to the International Society of Biomechanics (ISB) coordinate system (Wu et al., 2002). Movements in this coordinate system mimic movements of the lower limb in a clinical environment (Figure 2.3, page 10) with neutral flexion, rotation and ab/adduction equating to a standing upright position (when the ISB pelvic and femoral axes align). The alignment method is described fully in chapter 5. Flexion and abduction torques were applied by hanging weights and angular positions applied using screw clamps. Internal/external rotation torques/angles were controlled by the rotating axis of a dual-axis servo-hydraulic materials-testing-machine (model 8874, software MAX v9.3, Instron Ltd, High Wycombe, UK) equipped with a two-degrees-of-freedom (tension/torsion) load-cell. Throughout testing, a fixed joint compression force of 110 N angled 20° medially/proximally relative to the mechanical axis of the femur was applied using the servo-hydraulic machine's vertical axis and a horizontal hanging weight. This testing rig, which is described in more detail in chapter 4, only deflects 0.4 mm under this loading condition. This load is similar to the direction of the peak hip joint contact force measured for a variety of functional tasks (Bergmann et al., 2001) as described in appendix A6.2 (page 244). Translations were not applied but were free to occur in response to the applied load, by mounting the test fixture onto a freely-moving x-z table. For each specimen, all subsequent tests were performed on the same day, without removing the specimen from the testing rig. The tests were done at room temperature and the specimens were kept moist using regular water spray.

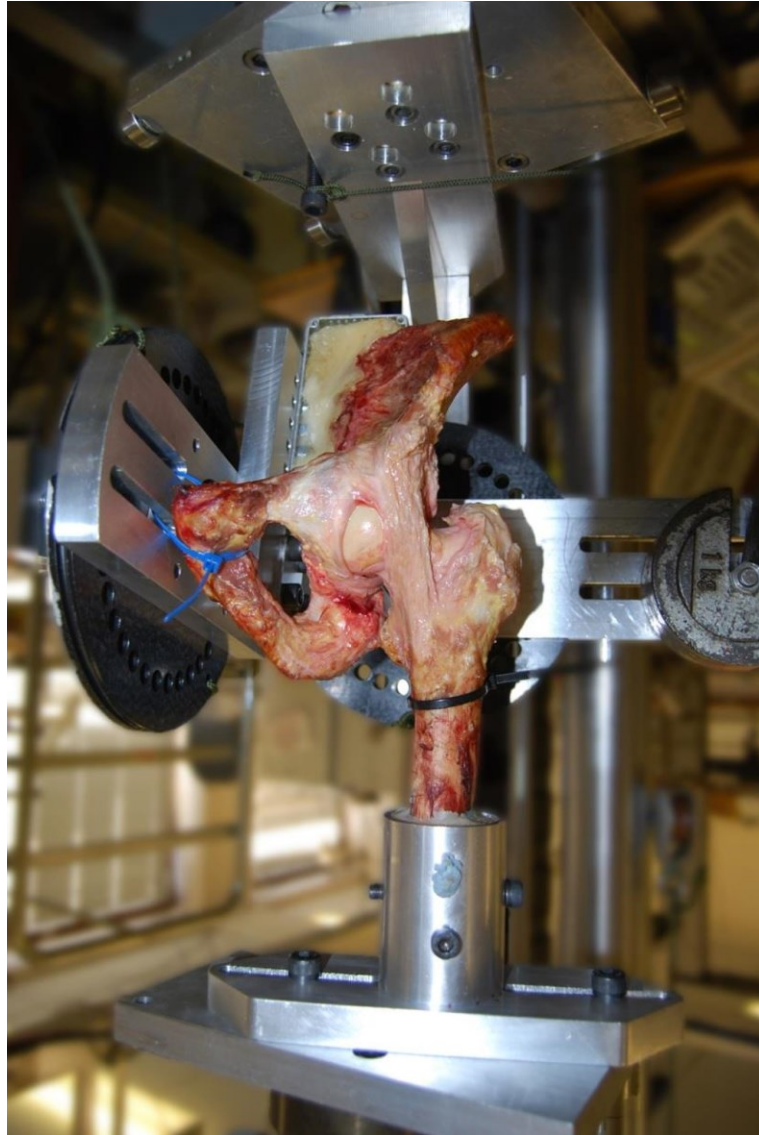


Figure 7.1 Anterior view of a left hemipelvis mounted in the custom built testing rig.

The hip is in neutral ad/abduction, extension and external rotation and all capsular ligaments have been resected except for the medial iliofemoral ligament which can be seen to be taut.

### *7.2.2 Testing protocol*

Specimens were preconditioned with ten internal/external rotation cycles as described in chapter 6 (page 108). For each specimen, the range of motion with the joint capsule intact was established by applying 5 Nm flexion/extension torques with the hip joint in neutral rotation and ab/adduction to define angles of maximum hip flexion (FLX) and extension (EXT). Then, with the joint still in neutral rotation, 5 Nm ab/adduction torques were applied at different positions of hip flexion (EXT, F0°, F30°, F60°, F90° and FLX) to define maximum hip adduction (ADD) and abduction (ABD) at each of the six flexion angles. Finally, 5 Nm torques were applied in external/internal rotation at all different positions of the hip (ADD, A0° and ABD at all six flexion/extension angles) to define maximum hip internal and external rotation (IR and ER respectively) for all 18 positions.

Importantly, throughout testing, the joint was never rotated beyond the angles determined by these initial 5 Nm passive resistance boundaries such that when a ligament was resected, the remaining ligaments did not experience increased strain.

One of the following ligaments was then resected: pubofemoral, medial arm of iliofemoral, lateral arm of iliofemoral, ischiofemoral or the ligamentum teres. The method used to identify and cut ligaments with shared origins and insertions is described in detail, with accompanying step-by-step pictures, in appendix A7.1 (page 257). For each of the 18 angular positions of flexion/extension and ab/adduction, the torque required to rotate the joint back to the intact IR and ER angular positions was measured. This process was then repeated after cutting another ligament until no ligaments remained. With all the ligaments resected, the passive resistance caused by labral impingement was measured in the same way. The cutting order for the capsular ligaments was varied such that each ligament was cut first and last at least once in different specimens with no pattern to the cutting order, however the intra-articular ligamentum teres had to be resected after the capsular ligaments as the joint had to be dislocated to access it. The principle of superposition was used to determine the contribution of each ligament and the labrum to rotational restraint by calculating the negative change in passive resistance torque after a ligament was cut as a percentage of the intact passive resistance (5 Nm) (Amis and Dawkins, 1991; Xerogeanes et al., 1995). This method of measuring ligament functions in a native joint is described in detail in 2.7.2 (page 47).

Pilot testing showed that in some cases the native hip could dislocate after resecting the capsular ligaments for some of the positions tested. If no capsular ligaments remained and adjacent non-dislocating trials had zero passive rotation resistance, a zero value was assumed for the dislocating trial as well. When this was not the case, subsequent measurements were taken by running the vertical axis of the servo-hydraulic machine in position control (instead of load control). This resulted in small fluctuations of the otherwise constant applied force (variations of 70-110 N and 20-32° in magnitude and angle respectively). In total, dislocation affected 5/9 hips but only 2.8 % (52/1836) of the measurements made.

Following all testing, all soft-tissue were resected and morphological measurements were made as outlined in section 6.2.3, page 108.

### *7.2.3 Statistical Analysis*

Internal and external rotation contributions analysed as separate dependent variables in SPSS version 21 (SPSS Inc., Chicago, Illinois). A Shapiro-Wilk's test of normality

## CHAPTER 7

was performed on the data's Studentized residuals. Normal data were analysed using a two-way repeated measures analysis of variance (RMANOVA) with independent variables of soft tissue state and hip position. Post hoc one-way RMANOVAs and paired t-tests with a Bonferroni correction were applied when differences across tests were found. The significance level was set to  $p < 0.05$ . For data which violated normality, non-parametric Friedman tests were used instead of RMANOVAs, and Wilcoxon Signed-Rank tests replaced the post-hoc t-tests.

Two analyses were performed: firstly, the contributions of extra- and intra-articular tissues (capsule, labrum and ligamentum teres) were compared against each other to determine their relative importance. Secondly, the effects of cutting the soft tissues (iliofemoral medial/lateral arms, ischiofemoral, pubofemoral, labrum and ligamentum teres) were examined to determine where each tissue made a significant contribution to rotation restraint.

A primary restraint was defined in each position as the tissue with the greatest statistically significant mean passive resistance contribution, and secondary stabilisers as any other ligaments with statistically significant mean contributions greater than 10 %. This 10 % figure is twice the root mean squared measurement error which is calculated in appendix A7.2 (page 257).

### 7.3 Results

External rotation data for one female specimen was lost due to a pull-out failure of the lateral iliofemoral ligament at its femoral attachment under the 5 Nm external rotation torque when the hip was in a position of full flexion and full abduction. A technical error lead to over-torqueing (close to 20 Nm), ligament rupture and persistent dislocation in another hip prevented collection ligament cut data in another female specimen. Thus, the results presented are for 8 specimens in external rotation and 9 specimens in internal rotation totalling 1836 torque measurements. Morphology measurements for these specimens are given in. An example of the resistive torque measured for a specimen in a single position as the ligaments were cut away is given in Figure 7.2.

For each hip position, it was found that approximately 1-in-12 of the measurement sets violated normality. To test the impact of these few violations of normality on the parametric RMANOVA and t-test results, both the parametric and non-parametric analysis were performed. Almost identical statistical differences were detected was found for both methods and so only results from the parametric tests are presented (RMANOVAs and t-tests) (Lund-Research-Ltd, 2013).

Table 7.1 Morphological measurements of the nine hips included in the data analysis.

Measurement	Mean $\pm$ S.D.	Range
Age	76 $\pm$ 9	61 to 89
Femoral head diameter (mm)	50 $\pm$ 5	43 to 57
Femoral anteversion ( $^{\circ}$ )	9 $\pm$ 10	-6 to 23
Femoral neck-shaft angle ( $^{\circ}$ )	130 $\pm$ 8	112 to 140
Femoral offset (mm)	36 $\pm$ 9	24 to 46
Femoral head/neck ratio	1.37 $\pm$ 0.07	1.29 to 1.49
Femoral anterior neck offset ratio	0.18 $\pm$ 0.02	0.15 to 0.21
Femoral alpha angle ( $^{\circ}$ )	51 $\pm$ 7	40 to 64
Femoral beta angle ( $^{\circ}$ )	45 $\pm$ 4	37 to 50
Acetabular centre edge angle ( $^{\circ}$ )	42 $\pm$ 9	32 to 57
Acetabular depth/width ratio	284 $\pm$ 32	254 to 348

### 7.3.1 Contributions of the capsular ligaments (combined), ligamentum teres and labrum

The capsular ligaments provided primary internal and external rotation restraint throughout a complete range of hip motion (Figure 7.3), protecting the hip from labral impingements. The contribution of the ligaments was greater than that from the labrum and ligamentum teres in all hip positions ( $p < 0.05$ , all  $\eta_p^2 > 0.686$ ); full tables for the post-hoc analyses are given in appendix A7.3 (page 260). Labral impingements only provided secondary restraint in the native hip and only when it was positioned in: high flexion ( $\geq 60^{\circ}$ ), full abduction and internal rotation; in low flexion ( $\leq 30^{\circ}$ ), full abduction and external rotation; or in extension, any ad/abduction and external rotation (Figure 7.3). The ligamentum teres also had a small secondary role restraining external rotation when the hip was in high flexion ( $\geq 30^{\circ}$ ) with neutral/full adduction (Figure 7.3).

### 7.3.2 Contributions of the individual capsular ligaments

The contribution of the capsular ligaments was not uniform: the ischiofemoral ligament provided primary internal rotation restraint in more than half the tested positions and was particularly prominent in high flexion ( $\geq 30^{\circ}$ ), adduction and internal rotation, or low flexion ( $\leq 30^{\circ}$ ), abduction and internal rotation (Figure 7.4). The iliofemoral ligament provided primary external rotation restraint in all hip positions, and both primary internal and external rotation restraint when the hip was extended or in neutral hip flexion (Figure 7.4). The medial arm of the iliofemoral ligament dominated in neutral flexion or extension, and the lateral arm in all other positions (Figure 7.4). The pubofemoral ligament only contributed to rotational restraint when the hip was fully abducted, contributing to external rotation restraint in extension, and internal rotation restraint in

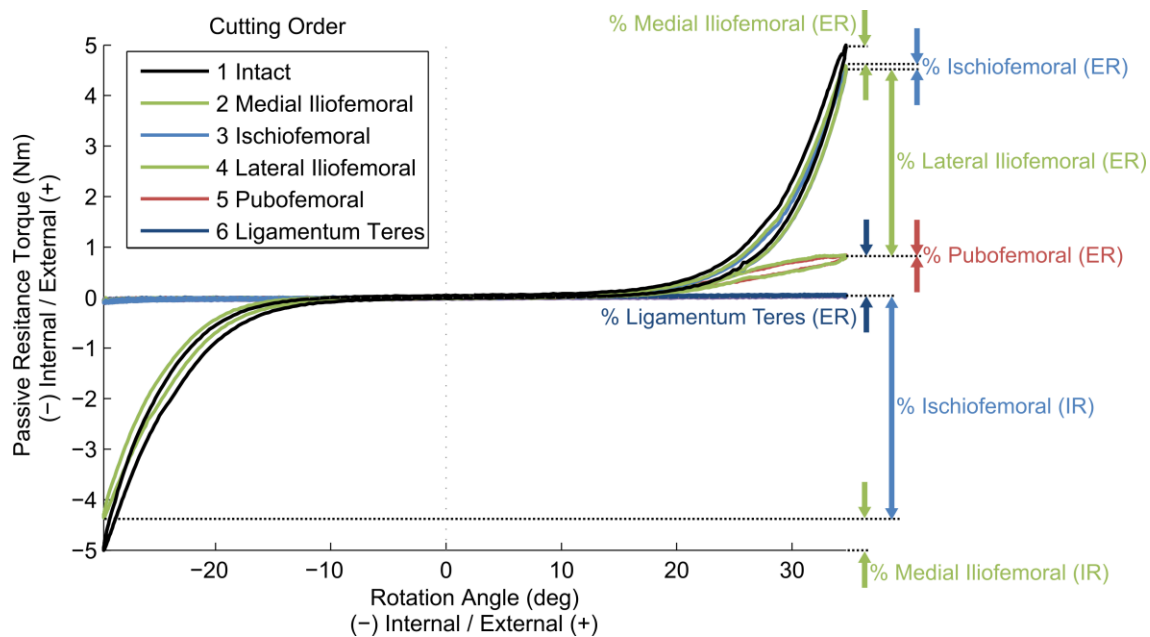


Figure 7.2 An internal/external rotation cycle showing the change in torque as different ligaments are resected for one specimen positioned at 60° flexion and full adduction.

The graph shows data exported directly from the material-testing-machine; there has been no filtering or smoothing function applied. Percentage changes not labelled (including the labrum) all lie on the zero torque axis. It can be seen that cutting the ischiofemoral and lateral iliofemoral ligaments caused the largest drops in internal and external passive rotation resistance respectively.

hip flexion (Figure 7.4). An extensive array of high resolution photos of all the ligaments in their functional positions is included in appendix A7.4 (page 262-268).

### 7.3.3 Subluxation and dislocation

Dislocations were only recorded in high flexion ( $\geq 60^\circ$ ) with neutral/full adduction and only after resection of the ischiofemoral ligament, indicating that tension in this ligament as it wrapped around the femoral head provided a net force that restrained the head from subluxing out of the acetabulum (Figure 7.5). For one hip, dislocation occurred in high flexion and adduction after resection of the joint capsule but stopped occurring following resection of the ligamentum teres; the ligamentum teres was wrapping around the posterior femoral head in external rotation causing the head to sublux laterally and inferiorly out of the acetabulum in a sling-shot like mechanism. This specific hip had an unusually high percentage contribution to external rotation from the ligamentum teres, however non-dislocating subluxations caused by the ligamentum teres in high flexion and adduction were also observed in other hips following resection of the joint capsule; appendix A7.5 (page 268) illustrates this subluxation with photographs.



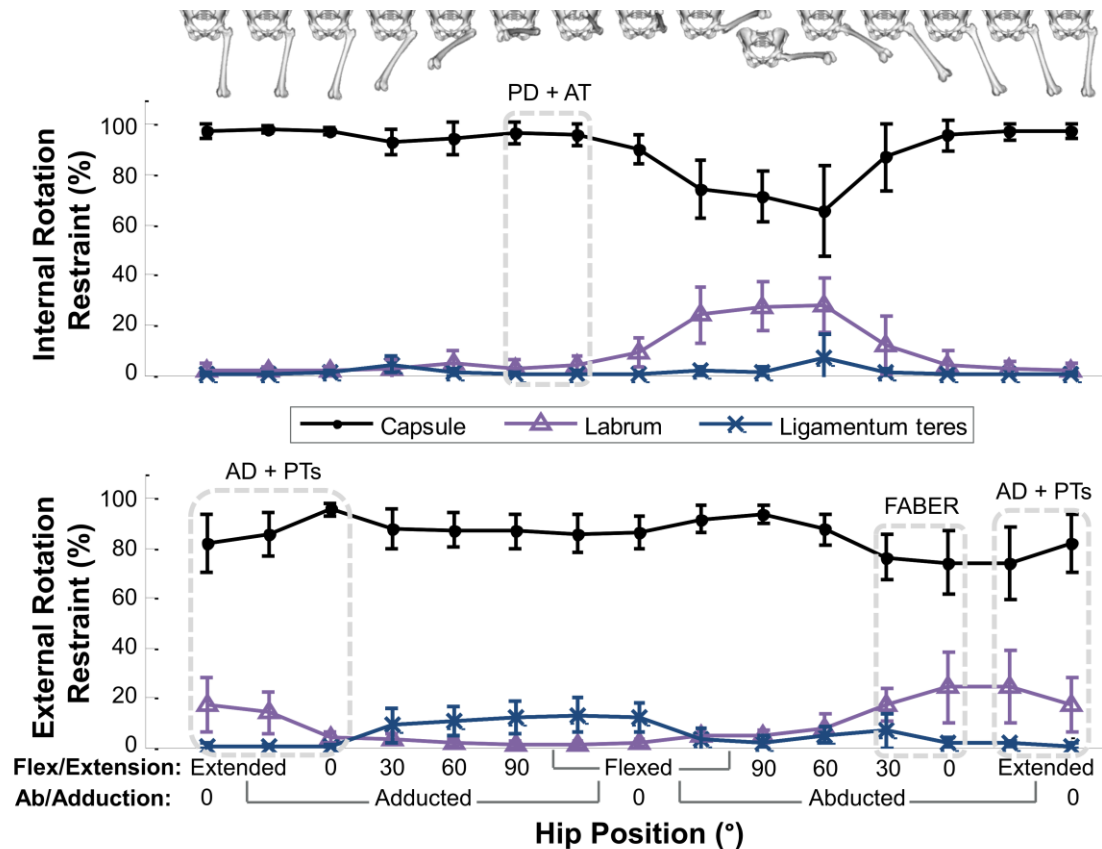


Figure 7.3 Mean percentage internal and external rotation restraint with 95 % confidence intervals provided by the hip capsule, labrum and ligamentum teres for a complete range of motion.

The hip images illustrate the positions on the x-axis. The dashed boxes highlight at risk positions for THA anterior/posterior dislocation (AD/PD),<sup>12</sup> and physical tests for FAI including the: anterior impingement test (AT), hyperextension, log-roll and posterior impingement tests (PTs) and the end point of a FABER test (Tijssen et al., 2012).

## 7.4 Discussion

This is a small cadaveric study, so conclusions can only be applied clinically with caution. However, we show a difference in importance between structures, overturning the null hypothesis with confidence.

### 7.4.1 Most important findings

Capsular ligaments provide primary rotational restraint and prevent labral impingements around the limits of a complete range of hip motion (Figure 7.3). Within the capsule, the ischiofemoral and iliofemoral ligaments are the dominant restraints for internal and external rotation respectively, accounting for more than two thirds of the possible hip positions (Figure 7.4). The ischiofemoral ligament also cradles the femoral head in deep hip flexion, stabilising the hip against posterior subluxation and dislocation (Figure 7.5). Damage to these two ligaments in particular could be a cause of labral impingement, hip instability or damaging loads to the cartilage. These

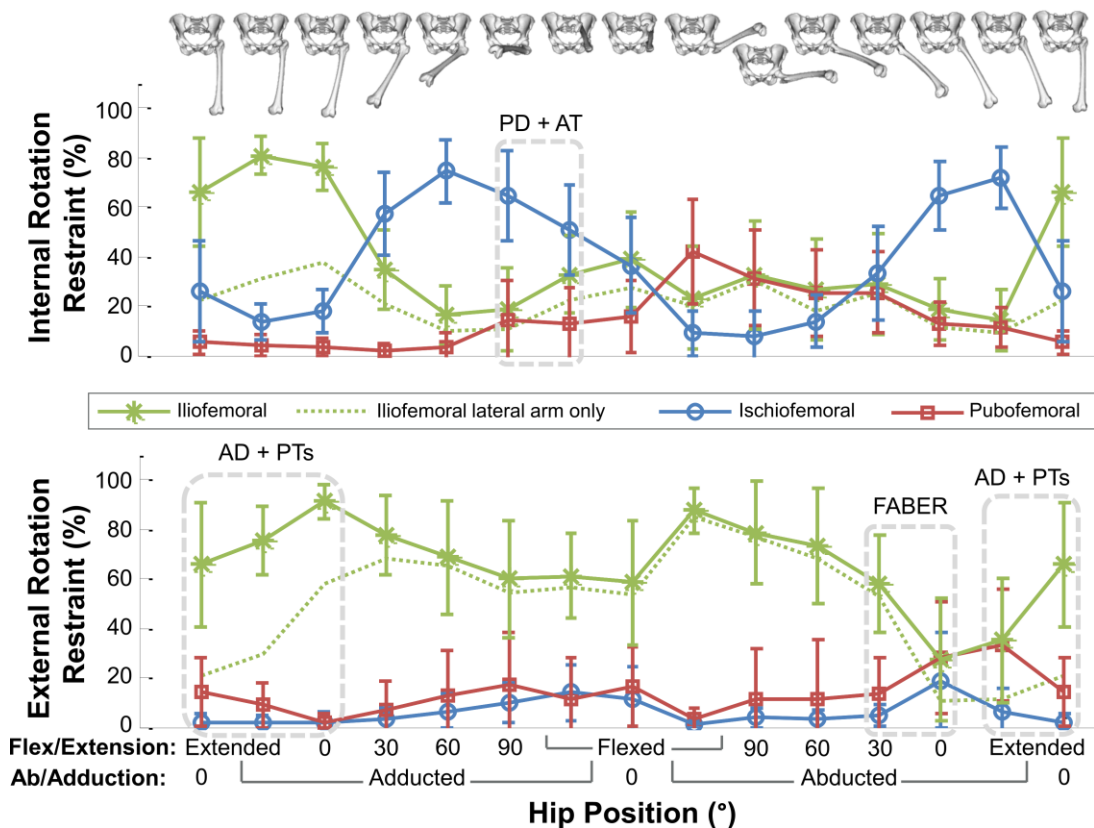


Figure 7.4 Mean percentage contributions to internal (top) and external (bottom) rotation restraint with 95 % confidence intervals provided by individual capsular ligaments for a complete range of hip motion.

The hip images illustrate the hip positions on the x-axis and the dashed boxes are equivalent to those presented in Figure 7.3.

ligaments should be a priority during surgery to maintain/restore normal hip mechanics, with their functional significance born in mind if early restoration of function is a priority.

Labral impingement only contributed to resisting hip rotation in a limited number of positions by providing a soft buffer against bony impingement. These labral impingements triggered small subluxations of the femoral head out of the acetabulum. However, the restraint provided by the labrum was always less than the sum of contributions from the capsular ligaments (Figure 7.3). Thus the capsule protects the labrum against the full force of impingement by providing most of the rotational restraint. Release of the posterosuperior capsule at hip arthroscopy could therefore increase the postoperative load on the labrum.

The ligamentum teres has a small role in limiting external rotation, but its contribution is considerably less than that of the lateral iliofemoral ligament (Figure 7.3), indicating that repair of the ligamentum teres to restore native restraint should only be considered second to repair of any deficiencies in the anterior joint capsule. In the complete absence of the joint capsule, the ligamentum teres can wrap around the femoral head and cause a destabilising subluxation in high flexion, adduction and external rotation,

potentially leading to dislocation. Thus, with the capsular ligaments intact, this destabilising subluxation caused by ligamentum teres tension will be resisted by opposing tension from the capsular ligaments resulting in a very stiff joint with high passive stability.

#### 7.4.2 Limitations

By skeletonising the hip, this study was limited to measuring the contributions of the capsular ligament, ligamentum teres and the labrum only and not any resistance caused by other soft tissues such as muscles/fat. This study only included a small number of specimens and while visual observation suggested subjectively that the primary restraints for both male and female hips were similar (see appendix A7.6, page

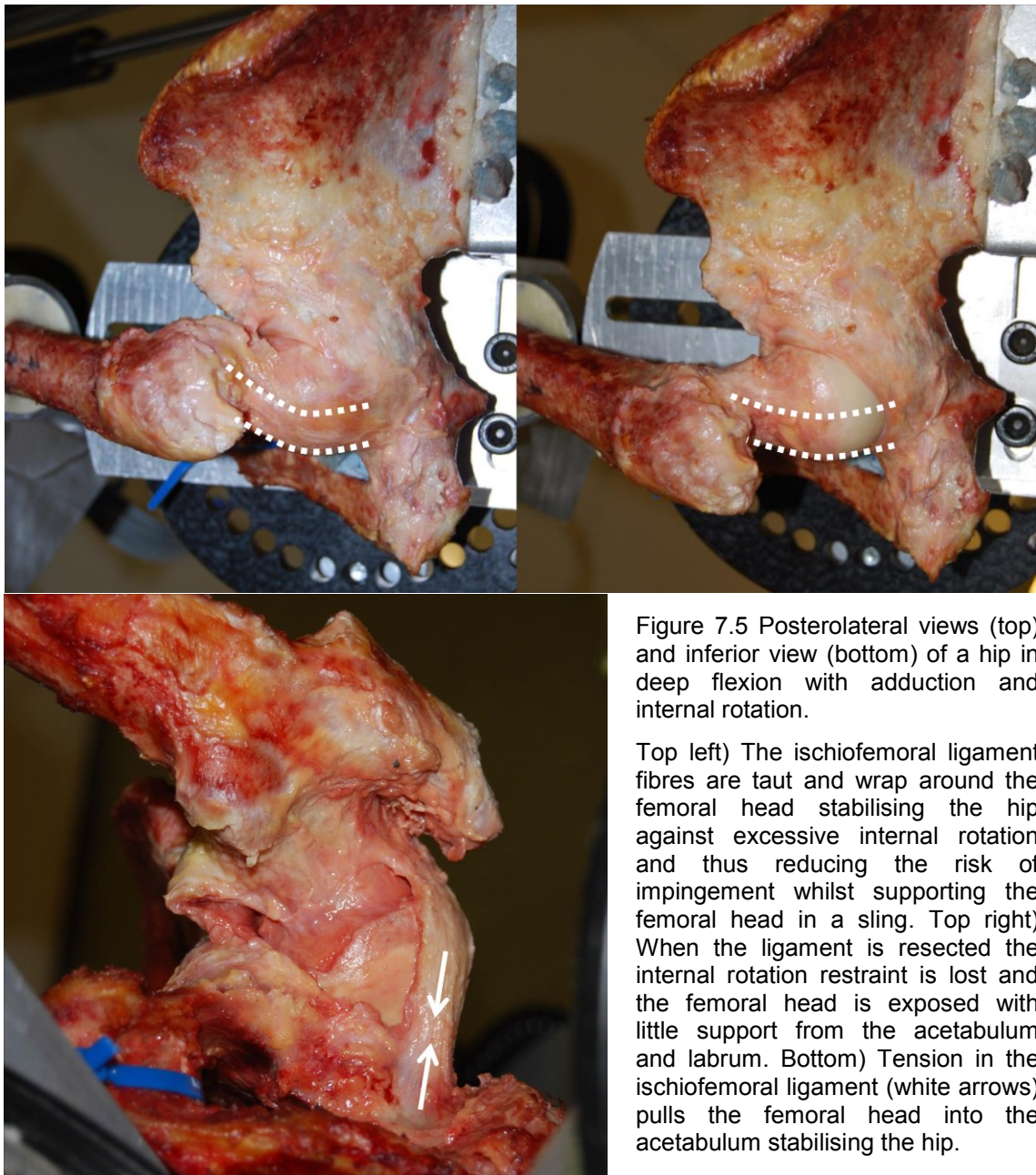


Figure 7.5 Posterolateral views (top) and inferior view (bottom) of a hip in deep flexion with adduction and internal rotation.

Top left) The ischiofemoral ligament fibres are taut and wrap around the femoral head stabilising the hip against excessive internal rotation and thus reducing the risk of impingement whilst supporting the femoral head in a sling. Top right) When the ligament is resected the internal rotation restraint is lost and the femoral head is exposed with little support from the acetabulum and labrum. Bottom) Tension in the ischiofemoral ligament (white arrows) pulls the femoral head into the acetabulum stabilising the hip.

269), larger numbers would be needed to draw a significant conclusion on any differences between the genders. We also only modelled a single compressive loading condition whereas in-vivo the magnitude and direction of this force varies for different activities (Bergmann et al., 2001) and could act to increase/decrease subluxation and loading on the labrum. Another limitation is that the technique of superposition requires the kinematics to be exactly repeated so that all tissues experience the same strain though however we did not control translations; indeed, the hip dislocated after resecting the ischiofemoral ligament. The effects of this limitation on the conclusion are likely to be small for a number of reasons: firstly, this study primarily draws conclusions about rotational restraint and angular position was tightly controlled. Secondly, the distance the ligaments' femoral insertions moved due to the arc of rotation will have been greater than the translation within the hip which other studies have measured to be small (1-2 mm) during rotation movements similar to those applied in this study (Myers et al., 2011); thirdly, the translations would have occurred in response to the applied load and the loading direction used in this experiment was representative of common hip joint activities (appendix A6.2, page 244). Moreover, in nearly all hip positions (except for those where the hip dislocated), the applied load would have forced the hip to be concentric and the hip approximates well to a ball and socket joint thus minimising translations (Cereatti et al., 2010). Finally, we randomised the cutting order which means that all capsular ligaments had equal opportunity to influence the results.

The results also assume that the ligaments were in the linear and not the toe-region of their torque-rotation curve because the principal of superposition is only valid in this elastic, linear region. The data analysis involved plotting all the torque-rotation data to verify that the gradient measurements in chapter 6 were calculated correctly by the MatLab script. These plots confirmed that the ligaments were indeed in this linear region when the capsule was intact (Figure 7.2). Moreover, the results were highly repeatable when multiple load cycles were performed, an example is shown in figure (Figure 6.2, page 110). However, in some cases, the secondary or tertiary restraints were not linear region, particularly when the contribution was low (<10 %) or when the labrum impinged and hence this is a limitation of the research. Importantly, the measurements based on the entire capsule, and those for the primary restraints, were in the linear region.

Finally, this study was also limited in that the tests were performed on cadaveric specimens with a mean age higher than that of patients undergoing hip arthroscopy so the true contribution of the ligamentum teres in these patients may be higher than

measured here as it can degenerate with age (Tan and Wong, 1990). An intact capsule was necessary for ligamentum teres tension to develop without subluxation, and so our measurement of ligamentum teres contributions may be artificially reduced due to cutting order bias, having always been resected after the capsular ligaments for practical reasons.

#### *7.4.3 Comparison with published research*

For the joint capsule, these results agree with a laxity based cadaveric model which quantified their function in low flexion/extension (Martin et al., 2008). They also agree with a detailed anatomical description of where the ligaments are taut throughout a complete range of motion (Fuss and Bacher, 1991). For the labrum, the results corroborate a study which found that it only provides secondary stability in low hip flexion/extension, with primary stability coming from the iliofemoral ligament (Myers et al., 2011). The position of deep flexion, full abduction and internal rotation where labral impingements were recorded in this study correlate well with those measured in ballet dancers with normal hip anatomy and normal passive range of hip motion during extreme dancing positions (Charbonnier et al., 2011). For the ligamentum teres, the findings support some results from a simple string model (Martin et al., 2012) and arthroscopic observations that it tightens in flexion, adduction and external rotation (Kelly et al., 2003). Recent work also suggested that it has a role in preventing hip subluxation in high flexion and abduction, and low flexion/extension and external rotation (Kivlan et al., 2013; Martin et al., 2013) in these positions we found that indeed the hip was at risk of impingement and subluxation (Figure 7.1) but did not find that the ligamentum teres provided consistent rotational restraint.

#### *7.4.4 Clinical relevance*

The iliofemoral ligament may be cut during FAI treatment when performed by either open (Leunig and Ganz, 2014) or arthroscopic (Domb et al., 2013) surgery. Some reports indicate that hip instability is not a problem after these procedures (Ilizaliturri, 2009), while others have found that capsular defects (McCormick et al., 2014) and instability (Philippon et al., 2007d) are common in patients requiring revision hip arthroscopy and that postoperative subluxations are underreported (Domb et al., 2013). The current study did not find an increase in dislocation risk after resection of the iliofemoral ligament, but the loss of primary external rotational restraint across the complete range of motion (Figure 7.3) could increase the load on the labrum through impingement in extension or abduction which may be perceived as pain and lead to subluxation, and we have not measured the hip in an unloaded environment, where

conditions may be more severe. Thus, we advocate repair of the capsular ligaments during early intervention surgery to reduce the risk of hip subluxation and labral overloading. This is particularly relevant when treating dysplastic hips, or trimming the rim of the acetabulum to treat FAI with a cam-pincer diagnosis (Masjedi et al., 2013) because an insufficient acetabulum increases the risk of hip instability (Benali and Katthagen, 2009; Ilizaliturri, 2009; Mei Dan et al., 2012).

The internal rotation restraint and supporting sling protecting against subluxation (Figure 7.4 and Figure 7.5) offered by the ischiofemoral ligament in deep hip flexion would benefit THA patients by passively stabilising the hip in a position where few muscles have favourable lines of action (chapter 3). This reduces the risk of dislocation but could also prevent posterior edge loading of THA that, by damaging the bearing surfaces, has been identified as a causative factor in ceramic hip squeaking (Esposito et al., 2012). This benefit will increase with increasing bearing couple sizes: less subluxation means less edge loading (De Haan et al., 2008a) but also a reduction in the pumping action which potentially expels joint fluid and edge loading wear debris into neighbouring soft tissues (Wroblewski et al., 2012). This study therefore supports repair of the ischiofemoral ligament after using a posterior approach for THA, particularly if a larger diameter bearing couple is used.

### *7.4.5 Conclusion*

In conclusion, the iliofemoral and ischiofemoral capsular ligaments are important passive rotational restraints to hip motion. The integrity of these ligaments appears to be important for maintaining normal hips mechanics and preventing excessive hip rotation. Preservation of them may prevent both impingement and hip instability.

## **7.5 Acknowledgements**

This study was funded by the Wellcome Trust and EPSRC [088844/Z/09/Z] and the Institution of Mechanical Engineers. The dual-axis Instron materials-testing-machine was provided by an equipment grant from Arthritis Research UK.

## **8 Discussion**

### **8.1 Most important findings**

The most important finding of this PhD was that the active and passive soft-tissues have complementary functions that help protect the hip from subluxation, edge loading and dislocation. In the mid-range of hip motion, all the hip muscles' lines of action were found to point inbound, within the acetabular rim, and thus could contribute compressive hip forces that would keep a femoral head concentric with an acetabular cup (chapter 3). In these hip positions, the hip was found to be within the ligaments' slack region with no passive contribution to hip motion (chapter 6). This would allow a hip to move freely under the action of the hip muscles resulting in efficient yet stable hip motion. However, at the extremes of the range of hip motion, where impingement could occur and where up to 50 % of the muscles were found to have unfavourable lines of action that could encourage edge loading or even dislocation (chapter 3), the hip ligaments were found to become taut and restrain excessive hip movement (chapter 6). This passive restraint could help protect the hip from subluxation, edge loading and dislocation in three ways: firstly, by preventing the hip from moving into positions where muscle lines of action were unfavourable. Secondly, by restraining excessive movements that could cause impingement, lever-out and subluxation of the femoral head out of the acetabulum. Thirdly, by contributing a stabilising force that helps maintain a joint reaction force that is inbound and away from the acetabular rim, though further work is needed to verify this. The ischiofemoral and iliofemoral ligaments were identified as the most important passive soft-tissues for maintaining this natural passive restraint (chapter 7). Indeed, cutting the ischiofemoral ligament alone was sufficient to destabilise over half of the hip joints tested to the point where dislocation occurred (chapter 7). Therefore, it is recommended that the ischiofemoral and iliofemoral ligaments should be protected or repaired during any intra-articular hip surgery where impingement, subluxation/micro-separation, edge loading or dislocation is a concern. This includes joint preserving hip surgery to treat abnormal hip shapes in young adults as well as hip replacement procedures.

### **8.2 Limitations**

A combination of computational and experimental methods was used to investigate different aspects of hip mechanics throughout the range of hip motion. Individual limitations for each study are discussed extensively in the main chapters and include: using geometrical analyses based on simplified muscle architecture and wrapping



## CHAPTER 8

mechanics (chapter 3), using a testing rig that could fail under high physiological loads (chapter 4), using synthetic bones to validate cadaveric testing methodology (chapter 5), using a small number of elderly cadaveric tissue samples to draw conclusions at the population level (chapters 6 and 7) and skeletonising test specimens thus ignoring passive restraint from other soft tissues such as skin, muscles and fat (chapter 7). In addition to these limitations, it should also be noted that the musculoskeletal model was used to study an artificially replaced hip whereas the in-vitro model studied the native hip and results for a native/replaced hip may not be directly comparable.

These individual limitations also highlight the largest overall limitation: all the methods used (both computational and experimental) are modelling techniques and hence represent simplified cases of the true *in vivo* scenario. Therefore, results should be applied clinically with caution until the findings can be verified with appropriate clinical research. Indeed, to date the clinical evidence supports the findings from these studies, for example, capsular repair improves outcomes following both joint preservation (Frank et al., 2014) and hip replacement surgery (Kwon et al., 2006), but more evidence is needed until decisive conclusions can be drawn about all aspects of the research, particularly in the role of certain muscles/ligaments in preventing edge loading.

### 8.3 Comparison to clinical research

Edge loading and high wear has been identified in the majority of hard hip replacement retrievals, including metal-on-metal hips revised for pseudotumours (Kwon et al., 2010), and ceramic-on-ceramic hips revised for a number reasons (Esposito et al., 2012). However, the majority of this wear is reported in the absence of impingement (Esposito et al., 2012) and is believed to occur primarily in deep flexion (Walter et al., 2004). The finding that muscle lines of action are unfavourable in these hip positions provides a possible mechanism for this high reported wear (chapter 3). An exception for this is metal-on-metal devices which could wear during gait (Kwon et al., 2012; Mellon et al., 2013). Indeed, the results suggest that the gluteus medius and minimus could have important roles in preventing this wear mechanism and provides an interesting avenue for future research (see chapter 9).

For hip replacement patients, it is well known that repairing/protecting the posterior soft-tissues can help prevent dislocation (Chiu et al., 2000; Kwon et al., 2006; Kumar et al., 2014). This is corroborated by results from this thesis which found that the capsular ligaments tauten and wrap around the femoral head in this position restraining the hip



against excessive movements, and potentially providing protection against subluxation (chapters 6 and 7).

Finally, recent evidence from joint preserving surgery suggests improved outcomes when patients receive an anatomical repair of the iliofemoral ligament during surgery (Frank et al., 2014). What is more, cases of dislocation are only reported when the ligament has been damaged (Matsuda, 2009; Ranawat et al., 2009; Sansone et al., 2013; Austin et al., 2014) and patients who require revision hip arthroscopy have been found to have capsular laxity/defects (Philippon et al., 2007d; Frank et al., 2014; McCormick et al., 2014). These clinical observations are supported by the research conducted for this thesis which shows that the iliofemoral ligament, which is cut during both open and arthroscopic early intervention techniques, is the primary restraint for nearly all external rotation, and some internal rotation movements (chapter 7).

#### **8.4 Innovative methodology developed**

To identify the most important findings, this PhD necessitated the development of new methodologies that could be useful for future work. This included the design and validation of a six-degrees-of-freedom in-vitro testing system that allowed for application of torques/rotations in all three rotatory degrees of freedom whilst applying loading in a physiological direction (chapter 4). Importantly, the testing system recreated the ISB coordinate system allowing easy translation of the results to a clinical (and a modelling) environment (chapter 5). This rig was instrumental in adapting well established techniques developed for knee research (section 2.7.2) to the hip for the first time (chapters 6 and 7). This thesis also extended the use of established musculoskeletal models using a new geometrical approach to allow investigation of hip mechanics for activities with unmeasured/unknown hip loading/kinematics (chapter 3). This methodology was not intended to replace existing optimisation techniques, but provided a useful complimentary technique.

#### **8.5 Research impact**

This research has been well received both academically and with clinicians. A highlight of the work was receiving the Student Biomechanics Award for the work presented in chapter 7 at ISTA 2014. The research won the award with a unanimous vote from the judging panel which included leading clinicians and academics. This helped demonstrate the rigor, timeliness and relevance of the work. In addition to this award, two original research articles, a review article, six international conference podium presentations, a conference poster presentation and a book chapter have been published based on work presented in this thesis. The greatest success however could

## CHAPTER 8

come in ten years' time if this work plays even a small role in influencing clinical practise and results in the improved treatment of hip disease and better outcomes for patients.

### **8.6 Conclusion**

Passive restraint from the hip ligaments have an important, complementary role to the hip muscles which together enable normal hip mechanics and help protect the hip from adverse loading conditions such as edge loading. Therefore, the ischiofemoral and iliofemoral ligaments should be protected and/or repaired during normal hip surgery to help maintain/restore normal hip function in the native or replaced hip.

## 9 Future Work

### 9.1 Muscle contribution to edge loading

#### *9.1.1 The effect of surgery on the muscle contribution to edge loading*

Both lateral and posterior approaches, the two most common surgical approaches for hip replacement surgery (Masonis and Bourne, 2002; NJR, 2011), damage muscles which have lines of action that could protect against edge loading: the gluteus medius and minimus, and the short external rotators (Figure 3.3, page 61). Conversely, an anterior approach does not (Lovell, 2008). It would be interesting to conduct further research into the model to see how these surgical approaches could affect edge loading risk. This research could be conducted by recording movement kinematics and ground reaction forces in a matched-cohort of patients who have undergone different surgical approaches and using this to calculate muscle forces and the joint reaction force using a musculoskeletal model and an optimisation routine. The line of action of this force could be used to calculate the joint reaction force and this could be used to calculate the risk of edge loading for these activities using a method similar to that presented in Chapter 3 and by Mellon et al. (Mellon et al., 2013). The accuracy of such an experiment would depend greatly on the muscle physiological cross sectional areas used in the model and hence an ideal experiment would measure these for key-muscle using post-operative imaging and develop patient specific models (Neal and Kerckhoffs, 2010).

Alternatively, muscle weakness could be introduced into the musculoskeletal models by changing the muscles maximum isometric contraction force and investigating how this affects the optimisation solution. This approach is explored in greater detail in the following section.

#### *9.1.2 The protective effect of gluteus medius activity*

Chapter 3 demonstrated that the gluteus medius and minimus, the primary hip abductors, never contribute to edge loading, whereas the distally inserting tensor fascia lata, a hip flexor and abductor (Dostal et al., 1986), could contribute to superior edge loading if the cup is orientated with high inclination. Thus if gluteal weakness was compensated for with increased activity in the tensor fascia lata then there could be an increased risk of superior edge loading following total hip replacement.

This has clinical relevance as the gluteus medius and minimus are damaged during a lateral approach (Masonis and Bourne, 2002), which accounts for one third of all hip

replacement procedures (NJR, 2013). A strong association between gluteal deficiency, abductor weakness and symptomatic gait adaptations has been reported by many authors (Perron et al., 2000; Bach et al., 2002; Madsen et al., 2004; Foucher et al., 2007; Mont et al., 2007; Grimaldi et al., 2009; Beaulieu et al., 2010; Ewen et al., 2012; Zeni et al., 2014) and recent evidence suggests that differences in gait could affect the risk of edge loading (Mellon et al., 2011; Kwon et al., 2012; Mellon et al., 2013). Consequently rehabilitation strategies to improve abductor strength are well established (Vaz et al., 1993) and thus should gluteal weakness be associated with an increased risk of edge loading then this could provide a new non-operative treatment strategy to try and minimise the risk of excessive edge loading wear in metal-on-metal hip replacements.

A compensatory mechanism substitution for gluteal weakness with a tensor fascia lata is plausible as it is known cause of iliotibial band syndrome in runners (Fredericson et al., 2000). Moreover, anatomy research suggests that whilst both muscles can abduct the hip, the gluteus medius and minimus are better aligned to stabilise the hip whilst the tensor fascia lata muscle is at a mechanical advantage to balance bodyweight (Gottschalk et al., 1989). Therefore, it is hypothesized that weakness in the gluteus medius and minimus would result in increased activity in the tensor fascia lata muscle to compensate for the loss in abductor moment.

A simple pilot study was conducted to confirm whether this hypothesis warrants further study or not and is described in detail in appendix A3.9 (page 201). It found that increased activity in the tensor fascia lata was needed to compensate for reduced force capacity in the gluteus medius when solving a musculoskeletal model for the same gait cycle. What is more, there was a small decrease in the angle the joint reaction forces makes with the edge of a well-positioned cup at heel strike demonstrating that a change in the optimum balance of muscle forces could lead to change in the direction of the joint reaction force. The difference detected was small but may be larger for other activities such as sit-to-stand. Whilst this pilot work has many limitations as described in the appendix (A3.9.3, page 202), it provides some preliminary data to support that the hypothesis warrants further work. This would ideally involve collecting kinematic and kinetic data for patients both with and without pathology during activities such as gait, stair climbing and sit to stand, and then inducing muscle weakness or strengthening as appropriate (combining this section with the previous, 9.1.1).

## 9.2 Capsular ligament research

### 9.2.1 Improvements to the rig and experimental set-up

There are a number of small improvements that could be made to the rig. For example, whilst the pulleys could be fixed to an accuracy of  $1^\circ$ , this required use of g-clamps as the rig only had screw-holes every  $10^\circ$ ; it would have been much quicker and easier with additional holes. Therefore, a smaller size hole, or staggered holes could be used to allow clamping at a finer resolution than  $10^\circ$ . The rig could also be improved by reducing the clearance on the clamping holes so that when clamped, there is no possible rotation. Re-building the rig out of stainless-steel would also serve to improve the rig as it would be stiffer (less translation at the level of the joint under an applied load) and could tolerate higher loads. However, by far the best improvement that could be made to the rig would be the addition of features upon which optical trackers could be mounted, or the addition of LVDTs, as commonly applied to knee ligament research (Stephen et al., 2012), to the x-z bearing table so that translation in the horizontal plane could also be tracked. This improvement could be taken one step further by combining CT-scans with optical trackers data to reconstruct the movements in a CAD model after the experiment; this method has been developed by Phil Noble's research group and would be a valuable addition to the rig method (Crawford et al., 2007; Dwyer et al., 2015).

### 9.2.2 Experimental measurement of ligament length changes and properties

LDVT's, or optical tracking and CAD reconstruction of the hip, could also be used to quantify ligament length changes during the testing. This would help address a limitation of Chapter 6 and 7 where only torque-rotation and not stress-strain curves were analysed. However, to fully calculate stresses and strains it is also necessary to know the ligament fibre lengths and cross-sectional areas. These measurements are challenging to take for the capsular ligaments as the shared origin and insertion points prevent simple resection of all the ligaments in a single specimen without risking damaging a neighbouring ligament (appendix A7.1, page 257). Previous research has attempted to do this (Hewitt et al., 2001; Hewitt et al., 2002), however it is unclear how (or even if) the authors circumnavigated this problem. Therefore, the goal of a future study could be develop appropriate methodology to reliably measure the fibre lengths and cross-sectional areas of all the capsular ligaments in the same specimen. If achieved, it would allow for not only the calculation of stress-strain curves for the intact joint, but also for accurate mechanical testing of the ligament properties to build on the

existing datasets from a limited number of specimens (Hewitt et al., 2001; Hewitt et al., 2002; Stewart et al., 2002).

### *9.2.3 Investigating the effects of surgical approaches on ligamentous restraint*

Another interesting extension of the capsular ligament research would be to combine a reconstructed 3D motion-tracked model (9.2.1) with measured mechanical properties of the ligaments (9.2.2) to develop a finite element/rigid body model of the capsular ligaments. This model could be validated against the data for the intact hip and then used to investigate the effects of hip surgery on passive restraint. This would be a great improvement over existing cutting edge research (Elkins et al., 2011b; Bunn et al., 2014) which relies on ligament data collect from a single study (Hewitt et al., 2002), and validation from a single movement (Chapter 7 shows that different ligaments are recruited to restrain different movements and hence a validation would need to encompass multiple movements).

### *9.2.4 Investigating the role of capsular ligaments following total hip arthroplasty*

Chapter 7 finds that the ischiofemoral and iliofemoral ligaments are primary restraints for hip internal rotation in deep flexion and external rotation in extension respectively. This is important with reference to hip arthroplasty as these are movements which expose the hip to a risk of dislocation. It would be interesting to test if a hip replacement can be manipulated to restore this advantageous native hip rotation restraint.

It is hypothesised that for a given angle of rotation, the capsular ligaments would offer less rotational restraint following total hip arthroplasty, even if perfectly repaired, due to the decrease in femoral head size affecting the mechanics of ligament wrapping. It is also hypothesized that increasing the femoral head size could thus restore more of the native restraint and similarly increasing femoral offset could act to tighten the ligaments and reduce the rotational restraint envelope to levels similar to the intact case; however increasing hip anteversion or valgus could serve to widen the rotational restraint envelope by effectively reducing femoral offset. These hypotheses could be tested using the set-up described in this thesis and thus provide an interesting avenue for further work. Such a test would measure the passive restraint envelope for a native hip (ideally with osteoarthritis as this is the leading indication for total hip replacement) before performing a total hip replacement with a modular hip stem. The passive restraint envelope could then be measured in the replaced hip for different levels of anteversion, varus/valgus, neck offset and head size by changing the modular components. The measured values could be compared to each other and the intact

case to determine which best restores native restraint. This model could also be used to assess the efficacy of soft-tissue repair strategies.

#### *9.2.5 Investigating the role of the capsular ligaments in hip stability*

Chapters 6 and 7 described the regions where the capsular ligaments are taut, and their relative contributions to rotational restraint and how this could affect impingement. However, an important function of the ligaments could also be to help stabilise the hip. Previous work suggested that capsule has an important stabilising role, resisting distraction of the hip in a neutral position (Ito et al., 2009; Smith et al., 2014), and controlling displacements when the hip is rotated in the absence of load (Myers et al., 2011; Safran et al., 2013) but more research is needed.

For example, chapter 6 found that the joint is relative slack in the position where existing experiments measure its resistance to distraction (Ito et al., 2009; Smith et al., 2014). It is hypothesised that as the capsular ligaments tighten at the limits of the range of hip motion, the joint will stiffen and thus provide greater resistance to distraction – the hip rig could be used to test this hypothesis.

Moreover, Figure 7.5 (page 133) shows visually how the ligaments wrapping around the femoral head could contribute a stabilising force even whilst the femoral head is concentric with this acetabulum. Indeed, the hip position for where this photo was taken (deep flexion with adduction) is also the position where chapter 3 found the highest number of muscles that could contribute to edge loading. Thus an important role of the capsular ligaments could be to contribute a force that helps keep the joint reaction force inbound and away from the edge of the acetabulum thus protecting the hip against edge loading in the absence of impingement. In other words, for the native hip passive stability may prevent edge loading in positions where it could occur from active muscular contributions. It is hypothesised that cutting the ischiofemoral ligament in deep flexion, adduction and internal rotation, and cutting the iliofemoral ligament in extension and external rotation will result in a force that is closer to the edge of the acetabulum as the beneficial force component from the ligaments is lost.

This hypothesis could be tested using computational modelling, however such a finite element model would be difficult to validate and hence could be unreliable for determining absolute contribution values. An interesting way to test this hypothesis experimentally could be to test the intact case using a similar protocol as described in chapters 6 and 7; however instead of using a test rig mounted in a dual-axis materials-testing-machine, apply known forces and torques in all six-degrees-of-freedom with a robotic actuator which could simultaneously record the exact kinematics for the

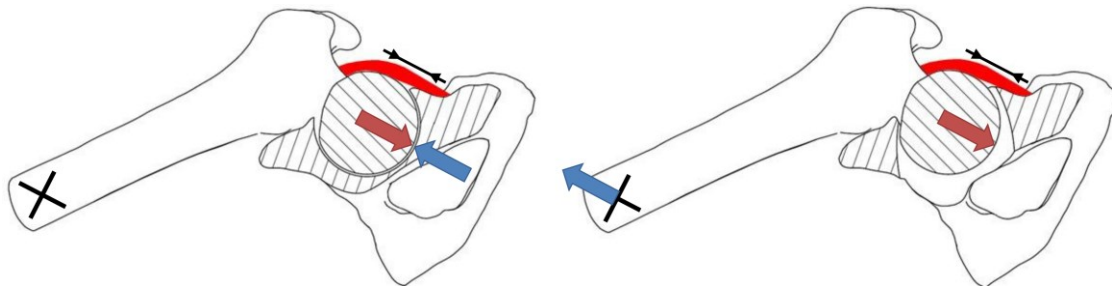


Figure 9.1 A diagram showing how a robotic actuator can be used to directly measure ligament forces by resecting the acetabulum.

Left) First, the robotic actuator (attached at point 'x') applies physiological torques to move the joint whilst recording the kinematics. The movement is such that the capsular ligaments become taut (black arrows) but any stabilising force generated by the ligaments (red arrow) is resisted by the acetabulum (blue arrow) and hence cannot be measured externally. Right) The robotic actuator repeats the learned movement exactly as before thus generating the same tension in the capsular ligaments (black arrows); however the acetabulum has been resected and hence the robot has to provide additional force to resist the stabilising forces generated by the ligaments and hence the force can be measured directly

movement. Then the acetabulum could be completely cut away using a burr tool and/or patient specific cutting guides through the medial side of the pelvis, thus leaving the femoral head and capsular ligaments intact. Then, if the recorded kinematics were exactly repeated, any forces recorded by the external load-cell would equal the contribution from the capsular ligaments because the equal and opposite reaction force from the acetabulum would have been removed (Figure 9.1). This allows for the capsular contribution to the joint reaction force to be measured directly. A key part of this method is to repeat the kinematics exactly and hence requires a full six-degrees-of-freedom robotic actuator with accompanying load cell instead of the two-axis servo-hydraulic machine used for this thesis.



## 10 Bibliography

Aalco-Metals-Ltd, 2013. Aluminium Alloy 6082 T6 Extrusion Datasheet (BS EN 755-2:2008). <http://www.aalco.co.uk/datasheets/> (Last accessed: 05/02/2015).

Aalco-Metals-Ltd, 2014a. Aluminium Alloy: EN Standards for Aluminium Extrusions. <http://www.aalco.co.uk/datasheets/> (Last accessed: 05/02/2015).

Aalco-Metals-Ltd, 2014b. Stainless Steel 1.4305 (BS 303S31) Bar Datasheet (BS EN 10088-3:2005). <http://www.aalco.co.uk/datasheets/> (Last accessed: 05/02/2015).

Abraham, C.L., Maas, S.A., Weiss, J.A., Ellis, B.J., Peters, C.L., Anderson, A.E., 2013. A new discrete element analysis method for predicting hip joint contact stresses. *Journal of Biomechanics* 46(6):1121-1127.

Accardi, M.A., Dini, D., Cann, P.M., 2011. Experimental and numerical investigation of the behaviour of articular cartilage under shear loading-Interstitial fluid pressurisation and lubrication mechanisms. *Tribology International* 44(5):565-578.

Affatato, S., Traina, F., Toni, A., 2011. Microseparation and stripe wear in alumina-on-alumina hip implants. *International Journal of Artificial Organs* 34(6):506-512.

Afoke, N.Y., Byers, P.D., Hutton, W.C., 1980. The incongruous hip joint. A casting study. *Journal of bone and joint surgery. British volume* 62-B(4):511-514.

Afoke, N.Y., Byers, P.D., Hutton, W.C., 1984. The incongruous hip joint: a loading study. *Annals of the rheumatic diseases* 43(2):295-301.

Afoke, N.Y., Byers, P.D., Hutton, W.C., 1987. Contact pressures in the human hip joint. *Journal of bone and joint surgery. British volume* 69(4):536-541.

Al Hajjar, M., Leslie, I., Tipper, J., Williams, S., Fisher, J., Jennings, L., 2010. Effect of cup inclination angle during microseparation and rim loading on the wear of BIOLOX® delta ceramic-on-ceramic total hip replacement. *Journal of biomedical materials research. Part B, Applied biomaterials* 95(2):263-268.

Amis, A., 2012. The functions of the fibre bundles of the anterior cruciate ligament in anterior drawer, rotational laxity and the pivot shift. *Knee surgery, sports traumatology, arthroscopy* 20(4):613-620.

## CHAPTER 10

Amis, A., Dawkins, G., 1991. Functional anatomy of the anterior cruciate ligament. Fibre bundle actions related to ligament replacements and injuries. *Journal of Bone & Joint Surgery, British Volume* 73-B(2):260-267.

Amis, A.A., Firer, P., Mountney, J., Senavongse, W., Thomas, N.P., 2003. Anatomy and biomechanics of the medial patellofemoral ligament. *The Knee* 10(3):215-220.

Amstutz, H., Ludwig, R., Schurman, D.H., A, 1975. Range of motion studies for total hip replacements: A comparative study with a new experimental apparatus. *Clinical Orthopaedics & Related Research* 111:124-130.

Amstutz, H.C., Ball, S.T., Le Duff, M.J., Dorey, F.J., 2007. Resurfacing THA for patients younger than 50 years - Results of 2- to 9-year followup. *Clinical Orthopaedics and Related Research*(460):159-164.

Amstutz, H.C., Le Duff, M.J., 2006. Background of metal-on-metal resurfacing. *Proceedings of the Institution of Mechanical Engineers; Part H; Journal of Engineering in Medicine* 220(2):85-94.

Anderson, A., Peters, C., Tuttle, B., Weiss, J., 2005. Subject-specific finite element model of the pelvis: development, validation and sensitivity studies. *Journal of biomechanical engineering* 127(3):364-373.

Anderson, A.E., Ellis, B.J., Maas, S.A., Peters, C.L., Weiss, J.A., 2008. Validation of finite element predictions of cartilage contact pressure in the human hip joint. *Journal of Biomechanical Engineering-Transactions of the Asme* 130(5).

Anderson, A.E., Ellis, B.J., Maas, S.A., Weiss, J.A., 2010. Effects of idealized joint geometry on finite element predictions of cartilage contact stresses in the hip. *Journal of Biomechanics* 43(7):1351-1357.

Archibeck, M.J., Jacobs, J.J., Roebuck, K.A., Glant, T.T., 2000. The basic science of periprosthetic osteolysis. *Journal of Bone and Joint Surgery-American Volume* 82A(10):1478-1489.

Arnold, E., Ward, S., Lieber, R., Delp, S., 2010. A Model of the Lower Limb for Analysis of Human Movement. *Annals of Biomedical Engineering* 38(2):269-279.

- Arun, K.S., Huang, T.S., Blostein, S.D., 1987. Least-Squares Fitting of Two 3-D Point Sets. *Pattern Analysis and Machine Intelligence*, IEEE Transactions on PAMI-9(5):698-700.
- Athwal, K.K., Takeda, R., El Daou, H., Kawaguchi, Y., Hunt, N.C., Deehan, D.J., Amis, A., 2014. In Vitro Evaluation of Knee Kinematics and Soft Tissue Restraint using a Robotic System, BASK Annual Meeting 2014, Norwich.
- Audenaert, E.A., Mahieu, P., Pattyn, C., 2011. Three-Dimensional Assessment of Cam Engagement in Femoroacetabular Impingement. *Arthroscopy: The Journal of Arthroscopic & Related Surgery* 27(2):167-171.
- Audenaert, E.A., Peeters, I., Vigneron, L., Baelde, N., Pattyn, C., 2012. Hip Morphological Characteristics and Range of Internal Rotation in Femoroacetabular Impingement. *The American Journal of Sports Medicine* 40(6):1329-1336.
- Austin, D.C., Horneff Iii, J.G., Kelly Iv, J.D., 2014. Anterior Hip Dislocation 5 Months After Hip Arthroscopy. *Arthroscopy: The Journal of Arthroscopic & Related Surgery* 30(10):1380-1382.
- Bach, C.M., Winter, P., Nogler, M., Göbel, G., Wimmer, C., Ogon, M., 2002. No functional impairment after Robodoc total hip arthroplasty. *Acta orthopaedica* 73(4):386-391.
- Bardakos, N.V., Villar, R.N., 2009. The ligamentum teres of the adult hip. *Journal of bone and joint surgery. British volume* 91(1):8-15.
- Bartz, R.L., Noble, P.C., Kadakia, N.R., Tullos, H.S., 2000. The effect of femoral component head size on posterior dislocation of the artificial hip joint. *Journal of Bone and Joint Surgery-American Volume* 82A(9):1300-1307.
- Basmajian, J.V., De Luca, C., 1985. *Muscles Alive: Their Functions Revealed by Electromyography*, 5th ed. Lippincott Williams and Wilkins.
- Bauer, R., Kerschbaumer, F., Poisel, S., Oberthaler, W., 1979. The Transgluteal Approach to the Hip Joint. *Archives of orthopaedic and traumatic surgery* 95(1-2):47-49.

## CHAPTER 10

Beaulieu, M.L., Lamontagne, M., Beaulé, P.E., 2010. Lower limb biomechanics during gait do not return to normal following total hip arthroplasty. *Gait & Posture* 32(2):269-273.

Beck, M., Kalhor, M., Leunig, M., Ganz, R., 2005. Hip morphology influences the pattern of damage to the acetabular cartilage - Femoroacetabular impingement as a cause of early osteoarthritis of the hip. *Journal of Bone and Joint Surgery-British Volume* 87B(7):1012-1018.

Beck, M., Leunig, M., Parvizi, J., Boutier, V., Wyss, D., Ganz, R., 2004. Anterior femoroacetabular impingement Part II. Midterm results of surgical treatment. *Clinical Orthopaedics and Related Research*(418):67-73.

Bedi, A., Dolan, M., Hetsroni, I., Magennis, E., Lipman, J., Buly, R., Kelly, B.T., 2011a. Surgical Treatment of Femoroacetabular Impingement Improves Hip Kinematics A Computer-Assisted Model. *American Journal of Sports Medicine* 3943S-49S.

Bedi, A., Galano, G., Walsh, C., Kelly, B., 2011b. Capsular management during hip arthroscopy: from femoroacetabular impingement to instability. *Arthroscopy* 27(12):1720-1731.

Bedi, A., Kelly, B.T., Khanduja, V., 2013. Arthroscopic hip preservation surgery: Current concepts and perspective. *Bone & Joint Journal* 95-B(1):10-19.

Benali, Y., Katthagen, B., 2009. Hip subluxation as a complication of arthroscopic debridement. *Arthroscopy* 25(4):405-407.

Bergmann, G., 2008. OrthoLoad. Charite – Universitaetsmedizin Berlin.

Bergmann, G., 2010. OrthoLoad Manual. Charite – Universitaetsmedizin Berlin.

Bergmann, G., Deuretzbacher, G., Heller, M., Graichen, F., Rohlmann, A., Strauss, J., Duda, G.N., 2001. Hip contact forces and gait patterns from routine activities. *Journal of Biomechanics* 34(7):859-871.

Bergmann, G., Graichen, F., Rohlmann, A., Bender, A., Heinlein, B., 2010. Realistic loads for testing hip implants. *Bio-medical materials and engineering* 20(2):65-75.

Biomechanics-European-Laboratory, 2009. Visible Human Male - CT Frozen - Ileum and Femur.

- Blankevoort, L., Huiskes, R., de Lange, A., 1988. The envelope of passive knee joint motion. *Journal of Biomechanics* 21(9):705-720.
- Blemker, S., Delp, S., 2005. Three-dimensional representation of complex muscle architectures and geometries. *Annals of Biomedical Engineering* 33(5):661-673.
- Boone, D.C., Azen, S.P., 1979. Normal range of motion of joints in male subjects. *Journal of Bone and Joint Surgery; American volume* 61(5):756-759.
- Brand, R.A., Crowninshield, R.D., Wittstock, C.E., Pedersen, D.R., Clark, C.R., van Krieken, F.M., 1982. A model of lower extremity muscular anatomy. *Journal of biomechanical engineering* 104(4):304-310.
- Brand, R.A., Pedersen, D.R., Davy, D.T., Kotzar, G.M., Heiple, K.G., Goldberg, V.M., 1994. Comparison of hip force calculations and measurements in the same patient. *The Journal of Arthroplasty* 9(1):45-51.
- Brown, T.D., Callaghan, J.J., 2008. Impingement in total hip replacement: mechanisms and consequences. *Current Orthopaedics* 22(6):376-391.
- Bunn, A., Colwell, C.W., D'Lima, D.D., 2014. Effect of head diameter on passive and active dynamic hip dislocation. *Journal of Orthopaedic Research* n/a-n/a.
- Burroughs, B., Hallstrom, B., Golladay, G., Hoeffel, D., Harris, W., 2005. Range of motion and stability in total hip arthroplasty with 28-, 32-, 38-, and 44-mm femoral head sizes. *The Journal of Arthroplasty* 20(1):11-19.
- Butler, D.L., Noyes, F.R., Grood, E.S., 1980. Ligamentous restraints to anterior-posterior drawer in the human knee. A biomechanical study. *Journal of Bone and Joint Surgery; American volume* 62(2):259-270.
- Cadet, E., Chan, A., Vorys, G., Gardner, T., Yin, B., 2012. Investigation of the preservation of the fluid seal effect in the repaired, partially resected, and reconstructed acetabular labrum in a cadaveric hip model. *American Journal of Sports Medicine* 40(10):2218-2223.
- Cappozzo, A., Della Croce, U., Leardini, A., Chiari, L., 2005. Human movement analysis using stereophotogrammetry. Part 1: theoretical background. *Gait & Posture* 21(2):186-196.

## CHAPTER 10

Cashin, M., Uhthoff, H., O'Neill, M., Beaul, P.E., Beaul, P.E., 2008. Embryology of the acetabular labral-chondral complex. *Journal of bone and joint surgery. British volume* 90(8):1019-1024.

Cashman, P.M.M., Baring, T., Reilly, P., Emery, R.J.H., Amis, A.A., 2010. Measurement of migration of soft tissue by modified Roentgen stereophotogrammetric analysis (RSA): validation of a new technique to monitor rotator cuff tears. *Journal of medical engineering & technology* 34(3):159-165.

Cereatti, A., Margheritini, F., Donati, M., Cappozzo, A., 2010. Is the human acetabulofemoral joint spherical? *Journal of Bone & Joint Surgery, British Volume* 92-B(2):311-314.

Cerezal, L., Kassarian, A., Canga, A., Carmen Dobado, M., Antonio Montero, J., Dobado, M., Montero, J., Llopis, E., Roln, A., Prez-Carro, L., 2010. Anatomy, biomechanics, imaging, and management of ligamentum teres injuries. *Radiographics* 30(6):1637-1651.

Challis, J.H., 1995. A procedure for determining rigid body transformation parameters. *J Biomech* 28(6):733-737.

Charbonnier, C., Assassi, L., Volino, P., Magnenat-Thalmann, N., 2009. Motion study of the hip joint in extreme postures. *Visual Computer* 25(9):873-882.

Charbonnier, C., Kolo, F.C., Duthon, V.B., Magnenat-Thalmann, N., Becker, C.D., Hoffmeyer, P., Menetrey, J., 2011. Assessment of Congruence and Impingement of the Hip Joint in Professional Ballet Dancers: A Motion Capture Study. *The American Journal of Sports Medicine* 39(3):557-566.

Charnley, J., 1970. Total Hip Replacement by Low-Friction Arthroplasty. *Clinical Orthopaedics and Related Research* 727-21.

Charnley, J., 1972. The long-term results of low-friction arthroplasty of the hip performed as a primary intervention. *Journal of Bone & Joint Surgery, British Volume* 54-B(1):61-76.

Chegini, S., Beck, M., Ferguson, S.J., 2009. The Effects of Impingement and Dysplasia on Stress Distributions in the Hip Joint during Sitting and Walking: A Finite Element Analysis. *Journal of Orthopaedic Research* 27(2):195-201.

- Chiu, F.Y., Chen, T.H., Chen, C.M., Chung, T.Y., Lo, W.H., 2000. The effect of posterior capsulorrhaphy in primary total hip arthroplasty: a prospective randomized study. *The Journal of Arthroplasty* 15(2):194-199.
- Clohisy, J., Carlisle, J., Beaul, P., Kim, Y.-J., Trousdale, R., Beaul, P., Sierra, R., Leunig, M., Schoenecker, P., Millis, M., 2008. A systematic approach to the plain radiographic evaluation of the young adult hip. *Journal of Bone and Joint Surgery; American volume* 90 Suppl 447-66.
- Clohisy, J., St John, L., Schutz, A., 2010. Surgical treatment of femoroacetabular impingement: a systematic review of the literature. *Clinical Orthopaedics and Related Research* 468(2):555-564.
- Clyburn, T.A., Weitz-Marshall, A., Ambrose, C.G., 2003. Constrained acetabular cups - A cadaveric biomechanical evaluation. *Journal of Arthroplasty* 18(4):466-470.
- Cobb, J., Kannan, V., Brust, K., Thevendran, G., 2007. Navigation reduces the learning curve in resurfacing total hip arthroplasty. *Clinical Orthopaedics and Related Research*(463):90-97.
- Cobb, J., Logishetty, K., Davda, K., Iranpour, F., 2010. Cams and Pincer Impingement Are Distinct, Not Mixed: The Acetabular Pathomorphology of Femoroacetabular Impingement. *Clinical Orthopaedics and Related Research®* 468(8):2143-2151.
- Cohen, D., 2011. MEDICAL DEVICES Out of joint: The story of the ASR. *British Medical Journal* 342.
- Colbrunn, R.W., Bottros, J.J., Butler, R.S., Klika, A.K., Bonner, T.F., Greeson, C., van den Bogert, A.J., Barsoum, W.K., 2013. Impingement and Stability of Total Hip Arthroplasty Versus Femoral Head Resurfacing Using a Cadaveric Robotics Model. *Journal of Orthopaedic Research* 31(7):1108-1115.
- Colgan, D., Trench, P., McTague, D., Finlay, J.B., O'Donnell, P., Little, E.G., 1994. A review of joint and muscle load simulation relevant to in-vitro stress analysis of the hip. *Strain* 30(2):47-62.
- Cooperman, D., 2013. What is the evidence to support acetabular dysplasia as a cause of osteoarthritis? *J Pediatr Orthop* 33 Suppl 1S2-7.

## CHAPTER 10

Cooperman, D.R., Wallensten, R., Stulberg, S.D., 1983. Acetabular dysplasia in the adult. *Clinical Orthopaedics and Related Research* 17579-85.

Correa, T.A., Crossley, K.M., Kim, H.J., Pandy, M.G., 2010. Contributions of individual muscles to hip joint contact force in normal walking. *Journal of Biomechanics* 43(8):1618-1622.

Crawford, M.J., Dy, C.J., Alexander, J.W., Thompson, M., Schroder, S.J., Vega, C.E., Patel, R.V., Miller, A.R., McCarthy, J.C., Lowe, W.R., Noble, P.C., 2007. The 2007 Frank Stinchfield Award. The biomechanics of the hip labrum and the stability of the hip. *Clinical Orthopaedics and Related Research* 46516-22.

Cristofolini, L., 1997. A critical analysis of stress shielding evaluation of hip prostheses. *Critical reviews in biomedical engineering* 25(4-5):409-483.

Cross, M., Shindle, M., Kelly, B., 2010. Arthroscopic Anterior and Posterior Labral Repair After Traumatic Hip Dislocation: Case Report and Review of the Literature. *HSS Journal* 6(2):223-227.

Culliford, D.J., Maskell, J., Kiran, A., Judge, A., Javaid, M.K., Cooper, C., Arden, N.K., 2012. The lifetime risk of total hip and knee arthroplasty: results from the UK general practice research database. *Osteoarthritis and Cartilage* 20(6):519-524.

D'Lima, D.D., Urquhart, A.G., Buehler, K.O., Walker, R.H., Colwell, C.W., 2000. The effect of the orientation of the acetabular and femoral components on the range of motion of the hip at different head-neck ratios. *Journal of Bone and Joint Surgery; American volume* 82(3):315-321.

Dall, P., Kerr, A., 2010. Frequency of the sit to stand task: An observational study of free-living adults. *Applied Ergonomics* 41(1):58-61.

De Haan, R., Campbell, P.A., Su, E.P., De-Smet, K.A., De Smet, K.A., 2008a. Revision of metal-on-metal resurfacing arthroplasty of the hip: the influence of malpositioning of the components. *Journal of bone and joint surgery. British volume* 90(9):1158-1163.

De Haan, R., Pattyn, C., Gill, H.S., Murray, D.W., Campbell, P.A., De Smet, K., 2008b. Correlation between inclination of the acetabular component and metal ion levels in metal-on-metal hip resurfacing replacement. *Journal of Bone and Joint Surgery-British Volume* 90B(10):1291-1297.



- Delp, S., Anderson, F., Arnold, A., Loan, P., Habib, A., John, C., Guendelman, E., Thelen, D., 2007. OpenSim: open-source software to create and analyze dynamic simulations of movement. *IEEE Transactions on Biomedical Engineering* 54(11):1940-1950.
- Delp, S.L., Hess, W.E., Hungerford, D.S., Jones, L.C., 1999. Variation of rotation moment arms with hip flexion. *Journal of Biomechanics* 32(5):493-501.
- Delp, S.L., Loan, J.P., Hoy, M.G., Zajac, F.E., Topp, E.L., Rosen, J.M., 1990. An interactive graphics-based model of the lower extremity to study orthopaedic surgical procedures. *IEEE Transactions on Biomedical Engineering* 37(8):757-767.
- Demange, M.K., 2007. Influence of the femoral head ligament on hip mechanical function. *Acta Ortopédica Brasileira* 15(4):187.
- DeMers, M., 2011. Webinar - Estimating Joint Reaction Loads. <http://opensim.stanford.edu/> (Last accessed: 11/12/2014).
- Dennison, C.R., Wild, P.M., Wilson, D.R., Gilbert, M.K., 2010. An in-fiber Bragg grating sensor for contact force and stress measurements in articular joints. *Measurement Science & Technology* 21(11).
- Dickinson, A.S., Browne, M., Wilson, K.C., Jeffers, J.R.T., Taylor, A.C., 2011a. Pre-clinical evaluation of ceramic femoral head resurfacing prostheses using computational models and mechanical testing. *Proceedings of the Institution of Mechanical Engineers Part H-Journal of Engineering in Medicine* 225(H9):866-876.
- Dickinson, A.S., Taylor, A.C., Browne, M., 2012. The influence of acetabular cup material on pelvis cortex surface strains, measured using digital image correlation. *Journal of Biomechanics* 45(4):719-723.
- Dickinson, A.S., Taylor, A.C., Ozturk, H., Browne, M., 2011b. Experimental Validation of a Finite Element Model of the Proximal Femur Using Digital Image Correlation and a Composite Bone Model. *Journal of biomechanical engineering* 133(1):014504-014506.
- Dieppe, P.A., Lohmander, L.S., 2005. Pathogenesis and management of pain in osteoarthritis. *The Lancet* 365(9463):965-973.

## CHAPTER 10

Dimitriou, D., Tsai, T.-Y., Li, J.S., Nam, K.W., Park, K.K., Kwon, Y.-M., 2015. In vivo kinematic evaluation of Total Hip Arthroplasty during stair climbing. *Journal of Orthopaedic Research* n/a-n/a.

Doherty, M., Courtney, P., Doherty, S., Jenkins, W., Maciewicz, R.A., Muir, K., Zhang, W., 2008. Nonspherical femoral head shape (pistol grip deformity), neck shaft angle, and risk of hip osteoarthritis: A case–control study. *Arthritis & rheumatism* 58(10):3172-3182.

Domb, B., Philippon, M., Giordano, B., 2013. Arthroscopic capsulotomy, capsular repair, and capsular plication of the hip: relation to atraumatic instability. *Arthroscopy* 29(1):162-173.

Doorenbosch, C.A.M., Harlaar, J., Roebroek, M.E., Lankhorst, G.J., 1994. Two strategies of transferring from sit-to-stand; The activation of monoarticular and biarticular muscles. *Journal of Biomechanics* 27(11):1299-1307.

Dostal, W.F., Soderberg, G.L., Andrews, J.G., 1986. Actions of hip muscles. *Physical Therapy* 66(3):351-359.

Dowson, D., Wang, F.C., Wang, W.Z., Jin, Z.M., 2007. A predictive analysis of long-term friction and wear characteristics of metal-on-metal total hip replacements. *Proceedings of the Institution of Mechanical Engineers, Part J, Journal of engineering tribology* 221(J3):367-378.

Duthon, V., Charbonnier, C., Kolo, F., Magnenat Thalmann, N., Becker, C., 2013. Correlation of Clinical and Magnetic Resonance Imaging Findings in Hips of Elite Female Ballet Dancers. *Arthroscopy* 29(3):411-419.

Dwyer, M., Jones, H., Field, R., McCarthy, J., Noble, P., 2015. Femoroacetabular Impingement Negates the Acetabular Labral Seal During Pivoting Maneuvers but Not Gait. *Clinical Orthopaedics and Related Research®* 473(2):602-607.

Dwyer, M.K., Jones, H.L., Hogan, M.G., Field, R.E., McCarthy, J.C., Noble, P.C., 2014. The Acetabular Labrum Regulates Fluid Circulation of the Hip Joint During Functional Activities. *The American Journal of Sports Medicine* 42(4):812-819.

Dy, C.J., Thompson, M.T., Crawford, M.J., Alexander, J.W., McCarthy, J.C., Noble, P.C., 2008. Tensile strain in the anterior part of the acetabular labrum during

provocative maneuvering of the normal hip. *Journal of Bone and Joint Surgery-American* Volume 90A(7):1464-1472.

Eckstein, F., vonEisenhartRothe, R., Landgraf, J., Adam, C., Loehe, F., Putz, R., MÃ¼ller Gerbl, M., 1997. Quantitative analysis of incongruity, contact areas and cartilage thickness in the human hip joint. *Acta Anatomica* 158(3):192-204.

Elkins, J., Kruger, K., Pedersen, D., Callaghan, J., Brown, T., 2012. Edge-loading severity as a function of cup lip radius in metal-on-metal total hips--a finite element analysis. *Journal of Orthopaedic Research* 30(2):169-177.

Elkins, J.M., O'Brien, M.K., Stroud, N.J., Pedersen, D.R., Callaghan, J.J., Brown, T.D., 2011a. Hard-on-Hard Total Hip Impingement Causes Extreme Contact Stress Concentrations. *Clinical Orthopaedics and Related Research* 469(2):454-463.

Elkins, J.M., Stroud, N.J., Rudert, M.J., Tochigi, Y., Pedersen, D.R., Ellis, B.J., Callaghan, J.J., Weiss, J.A., Brown, T.D., 2011b. The Capsule's Contribution to Total Hip Construct Stability - A Finite Element Analysis. *Journal of Orthopaedic Research* 29(11):1642-1648.

Ellis, A.R., Noble, P.C., Schroder, S.J., Thompson, M.T., Stocks, G.W., 2011. The Cam Impinging Femur Has Multiple Morphologic Abnormalities. *Journal of Arthroplasty* 26(6):59-65.

Erb, R.E., 2001. Current concepts in imaging the adult hip. *Clinics in sports medicine* 20(4):661-696.

Espinosa, N., Rothenfluh, D., Beck, M., Ganz, R., Leunig, M., 2006. Treatment of femoro-acetabular impingement: preliminary results of labral refixation. *Journal of Bone and Joint Surgery; American* volume 88(5):925-935.

Esposito, C.I., Walter, W.L., Roques, A., Tuke, M.A., Zicat, B.A., Walsh, W.R., Walter, W.K., 2012. Wear in alumina-on-alumina ceramic total hip replacements: a retrieval analysis of edge loading. *Journal of Bone and Joint Surgery-British* Volume 94-B(7):901-907.

Ewen, A.M., Stewart, S., St Clair Gibson, A., Kashyap, S.N., Caplan, N., 2012. Post-operative gait analysis in total hip replacement patients—A review of current literature and meta-analysis. *Gait & Posture* 36(1):1-6.

## CHAPTER 10

Ferguson, S.J., Bryant, J.T., Ganz, R., Ito, K., 2000a. The acetabular labrum seal: a poroelastic finite element model. *Clinical Biomechanics* 15(6):463-468.

Ferguson, S.J., Bryant, J.T., Ganz, R., Ito, K., 2000b. The influence of the acetabular labrum on hip joint cartilage consolidation: a poroelastic finite element model. *Journal of Biomechanics* 33(8):953-960.

Ferguson, S.J., Bryant, J.T., Ganz, R., Ito, K., 2003. An in vitro investigation of the acetabular labral seal in hip joint mechanics. *Journal of Biomechanics* 36(2):171-178.

Fisher, J., 2011. Bioengineering reasons for the failure of metal-on-metal hip prostheses: An engineer's perspective. *Journal of Bone and Joint Surgery-British Volume* 93B(8):1001-1004.

Fitzgerald, R.H., 1995. Acetabular labrum tears. Diagnosis and treatment. *Clinical Orthopaedics and Related Research*(311):60-68.

Foucher, K.C., Hurwitz, D.E., Wimmer, M.A., 2007. Preoperative gait adaptations persist one year after surgery in clinically well-functioning total hip replacement patients. *Journal of Biomechanics* 40(15):3432-3437.

Frank, R.M., Lee, S., Bush-Joseph, C.A., Kelly, B.T., Salata, M.J., Nho, S.J., 2014. Improved Outcomes After Hip Arthroscopic Surgery in Patients Undergoing T-Capsulotomy With Complete Repair Versus Partial Repair for Femoroacetabular Impingement: A Comparative Matched-Pair Analysis. *The American Journal of Sports Medicine* 42(11):2634-2642.

Fredericson, M., Cookingham, C.L., Chaudhari, A.M., Dowdell, B.C., Oestreicher, N., Sahrmann, S.A., 2000. Hip abductor weakness in distance runners with iliotibial band syndrome. *Clin J Sport Med* 10(3):169-175.

Furman, W., Marshall, J.L., Girgis, F.G., 1976. The anterior cruciate ligament. A functional analysis based on postmortem studies. *The Journal of Bone & Joint Surgery* 58(2):179-185.

Fuss, F.K., Bacher, A., 1991. New aspects of the morphology and function of the human hip joint ligaments. *American Journal of Anatomy* 192(1):1-13.

Ganz, R., Gautier, E., Ganz, K., Krugel, N., Gill, T.J., Krgel, N., Berlemann, U., 2001. Surgical dislocation of the adult hip a technique with full access to the femoral head

and acetabulum without the risk of avascular necrosis. Journal of bone and joint surgery. British volume 83(8):1119-1124.

Ganz, R., Klaue, K., Vinh, T.S., Mast, J.W., 1988. A new periacetabular osteotomy for the treatment of hip dysplasias - technique and preliminary results. Clinical Orthopaedics and Related Research(232):26-36.

Ganz, R., Leunig, M., Leunig-Ganz, K., Harris, W.H., 2008. The etiology of osteoarthritis of the hip - An integrated mechanical concept. Clinical Orthopaedics and Related Research 466(2):264-272.

Ganz, R., Parvizi, J., Beck, M., Leunig, M., Notzli, H., Siebenrock, K.A., 2003. Femoroacetabular impingement - A cause for osteoarthritis of the hip. Clinical Orthopaedics and Related Research(417):112-120.

Genovese, K., Lee, Y.U., Humphrey, J.D., 2011a. Novel optical system for in vitro quantification of full surface strain fields in small arteries: I. Theory and design. Computer Methods in Biomechanics and Biomedical Engineering 14(3):213-225.

Genovese, K., Lee, Y.U., Humphrey, J.D., 2011b. Novel optical system for in vitro quantification of full surface strain fields in small arteries: II. Correction for refraction and illustrative results. Computer Methods in Biomechanics and Biomedical Engineering 14(3):227-237.

Gibson, A., 1950. Posterior Exposure of the Hip Joint. Journal of Bone & Joint Surgery, British Volume 32-B(2):183-186.

Gioe, T.J., Sharma, A., Tatman, P., Mehle, S., 2011. Do "Premium" Joint Implants Add Value? Analysis of High Cost Joint Implants in a Community Registry. Clinical Orthopaedics and Related Research 469(1):48-54.

Giorgi, M., Carriero, A., Shefelbine, S.J., Nowlan, N.C., 2014. Mechanobiological simulations of prenatal joint morphogenesis. Journal of Biomechanics 47(5):989-995.

Glitsch, U., Baumann, W., 1997. The three-dimensional determination of internal loads in the lower extremity. Journal of Biomechanics 30(11-12):1123-1131.

Golub, G.H., Reinsch, C., 1970. Singular value decomposition and least squares solutions. Numerische Mathematik 14(5):403-420.

## CHAPTER 10

Goodman, S., Adler, S., Fyhrie, D., Schurman, D., 1988. The acetabular teardrop and its relevance to acetabular migration. *Clinical Orthopaedics and Related Research* 236:199-204.

Gosvig, K.K., Jacobsen, S., Palm, H., Sonne Holm, S., Magnusson, E., 2007. A new radiological index for assessing asphericity of the femoral head in cam impingement. *Journal of bone and joint surgery. British volume* 89(10):1309-1316.

Gosvig, K.K., Jacobsen, S., Sonne Holm, S., Gebuhr, P., 2008. The prevalence of cam-type deformity of the hip joint: a survey of 4151 subjects of the Copenhagen Osteoarthritis Study. *Acta Radiologica* 49(4):436-441.

Gottschalk, F., Kourosh, S., Leveau, B., 1989. The functional anatomy of tensor fasciae latae and gluteus medius and minimus. *Journal of anatomy* 166:179-189.

Grammatopoulos, G., Pandit, H., Glyn-Jones, S., McLardy-Smith, P., Gundle, R., Whitwell, D., Gill, H.S., Murray, D.W., 2010a. Optimal acetabular orientation for hip resurfacing. *Journal of Bone and Joint Surgery-British Volume* 92B(8):1072-1078.

Grammatopoulos, G., Pandit, H., Hip, O., Group, K., Murray, D.W., Gill, H.S., 2010b. The relationship between head-neck ratio and pseudotumour formation in metal-on-metal resurfacing arthroplasty of the hip. *Journal of Bone & Joint Surgery, British Volume* 92-B(11):1527-1534.

Gray, A.J., Villar, R.N., 1997. The ligamentum teres of the hip: an arthroscopic classification of its pathology. *Arthroscopy* 13(5):575-578.

Gray, H., 1918. *Gray's Anatomy of the Human Body*, 20th ed. (Lewis, W.H. Ed.) Lea & Febiger, Philadelphia.

Gray, H., 2008. *Gray's Anatomy*, 40th ed. (Standring, S. Ed.) Churchill Livingstone, London.

Greaves, L.L., Gilbert, M.K., Yung, A.C., Kozlowski, P., Wilson, D.R., 2010. Effect of acetabular labral tears, repair and resection on hip cartilage strain: A 7 T MR study. *Journal of Biomechanics* 43(5):858-863.

Griffin, W.L., Nanson, C.J., Springer, B.D., Davies, M.A., Fehring, T.K., 2010. Reduced Articular Surface of One-piece Cups A Cause of Runaway Wear and Early Failure. *Clinical Orthopaedics and Related Research* 468(9):2328-2332.

- Grimaldi, A., Richardson, C., Stanton, W., Durbridge, G., Donnelly, W., Hides, J., 2009. The association between degenerative hip joint pathology and size of the gluteus medius, gluteus minimus and piriformis muscles. *Manual Therapy* 14(6):605-610.
- Gross, T.P., Liu, F., 2012. The HAP Paul Award: a Safe Zone for Acetabular Component Position in Metal-on-Metal Hip Resurfacing Arthroplasty, 25th Annual Congress of the International Society for Technology in Arthroplasty, Sydney, Australia.
- Gupte, C.M., Bull, A.M.J., Thomas, R.d., Amis, A.A., 2003. A review of the function and biomechanics of the meniscomfemoral ligaments. *Arthroscopy: The Journal of Arthroscopic & Related Surgery* 19(2):161-171.
- Haemer, J., Carter, D., Giori, N., 2012. The low permeability of healthy meniscus and labrum limit articular cartilage consolidation and maintain fluid load support in the knee and hip. *Journal of Biomechanics* 45(8):1450-1456.
- Hannouche, D., Zaoui, A., Zadegan, F., Sedel, L., Nizard, R., 2011. Thirty years of experience with alumina-on-alumina bearings in total hip arthroplasty. *International Orthopaedics* 35(2):207-213.
- Hardinge, K., 1982. The direct lateral approach to the hip. *Journal of Bone & Joint Surgery, British Volume* 64-B(1):17-19.
- Harris, J.D., McCormick, F.M., Abrams, G.D., Gupta, A.K., Ellis, T.J., Bach Jr, B.R., Bush-Joseph, C.A., Nho, S.J., 2013. Complications and Reoperations During and After Hip Arthroscopy: A Systematic Review of 92 Studies and More Than 6,000 Patients. *Arthroscopy: The Journal of Arthroscopic & Related Surgery* 29(3):589-595.
- Harris, M., Anderson, A., Henak, C., Ellis, B., Peters, C., Weiss, J., 2012. Finite element prediction of cartilage contact stresses in normal human hips. *Journal of Orthopaedic Research* 30(7):1133-1139.
- Hart, A., Skinner, J., Henckel, J., Sampson, B., Gordon, F., 2011a. Insufficient acetabular version increases blood metal ion levels after metal-on-metal hip resurfacing. *Clinical Orthopaedics and Related Research* 469(9):2590-2597.
- Hart, A.J., Ilo, K., Underwood, R., Cann, P., Henckel, J., Lewis, A., Cobb, J., Skinner, J., 2011b. The relationship between the angle of version and rate of wear of retrieved metal-on-metal resurfacings: a prospective, CT-based study. *Journal of bone and joint surgery. British volume* 93(3):315-320.

## CHAPTER 10

Haversath, M., Hanke, J., Landgraeber, S., Herten, M., Zilkens, C., Krauspe, R., Jäger, M., 2013. The distribution of nociceptive innervation in the painful hip: A histological investigation. *Bone & Joint Journal* 95-B(6):770-776.

Heller, M., Kratzstein, S., Ehrig, R., Wassilew, G., Duda, G., Taylor, W., 2011. The weighted optimal common shape technique improves identification of the hip joint center of rotation in vivo. *Journal of Orthopaedic Research* 29(10):1470-1475.

Heller, M.O., 2005. Determination of muscle loading at the hip joint for use in pre-clinical testing. *Journal of Biomechanics* 38(5):1155.

Heller, M.O., Bergmann, G., Deuretzbacher, G., Dürselen, L., Pohl, M., Claes, L., Haas, N.P., Duda, G.N., 2001. Musculo-skeletal loading conditions at the hip during walking and stair climbing. *Journal of Biomechanics* 34(7):883-893.

Henak, C.R., Ellis, B.J., Harris, M.D., Anderson, A.E., Peters, C.L., Weiss, J.A., 2011. Role of the acetabular labrum in load support across the hip joint. *Journal of Biomechanics* 44(12):2201-2206.

Hewitt, J., Glisson, R., Guilak, F., Vail, T.P., 2002. The mechanical properties of the human hip capsule ligaments. *The Journal of Arthroplasty* 17(1):82-89.

Hewitt, J., Guilak, F., Glisson, R., Vail, T.P., 2001. Regional material properties of the human hip joint capsule ligaments. *Journal of Orthopaedic Research* 19(3):359-364.

Hlavacek, M., 2002. The influence of the acetabular labrum seal, intact articular superficial zone and synovial fluid thixotropy on squeeze-film lubrication of a spherical synovial joint. *Journal of Biomechanics* 35(10):1325-1335.

Hodge, W.A., Carlson, K.L., Fijan, R.S., Burgess, R.G., Riley, P.O., Harris, W.H., Mann, R.W., 1989. Contact pressures from an instrumented hip endoprosthesis. *Journal of Bone and Joint Surgery; American volume* 71(9):1378-1386.

Hodge, W.A., Fijan, R.S., Carlson, K.L., Burgess, R.G., Harris, W.H., Mann, R.W., 1986. Contact pressures in the human hip-joint measured in vivo. *Proceedings of the National Academy of Sciences of the United States of America* 83(9):2879-2883.

Hogervorst, T., Bouma, H., de Vos, J., 2009. Evolution of the hip and pelvis. *Acta orthopaedica. Supplementum* 80(336):1-39.



- Holland, J.P., Langton, D.J., Hashmi, M., 2012. Ten-year clinical, radiological and metal ion analysis of the Birmingham Hip Resurfacing: from a single, non-designer surgeon. *Journal of bone and joint surgery. British volume* 94(4):471-476.
- Hoy, M.G., Zajac, F.E., Gordon, M.E., 1990. A musculoskeletal model of the human lower extremity: the effect of muscle, tendon, and moment arm on the moment-angle relationship of musculotendon actuators at the hip, knee, and ankle. *Journal of Biomechanics* 23(2):157-169.
- Huang, H., Zhang, J., Sun, K., Zhang, X., Tian, S., 2011. Effects of repetitive multiple freeze-thaw cycles on the biomechanical properties of human flexor digitorum superficialis and flexor pollicis longus tendons. *Clinical Biomechanics* 26(4):419-423.
- Hunt, N.C., Ghosh, K.M., Blain, A.P., Athwal, K.K., Rushton, S.P., Amis, A.A., Longstaff, L.M., Deehan, D.J., 2014. How does laxity after single radius total knee arthroplasty compare with the native knee? *Journal of Orthopaedic Research* 32(9):1208-1213.
- Ilizaliturri, V., 2009. Complications of arthroscopic femoroacetabular impingement treatment: a review. *Clinical Orthopaedics and Related Research* 467(3):760-768.
- Impellizzeri, F.M., Mannion, A.F., Naal, F.D., Hersche, O., Leunig, M., 2012. The early outcome of surgical treatment for femoroacetabular impingement: success depends on how you measure it. *Osteoarthritis and Cartilage* 20(7):638-645.
- Incavo, S., Thompson, M., Gold, J., Patel, R., Icenogle, K., Noble, P., 2011. Which procedure better restores intact hip range of motion: total hip arthroplasty or resurfacing? A combined cadaveric and computer simulation study. *The Journal of Arthroplasty* 26(3):391-397.
- Isaac, G.H., Schmalzried, T.P., Vail, T.P., 2009. Component mal-position: The 'Achilles' heel' of bearing surfaces in hip replacement. *Proceedings of the Institution of Mechanical Engineers, Part J: Journal of Engineering Tribology* 223(3):275-286.
- Ito, H., Song, Y., Lindsey, D., Safran, M., Giori, N., 2009. The proximal hip joint capsule and the zona orbicularis contribute to hip joint stability in distraction. *Journal of Orthopaedic Research* 27(8):989-995.
- Jacobsen, S., 2006. Adult hip dysplasia and osteoarthritis: studies in radiology and clinical epidemiology. *Acta orthopaedica* 77(sup324):2-37.

## CHAPTER 10

Jalali Vahid, D., Jagatia, M., Dowson, D., Jin, Z.M., 2001. Prediction of lubricating film thickness in UHMWPE hip joint replacements. *Journal of Biomechanics* 34(2):261-266.

Jansson, K., Michalski, M., Smith, S., LaPrade, R., Wijdicks, C., 2013. Tekscan pressure sensor output changes in the presence of liquid exposure. *Journal of Biomechanics* 46(3):612-614.

Jarrett, C., Ranawat, A., Bruzzone, M., Blum, Y., Rodriguez, J., Ranawat, C., 2009. The squeaking hip: a phenomenon of ceramic-on-ceramic total hip arthroplasty. *Journal of Bone and Joint Surgery; American volume* 91(6):1344-1349.

Jazrawi, L.M., Bogner, E., Della Valle, C.J., Chen, F.S., Pak, K.I., Stuchin, S.A., Frankel, V.H., Di Cesare, P.E., 1999. Wear rates of ceramic-on-ceramic bearing surfaces in total hip implants: a 12-year follow-up study. *The Journal of Arthroplasty* 14(7):781-787.

Jeffers, J.R., 2012. The role of biomechanics and engineering in total hip replacement. Why surgeons need technical help. *Proceedings of the Institution of Mechanical Engineers, Part H: Journal of Engineering in Medicine*.

Jeffers, J.R., Roques, A., Taylor, A., Tuke, M.A., 2009. The problem with large diameter metal-on-metal acetabular cup inclination. *Bull NYU Hosp Jt Dis* 67(2):189-192.

Jeffers, J.R.T., Walter, W.L., 2012. Ceramic-on-ceramic bearings in hip arthroplasty: State of the art and the future. *Journal of bone and joint surgery. British volume* 94(6):735-745.

Johnston, R.C., Smidt, G.L., 1970. Hip motion measurements for selected activities of daily living. *Clinical Orthopaedics and Related Research*(72):205-&.

Kadaba, M.P., Ramakrishnan, H.K., Wootten, M.E., 1990. Measurement of lower-extremity kinematics during level walking. *Journal of Orthopaedic Research* 8(3):383-392.

Kapandji, I.A., 1978. The physiology of the ligamentum teres, in, *The physiology of the joints*, 2nd ed. Churchill Livingstone, New York.

- Kaptein, B., Valstar, E., Stoel, B., Reiber, H., Nelissen, R., 2007. Clinical validation of model-based RSA for a total knee prosthesis. *Clinical Orthopaedics and Related Research*(464):205-209.
- Kaptein, B.L., Reiber, J.H.C., Valstar, E.R., Stoel, B.C., Rozing, P.M., 2003. A new model-based RSA method validated using CAD models and models from reversed engineering. *Journal of Biomechanics* 36(6):873-882.
- Katta, J., Jin, Z., Ingham, E., Fisher, J., 2008. Biotribology of articular cartilage--a review of the recent advances. *Medical Engineering & Physics* 30(10):1349-1363.
- Kelly, B., Williams, R., Philippon, M., 2003. Hip arthroscopy: current indications, treatment options, and management issues. *American Journal of Sports Medicine* 31(6):1020-1037.
- Kelly, B.T., Weiland, D.E., Schenker, M.L., Philippon, M.J., 2005. Arthroscopic Labral Repair in the Hip: Surgical Technique and Review of the Literature. *Arthroscopy: The Journal of Arthroscopic & Related Surgery* 21(12):1496-1504.
- Kessler, O., Pati, S., Stefan, W., Mayr, E., Colwell, C., Patil, S., Wirth, S., D'Lima, D., 2008. Bony impingement affects range of motion after total hip arthroplasty: A subject-specific approach. *Journal of Orthopaedic Research* 26(4):443-452.
- Khan, R., Konyves, A., Rama, K.R.B.S., Thomas, R., Amis, A.A., 2006. RSA can measure ACL graft stretching and migration - Development of a new method. *Clinical Orthopaedics and Related Research*(448):139-145.
- Kivlan, B., Richard Clemente, F., Martin, R., Martin, H., 2013. Function of the ligamentum teres during multi-planar movement of the hip joint. *Knee surgery, sports traumatology, arthroscopy* 21(7):1664-1668.
- Klein Horsman, M.D., Koopman, H.F., van der Helm, F.C., Prose, L.P., Veeger, H.E., 2007. Morphological muscle and joint parameters for musculoskeletal modelling of the lower extremity. *Clinical Biomechanics* 22(2):239-247.
- Kluess, D., Martin, H., Mittelmeier, W., Schmitz, K.P., Bader, R., 2007. Influence of femoral head size on impingement, dislocation and stress distribution in total hip replacement. *Medical Engineering & Physics* 29(4):465-471.

## CHAPTER 10

Kluess, D., Zietz, C., Lindner, T., Mittelmeier, W., Schmitz, K.-P., Bader, R., 2008. Limited range of motion of hip resurfacing arthroplasty due to unfavorable ratio of prosthetic head size and femoral neck diameter. *Acta orthopaedica* 79(6):748-754.

Kondo, E., Merican, A., Yasuda, K., Amis, A., 2010. Biomechanical comparisons of knee stability after anterior cruciate ligament reconstruction between 2 clinically available transtibial procedures: anatomic double bundle versus single bundle. *American Journal of Sports Medicine* 38(7):1349-1358.

Konrath, G.A., Hamel, A.J., Olson, S.A., Bay, B., Sharkey, N.A., 1998. The role of the acetabular labrum and the transverse acetabular ligament in load transmission in the hip. *Journal of Bone and Joint Surgery-American Volume* 80A(12):1781-1788.

Koyanagi, J., Sakai, T., Yamazaki, T., Watanabe, T., Akiyama, K., Sugano, N., Yoshikawa, H., Sugamoto, K., 2011. In vivo kinematic analysis of squatting after total hip arthroplasty. *Clinical Biomechanics* 26(5):477-483.

Krebs, V., Incavo, S., Shields, W., 2009. The Anatomy of the Acetabulum: What is Normal? *Clinical Orthopaedics and Related Research*® 467(4):868-875.

Kroeber, M., Ries, M., Suzuki, Y., Renowitzky, G., Ashford, F., Lotz, J., 2002. Impact biomechanics and pelvic deformation during insertion of press-fit acetabular cups. *The Journal of Arthroplasty* 17(3):349-354.

Kubiak-Langer, M., Tannast, M., Murphy, S.B., Siebenrock, K.A., Langlotz, F., 2007. Range of Motion in Anterior Femoroacetabular Impingement. *Clinical Orthopaedics and Related Research* 458:117-124.

Kumar, V., Sharma, S., James, J., Hodgkinson, J.P., Hemmady, M.V., 2014. Total hip replacement through a posterior approach using a 22 mm diameter femoral head: The role of the transverse acetabular ligament and capsular repair in reducing the rate of dislocation. *Bone & Joint Journal* 96-B(9):1202-1206.

Kwon, M.S., Kuskowski, M., Mulhall, K.J., Macaulay, W., Brown, T.E., Saleh, K.J., 2006. Does surgical approach affect total hip arthroplasty dislocation rates? *Clinical Orthopaedics and Related Research*(447):34-38.

Kwon, Y.-H., 1998. Transformation Matrix.  
<http://www.kwon3d.com/theory/transform/transform.html> (Last accessed: 22/01/2015).

- Kwon, Y.-M., Mellon, S.J., Monk, P., Murray, D.W., Gill, H.S., 2012. In vivo evaluation of edge-loading in metal-on-metal hip resurfacing patients with pseudotumours. *Bone and Joint Research* 1(4):42-49.
- Kwon, Y.M., Glyn-Jones, S., Simpson, D.J., Kamali, A., McLardy-Smith, P., Gill, H.S., Murray, D.W., 2010. Analysis of wear of retrieved metal-on-metal hip resurfacing implants revised due to pseudotumours. *Journal of Bone and Joint Surgery-British Volume* 92B(3):356-361.
- Langton, D.J., Jameson, S.S., Joyce, T.J., Gandhi, J.N., Sidaginamale, R., Mereddy, P., Lord, J., Nargol, A.V.F., 2011a. Accelerating failure rate of the ASR total hip replacement. *Journal of Bone & Joint Surgery, British Volume* 93-B(8):1011-1016.
- Langton, D.J., Jameson, S.S., Joyce, T.J., Webb, J., Nargol, A.V.F., 2008. The effect of component size and orientation on the concentrations of metal ions after resurfacing arthroplasty of the hip. *Journal of bone and joint surgery. British volume* 90(9):1143-1151.
- Langton, D.J., Joyce, T.J., Jameson, S.S., Lord, J., Van Orsouw, M., Holland, J.P., De Smet, K.A., 2011b. Adverse reaction to metal debris following hip resurfacing: the influence of component type, orientation and volumetric wear. *Journal of bone and joint surgery. British volume* 93(2):164-171.
- Langton, D.J., Sprowson, A.P., Joyce, T.J., Reed, M., Carluke, I., Partington, P., 2009. Blood metal ion concentrations after hip resurfacing arthroplasty: a comparative study of articular surface replacement and Birmingham Hip Resurfacing arthroplasties. *Journal of bone and joint surgery. British volume* 91(10):1287-1295.
- Larson, C., Giveans, M.R., 2009. Arthroscopic debridement versus refixation of the acetabular labrum associated with femoroacetabular impingement. *Arthroscopy* 25(4):369-376.
- Lavigne, M., Parvizi, J., Beck, M., Siebenrock, K.A., Ganz, R., Leunig, M., 2004. Anterior femoroacetabular impingement Part I. Techniques of joint preserving surgery. *Clinical Orthopaedics and Related Research*(418):61-66.
- Lee, G., Kumar, A., Berkson, E., Verma, N., Bach, B.R., Hallab, N., 2009. A biomechanical analysis of bone-patellar tendon-bone grafts after repeat freeze-thaw cycles in a cyclic loading model. *The journal of knee surgery* 22(2):111-113.

## CHAPTER 10

Lee, S., Wuerz, T.H., Shewman, E., McCormick, F.M., Salata, M.J., Philippon, M.J., Nho, S.J., 2015. Labral Reconstruction With Iliotibial Band Autografts and Semitendinosus Allografts Improves Hip Joint Contact Area and Contact Pressure: An In Vitro Analysis. *The American Journal of Sports Medicine* 43(1):98-104.

Lee, Y.K., Ha, Y.C., Yoo, J.J., Koo, K.H., Yoon, K.S., Kim, H.J., 2010. Alumina-on-Alumina Total Hip Arthroplasty A Concise Follow-up, at a Minimum of Ten Years, of a Previous Report. *Journal of Bone and Joint Surgery-American Volume* 92A(8):1715-1719.

Leslie, I., Williams, S., Isaac, G., Ingham, E., Fisher, J., 2009. High cup angle and microseparation increase the wear of hip surface replacements. *Clinical Orthopaedics and Related Research* 467(9):2259-2265.

Leunig, M., Beaule, P.E., Ganz, R., 2009. The Concept of Femoroacetabular Impingement: Current Status and Future Perspectives. *Clinical Orthopaedics and Related Research* 467(3):616-622.

Leunig, M., Beck, M., Stauffer, E., Hertel, R., Ganz, R., 2000. Free nerve endings in the ligamentum capitis femoris. *Acta Orthopaedica Scandinavica* 71(5):452-454.

Leunig, M., Ganz, R., 2014. The evolution and concepts of joint-preserving surgery of the hip. *Bone & Joint Journal* 96-B(1):5-18.

Lewinnek, G.E., Lewis, J.L., Tarr, R., Compere, C.L., Zimmerman, J.R., 1978. Dislocations after total hip-replacement arthroplasties. *Journal of Bone and Joint Surgery; American volume* 60(2):217-220.

Liechti, E.F., Ferguson, S.J., Tannast, M., 2014. Protrusio acetabuli: Joint loading with severe pincer impingement and its theoretical implications for surgical therapy. *Journal of Orthopaedic Research* n/a-n/a.

Lohmander, L.S., Englund, P.M., Dahl, L., Roos, E., 2007. The long-term consequence of anterior cruciate ligament and meniscus injuries: osteoarthritis. *American Journal of Sports Medicine* 35(10):1756-1769.

Lombardi, A.V., Mallory, T.H., Dennis, D.A., Komistek, R.D., Fada, R.A., Northcut, E.J., 2000. An in vivo determination of total hip arthroplasty pistoning during activity. *The Journal of Arthroplasty* 15(6):702-709.

- Lopomo, N., Sun, L., Zaffagnini, S., Giordano, G., Safran, M., 2010. Evaluation of formal methods in hip joint center assessment: an in vitro analysis. *Clinical Biomechanics* 25(3):206-212.
- Lovell, T.P., 2008. Single-Incision Direct Anterior Approach for Total Hip Arthroplasty Using a Standard Operating Table. *The Journal of Arthroplasty* 23(7, Supplement):64-68.
- Lu, T.W., O'Connor, J.J., 1999. Bone position estimation from skin marker co-ordinates using global optimisation with joint constraints. *Journal of Biomechanics* 32(2):129-134.
- Lund-Research-Ltd, 2013. Laerd Statistics: SPSS Guide. <https://statistics.laerd.com> (Last accessed: 03/07/2015).
- Lusty, P.J., Tai, C.C., Sew-Hoy, R.P., Walter, W.L., Walter, W.K., Zicat, B.A., 2007a. Third-generation alumina-on-alumina ceramic bearings in cementless total hip arthroplasty. *Journal of Bone and Joint Surgery-American Volume* 89A(12):2676-2683.
- Lusty, P.J., Watson, A., Tuke, M.A., Walter, W.L., Walter, W.K., Zicat, B., 2007b. Orientation and wear of the acetabular component in third generation alumina-on-alumina ceramic bearings - An analysis of 33 retrievals. *Journal of Bone and Joint Surgery-British Volume* 89B(9):1158-1164.
- Madsen, M.S., Ritter, M.A., Morris, H.H., Meding, J.B., Berend, M.E., Faris, P.M., Vardaxis, V.G., 2004. The effect of total hip arthroplasty surgical approach on gait. *Journal of Orthopaedic Research* 22(1):44-50.
- Mak, M., Jin, Z.M., Fisher, J., Stewart, T.D., 2011. Influence of Acetabular Cup Rim Design on the Contact Stress During Edge Loading in Ceramic-on-Ceramic Hip Prostheses. *Journal of Arthroplasty* 26(1):131-136.
- Mak, M.M., Jin, Z.M., 2002. Analysis of contact mechanics in ceramic-on-ceramic hip joint replacements. *Proceedings of the Institution of Mechanical Engineers; Part H; Journal of Engineering in Medicine* 216(4):231-236.
- Marchetti, E., Krantz, N., Berton, C., Bocquet, D., Fouilleron, N., 2011. Component impingement in total hip arthroplasty: Frequency and risk factors. A continuous retrieval analysis series of 416 cup. *Orthopaedics & Traumatology: Surgery & Research* 97(2):127-133.

## CHAPTER 10

Markley, F.L., 1988. Attitude determination using vector observations and the singular value decomposition. *The Journal of the astronautical sciences* 36(3):245-258.

Martin, H., Savage, A., Braly, B., Palmer, I., Beall, D., Kelly, B., 2008. The function of the hip capsular ligaments: a quantitative report. *Arthroscopy* 24(2):188-195.

Martin, R., Kivlan, B., Clemente, F.R., 2013. A cadaveric model for ligamentum teres function: a pilot study. *Knee surgery, sports traumatology, arthroscopy* 21(7):1689-1693.

Martin, R., Palmer, I., Martin, H., 2012. Ligamentum teres: a functional description and potential clinical relevance. *Knee surgery, sports traumatology, arthroscopy* 20(6):1209-1214.

Martínez, H., Obst, T., Ulbrich, H., Burgkart, R., 2013. A novel application of direct force control to perform in-vitro biomechanical tests using robotic technology. *Journal of Biomechanics* 46(7):1379-1382.

Masjedi, M., Nightingale, C.L., Azimi, D.Y., Cobb, J.P., 2013. The three-dimensional relationship between acetabular rim morphology and the severity of femoral cam lesions. *Bone & Joint Journal* 95-B(3):314-319.

Masonis, J.L., Bourne, R.B., 2002. Surgical approach, abductor function, and total hip arthroplasty dislocation. *Clinical Orthopaedics and Related Research* (405)46-53.

Masouros, S.D., McDermott, I.D., Amis, A.A., Bull, A.M.J., 2008. Biomechanics of the meniscus-meniscal ligament construct of the knee. *Knee surgery, sports traumatology, arthroscopy* 16(12):1121-1132.

Matar, W.Y., Restrepo, C., Parvizi, J., Kurtz, S.M., Hozack, W.J., 2010. Revision Hip Arthroplasty for Ceramic-on-Ceramic Squeaking Hips Does Not Compromise the Results. *Journal of Arthroplasty* 25(6):81-86.

Matsuda, D.K., 2009. Acute Iatrogenic Dislocation Following Hip Impingement Arthroscopic Surgery. *Arthroscopy: The Journal of Arthroscopic & Related Surgery* 25(4):400-404.

Matta, J.M., Shahrदार, C., Ferguson, T., 2005. Single-incision anterior approach for total hip arthroplasty on an orthopaedic table. *Clinical Orthopaedics and Related Research*(441):115-124.



- Matthies, A., Skinner, J., Osmani, H., Henckel, J., Hart, A., 2012. Pseudotumors are common in well-positioned low-wearing metal-on-metal hips. *Clinical Orthopaedics and Related Research* 470(7):1895-1906.
- McCarthy, J., Noble, P., Aluisio, F., Schuck, M., Wright, J., Lee, J.-a., 2003. Anatomy, pathologic features, and treatment of acetabular labral tears. *Clinical Orthopaedics and Related Research*(406):38-47.
- McCarthy, J.C., Noble, P.C., Schuck, M.R., Wright, J., Lee, J., 2001a. The role of labral lesions to development of early degenerative hip disease. *Clinical Orthopaedics and Related Research*(393):25-37.
- McCarthy, J.C., Noble, P.C., Schuck, M.R., Wright, J., Lee, J., 2001b. The watershed labral lesion: Its relationship to early arthritis of the hip. *The Journal of Arthroplasty* 16(8, Supplement 1):81-87.
- McCormick, F., Slikker, W., III, Harris, J., Gupta, A., Abrams, G., Frank, J., Bach, B., Jr., Nho, S., 2014. Evidence of capsular defect following hip arthroscopy. *Knee surgery, sports traumatology, arthroscopy* 22(4):902-905.
- McDermott, I.D., Amis, A.A., 2006. The consequences of meniscectomy. *Journal of bone and joint surgery. British volume* 88(12):1549-1556.
- McDonnell, S.M., Boyce, G., Baré, J., Young, D., Shimmin, A.J., 2013. The incidence of noise generation arising from the large-diameter Delta Motion ceramic total hip bearing. *Bone & Joint Journal* 95-B(2):160-165.
- McGrory, B., Morrey, B., Cahalan, T., An, K., Cabanela, M., 1995. Effect of femoral offset on range of motion and abductor muscle strength after total hip arthroplasty. *Journal of Bone & Joint Surgery, British Volume* 77-B(6):865-869.
- McKellop, H., Shen, F.-w., Lu, B., Campbell, P., Salovey, R., 1999. Development of an extremely wear-resistant ultra high molecular weight polyethylene for total hip replacements. *Journal of Orthopaedic Research* 17(2):157-167.
- McMinn, D.J.W., Daniel, J., Ziaee, H., Pradhan, C., 2011. Indications and results of hip resurfacing. *International Orthopaedics* 35(2):231-237.

## CHAPTER 10

Mei Dan, O., McConkey, M., Brick, M., 2012. Catastrophic failure of hip arthroscopy due to iatrogenic instability: can partial division of the ligamentum teres and iliofemoral ligament cause subluxation? *Arthroscopy* 28(3):440-445.

Mellon, S.J., Grammatopoulos, G., Andersen, M.S., Pandit, H.G., Gill, H.S., Murray, D.W., 2015. Optimal acetabular component orientation estimated using edge-loading and impingement risk in patients with metal-on-metal hip resurfacing arthroplasty. *Journal of Biomechanics* 48(2):318-323.

Mellon, S.J., Grammatopoulos, G., Andersen, M.S., Pegg, E.C., Pandit, H.G., Murray, D.W., Gill, H.S., 2013. Individual motion patterns during gait and sit-to-stand contribute to edge-loading risk in metal-on-metal hip resurfacing. *Proceedings of the Institution of Mechanical Engineers, Part H: Journal of Engineering in Medicine* 227(7):799-810.

Mellon, S.J., Kwon, Y.M., Glyn Jones, S., Murray, D.W., Gill, H.S., 2011. The effect of motion patterns on edge-loading of metal-on-metal hip resurfacing. *Medical Engineering & Physics* 33(10):1212-1220.

Mesko, J.W., D'Antonio, J., Capello, W., Bierbaum, B., Naughton, M., 2011. Ceramic-on-ceramic hip outcome at a 5- to 10-year interval: has it lived up to its expectations? *The Journal of Arthroplasty* 26(2):172-177.

Meyer, D.C., Beck, M., Ellis, T., Ganz, R., Leunig, M., 2006. Comparison of six radiographic projections to assess femoral head/neck asphericity. *Clin Orthop Relat Res* 445:181-185.

MHRA, 2010. Medical Device Alert: DePuy ASR™ hip replacement implants. Medicines and Healthcare products Regulatory Agency.

Mihalko, W.M., Whiteside, L.A., 2004. Hip mechanics after posterior structure repair in total hip arthroplasty. *Clinical Orthopaedics and Related Research*(420):194-198.

Mindivan, H., Sabri Kayali, E., Cimenoglu, H., 2008. Tribological behavior of squeeze cast aluminum matrix composites. *Wear* 265(5–6):645-654.

Modenese, L., 2012. Hip contact force prediction using a musculoskeletal model of the lower limb. Ph.D, Imperial College London, London.

- Modenese, L., Gopalakrishnan, A., Phillips, A.T.M., 2013. Application of a falsification strategy to a musculoskeletal model of the lower limb and accuracy of the predicted hip contact force vector. *Journal of Biomechanics* 46(6):1193-1200.
- Modenese, L., Phillips, A.M., 2012. Prediction of hip contact forces and muscle activations during walking at different speeds. *Multibody System Dynamics* 28(1-2):157-168.
- Modenese, L., Phillips, A.T.M., Bull, A.M.J., 2011. An open source lower limb model: Hip joint validation. *Journal of Biomechanics* 44(12):2185-2193.
- Modenese, L., Phillips, A.T.M., Thibon, A., 2012. OpenSim plugin to extract the muscle lines of action. [https://simtk.org/home/force\\_direction/](https://simtk.org/home/force_direction/) (Last accessed: 16 Jan 2013).
- Mont, M.A., Seyler, T.M., Ragland, P.S., Starr, R., Erhart, J., Bhav, A., 2007. Gait Analysis of Patients with Resurfacing Hip Arthroplasty Compared with Hip Osteoarthritis and Standard Total Hip Arthroplasty. *The Journal of Arthroplasty* 22(1):100-108.
- Moon, D., Woo, S.L.Y., Takakura, Y., Gabriel, M., Abramowitch, S., 2006. The effects of refreezing on the viscoelastic and tensile properties of ligaments. *Journal of Biomechanics* 39(6):1153-1157.
- Morlock, M., Schneider, E., Bluhm, A., Vollmer, M., Bergmann, G., Muller, V., Honl, M., 2001. Duration and frequency of every day activities in total hip patients. *Journal of Biomechanics* 34(7):873-881.
- Murphy, A.J., Bull, A.M.J., McGregor, A.H., 2011. Predicting the lumbosacral joint centre location from palpable anatomical landmarks. *Proceedings of the Institution of Mechanical Engineers; Part H; Journal of Engineering in Medicine* 225(11):1078-1083.
- Murphy, L.B., Helmick, C.G., Schwartz, T.A., Renner, J.B., Tudor, G., Koch, G.G., Dragomir, A.D., Kalsbeek, W.D., Luta, G., Jordan, J.M., 2010. One in four people may develop symptomatic hip osteoarthritis in his or her lifetime. *Osteoarthritis and Cartilage* 18(11):1372-1379.
- Murray, D.W., 1993. The definition and measurement of acetabular orientation. *Journal of bone and joint surgery. British volume* 75(2):228-232.

## CHAPTER 10

Murray, D.W., Grammatopoulos, G., Pandit, H., Gundle, R., Gill, H.S., McLardy-Smith, P., 2012. The ten-year survival of the Birmingham hip resurfacing: An independent series. *Journal of Bone & Joint Surgery, British Volume* 94-B(9):1180-1186.

Murray, D.W., O'Connor, J.J., 1998. Superolateral wear of the acetabulum. *Journal of bone and joint surgery. British volume* 80(2):197-200.

Myant, C., Underwood, R., Fan, J., Cann, P.M., 2012. Lubrication of metal-on-metal hip joints: the effect of protein content and load on film formation and wear. *Journal of the mechanical behavior of biomedical materials* 630-40.

Myers, C.A., Register, B.C., Lertwanich, P., Ejnisman, L., Pennington, W.W., Giphart, J.E., LaPrade, R.F., Philippon, M.J., 2011. Role of the Acetabular Labrum and the Iliofemoral Ligament in Hip Stability An In Vitro Biplane Fluoroscopy Study. *American Journal of Sports Medicine* 3985S-91S.

Nadzadi, M.E., Pedersen, D.R., Yack, H.J., Callaghan, J.J., Brown, T.D., 2003. Kinematics, kinetics, and finite element analysis of commonplace maneuvers at risk for total hip dislocation. *Journal of Biomechanics* 36(4):577-591.

Nakahara, I., Takao, M., Sakai, T., Nishii, T., Yoshikawa, H., Sugano, N., 2011. Gender differences in 3D morphology and bony impingement of human hips. *Journal of Orthopaedic Research* 29(3):333-339.

Neal, M.L., Kerckhoffs, R., 2010. Current progress in patient-specific modeling. *Briefings in Bioinformatics* 11(1):111-126.

Németh, G., Ohlsén, H., 1985. In vivo moment arm lengths for hip extensor muscles at different angles of hip flexion. *Journal of Biomechanics* 18(2):129-140.

Nevelos, J., Ingham, E., Doyle, C., Streicher, R., Nevelos, A., Walter, W., Fisher, J., 2000. Microseparation of the centers of alumina-alumina artificial hip joints during simulator testing produces clinically relevant wear rates and patterns. *Journal of Arthroplasty* 15(6):793-795.

Nevelos, J.E., Ingham, E., Doyle, C., Fisher, J., Nevelos, A.B., 1999. Analysis of retrieved alumina ceramic components from Mittelmeier total hip prostheses. *Biomaterials* 20(19):1833-1840.

- Ng, F., Zhang, J., Chiu, K., Yan, C., 2011. A cadaveric study of posterior dislocation after total hip replacement-effects of head diameter and acetabular anteversion. *International Orthopaedics* 35(3):325-329.
- Ng, V.Y., Arora, N., Best, T.M., Pan, X., Ellis, T.J., 2010. Efficacy of Surgery for Femoroacetabular Impingement A Systematic Review. *American Journal of Sports Medicine* 38(11):2337-2345.
- Nizard, R., Pourreyron, D., Raoult, A., Hannouche, D., Sedel, L., 2008. Alumina-on-alumina hip arthroplasty in patients younger than 30 years old. *Clinical Orthopaedics and Related Research* 466(2):317-323.
- NJR, 2011. 8th Annual Report. National Joint Registry for England and Wales.
- NJR, 2013. 10th Annual Report. National Joint Registry for England and Wales.
- NJR, 2014. 11th Annual Report. National Joint Registry for England and Wales.
- Nowlan, N.C., Chandaria, V., Sharpe, J., 2014. Immobilized chicks as a model system for early-onset developmental dysplasia of the hip. *Journal of Orthopaedic Research* 32(6):777-785.
- Nussbaumer, S., Leunig, M., Glatthorn, J., Stauffacher, S., Gerber, H., Maffiuletti, N., 2010. Validity and test-retest reliability of manual goniometers for measuring passive hip range of motion in femoroacetabular impingement patients. *BMC musculoskeletal disorders* 11(1):194.
- NZJR, 2014. 14th Annual Report. New Zealand Joint Registry.
- Ohara, B., 2006. Muscles of the Hip. [http://commons.wikimedia.org/wiki/File%3AAnterior\\_Hip\\_Muscles\\_2.PNG](http://commons.wikimedia.org/wiki/File%3AAnterior_Hip_Muscles_2.PNG); CC-BY-SA-3.0 (<http://creativecommons.org/licenses/by-sa/3.0/>) (Last accessed:
- Panagopoulos, C.N., Georgiou, E.P., Gavras, A.G., 2009. Corrosion and wear of 6082 aluminum alloy. *Tribology International* 42(6):886-889.
- Pandit, H., Glyn-Jones, S., McLardy-Smith, P., Gundle, R., Whitwell, D., Gibbons, C.L.M., Ostlere, S., Athanasou, N., Gill, H.S., Murray, D.W., 2008. Pseudotumours associated with metal-onmetal hip resurfacings. *Journal of Bone and Joint Surgery-British Volume* 90B(7):847-851.

## CHAPTER 10

Panjabi, M.M., Krag, M., Summers, D., Videman, T., 1985. Biomechanical time-tolerance of fresh cadaveric human spine specimens. *Journal of Orthopaedic Research* 3(3):292-300.

Papalia, R., Del Buono, A., Franceschi, F., Marinozzi, A., Maffulli, N., Denaro, V., 2012. Femoroacetabular impingement syndrome management: arthroscopy or open surgery? *International Orthopaedics* 36(5):903-914.

Park, S., Krebs, D.E., Mann, R.W., 1999. Hip muscle co-contraction: evidence from concurrent in vivo pressure measurement and force estimation. *Gait & Posture* 10(3):211-222.

Pedersen, D.R., Callaghan, J.J., Brown, T.D., 2005. Activity-dependence of the "safe zone" for impingement versus dislocation avoidance. *Medical Engineering & Physics* 27(4):323-328.

Perron, M., Malouin, F., Moffet, H., McFadyen, B.J., 2000. Three-dimensional gait analysis in women with a total hip arthroplasty. *Clinical Biomechanics* 15(7):504-515.

Peters, C., Erickson, J., 2006. Treatment of femoro-acetabular impingement with surgical dislocation and débridement in young adults. *Journal of Bone and Joint Surgery; American volume* 88(8):1735-1741.

Petersen, W., Petersen, F., Tillmann, B., 2003. Structure and vascularization of the acetabular labrum with regard to the pathogenesis and healing of labral lesions. *Archives of Orthopaedic and Trauma Surgery* 123(6):283-288.

Philippon, M., Schenker, M., Briggs, K., Kuppersmith, D., 2007a. Femoroacetabular impingement in 45 professional athletes: associated pathologies and return to sport following arthroscopic decompression. *Knee surgery, sports traumatology, arthroscopy* 15(7):908-914.

Philippon, M., Stubbs, A., Schenker, M., Maxwell, R.B., Ganz, R., Leunig, M., 2007b. Arthroscopic management of femoroacetabular impingement: osteoplasty technique and literature review. *American Journal of Sports Medicine* 35(9):1571-1580.

Philippon, M.J., Arnoczky, S.P., Torrie, A., 2007c. Arthroscopic Repair of the Acetabular Labrum: A Histologic Assessment of Healing in an Ovine Model. *Arthroscopy: The Journal of Arthroscopic & Related Surgery* 23(4):376-380.

- Philippon, M.J., Schenker, M.L., Briggs, K.K., Kuppersmith, D.A., Maxwell, R.B., Stubbs, A.J., 2007d. Revision hip arthroscopy. *American Journal of Sports Medicine* 35(11):1918-1921.
- Phillips, A., Bartlett, G., Norton, M., Fern, D., 2012. Hip stability after ligamentum teres resection during surgical dislocation for cam impingement. *Hip International* 22(3):329-334.
- Ranawat, A.S., McClincy, M., Sekiya, J.K., 2009. Anterior Dislocation of the Hip After Arthroscopy in a Patient with Capsular Laxity of the Hip A Case Report. *The Journal of Bone & Joint Surgery* 91(1):192-197.
- Rao, J., Zhou, Y.X., Villar, R.N., 2001. Injury to the ligamentum teres. Mechanism, findings, and results of treatment. *Clinics in sports medicine* 20(4):791-799, vii.
- Register, B., Pennock, A.T., Ho, C.P., Strickland, C.D., Lawand, A., Philippon, M.J., 2012. Prevalence of Abnormal Hip Findings in Asymptomatic Participants: A Prospective, Blinded Study. *The American Journal of Sports Medicine* 40(12):2720-2724.
- Ren, D., Sun, K., Tian, S., Yang, X., Zhang, C., Wang, W., Huang, H., Zhang, J., Deng, Y., 2012. Effects of gamma irradiation and repetitive freeze-thaw cycles on the biomechanical properties of human flexor digitorum superficialis tendons. *Journal of Biomechanics* 45(2):252-256.
- Reynolds, D., Lucas, J., Klaue, K., 1999. Retroversion of the acetabulum: A CAUSE OF HIP PAIN. *Journal of Bone & Joint Surgery, British Volume* 81-B(2):281-288.
- Roach, K.E., Miles, T.P., 1991. Normal hip and knee active range of motion: the relationship to age. *Physical Therapy* 71(9):656-665.
- Rushfeld, P.D., 1979. Influence of cartilage geometry on the pressure distribution in the human hip joint. *Science* 204(4391):413.
- Safran, M., Lopomo, N., Zaffagnini, S., Signorelli, C., Vaughn, Z., Lindsey, D., Gold, G., Giordano, G., Marcacci, M., 2013. In vitro analysis of peri-articular soft tissues passive constraining effect on hip kinematics and joint stability. *Knee surgery, sports traumatology, arthroscopy* 21(7):1655-1663.

## CHAPTER 10

Safran, M.R., Giordano, G., Lindsey, D.P., Gold, G.E., Rosenberg, J., Zaffagnini, S., Giori, N.J., 2011. Strains Across the Acetabular Labrum During Hip Motion A Cadaveric Model. *American Journal of Sports Medicine* 39(2S):102S.

Sanders, A., Dudhiya, P., Brannon, R., 2012. Thin hard crest on the edge of ceramic acetabular liners accelerates wear in edge loading. *The Journal of Arthroplasty* 27(1):150-152.

Sansone, M., Ahldén, M., Jónasson, P., Swärd, L., Eriksson, T., Karlsson, J., 2013. Total dislocation of the hip joint after arthroscopy and ileopsoas tenotomy. *Knee surgery, sports traumatology, arthroscopy* 21(2):420-423.

Sariali, E., Stewart, T., Jin, Z.M., Fisher, J., 2010. In Vitro Investigation of Friction under Edge Loading Conditions for Ceramic-on-Ceramic Total Hip Prosthesis. *Journal of Orthopaedic Research* 28(8):979-985.

Schilders, E., Dimitrakopoulou, A., Bismil, Q., Marchant, P., Cooke, C., 2011. Arthroscopic treatment of labral tears in femoroacetabular impingement: a comparative study of refixation and resection with a minimum two-year follow-up. *Journal of Bone and Joint Surgery-British Volume* 93B(8):1027-1032.

Scifert, C., Brown, T., Pedersen, D., Heiner, A., Callaghan, J., 1999. Development and Physical Validation of a Finite Element Model of Total Hip Dislocation. *Computer Methods in Biomechanics and Biomedical Engineering* 2(2):139-147.

Scifert, C.F., Noble, P.C., Brown, T.D., Bartz, R.L., Kadakia, N., Sugano, N., Johnston, R.C., Pedersen, D.R., Callaghan, J.J., 2001. Experimental and computational simulation of total hip arthroplasty dislocation. *Orthopedic Clinics of North America* 32(4):553-567.

Seidel, G.K., Dijkers, M., Soutaslittle, R.W., Marchinda, D.M., Soutas Little, R.W., 1995. Hip joint center location from palpable bony landmarks--a cadaver study. *Journal of Biomechanics* 28(8):995-998.

Seldes, R.M., Tan, V., Hunt, J., Katz, M., Winiarsky, R., Fitzgerald, R.H., 2001. Anatomy, histologic features, and vascularity of the adult acetabular labrum. *Clinical Orthopaedics and Related Research*(382):232-240.



- Selvik, G., 1989. Roentgen stereophotogrammetry. A method for the study of the kinematics of the skeletal system. *Acta orthopaedica Scandinavica. Supplementum* 2321-51.
- Shabana, A.A., 2013. *Dynamics of Multibody Systems*, in. Cambridge University Press, pp. 67-68.
- Shaw, J., Hunter, S., Gayton, J.C., Boivin, G., Prayson, M., 2012. Repeated freeze-thaw cycles do not alter the biomechanical properties of fibular allograft bone. *Clinical Orthopaedics and Related Research* 470(3):937-943.
- Shelburne, K.B., Decker, M.J., Krong, J., Torry, M.R., Philippon, M.J., 2010a. Hip Joint Forces during Squatting Exercise Predicted with Subject-specific Modeling, *Transaction of the 56th Annual Meeting of the Orthopaedic Research Society*.
- Shelburne, K.B., Decker, M.J., Krong, J., Torry, M.R., Philippon, M.J., 2010b. Muscle Forces at the Hip during Squatting Exercise, *Transaction of the 56th Annual Meeting of the Orthopaedic Research Society*.
- Shon, W., Baldini, T., Peterson, M., Wright, T., Salvati, E., 2005. Impingement in total hip arthroplasty a study of retrieved acetabular components. *The Journal of Arthroplasty* 20(4):427-435.
- Siebenrock, K.A., Ferner, F., Noble, P.C., Santore, R.F., Werlen, S., Mamisch, T.C., 2011. The Cam-type Deformity of the Proximal Femur Arises in Childhood in Response to Vigorous Sporting Activity. *Clinical Orthopaedics and Related Research* 469(11):3229-3240.
- Siebenrock, K.A., Fiechter, R., Tannast, M., Mamisch, T.C., von Rechenberg, B., 2013. Experimentally induced cam impingement in the sheep hip. *Journal of Orthopaedic Research* 31(4):580-587.
- Siebenrock, K.A., Schoeniger, R., Ganz, R., 2003. Anterior femoro-acetabular impingement due to acetabular retroversion - Treatment with periacetabular osteotomy. *Journal of Bone and Joint Surgery-American Volume* 85A(2):278-286.
- Signorelli, C., Lopomo, N., Bonanzinga, T., Marcheggiani Muccioli, G.M., Safran, M., Marcacci, M., Zaffagnini, S., 2013. Relationship between femoroacetabular contact areas and hip position in the normal joint: an in vitro evaluation. *Knee surgery, sports traumatology, arthroscopy* 21(2):408-414.

## CHAPTER 10

Sioen, W., Simon, J.P., Labey, L., Van Audekercke, R., 2002. Posterior transosseous capsulotendinous repair in total hip arthroplasty - A cadaver study. *Journal of Bone and Joint Surgery-American Volume* 84A(10):1793-1798.

Smith, C.D., Masouros, S., Hill, A.M., Amis, A.A., Bull, A.M.J., 2009. A biomechanical basis for tears of the human acetabular labrum. *British Journal of Sports Medicine* 43(8):574-578.

Smith, C.D., Masouros, S., Hill, A.M., Wallace, A.L., Amis, A.A., Bull, A.M.J., 2008. Mechanical testing of intra-articular tissues. Relating experiments to physiological function. *Current Orthopaedics* 22(5):341-348.

Smith, I.M., 2002. Least-squares plane (orthogonal distance regression). <http://uk.mathworks.com/matlabcentral/fileexchange/> (Last accessed: 10/05/2013).

Smith, M.V., Costic, R.S., Allaire, R., Schilling, P.L., Sekiya, J.K., 2014. A biomechanical analysis of the soft tissue and osseous constraints of the hip joint. *Knee Surg Sports Traumatol Arthrosc* 22(4):946-952.

Smith, M.V., Panchal, H.B., Thiele, R.A.R., Sekiya, J.K., 2011. Effect of Acetabular Labrum Tears on Hip Stability and Labral Strain in a Joint Compression Model. *American Journal of Sports Medicine* 39103S-110S.

Söderkvist, I., Wedin, P.-Å., 1993. Determining the movements of the skeleton using well-configured markers. *Journal of Biomechanics* 26(12):1473-1477.

Song, Y., Ito, H., Kourtis, L., Safran, M., Carter, D., Giori, N., 2012. Articular cartilage friction increases in hip joints after the removal of acetabular labrum. *Journal of Biomechanics* 45(3):524-530.

Southgate, D.F.L., Hill, A., Alexander, S., Wallace, A., Hansen, U., Bull, A.M.J., 2009. The range of axial rotation of the glenohumeral joint. *Journal of Biomechanics* 42(9):1307-1312.

Sparks, D., Beason, D., Etheridge, B., Alonso, J., Eberhardt, A., 2005. Contact pressures in the flexed hip joint during lateral trochanteric loading. *Journal of Orthopaedic Research* 23(2):359-366.

Spera, D., Genovese, K., Voloshin, A., 2011. Application of Stereo-Digital Image Correlation to Full-Field 3-D Deformation Measurement of Intervertebral Disc. *Strain* 47E572-E587.

Stephen, J.M., Kader, D., Lumpaopong, P., Deehan, D.J., Amis, A.A., 2013. Sectioning the medial patellofemoral ligament alters patellofemoral joint kinematics and contact mechanics. *Journal of Orthopaedic Research* 31(9):1423-1429.

Stephen, J.M., Kaider, D., Lumpaopong, P., Deehan, D.J., Amis, A.A., 2014. The Effect of Femoral Tunnel Position and Graft Tension on Patellar Contact Mechanics and Kinematics After Medial Patellofemoral Ligament Reconstruction. *The American Journal of Sports Medicine* 42(2):364-372.

Stephen, J.M., Lumpaopong, P., Deehan, D.J., Kader, D., Amis, A.A., 2012. The Medial Patellofemoral Ligament: Location of Femoral Attachment and Length Change Patterns Resulting From Anatomic and Nonanatomic Attachments. *The American Journal of Sports Medicine* 40(8):1871-1879.

Stewart, K.J., Edmonds-Wilson, R.H., Brand, R.A., Brown, T.D., 2002. Spatial distribution of hip capsule structural and material properties. *Journal of Biomechanics* 35(11):1491-1498.

Stewart, T.D., Tipper, J.L., Insley, G., Streicher, R.M., Ingham, E., Fisher, J., 2003. Long-term wear of ceramic matrix composite materials for hip prostheses under severe swing phase microseparation. *Journal of Biomedical Materials Research Part B- Applied Biomaterials* 66B(2):567-573.

Sutton, M.A., Orteu, J.-J., Schreier, H., 2009. Image correlation for shape, motion and deformation measurements. Springer, New York.

Sztefek, P., Vanleene, M., Olsson, R., Collinson, R., Pitsillides, A.A., Shefelbine, S., 2010. Using digital image correlation to determine bone surface strains during loading and after adaptation of the mouse tibia. *Journal of Biomechanics* 43(4):599-605.

Taddei, F., Cristofolini, L., Martelli, S., Gill, H.S., Viceconti, M., 2006. Subject-specific finite element models of long bones: An in vitro evaluation of the overall accuracy. *Journal of Biomechanics* 39(13):2457-2467.

## CHAPTER 10

Takechi, H., Nagashima, H., Ito, S., 1982. Intra-articular pressure of the hip joint outside and inside the limbus. *Journal of the Japanese Orthopaedic Association* 56(6):529-536.

Tan, C.K., Wong, W.C., 1990. Absence of the ligament of head of femur in the human hip joint. *Singapore medical journal* 31(4):360-363.

Tan, V., Seldes, R.M., Katz, M.A., Freedhand, A.M., Klimkiewicz, J.J., Fitzgerald, R.H., Jr., 2001. Contribution of acetabular labrum to articulating surface area and femoral head coverage in adult hip joints: an anatomic study in cadavera. *American journal of orthopedics (Belle Mead, N.J.)* 30(11):809-812.

Tannast, M., Hanke, M., Ecker, T., Murphy, S., Albers, C., Puls, M., 2012. LCPD: Reduced Range of Motion Resulting From Extra- and Intraarticular Impingement. *Clinical Orthopaedics and Related Research®* 470(9):2431-2440.

Tannast, M., Kubiak Langer, M., Langlotz, F., Puls, M., Murphy, S., Siebenrock, K., 2007a. Noninvasive three-dimensional assessment of femoroacetabular impingement. *Journal of Orthopaedic Research* 25(1):122-131.

Tannast, M., Siebenrock, K.A., Anderson, S.E., 2007b. Femoroacetabular impingement: radiographic diagnosis—what the radiologist should know. *AJR, American journal of roentgenology* 188(6):1540.

Telleria, J.J.M., Lindsey, D., Giori, N., Safran, M., 2011. An anatomic arthroscopic description of the hip capsular ligaments for the hip arthroscopist. *Arthroscopy* 27(5):628-636.

Terayama, K., Takei, T., Nakada, K., 1980. Joint Space of the Human Knee and Hip Joint under a Static Load. *Engineering in Medicine* 9(2):67-74.

ThyssenKrupp-Materials, 2013. Aluminium and Stainless Steel Stocklist and Technical Information: EN 755 Aluminium Flat Bar Tolerances.

Tijssen, M., van Cingel, R., Willemsen, L., de Visser, E., 2012. Diagnostics of Femoroacetabular Impingement and Labral Pathology of the Hip: A Systematic Review of the Accuracy and Validity of Physical Tests. *Arthroscopy: The Journal of Arthroscopic & Related Surgery* 28(6):860-871.

- Tohnichi, 2012. Technical Data: Bolt Tightening. <http://tohnichi.jp/english/technical/index.html> (Last accessed: 05/02/2015).
- Toms, A.P., Marshall, T.J., Cahir, J., Darrah, C., Nolan, J., Donell, S.T., Barker, T., Tucker, J.K., 2008. MRI of early symptomatic metal-on-metal total hip arthroplasty: a retrospective review of radiological findings in 20 hips. *Clinical Radiology* 63(1):49-58.
- Tönnis, D., Legal, H., Graf, R., 1987. Congenital dysplasia and dislocation of the hip in children and adults. Springer-Verlag Berlin.
- Treacy, R.B.C., McBryde, C.W., Shears, E., Pynsent, P.B., 2011. Birmingham hip resurfacing: a minimum follow-up of ten years. *Journal of bone and joint surgery. British volume* 93(1):27-33.
- Turley, G.A., Ahmed, S.M.Y., Williams, M.A., Griffin, D.R., 2011. Establishing a range of motion boundary for total hip arthroplasty. *Proceedings of the Institution of Mechanical Engineers; Part H; Journal of Engineering in Medicine* 225(8):769-782.
- Udofia, I.J., Jin, Z.M., 2003. Elastohydrodynamic lubrication analysis of metal-on-metal hip-resurfacing prostheses. *Journal of Biomechanics* 36(4):537-544.
- Underwood, R., Matthies, A., Cann, P., Skinner, J.A., Hart, A.J., 2011. A comparison of explanted Articular Surface Replacement and Birmingham Hip Resurfacing components. *Journal of Bone and Joint Surgery-British Volume* 93B(9):1169-1177.
- Underwood, R., Zografos, A., Sayles, R., Hart, A., Cann, P., 2012. Edge loading in metal-on-metal hips: low clearance is a new risk factor. *Proceedings of the Institution of Mechanical Engineers; Part H; Journal of Engineering in Medicine* 226(H3):217-226.
- Unnanuntana, A., Toogood, P., Hart, D., Cooperman, D., Grant, R.E., 2010. Evaluation of proximal femoral geometry using digital photographs. *Journal of Orthopaedic Research* 28(11):1399-1404.
- Valstar, E.R., Reiber, J.H.C., de Jong, F.W., Vrooman, H.A., Rozing, P.M., 2001. Model-based Roentgen stereophotogrammetry of orthopaedic implants. *Journal of Biomechanics* 34(6):715-722.
- van Arkel, R., Amis, A., 2013. (i) Basics of orthopaedic biomechanics. *Orthopaedics and Trauma* 27(2):67-75.

## CHAPTER 10

van Arkel, R.J., Amis, A.A., Cobb, J.P., Jeffers, J.R.T., 2015. The capsular ligaments provide more hip rotational restraint than the acetabular labrum and the ligamentum teres: an experimental study. *Bone & Joint Journal* 97-B(4):484-491.

Van Ee, C.A., Chasse, A.L., Myers, B.S., 2000. Quantifying skeletal muscle properties in cadaveric test specimens: effects of mechanical loading, postmortem time, and freezer storage. *Journal of biomechanical engineering* 122(1):9-14.

Vanhegan, I.S., Malik, A.K., Jayakumar, P., Ul Islam, S., Haddad, F.S., 2012. A financial analysis of revision hip arthroplasty. *Journal of Bone & Joint Surgery, British Volume* 94-B(5):619-623.

Vaz, M.D., Kramer, J.F., Rorabeck, C.H., Bourne, R.B., 1993. Isometric Hip Abductor Strength Following Total Hip Replacement and Its Relationship to Functional Assessments. *Journal of Orthopaedic & Sports Physical Therapy* 18(4):526-531.

Viceconti, M., Clapworthy, G., Van Sint Jan, S., 2008. The Virtual Physiological Human - a European initiative for in silico human modelling. *Journal of Physiological Sciences* 58(7):441-446.

von Eisenhart-Rothe, R., Eckstein, F., Muller-Gerbl, M., Landgraf, J., Rock, C., Putz, R., 1997. Direct comparison of contact areas, contact stress and subchondral mineralization in human hip joint specimens. *Anat Embryol (Berl)* 195(3):279-288.

Wagner, F., Negrao, J., Campos, J., Ward, S., Haghighi, P., Trudell, D., Resnick, D., 2012. Capsular ligaments of the hip: anatomic, histologic, and positional study in cadaveric specimens with MR arthrography. *Radiology* 263(1):189-198.

Wahba, G., 1965. A Least Squares Estimate of Satellite Attitude. *SIAM Review* 7(3):409-409.

Walter, W.L., Insley, G.M., Walter, W.K., Tuke, M.A., 2004. Edge loading in third generation alumina ceramic-on-ceramic bearings. *Journal of Arthroplasty* 19(4):402-413.

Walter, W.L., Kurtz, S.M., Esposito, C., Hozack, W., Holley, K.G., Garino, J.P., Tuke, M.A., 2011. Retrieval analysis of squeaking alumina ceramic-on-ceramic bearings. *Journal of bone and joint surgery. British volume* 93(12):1597-1601.

- Walter, W.L., Waters, T.S., Gillies, M., Donohoo, S., Kurtz, S.M., Ranawat, A.S., Flozack, W.J., Tuke, M.A., 2008. Squeaking Hips. *Journal of Bone and Joint Surgery-American* Volume 90A102-111.
- Wassilew, G.I., Janz, V., Heller, M.O., Tohtz, S., Rogalla, P., Hein, P., Perka, C., 2013. Real time visualization of femoroacetabular impingement and subluxation using 320-slice computed tomography. *Journal of Orthopaedic Research* 31(2):275-281.
- Wearing, S.C., Hennig, E.M., Byrne, N.M., Steele, J.R., Hills, A.P., 2006. Musculoskeletal disorders associated with obesity: a biomechanical perspective. *Obesity Reviews* 7(3):239-250.
- Weidner, J., Büchler, L., Beck, M., 2012. Hip capsule dimensions in patients with femoroacetabular impingement: a pilot study. *Clinical Orthopaedics and Related Research* 470(12):3306-3312.
- Wertheimer, L.G., Sd, F., 1971. Arterial supply of the femoral head. A combined angiographic and histological study. *Journal of Bone and Joint Surgery; American* volume 53(3):545-556.
- White, R.E., Forness, T.J., Allman, J.K., Junick, D.W., 2001. Effect of posterior capsular repair on early dislocation in primary total hip replacement. *Clinical Orthopaedics and Related Research*(393):163-167.
- Whiteside, L.A., 2002. Soft tissue balancing: The knee. *The Journal of Arthroplasty* 17(4, Supplement 1):23-27.
- Wiadrowski, T.P., McGee, M., Cornish, B.L., Howie, D.W., 1991. Peripheral wear of Wagner resurfacing hip arthroplasty acetabular components. *The Journal of Arthroplasty* 6(2):103-107.
- Wik, T.S., Ostbyhaug, P.O., Klaksvik, J., Aamodt, A., stbyhaug, P.O., 2010. Increased strain in the femoral neck following insertion of a resurfacing femoral prosthesis. *Journal of bone and joint surgery. British* volume 92(3):461-467.
- Wilson, D.R., Feikes, J.D., Zavatsky, A.B., O'Connor, J.J., 2000. The components of passive knee movement are coupled to flexion angle. *Journal of Biomechanics* 33(4):465-473.

## CHAPTER 10

Won, Y.Y., Chung, I.H., Chung, N.S., Song, K.H., 2003. Morphological study on the acetabular labrum. *Yonsei Medical Journal* 44(5):855-862.

Woo, S.L., Gomez, M.A., Woo, Y.K., Akeson, W.H., 1982. Mechanical properties of tendons and ligaments. II. The relationships of immobilization and exercise on tissue remodeling. *Biorheology* 19(3):397-408.

Wroblewski, B.M., Siney, P.D., Fleming, P.A., 2012. Microseparation, fluid pressure and flow in failures of metal-on-metal hip resurfacing arthroplasties. *Bone and Joint Research* 1(3):25-30.

Wu, G., Siegler, S., Allard, P., Kirtley, C., Leardini, A., Siegler, S., Allard, P., Kirtley, C., Leardini, A., Rosenbaum, D., Whittle, M., D'Lima, D., Cristofolini, L., Witte, H., Schmid, O., Stokes, I., 2002. ISB recommendation on definitions of joint coordinate system of various joints for the reporting of human joint motion--part I: ankle, hip, and spine. International Society of Biomechanics. *Journal of Biomechanics* 35(4):543-548.

Wu, G., van der Helm, F.C.T., Veeger, H.E.J., Makhsous, M., Van Roy, P., Anglin, C., Nagels, J., Karduna, A.R., McQuade, K., Wang, X., Werner, F.W., Buchholz, B., 2005. ISB recommendation on definitions of joint coordinate systems of various joints for the reporting of human joint motion—Part II: shoulder, elbow, wrist and hand. *Journal of Biomechanics* 38(5):981-992.

Xerogeanes, J.W., Takeda, Y., Livesay, G.A., Ishibashi, Y., Kim, H.S., Fu, F.H., Woo, S.L.Y., 1995. Effect of knee flexion on the in situ force distribution in the human anterior cruciate ligament. *Knee surgery, sports traumatology, arthroscopy* 3(1):9-13.

Yoon, J.P., Duff, M.J.L., Johnson, A.J., Takamura, K.M., Ebrahimzadeh, E., Amstutz, H.C., 2012. Contact Patch to Rim Distance Predicts Metal Ion Levels in Hip Resurfacing. *Clinical Orthopaedics and Related Research*® 471(5):1615-1621.

Yoshioka, S., Nagano, A., Hay, D.C., Fukashiro, S., 2012. The minimum required muscle force for a sit-to-stand task. *Journal of Biomechanics* 45(4):699-705.

Yoshioka, S., Nagano, A., Himeno, R., Fukashiro, S., 2007. Computation of the kinematics and the minimum peak joint moments of sit-to-stand movements. *BioMedical Engineering OnLine* 6(1):26.

Yoshioka, Y., Siu, D., Cooke, T.D.V., 1987. The anatomy and functional axes of the femur. *Journal of Bone and Joint Surgery; American volume* 69(6):873-880.



- Young, E.Y., Gebhart, J., Cooperman, D., Ahn, N.U., 2012. Are the Left and Right Proximal Femurs Symmetric? *Clinical Orthopaedics and Related Research*® 471(5):1593-1601.
- Yuan, L.J., Shih, C.H., 1999. Dislocation after total hip arthroplasty. *Archives of Orthopaedic and Trauma Surgery* 119(5):263-266.
- Zeni, J., Pozzi, F., Abujaber, S., Miller, L., 2014. Relationship between physical impairments and movement patterns during gait in patients with end-stage hip osteoarthritis. *Journal of Orthopaedic Research* n/a-n/a.
- Zou, Z., Chávez-Arreola, A., Mandal, P., Board, T.N., Alonso-Rasgado, T., 2013. Optimization of the position of the acetabulum in a ganz periacetabular osteotomy by finite element analysis. *Journal of Orthopaedic Research* 31(3):472-479.



## 11 Appendices

### A3 Hip Abduction Prevents Edge Loading Appendices

#### A3.1 Muscle wrapping geometries

*Muscle wrapping surfaces i and ii were developed by my co-author, Dr Luca Modenese. Also, whilst I developed wrapping surface iii, the initial idea was Luca's and indeed he produced the first iteration of this wrapping surface for the inferior gluteus medius fibres. My modifications to his initial work on wrapping surface iii enabled viable fibre directions in deep hip flexion which had previously been problematic.*

The musculoskeletal model used in this investigation is based on the anatomical measurements collected by Klein Horsman et al. (Klein Horsman et al., 2007) from a single cadaveric specimen. The original dataset has been enhanced at the hip joint by including the following wrapping surfaces:

- i. The hip joint capsule was represented as a sphere centred in the hip joint centre (Figure 11.1). This modelling choice is consistent with the previous investigation of Brand et al. (Brand et al., 1994) and prevents muscle fibres of the gemelli and the obturator internus from crossing the femoral head at high hip flexion angles.
- ii. As medical images for the specimen dissected by Klein Horsman et al. (Klein Horsman et al., 2007) were not made available, the anatomical dataset released through the Living Human Digital Library project (LHDL) (Viceconti et al., 2008), and publicly available at <https://www.physiomespace.com> was used to redesign the gluteus maximus geometry. As this dataset makes available muscle fibre paths collected on the muscle surface, an ellipsoid was fitted in a least squares sense to the point cloud obtained from the gluteus maximus fibers. In order to take into account the flattening of the muscle due to the supine position of the specimen, the ellipsoid axes were varied under the constraint of constant volume and finally scaled to the dimensions of the Klein Horsman specimen using a scaling ratio based on the thigh length. The obtained surface was used for defining a wrapping surface for the upper bundles of gluteus maximus (Figure 11.1).
- iii. An additional wrapping surface representing the ischial tuberosity was included in the model in order to influence the paths of the gluteus maximus inferior bundles (Figure 11.1). A similar modelling choice can be found in a previously

published model of the lower limb (Shelburne et al., 2010b, a). Due to the difference in wraps for the superior and inferior fibre bundles of the gluteus maximus, it is reported in the main text as two different muscles to indicate how the different fibre bundles would contribute to the hip joint reaction force.

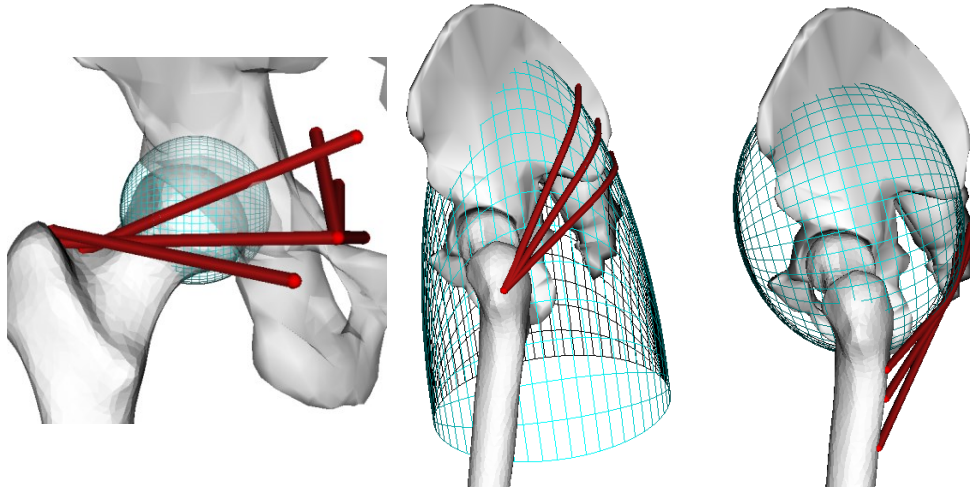


Figure 11.1 Wrapping surfaces included in the model in order to improve the muscle geometrical representation

(Left) the muscles surrounding the femoral head wrap around a capsular like structure (gemelli and obturator internus are shown); (middle) the superior bundles of the gluteus maximus and (right) the inferior bundles of the gluteus maximus.

### A3.2 Plugin overview

*This plug-in was developed solely by Dr Luca Modenese; whilst I used the plug-in extensively during for this study, I had no role in its design or development.*

#### A3.2.1 How it works

The MuscleForceDirection plugin executes a few simple operations. Given a selected body (or a set of bodies) included in an OpenSim model, the plugin:

- i. Identifies the muscles attached to the segment(s).
- ii. Retrieves the current path for each muscle, including wrapping points, by using the `GetPointForceDirections` method of the class `OpenSim::GeometryPath`.
- iii. Identifies the anatomical or effective muscle attachments according to the user selection and calculates the muscle force direction at that point.
- iv. Depending on the reference system chosen by the user (body reference system or global coordinate system), the plugin transforms the previously identified muscle attachment coordinates and force directions by using the methods of the `OpenSim::SimbodyEngine` class.

- v. Prints the muscle force directions and, if requested, the muscle attachments.

### A3.2.2 More information

Full documentation and the plugin can be downloaded for free from [https://simtk.org/home/force\\_direction](https://simtk.org/home/force_direction) (Modenese et al., 2012).

## A3.3 Modelling a hip replacement in MatLab

For the edge loading calculations (A3.4) it is necessary to know the location of the cup-axis in 3D space as well as three points on the edge loading risk-zone plane. The following sections describe how the cup was initialised and orientated and its position verified.

### A3.3.1 Initialising the cup

The cup-axis was initially defined as a superior-inferior unit vector, in the direction of the ISB pelvic Y-axis (Wu et al., 2002), located at the origin (the femoral head/acetabular cup centre). In this initial position, the centre point on the edge loading risk-zone plane is located at  $(0, d_y, 0)$  where  $d_y$  can be calculated using geometrical relationships below (see Figure 11.2 for definitions).

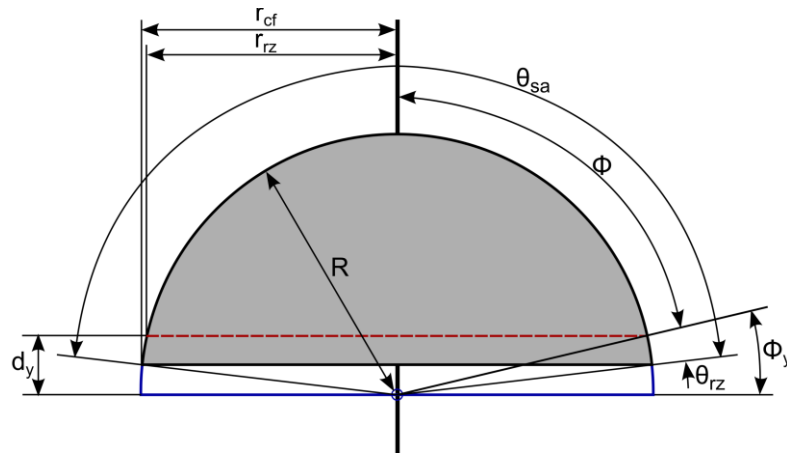


Figure 11.2 Defining an acetabular cup in MatLab

A cup with a subtended arc less than  $180^\circ$  is shown; the cup-axis is the thick black line. The outline of a cup with a  $180^\circ$  subtended arc and its cup-face centre (equivalent to the centre of the femoral head) are also shown in blue. The red-dashed line is the edge loading risk-zone plane (in/out of the page).  $\theta_{sa}$  is the subtended arc angle of the cup,  $\theta_{rz}$  is the edge load risk-zone angle,  $\phi$  is the edge loading safe zone angle and  $\phi_y$  is the angle used to find the risk-zone offset,  $d_y$ , the cup radius (and femoral head radius)  $R$ , the cup face radius  $r_{cf}$  (note that when  $\theta_{sa} < 180^\circ$ ,  $r_{cf} \neq R$ ), and the risk-zone radius,  $r_{rz}$ .

$$\phi = \frac{\theta_{sa}}{2} - \theta_{rz} \quad (11.1)$$

$$\phi_y = 90^\circ - \phi \quad (11.2)$$

$$d_y = R \sin \phi_y ; r_{rz} = R \cos \phi_y \quad (11.3)$$

$$r_{cf} = R \sin \left( \frac{\theta_{sa}}{2} \right) \quad (11.4)$$

### A3.3.2 Orientating the cup

The cup can be positioned according to the definitions published by Murray (Murray, 1993); isolated anteversion is equivalent to flexion about the ISB pelvic Z-axis, and isolated inclination equivalent to abduction about the ISB pelvic X-axis. Thus, two rotation matrices can be defined (for a right-hip acetabular cup) where  $a_v$  is the angle of anteversion and  $[AV]$  the anteversion rotation matrix, and  $i_n$  is the angle of inclination and  $[INC]$  the inclination rotation matrix:

$$[AV] = \begin{bmatrix} \cos a_v & -\sin a_v & 0 \\ \sin a_v & \cos a_v & 0 \\ 0 & 0 & 1 \end{bmatrix} \quad (11.5)$$

$$[INC] = \begin{bmatrix} 1 & 0 & 0 \\ 0 & \cos i_n & -\sin i_n \\ 0 & \sin i_n & \cos i_n \end{bmatrix} \quad (11.6)$$

Matrix multiplication is not commutative and hence the different orders of cup rotation results in different cups orientations. Murray defines operative anteversion as the angle between the cup-axis projected into the sagittal plane with the longitudinal axis of the patient (or the coronal plane), and operative inclination as the angle between the cup-axis and the sagittal plane. Thus, to position a cup in the operative definition first the cup needs to be inclined, and then anteverted:

$$\text{Operative:} \quad [c'] = [AV][INC][c] \quad (11.7)$$

Where  $c'$  is the new cup-axis/edge loading risk zone plane coordinates, and  $c$  is the original coordinates. The definition is analogous to those used to described hip kinematics in the ISB coordinate system (appendix A5.4.4, page 236) where  $[AV] = [Rz]$ ,  $[INC] = [Rx]$  and the hip internal/external rotation matrix set to the identity matrix ( $[Ry] = [I]$ ) as the cup is axis-symmetric about the y-axis in its original position so the internal/external rotation positioning is irrelevant.

For a radiographic definition, the inclination is the angle between the cup-axis projected in the coronal plane and the longitudinal axis of the patient (the sagittal plane); this projection is a result of the anterior view in a radiograph. Radiographic anteversion is equivalent to the angle between the acetabular axis and the coronal plane (Murray, 1993). Thus to orientate a cup in a radiographic position: first the cup is anteverted and then inclined:

$$\text{Radiographic:} \quad [c'] = [INC][AV][c] \quad (11.8)$$

These equations define how to orientate the cup for the purposes of the calculations in appendix A3.4 and also through creating spheres in MatLab they are also used to create the graphics in Figure 3.1 allowing a visual verification of the method.

### A3.3.3 Verification of the cup position

When the radiographic definition was used to orientate the cup, the cup orientation was verified by calculating the operative angles of the cup-axis in its new position using equations (11.9) and (11.10) which calculate the angle between the cup-axis and a plane, and project the cup-axis into a plane respectively (then the angle of the projected vector and a plane/normal to a plane can be calculated). The radiographic orientation was then calculated from these operative angles using the relationships published by Murray to verify that the desired position was achieved by using equations (11.11) and (11.12). To confirm correct orientation using an operative definition, the radiographic orientation of the new position was calculated using equations (11.9) and (11.10) and checked against the desired operative angles using the relevant relationships from Murray: equations (11.13), and (11.14). Cups were also plotted in 3D and the orientation of the acetabular-axis was visually checked.

$$\theta_{ap} = 90^\circ - \cos^{-1} \left( \frac{\mathbf{c}_a \cdot \mathbf{n}_p}{|\mathbf{c}_a| |\mathbf{n}_p|} \right) \quad (11.9)$$

$$\mathbf{c}_{ap} = \frac{\mathbf{n}_p \times (\mathbf{c}_a \times \mathbf{n}_p)}{|\mathbf{n}_p|^2} = \mathbf{c}_a - \frac{(\mathbf{c}_a \cdot \mathbf{n}_p) \mathbf{n}_p}{|\mathbf{n}_p|^2} \quad (11.10)$$

$$a_R = \sin^{-1}(\sin a_O \cos i_O) \quad (11.11)$$

$$i_R = \tan^{-1}(\sec a_O \tan i_O) \quad (11.12)$$

$$a_O = \tan^{-1}(\tan a_R \sec i_R) \quad (11.13)$$

$$i_O = \sin^{-1}(\cos a_R \sin i_R) \quad (11.14)$$

Where  $a_R$  and  $i_R$  are radiographic anteversion and inclination respectively,  $a_O$  and  $i_O$  are operative anteversion and inclination respectively,  $\theta_{ap}$ , is the angle between the cup-axis and a plane,  $\mathbf{c}_a$  is the cup axis vector,  $\mathbf{c}_{ap}$  is the cup-axis vector projected into plane  $p$  with normal  $\mathbf{n}_p$  (this denotes a normal to either the sagittal/coronal plane as required to match the definitions described in A3.3.2).

### A3.4 Calculation to determine if muscles edge loads in a given hip position

The calculation for determining if a muscle edge loads in a given hip position is critical for reliable results and hence was calculated independently using two different methods and the results were compared to ensure that the calculation was being performed correctly. For these calculations, the lines of action of the hip muscles are applied at the centre of the femoral head (equivalent to the joint reaction force for each muscle).

*A3.4.1 Method 1: Calculating the angle between the cup-axis and the muscle line of action*

To determine whether a muscle edge loads or not, the minimum angle,  $\theta_{mn}$ , between the vector of the cup-axis,  $\mathbf{n}_c$ , (normal to the cup-face plane) and the vector of the muscle line of action,  $\mathbf{m}_v$ , is calculated. If this angle is less than  $\phi$  (Figure 11.2), then the muscle does not contribute to edge loading; however if it is greater than or equal to  $\phi$ , then the muscle would contribute to edge loading in that hip position (Figure 11.3). The minimum angle between the cup-axis and the muscle line of action can be calculated using the vector dot product:

$$\theta_{mn} = \cos^{-1} \left( \frac{\mathbf{m}_v \cdot \mathbf{n}_c}{|\mathbf{m}_v| |\mathbf{n}_c|} \right) \quad (11.15)$$

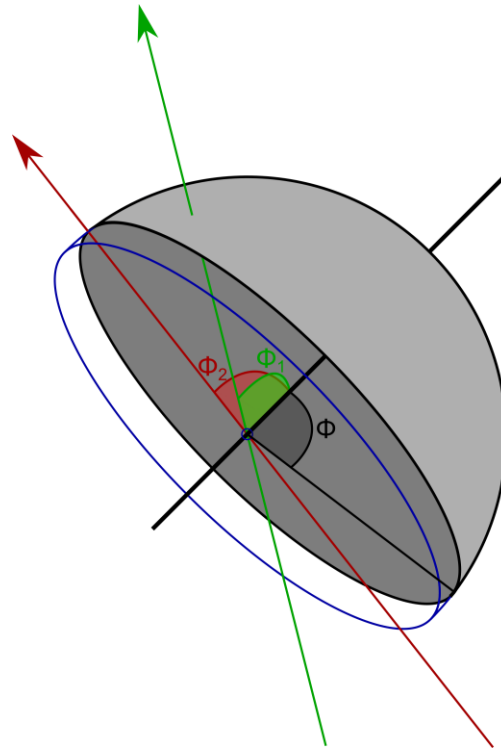


Figure 11.3 Calculating if a muscle edge loads based on the angle it makes with the cup axis

An anterior view of a right hip acetabular cup with a subtended arc less than  $180^\circ$  and the cup-axis is shown (thick black line). The outline of a cup with a  $180^\circ$  subtended arc and its cup-face centre (equivalent to the centre of the femoral head) are also shown (blue). The green muscle line of action is within the safe-zone in the acetabular cup and hence the angle it makes with the cup-axis ( $\phi_1$ ) is less than edge loading safe angle  $\phi$ . However the red muscle line of action would contribute to edge loading; the angle it makes with the cup-axis ( $\phi_2$ ) is greater than  $\phi$ . Note that to reduce complexity in this image, the edge load risk-zone ( $\theta_{rz}$  in Figure 11.2) in this diagram is set to zero such that  $\phi$  is equal to half the subtended arc of the acetabular cup.



#### A3.4.2 Method 2: Finding the intersection point between the cup-face and the muscle line of action

To determine whether a muscle edge loads or not, the intersection point between the muscle line of action and the edge loading risk zone plane can be calculated, then if the distance of this point to the risk-zone plane centre is less than the risk-zone radius then the muscle contributes a safe force; however if the distance is greater than the radius then the muscle would contribute to edge loading (Figure 11.4).

First, the edge loading risk-zone plane is expressed in parametric form:

$$\mathbf{p}_c = \mathbf{c}_0 + (\mathbf{c}_1 - \mathbf{c}_0)u + (\mathbf{c}_2 - \mathbf{c}_0)v \quad (11.16)$$

Where  $\mathbf{c}_0$ ,  $\mathbf{c}_1$  and  $\mathbf{c}_2$  are any three known points (with  $x, y, z$  coordinates) on the risk-zone plane and  $u$  and  $v$  are parameters that can be varied such that any point on the plane,  $\mathbf{p}_c$ , can be calculated using equation (11.16). Then the muscle lines of action are expressed in parametric form:

$$\mathbf{p}_m = \mathbf{m}_0 + (\mathbf{m}_1 - \mathbf{m}_0)t \quad (11.17)$$

Where  $\mathbf{m}_0$  and  $\mathbf{m}_1$  are any two known points (with  $x, y, z$  coordinates) on the muscle's line of action and  $t$  is a parameter that can be varied such that any point on the muscle line of action,  $\mathbf{p}_m$ , can be calculated using equation (11.17).

Then, for each muscle, its intersection point between the line of action and the cup-face plane,  $\mathbf{p}_{isp}$ , is given when  $\mathbf{p}_{isp} = \mathbf{p}_c = \mathbf{p}_m$ :

$$\mathbf{m}_0 + (\mathbf{m}_1 - \mathbf{m}_0)t_{isp} = \mathbf{c}_0 + (\mathbf{c}_1 - \mathbf{c}_0)u_{isp} + (\mathbf{c}_2 - \mathbf{c}_0)v_{isp} \quad (11.18)$$

Rearranging and expressing in matrix form to solve for  $t, u$  and  $v$ :

$$\begin{aligned} \mathbf{m}_0 - \mathbf{c}_0 &= (\mathbf{m}_1 - \mathbf{m}_0)t + (\mathbf{c}_1 - \mathbf{c}_0)u + (\mathbf{c}_2 - \mathbf{c}_0)v \\ [\mathbf{m}_0 - \mathbf{c}_0] &= [(\mathbf{m}_1 - \mathbf{m}_0) \quad (\mathbf{c}_1 - \mathbf{c}_0) \quad (\mathbf{c}_2 - \mathbf{c}_0)] \begin{bmatrix} t_{isp} \\ u_{isp} \\ v_{isp} \end{bmatrix} \\ \begin{bmatrix} t_{isp} \\ u_{isp} \\ v_{isp} \end{bmatrix} &= \begin{bmatrix} (m_{0x} - m_{1x}) & (c_{1x} - c_{0x}) & (c_{2x} - c_{0x}) \\ (m_{0y} - m_{1y}) & (c_{1y} - c_{0y}) & (c_{2y} - c_{0y}) \\ (m_{0z} - m_{1z}) & (c_{1z} - c_{0z}) & (c_{2z} - c_{0z}) \end{bmatrix}^{-1} \begin{bmatrix} m_{0x} - c_{0x} \\ m_{0y} - c_{0y} \\ m_{0z} - c_{0z} \end{bmatrix} \end{aligned} \quad (11.19)$$

Equation (11.19) can be solved in MatLab using the backslash (\) command provided that the line and the plane are not parallel or co-planar (which can be tested with if statements). Then the calculated parameters for the intersection point,  $t_{isp}$ ,  $u_{isp}$  and

$v_{isp}$ , can be substituted into either equation (11.16) or (11.17) to find the  $x, y, z$  coordinates of the intersection point. The scalar distance,  $d_{isp}$ , between the intersection point and the risk-zone centre,  $c_c$ , is calculated using equation (11.20) below and is compared to the risk-zone radius,  $r_{rz}$ , to determine if a muscle would contribute to edge loading; if  $d_{isp} \geq r_{rz}$  then the muscle would contribute to edge loading (Figure 11.4).

$$d_{isp} = \sqrt{(p_{isp_x} - c_{cx})^2 + (p_{isp_y} - c_{cy})^2 + (p_{isp_z} - c_{cz})^2} \quad (11.20)$$

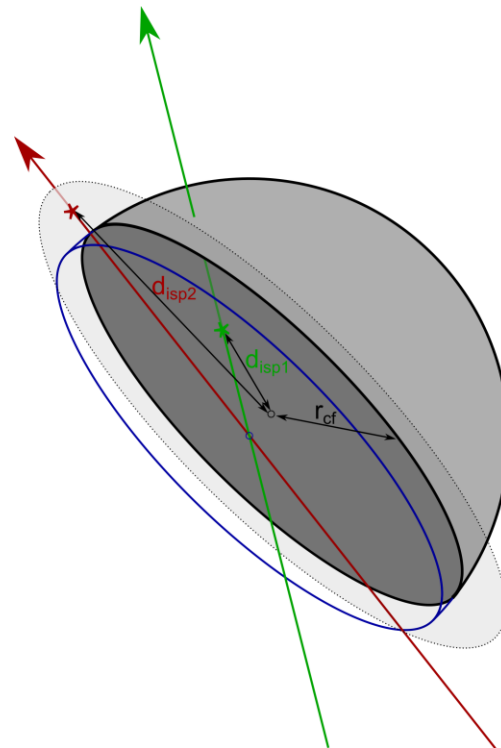


Figure 11.4 Calculating if a muscle edge loads based on its intersection point with the cup face plane.

An anterior view of a right hip acetabular cup with a subtended arc less than  $180^\circ$  and the cup-face plane is shown (transparent grey). The outline of a cup with a  $180^\circ$  subtended arc and its cup-face centre (equivalent to the centre of the femoral head) are also shown (blue). The green muscle line of action is within the safe-zone in the acetabular cup and hence the distance between the intersection point with the cup-face plane and the cup-face plane centre ( $d_{isp1}$ ) is less than the cup-face radius ( $r_{cf}$ ). However the red muscle line of action would contribute to edge loading; the distance between the intersection point with the cup-face plane and the cup-face centre ( $d_{isp2}$ ) is greater than the cup-face radius ( $r_{cf}$ ). Note that to reduce complexity in this figure, the edge load risk-zone ( $\theta_{rz}$  in Figure 11.2) is set to  $0^\circ$  so that risk-zone plane and the cup-face plane are equal (and  $r_{cf} = r_{rz}$ ).

### A3.5 Conversion between Bergmann's and the ISB's coordinate systems

Bergmann's HIP98 coordinate system uses the femoral shaft in the coronal plane for the femoral axis; however, the ISB y-axis uses the femur's mechanical axis (connecting

femoral head centre to mid-point of the epicondyles). For both male and female hips, the mean ( $\pm$ S.D.) shaft centre to mechanical axis angle in the coronal plane is  $5 \pm 1^\circ$  (Yoshioka et al., 1987) and hence this simple correction was applied. There is also a small difference between the definitions for the femoral z-axis; however, the principal results are affected by flexion/extension and ab/adduction hence this small difference in internal/external rotation was not corrected for.

### A3.6 The effects of internal and external rotation on the number of muscles that edge load

Varying the angle of internal and external rotation had a negligible effect on the percentage of muscles that have the potential to edge load Figure 11.5. This is primarily because it is the lines of actions of the long distal muscles that are affected by gross movements of the femur (Figure 3.3) and internal/external rotation only acts to rotate these muscles about the mechanical axis resulting in only small movements of the insertion point (flexion/extension and ab/adduction results in large movements of the femur and hence muscle insertions points and the lines of action).

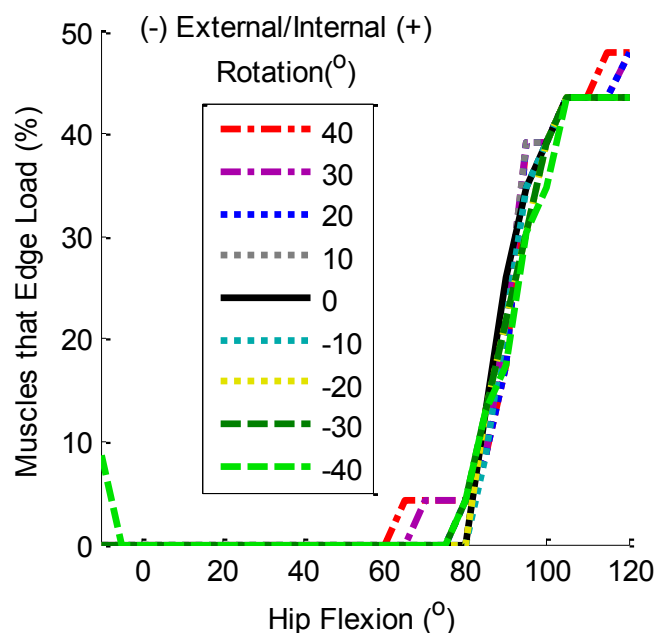


Figure 11.5 The percentage of muscles that can contribute to edge loading as a function of hip flexion with neutral ab/adduction and different hip rotation for a well-positioned cup

### A3.7 The effects of grouping muscle fibres together

For the edge loading analyses, muscle fibres were simplified into single muscles by taking the mean of their origins and lines of action; 92 muscle fibres were averaged to form 23 muscles (noting that the gluteus maximus was treated as two individual

muscles given the different wraps applied to the superior and inferior fibres). Figure 11.6 and Figure 11.8 show how this simplification does not affect the results. Indeed, presenting the results as individual muscles has the advantage that muscles with high/low numbers of fibres do not skew the results; for example the semitendinosus is represented as a single muscle fibre because it has a point insertion, whereas the gluteus medius is represented as 12 muscle fibres bundles to cover the area of its insertion. The disadvantage of presenting the results for individual muscles rather than muscle fibre bundles is that it gives all muscles an equal weighting, which means high force capacity muscles and weak muscles are given equal weighting. However, considering the maximum force capacity of each muscle, by multiplying it by its physiological cross section area, also has little effect on the results (Figure 11.7); the maximum force capacity of each muscle is directly proportional to its physiological cross-sectional area (Klein Horsman et al., 2007; Modenese et al., 2013). Importantly, the conclusion that activity modifications could prevent posterior edge loading of hip replacements, is unaffected by how the results are presented.

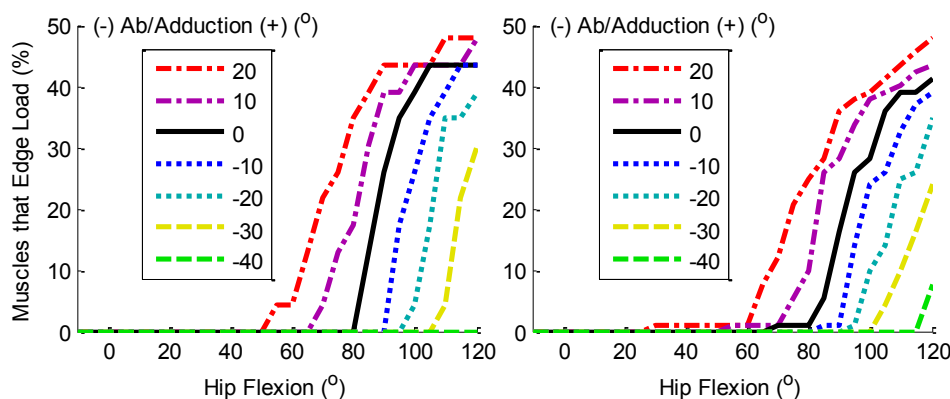


Figure 11.6 The percentage of muscles that can contribute to edge loading with muscle fibres are grouped as complete muscles (the original analysis, left) and each muscle fibre plotted individually (right). It can be seen that there is little difference between the two analyses.

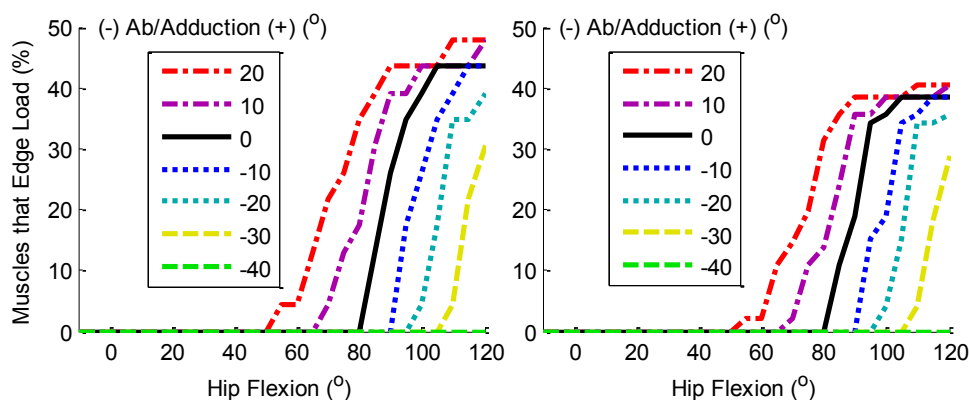


Figure 11.7 The percentage of the number of muscles that can contribute to edge loading (the original analysis, left) and the percentage of total force capacity at the hip that could contribute to edge loading (the percentage of physiological cross sectional area, right). It can be seen that there is little difference between the two analyses.

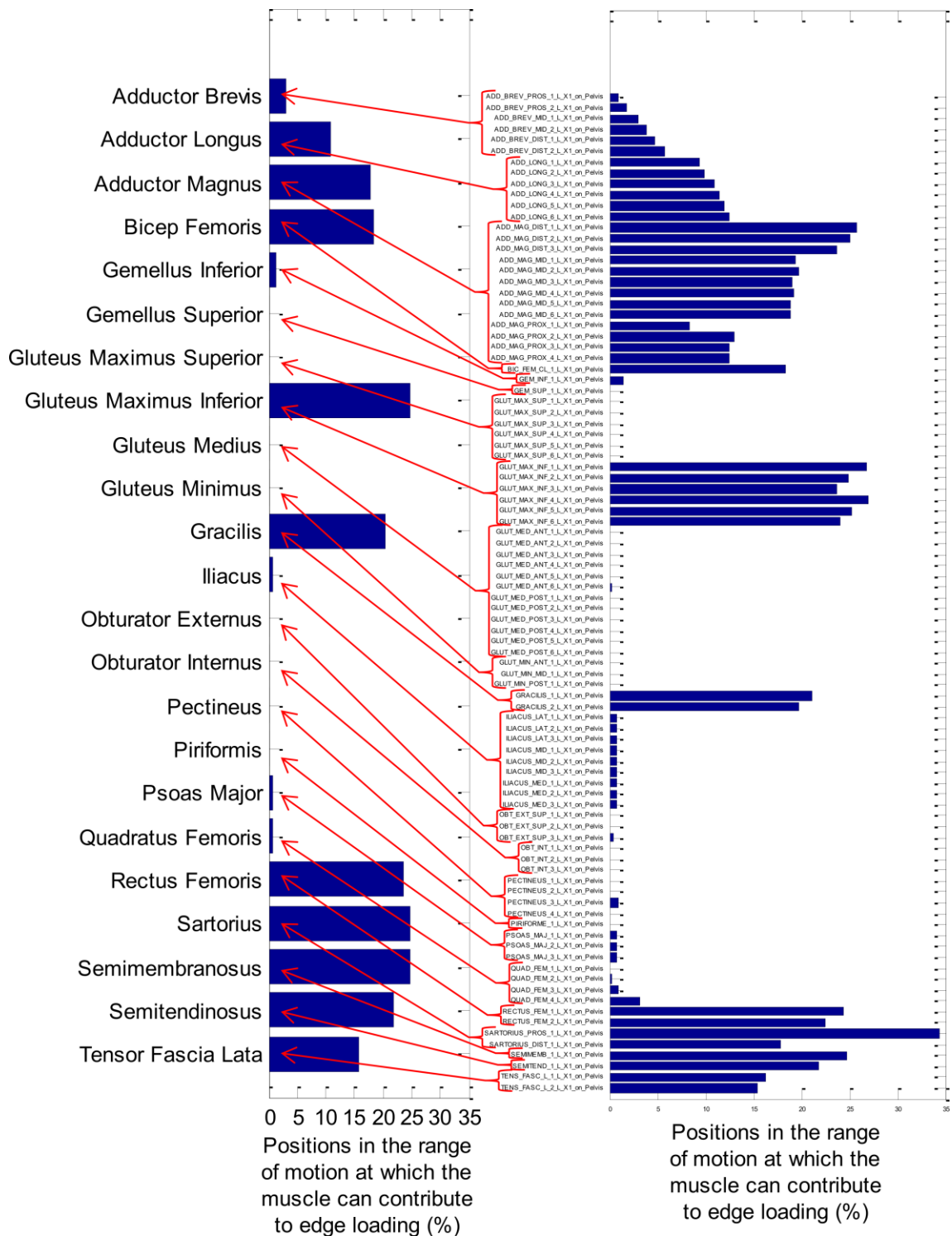


Figure 11.8 A comparison between the edge loading analysis based on whole muscles and muscle fibres.

A list of the muscles/fibres included in the study indicating the percentage of positions in the complete range of motion at which each muscle could contribute to an edge loading force vector in a well-positioned cup is shown. Left) muscle fibres are grouped to form whole muscles for the analysis. Right) Each muscle fibre is plotted individually; the x-axis labels are the same left and right (0 to 35) and the muscle fibres names are matched to corresponding complete muscle with red-arrows.

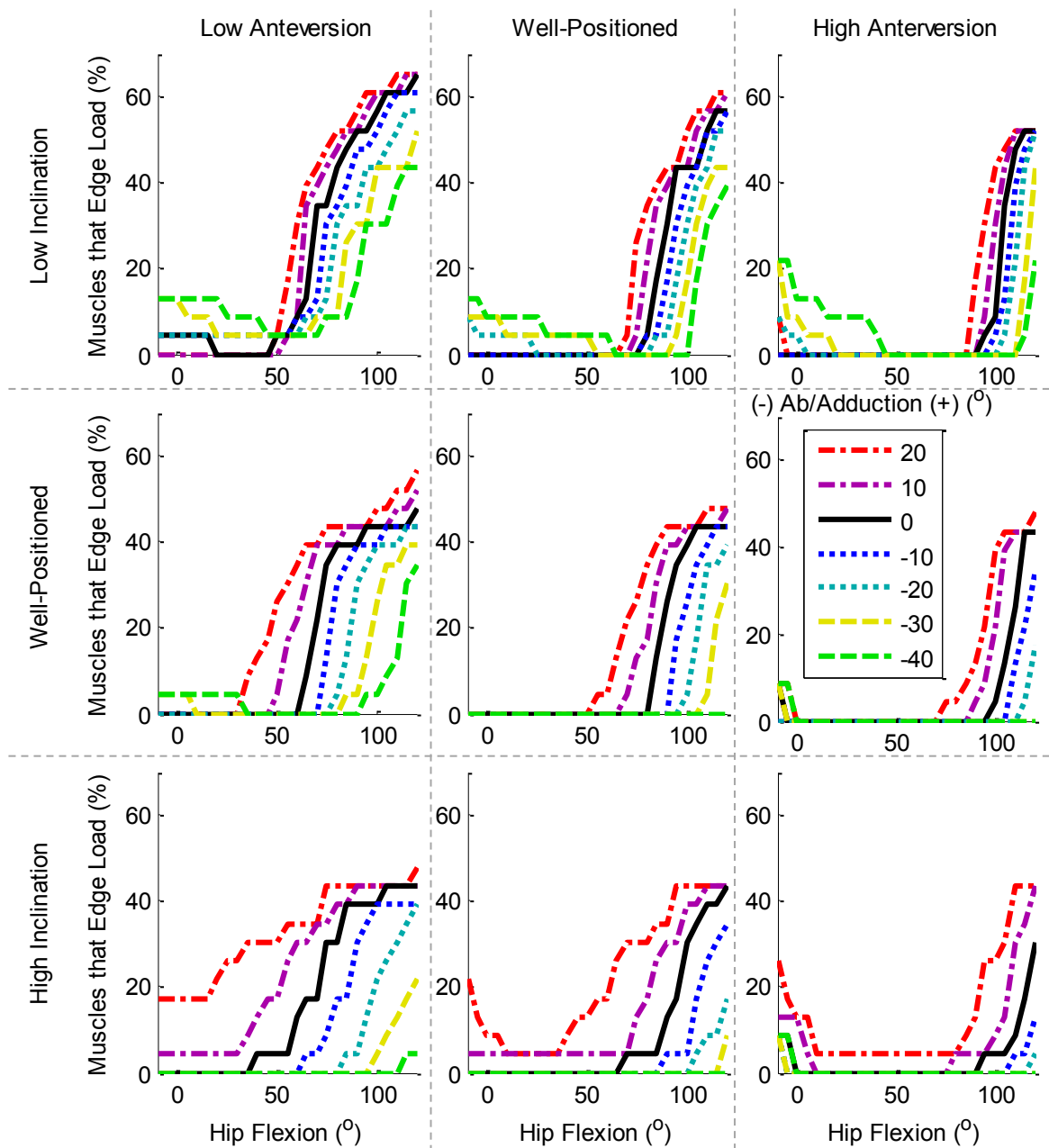
**A3.8 How cup position effects the risk of edge loading**

Figure 11.9 The percentage of muscles that can contribute to edge loading as a function of hip flexion with neutral internal/external rotation with varying cup position

Low anteverted (left column), normal anteversion (middle column) and high anteverted (right column), low inclination (top row), normal inclination (middle row) and high inclination (bottom row) are shown. It can be seen that low anteversion decreased the flexion angle at which edge loading could occur but had little effect on the maximum number of muscles that could edge load a hip; high anteversion had the opposite effect. Low inclination had two effects: it increased the maximum number of muscles that can cause edge loading forces and reduced the effect of abducting the hip in deep flexion; high inclination had the opposite effect and also allowed the distally inserting muscles to cause edge loading forces when the hip was adducted in low flexion or extension.

### **A3.9 Further work - how gluteal weakness could increase the risk of edge loading**

#### *A3.9.1 Materials and methods*

Example gait kinematic and kinetic data for a normal subject provided on the OpenSim website (Delp et al., 2007; DeMers, 2011) alongside an appropriately scaled version of the Delp et al. musculoskeletal model, with 92 muscles, 23 degrees of freedom (Delp et al., 1990), were used to analyse the effects of abductor (gluteus medius and minimus) muscle strength of direction of the hip joint reaction force.

First, the supplied files were analysed in their original form using static optimisation with a criterion of minimising the sum of muscle stresses squared to find the muscle forces and a subsequent joint reaction analyses to calculate the joint reaction force. Then, a MatLab script was used to change the maximum isometric strength of the gluteus medius and minimus muscle fibres in the musculoskeletal model; the strength of the gluteal abductors were varied from 0 % to 150 % of their original value at 10 % increments. This was the only change made to the model. The static optimisation and joint reaction analyses were then repeated for each of these modified models (using the same kinematics and kinetics data).

The joint reaction data were then imported into MatLab and the angle the force makes with the edge of the cup was calculated (see A3.3 and A3.4). A well-positioned cup orientation of 20° anteversion and 45° inclination was used for these pilot tests.

#### *A3.9.2 Results*

The model was unable to solve when the gluteal muscles were reduced to less than 40 % of their original strength hence only a strength range of 40-150 % was modelled. Also, as the abductor strengths were decreased, the model was unable to find solutions when both legs were in contact with the ground hence only the single leg stance phase of gait was analysed for the right hip only in the modified models.

#### Model Verification

The calculated hip joint reaction force (JRF) were similar to that which might be expected for a hip replacement patient for the first half of single leg stance; however it over-predicts the magnitude of the JRF in terminal stance (Figure 11.10). The shape for the angle the force makes with the pelvis is similar for the model and a hip replacement patient throughout the gait cycle; however the model calculated a force

that points more into the pelvis that may be observed in a hip replacement patient (Figure 11.10).

### The effects of gluteal weakening/strengthening on muscle forces during gait

As would be expected, reducing the maximum available strength of the gluteus medius and minimus muscle fibres reduced the force in these muscles during the gait cycle. This resulted in increased activity in the tensor fascia lata and superior fibres of the gluteus maximus (Figure 11.11). Increases in force contributions from other muscles' with a secondary abduction (Dostal et al., 1986) function in low flexion were also observed but these were small in comparison to those plotted in Figure 11.11. Overall, the joint reaction force increased as the available strength of the gluteus medius and minimus was decreased; the total hip abduction moment was constant (the same kinetic inputs were used for all models).

### The effects of gluteal weakening/strengthening on edge loading risk

Reducing the available muscle strength in the gluteus medius and minimus from 150 % to 40 % resulted in the joint reaction force passing closer to the edge of the cup at heel strike, thus increasing the risk of edge loading (Figure 11.12).

#### *A3.9.3 Discussion*

This pilot study demonstrated that a change in the line-of-action of the joint reaction force is possible if the balance of muscle strengths is changed: weakness in the gluteus medius and minimus could affect the optimum ratio of muscle forces in the hip and this may increase the risk of edge loading during gait. This is because the reduction in available strength for the gluteus medius and minimus is compensated for by increased activity in the tensor fascia lata and the superior fibres of the gluteus maximus which insert into the distally inserting iliotibial band (Figure 11.11). The lines of action of distally inserting muscles can contribute to edge loading (section 3.3.3) and therefore a gait strategy which relies on distally inserting muscles results in a joint reaction force that passes closer to the edge of the cup (Figure 11.12). However, only a small change was detected at heel strike whereas during gait the greatest risk of edge loading appears to be at toe-off (Figure 11.12). Thus further work looking at other daily activities such as stair climbing and sit-to-stand is necessary.

This pilot study is limited in that it assumes that reducing the strengths of the gluteus medius and minimus does not affect the way in which a patient would walk; constant kinetics and kinematics were used for all models. However, clinically, patients with reduced gluteal strength walk with different kinematics and kinetics (Madsen et al.,



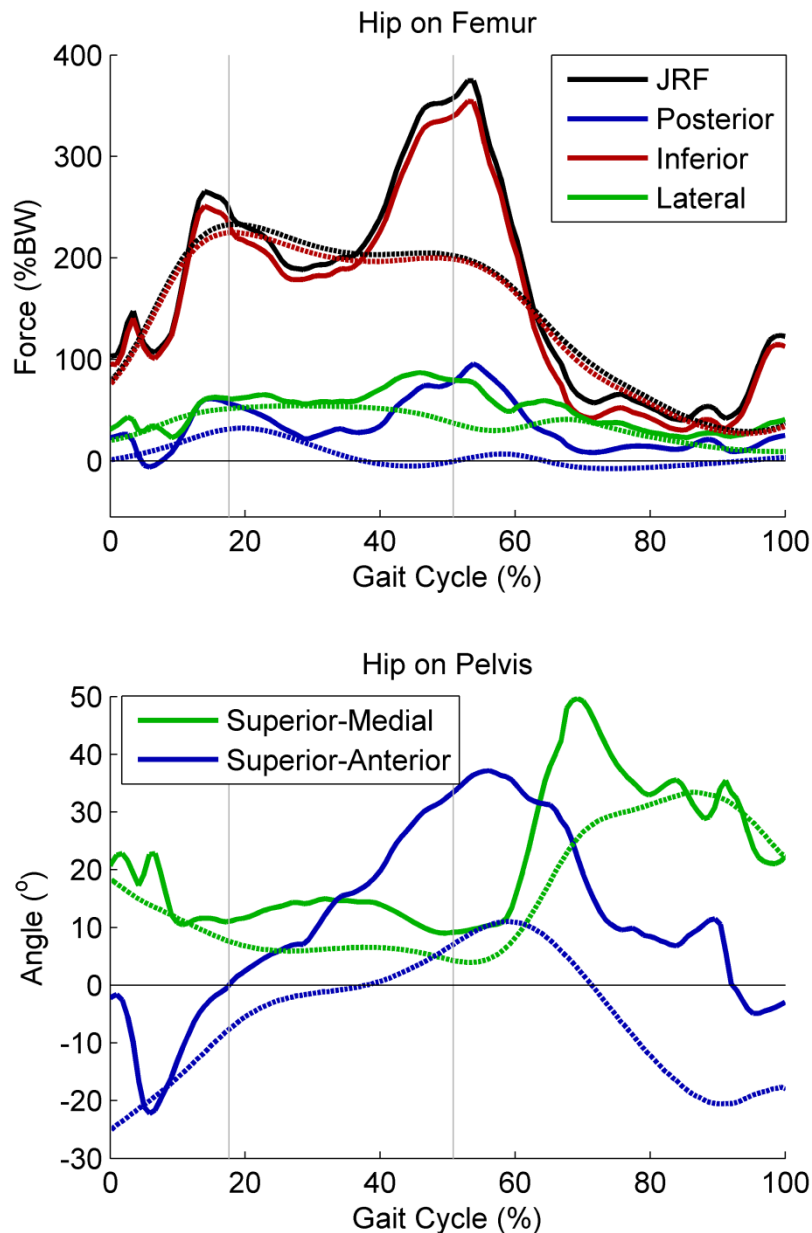


Figure 11.10 A comparison between the hip joint reaction forces for the unmodified Delp musculoskeletal model (solid lines) and Bergmann's in vivo forces for an average patient walking at their normal speed (dotted lines).

The solid vertical grey lines highlight the single leg stance phase of gait. Top) the hip joint reaction force applied by the hip onto the femur and its x, y, z (blue/red/green respectively) components in the reference frame of the femur; the legend describes the positive direction of the force acting from the hip onto the femur. Bottom) the angle of the force acting from the hip joint onto the pelvis in the pelvic reference frame; the legend describes the positive angle direction.

2004; Mont et al., 2007; Ewen et al., 2012; Zeni et al., 2014). This may explain why only a small change in the edge loading risk was detected. It also helps explain why there were no static optimisation solutions for very low ( $\leq 30\%$ ) gluteus medius and minimus muscle strengths: the tensor fascia lata muscle contributes to both a flexion and abduction moment, however the force capacity of the muscle saturates in models

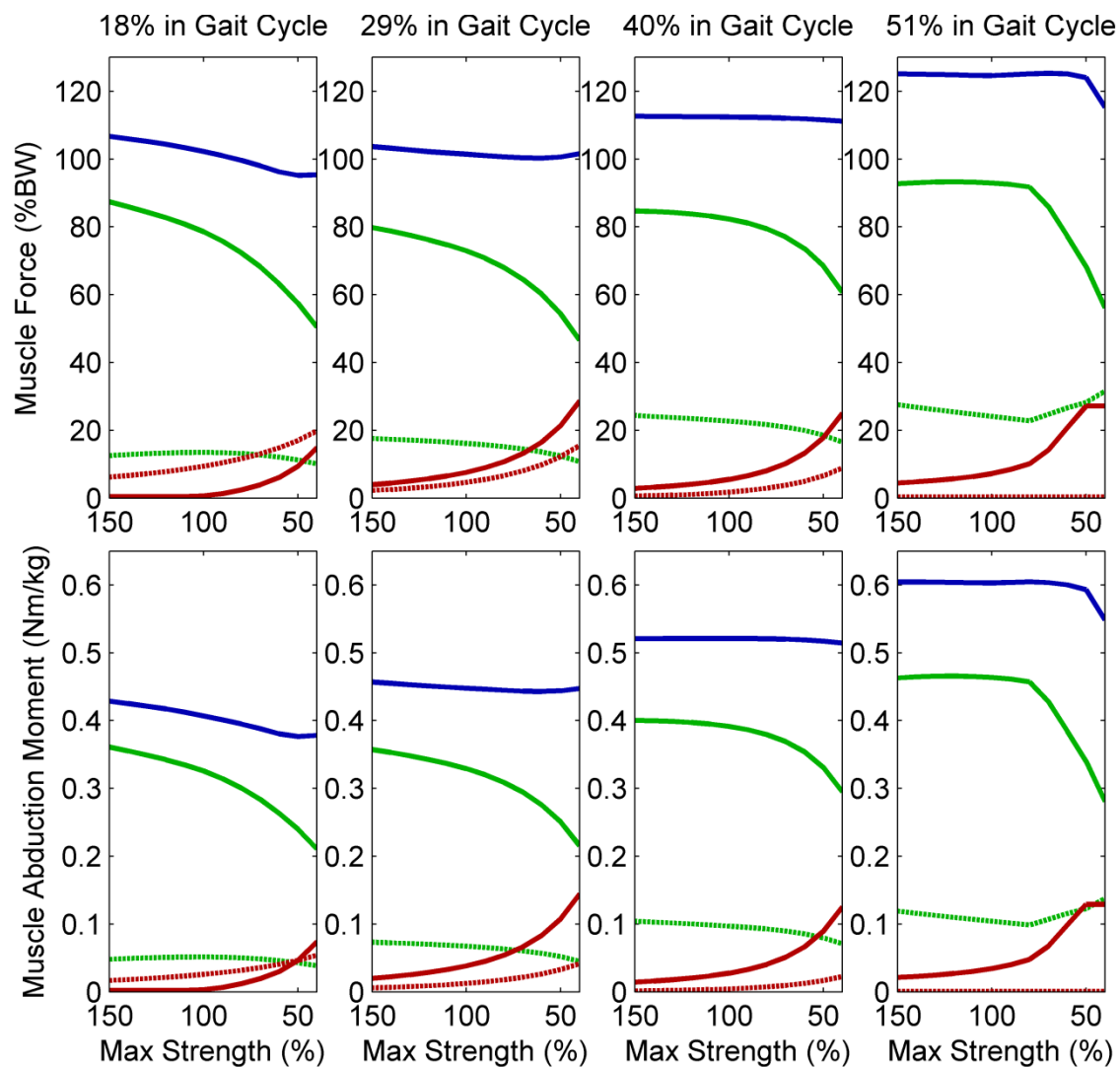


Figure 11.11 The effect of reducing the available maximum strength of the gluteus medius (solid green line) and minimus (dashed green line) on the forces (top) and abduction moments (bottom) provided by the muscles at the start (left), middle and end (right) of the single leg stance phase of gait.

Reducing the maximum available strength in the gluteus medius and minimus decreases the force and moment contributions from these muscles; it is substituted for by increased activity in the tensor fascia lata (solid red line) and the most superior fibres of the gluteus maximus (dashed red line). The total contribution from these four muscles summed together is near constant (blue line) demonstrating that changes in these muscles accounts for most of the variability caused by gluteal weakness/strengthening.

with low-gluteal strengths in terminal stance (Figure 11.11, 51 % gait cycle) which precludes a solution for the given kinetics and kinematics. In vivo, a patient could adapt their gait or use a walking aid to compensate for the severe gluteal weakness. Future work could address this limitation by examining the ratio of muscle forces in patients who suffer from a painful hip replacement as a consequence of edge loading and increase the force potential of the tensor fascia lata if necessary. This pilot study is also limited in that only a single gait cycle from a single normal subject was studied and the calculated force angles are greater than that which might be expected for a typical hip

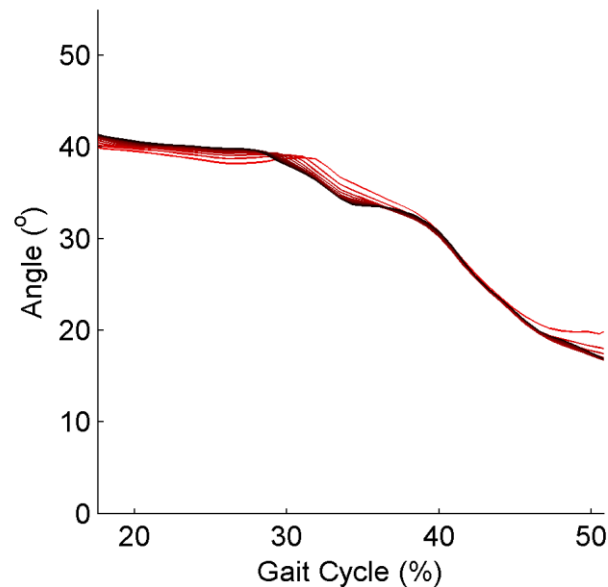


Figure 11.12 The angle between the joint reaction force and the edge of the acetabular cup for the same gait cycle as the maximum available strength in the gluteus medius and minimus was reduced in a musculoskeletal model.

The lines are coloured from black to red as the maximum strength is decreased from 150 % to 40 %. It can be seen that the joint reaction force passes closer to the edge of the cup at heel strike for models with the simulated abductor deficiency.

replacement patient (Figure 11.10). Moreover, recent research suggests that current musculoskeletal models are unable to find exact solutions for both the joint reaction force magnitude and direction (Modenese et al., 2013). Importantly, the shapes of the force angle curves are representative of that of a hip replacement patient (Figure 11.10) and hence indicate that the model is suitable for studying relative changes, but not absolute values.

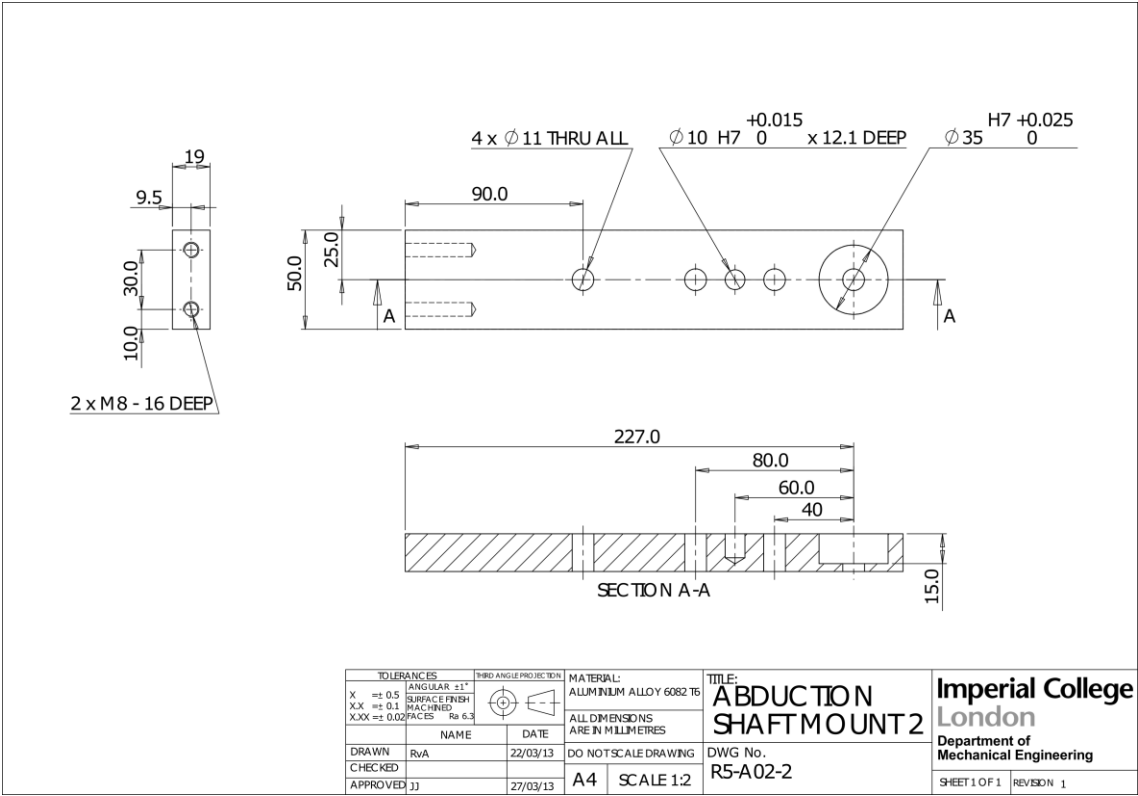
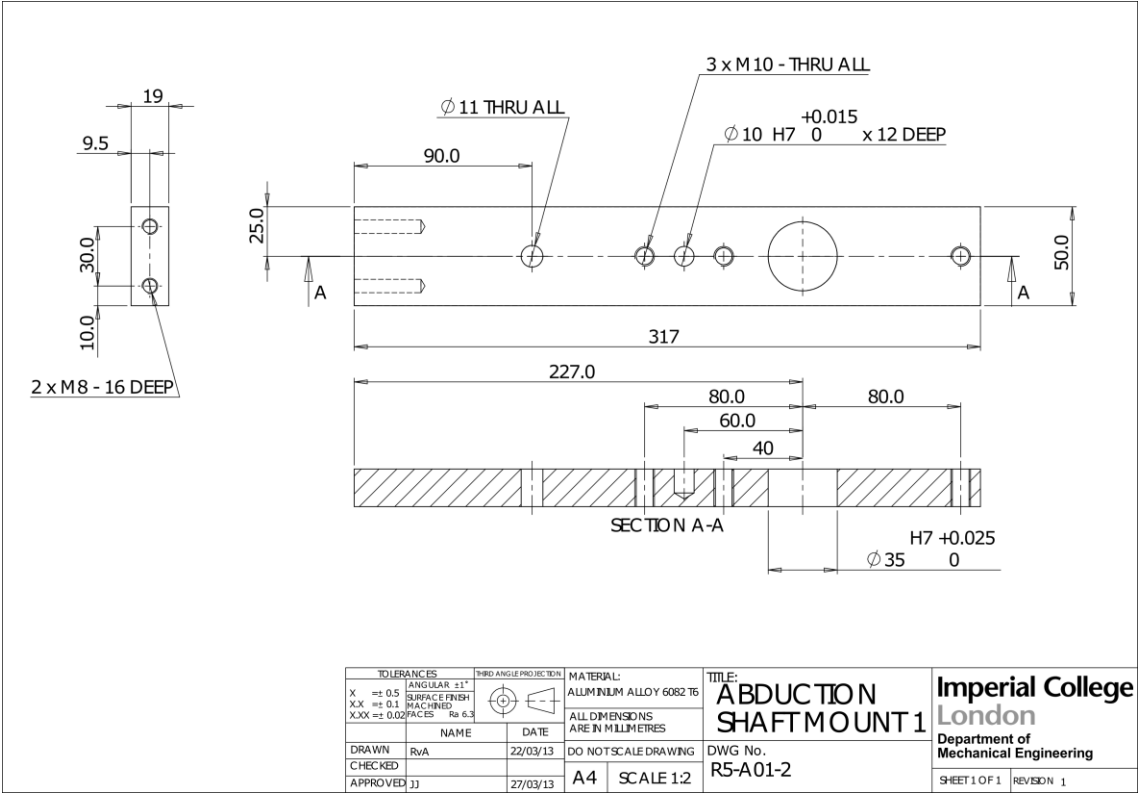
Mellon et al. have published a series of papers demonstrating how individual motion patterns can affect the edge loading risk in metal-on-metal hip replacement patients (Mellon et al., 2011; Kwon et al., 2012; Mellon et al., 2013). During the stance phase of gait, they report mean differences of cup-to-rim distances of 4.6 mm between patients with high/low metal ion concentrations who have similarly sized, mal-positioned cups (Mellon et al., 2013); for the average cup size in their study, Ø48 mm, this would equate to a joint reaction force that is 11° closer to the edge; the gluteal weakness modelled in this pilot study suggests a 50 % reduction in muscle strength could cause the joint reaction force to move >2° towards to cup-edge and thus could provide an explanation for these differences. Moreover, this variation in hip joint contact force direction could have clinical importance: the ASR had a subtended arc angle that was 10° less than the BHR and consequentially had significantly worse clinical results. This 10° difference would equate to only 5° difference the cup edge demonstrating that even small changes in edge loading risk could have large consequences for patients.

## CHAPTER 11

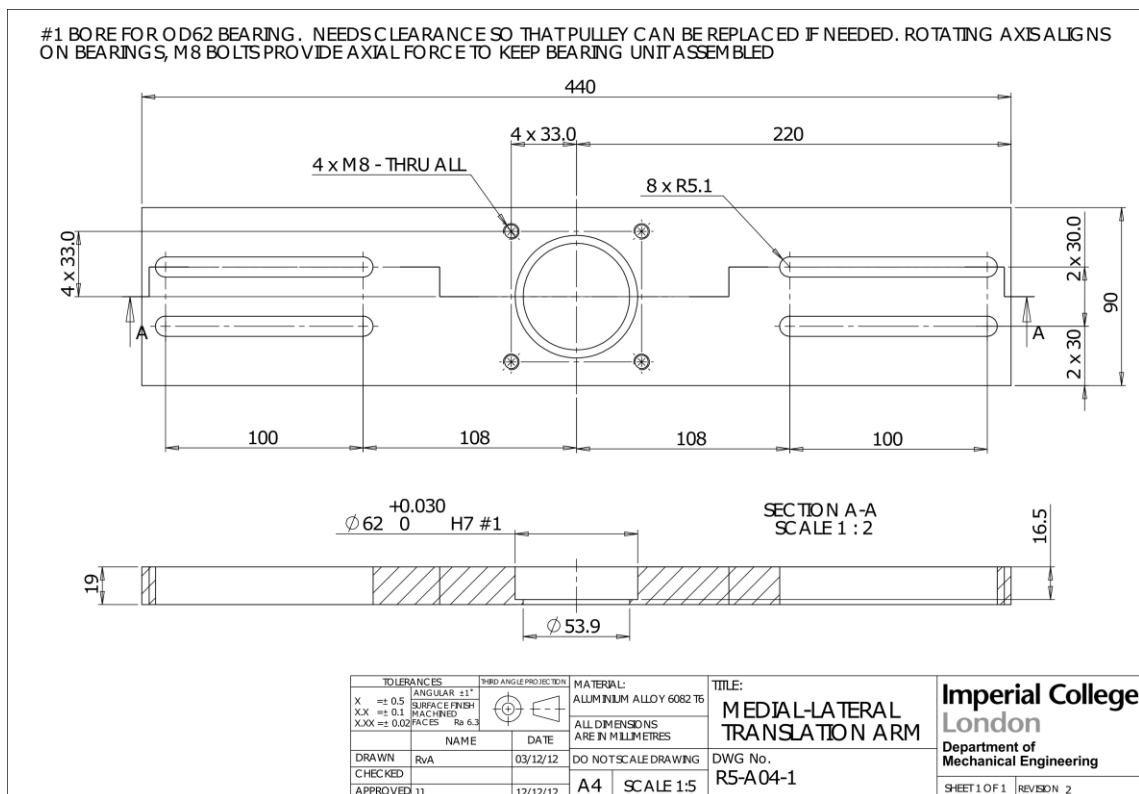
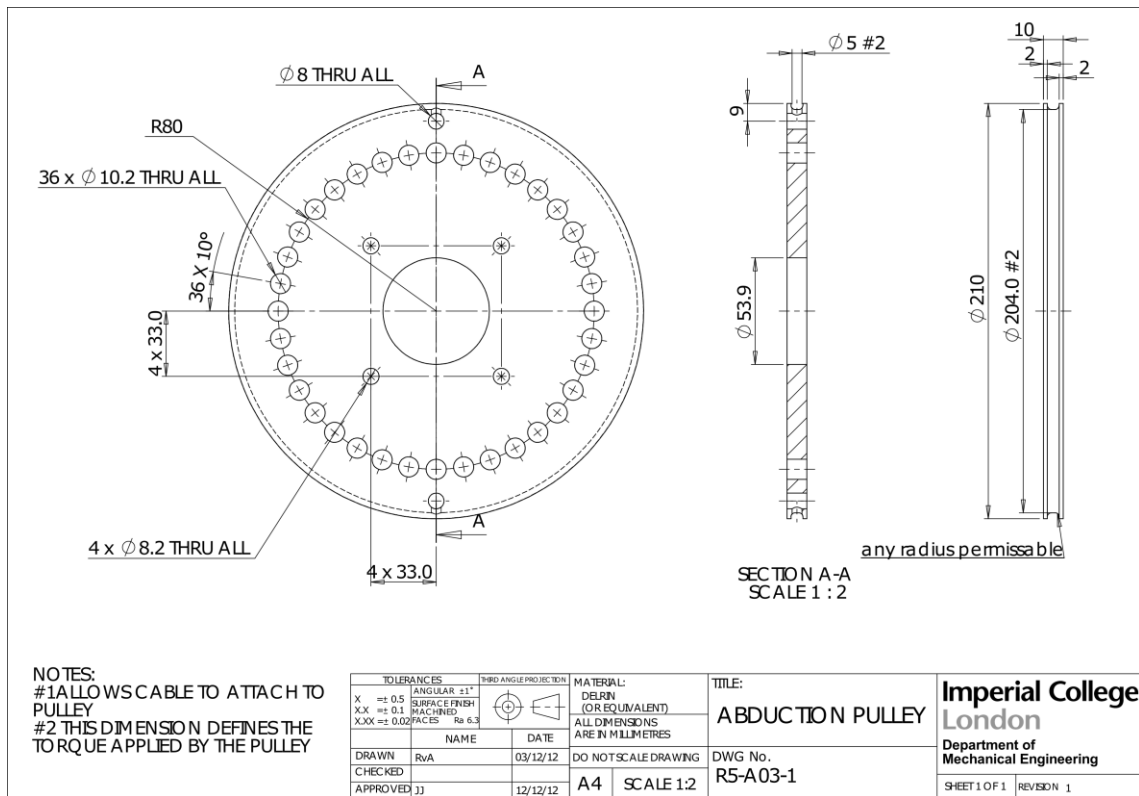
This pilot study quantifies how increasing hip abductor strength could reduce the risk of edge loading during gait. Abductor weakness is a common early problem following hip replacement and hence rehabilitation strategies to improve abductor strength are well established (Vaz et al., 1993). Therefore, this provides a promising line of research for investigating non-operative treatment courses for patients with metal-on-metal implants who are suffering from the consequences of high metal ions.

# A4 Six-degrees-of-freedom rig design appendices

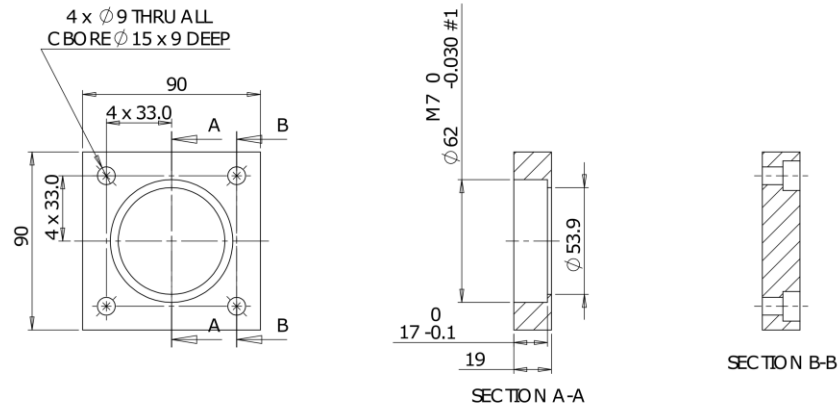
## A4.1 Component drawings



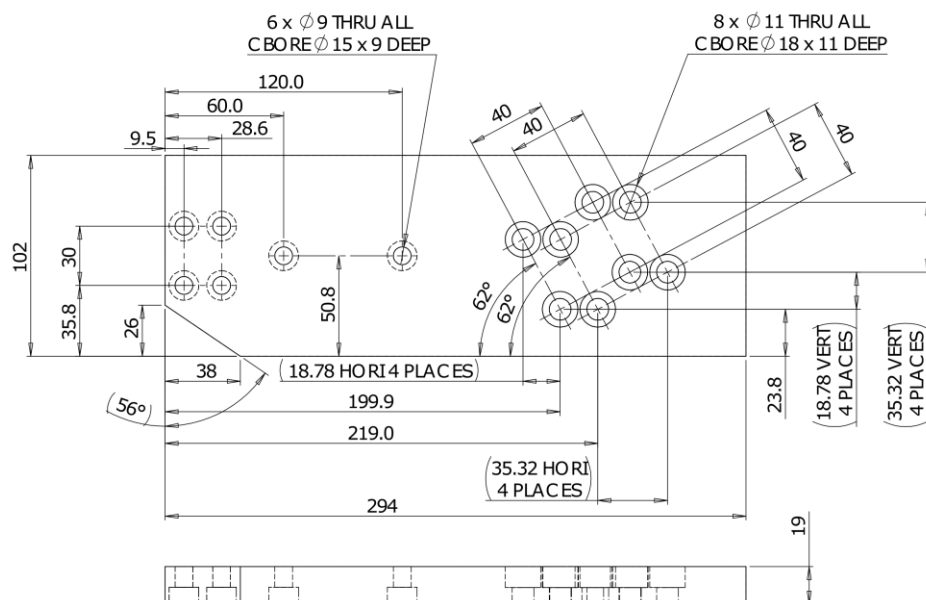
## CHAPTER 11



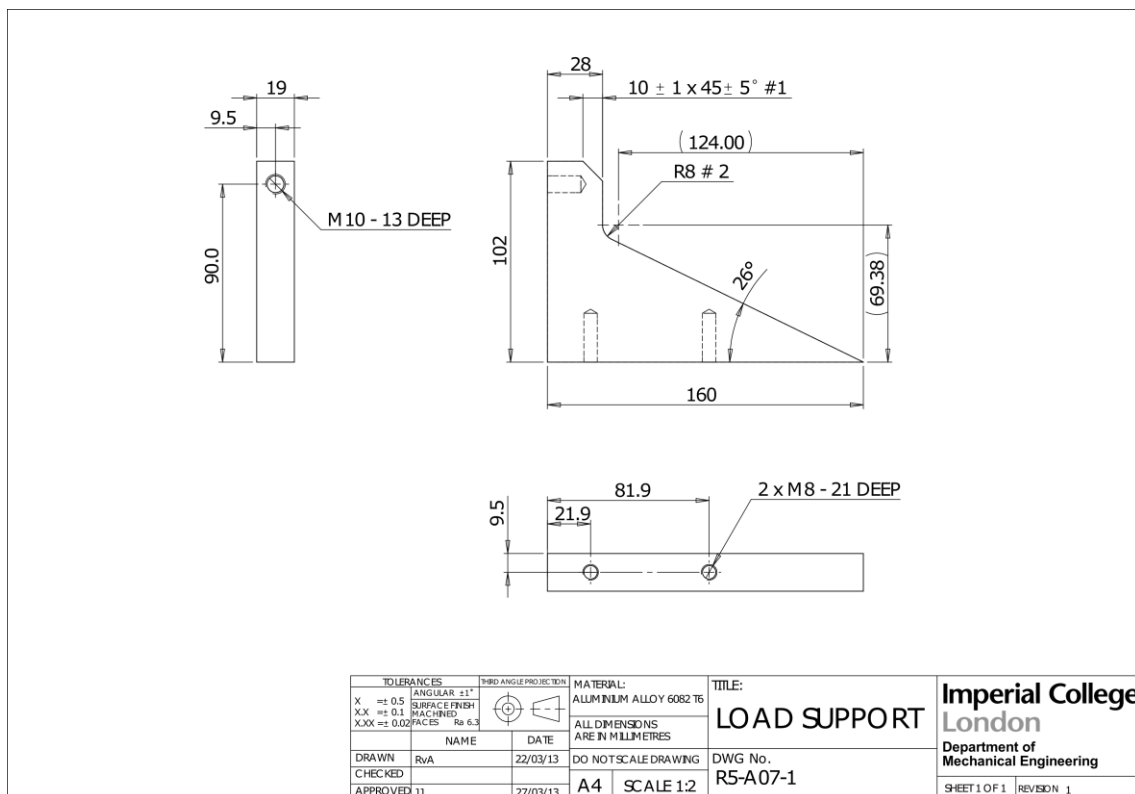
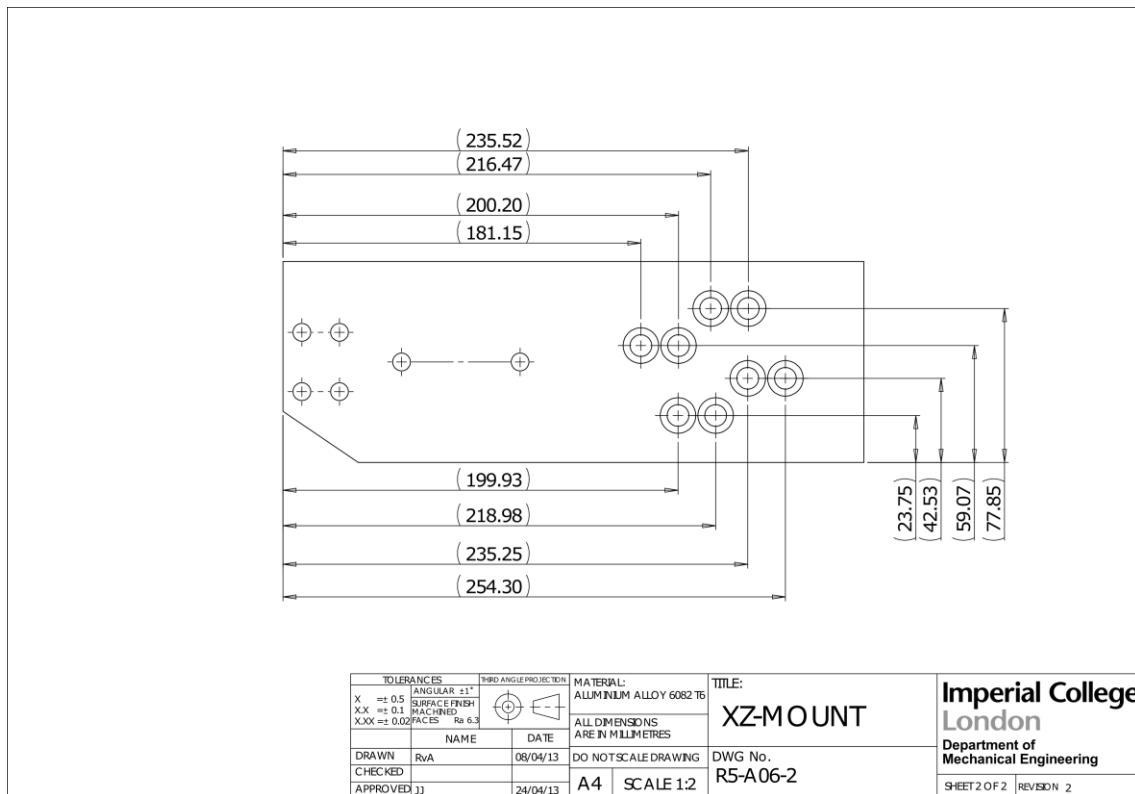
#1 BEARING BORE FOR OD62 BEARING. DOES NOT NEED TO DISASSEMBLE ONCE BEARING INSERTED



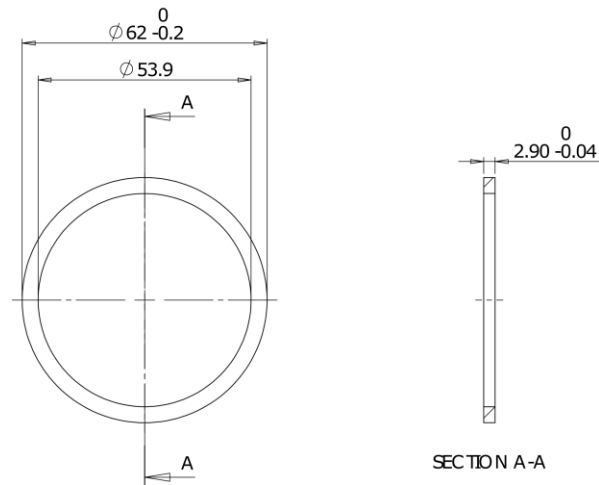
TOLERANCES		THIRD ANGLE PROJECTION	MATERIAL:	TITLE:	<div>Imperial College London</div> <div>Department of Mechanical Engineering</div> <div>SHEET 1 OF 1 REVISION 1</div>
X	± 0.5	ANGULAR ±1°	ALUMINUM ALLOY 6062 T6	BEARING HOUSING	
XX	± 0.1	SURFACE FINISH			
XXX	± 0.02	MACHINED FACES Ra 6.3	ALL DIMENSIONS ARE IN MILLIMETRES		
NAME		DATE	DO NOT SCALE DRAWING	DWG No. R5-A05-1	
DRAWN	RvA	03/12/12			
CHECKED			A4	SCALE 1:2	
APPROVED JJ		12/12/12			



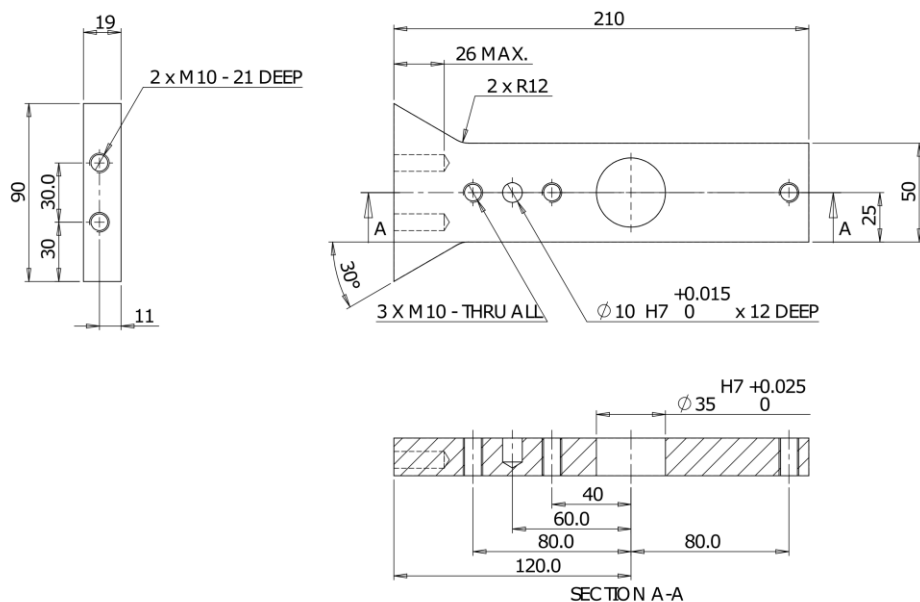
TOLERANCES		THIRD ANGLE PROJECTION	MATERIAL:	TITLE:	<div>Imperial College</div> <div>London</div> <div>Department of Mechanical Engineering</div> <div>SHEET 1 OF 2 REVISION 2</div>
X	± 0.5	ANGULAR ±1°	ALUMINUM ALLOY 6062 T6	XZ-MOUNT	
XX	± 0.1	SURFACE FINISH			
XXX	± 0.02	FACES Ra 6.3	ALL DIMENSIONS ARE IN MILLIMETRES		
NAME		DATE	DO NOT SCALE DRAWING	DWG No.	
DRAWN	RvA	08/04/13	A4	SCALE 1:2	R5-A06-2
CHECKED					
APPROVED JJ		24/04/13			



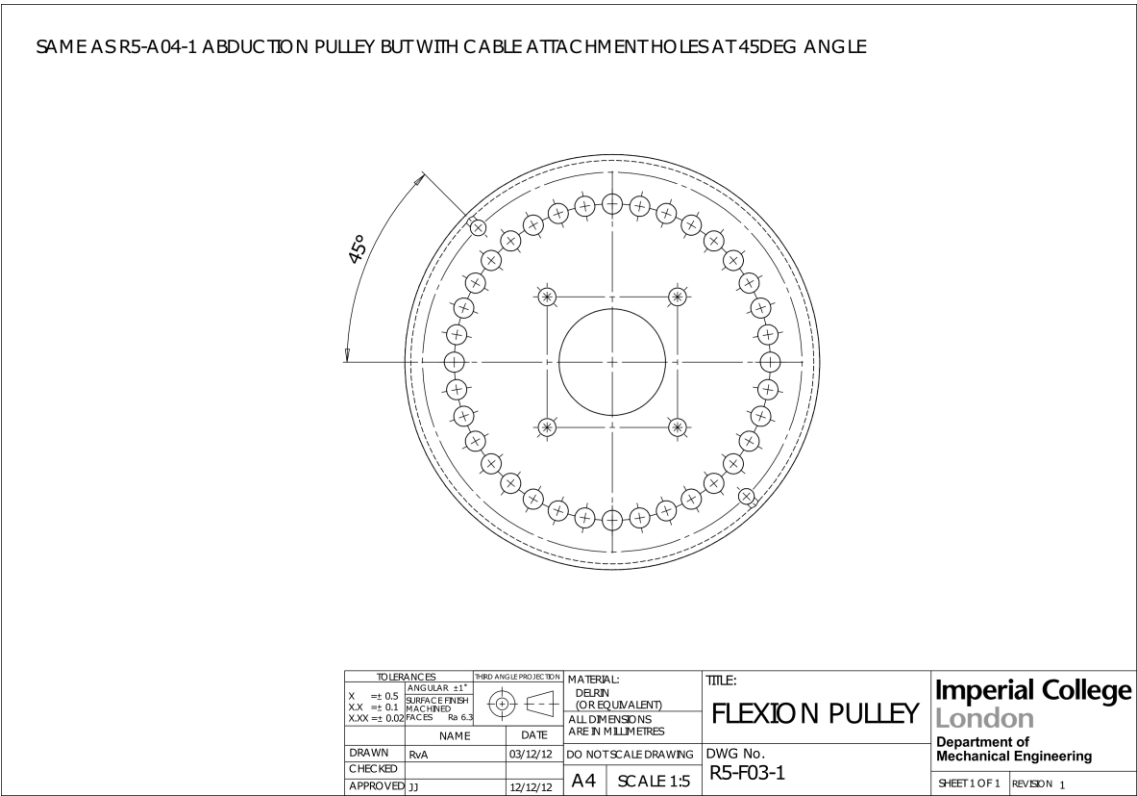
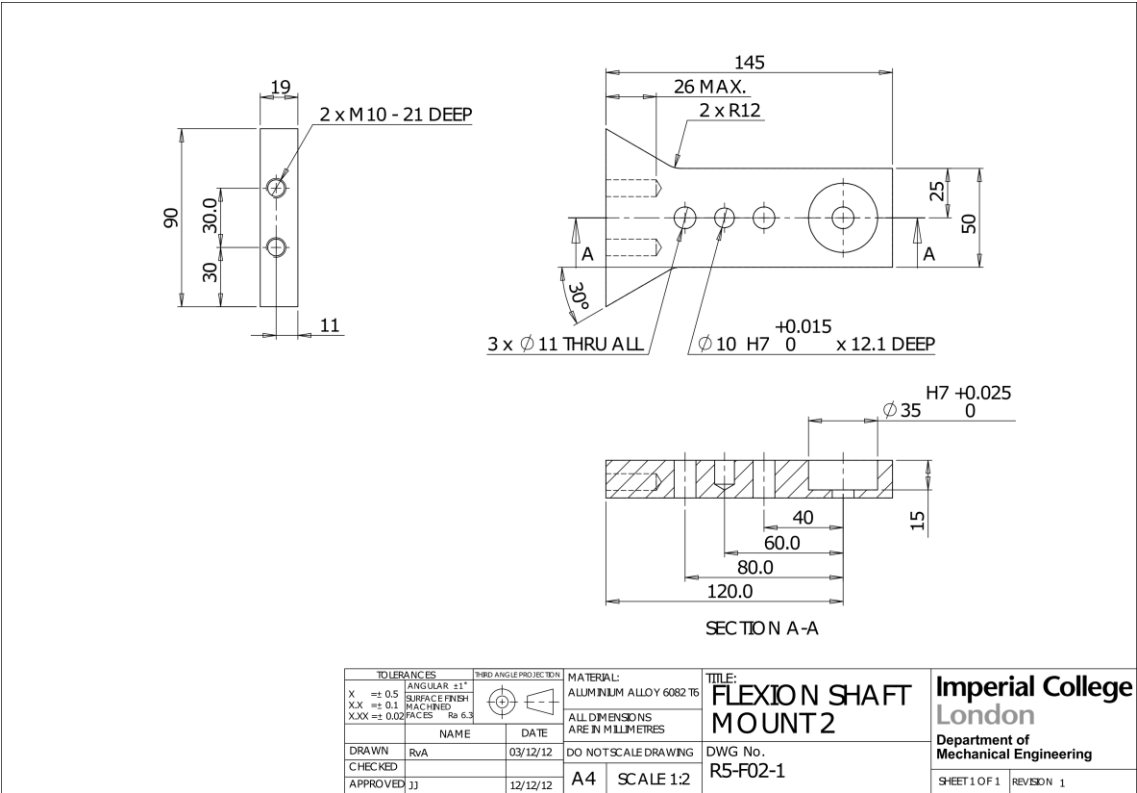




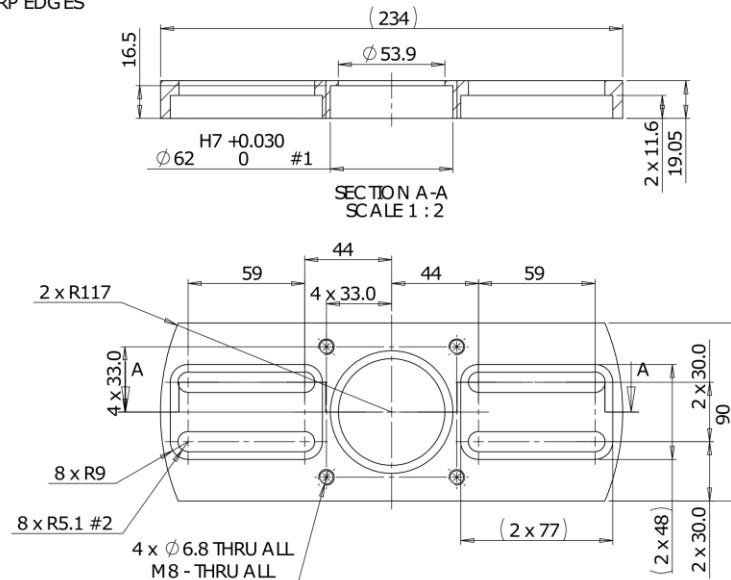
TOLERANCES		THIRD ANGLE PROJECTION	MATERIAL:	TITLE:	Imperial College London Department of Mechanical Engineering	
X	± 0.5	ANGULAR ±1°	STAINLESS STEEL 303	HOUSING SPACER		
XX	± 0.1	SURFACE FINISH		ALL DIMENSIONS ARE IN MILLIMETRES		DWG No. R-A08-1
XXX	± 0.02	FACES	DO NOT SCALE DRAWING			
NAME		DATE	DO NOT SCALE DRAWING		SHEET 1 OF 1    REVISION    1	
DRAWN	RvA	5/12/12	A4    SCALE 1:1			
CHECKED						
APPROVED JJ		12/12/12				



TOLERANCES		THIRD ANGLE PROJECTION		MATERIAL:	TITLE:	Imperial College London Department of Mechanical Engineering
X	± 0.5	ANGULAR	± 1°	ALUMINIUM ALLOY 6062 T6	FLEXION SHAFT MOUNT 1	
XX	± 0.1	SURFACE FINISH				
XXX	± 0.02	FACES		ALL DIMENSIONS ARE IN MILLIMETRES		
		Rz 6.3				
NAME		DATE		DO NOT SCALE DRAWING	DWG No.	
DRAWN	RvA	03/12/12		A4	SCALE 1:2	
CHECKED						
APPROVED	JJ			12/12/12		
					R5-F01-1	
						SHEET 1 OF 1 REVISION 1



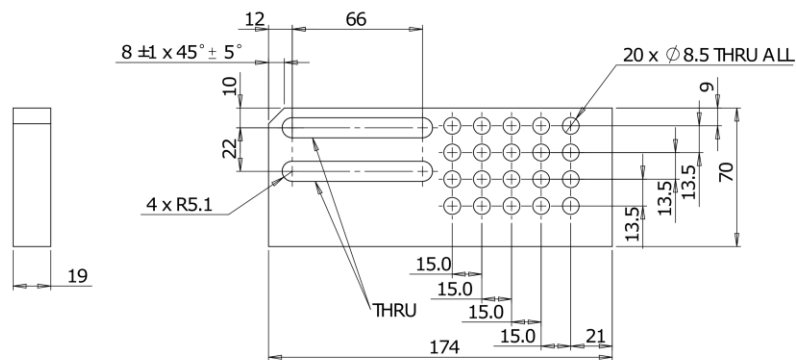
#1 BORE FOR OD 62 BEARING. NEEDS TO BE EASILY DISASSEMBLED SO CAN MOUNT DIFFERENT HIP SPECIMENS. ROTATING AXIS ALIGNS ON BEARING. M8 BOLTS PROVIDE AXIAL FORCE TO KEEP BEARING UNIT ASSEMBLED  
 #2 SLOTS PROVIDE CLEARANCE FOR M10 BOLTS  
 PLEASE DUBER SHARP EDGES



TOLERANCES	THIRD ANGLE PROJECTION	MATERIAL:
X $\pm 0.5$	ANGULAR $\pm 1^\circ$	ALUMINUM ALLOY 6062 T6
XX $\pm 0.1$	SURFACE FINISH	ALL DIMENSIONS ARE IN MILLIMETRES
XXX $\pm 0.02$	MACHINED	DO NOT SCALE DRAWING
	FACES	
	Re 6.3	
DRAWN	NAME	DATE
CHECKED	RvA	03/12/12
APPROVED JJ		12/12/12

TITLE:
ANTERIOR-POSTERIOR TRANSLATION ARM
DWG No.
R5-F04-1

**Imperial College  
London**  
 Department of  
Mechanical Engineering  
 SHEET 1 OF 1 REVISION 1

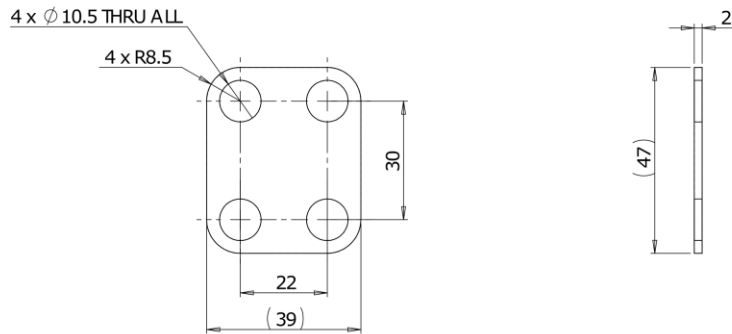



TOLERANCES	THIRD ANGLE PROJECTION	MATERIAL:
X $\pm 0.5$	ANGULAR $\pm 1^\circ$	ALUMINUM ALLOY 6062 T6
XX $\pm 0.1$	SURFACE FINISH	ALL DIMENSIONS ARE IN MILLIMETRES
XXX $\pm 0.02$	MACHINED	DO NOT SCALE DRAWING
	FACES	
	Re 6.3	
DRAWN	NAME	DATE
CHECKED	RvA	05/12/12
APPROVED JJ		12/12/12

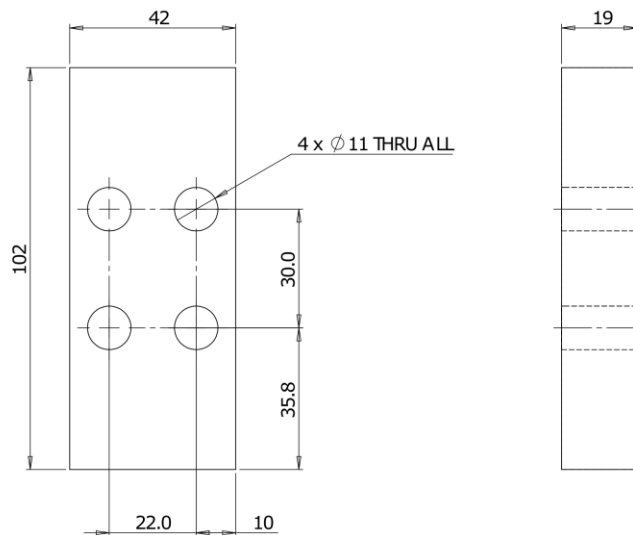
TITLE:
SUPERIOR-INFERIOR TRANSLATION ARM
DWG No.
R5-F05-1

**Imperial College  
London**  
 Department of  
Mechanical Engineering  
 SHEET 1 OF 1 REVISION 1

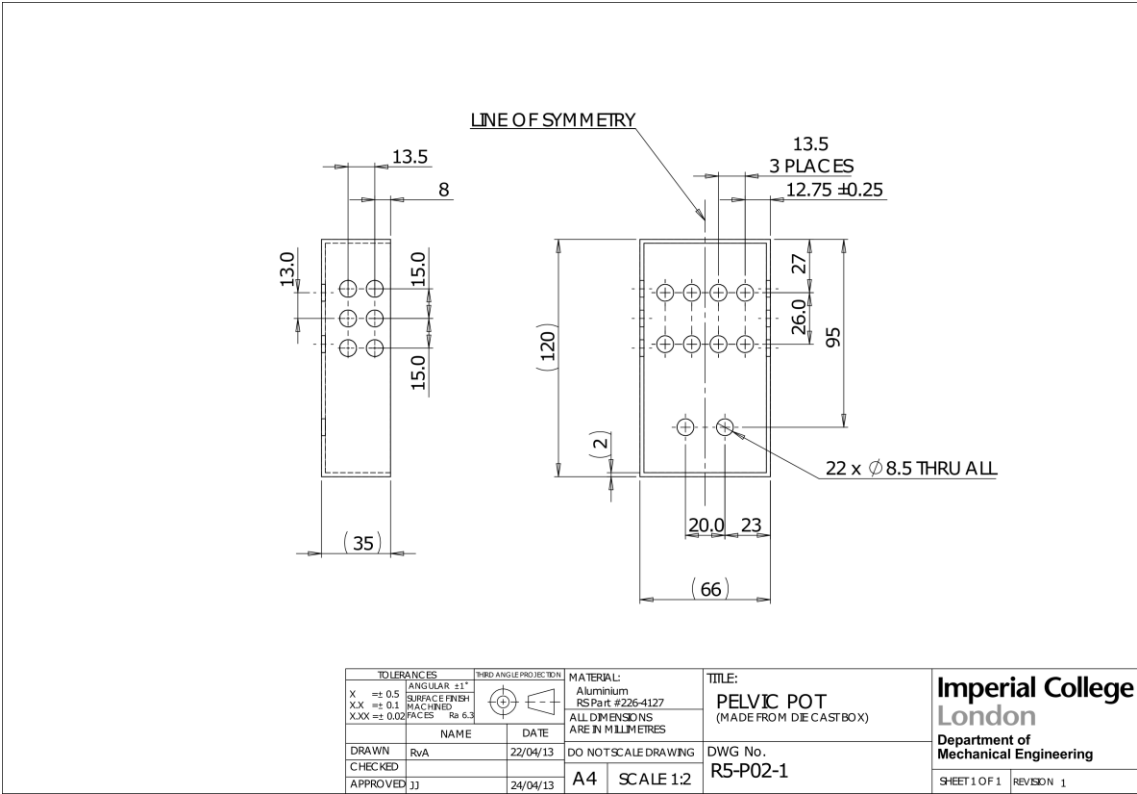
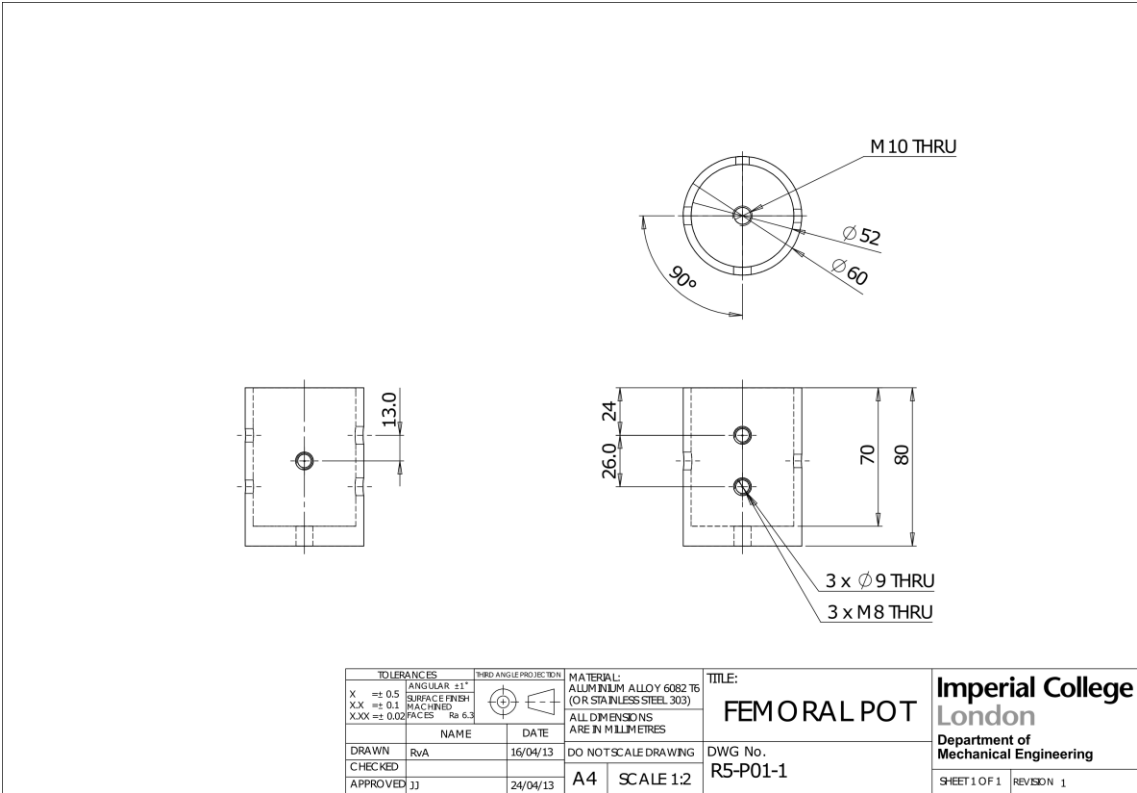
CAN BE MADE FROM ANY NON-RUSTING METAL SHEET

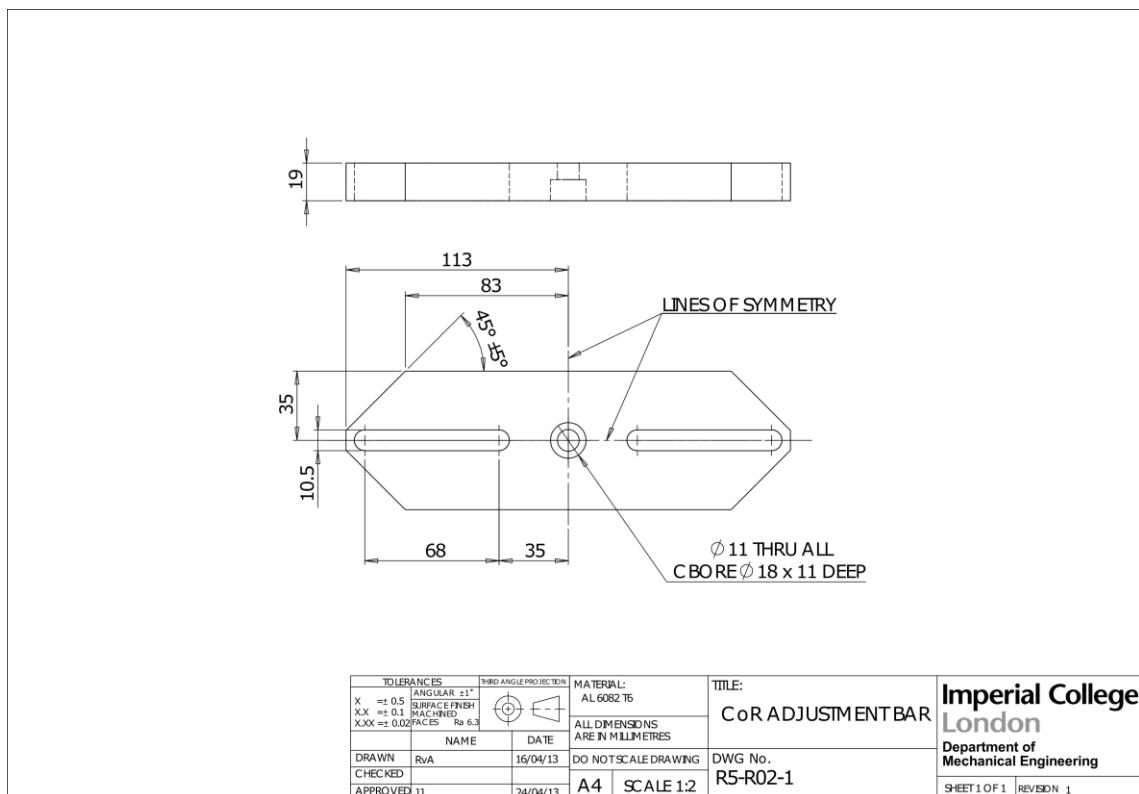
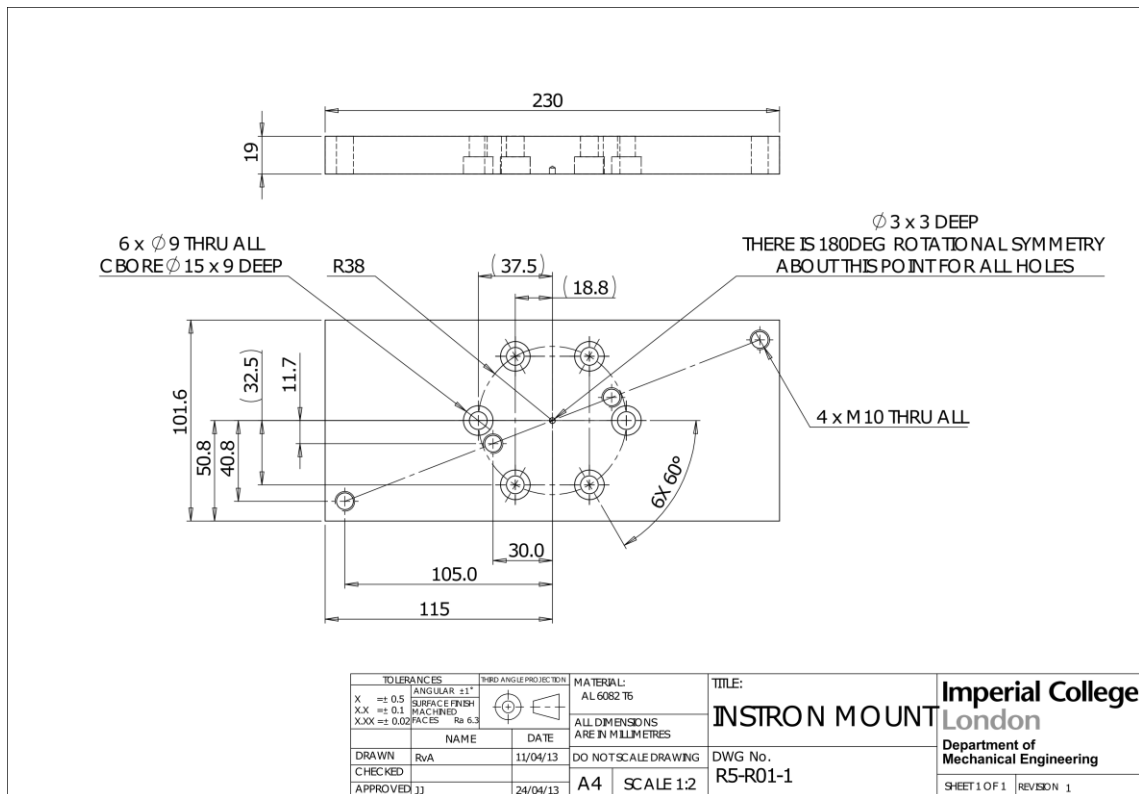


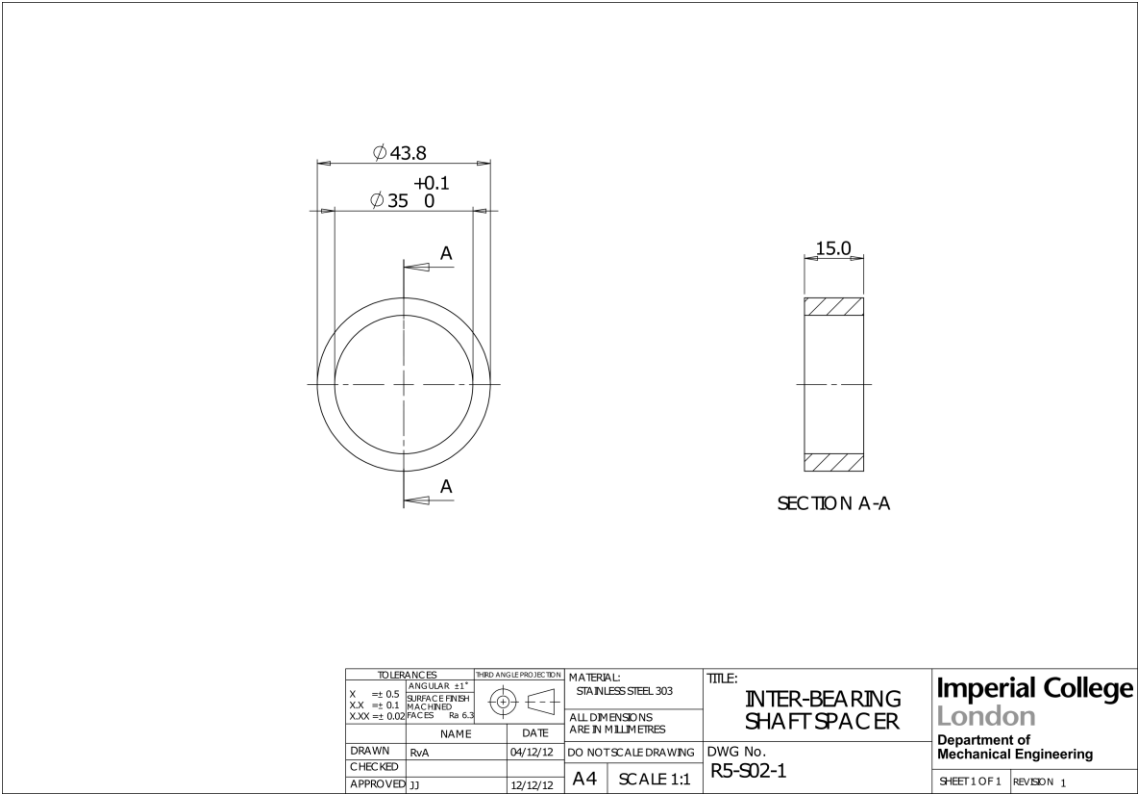
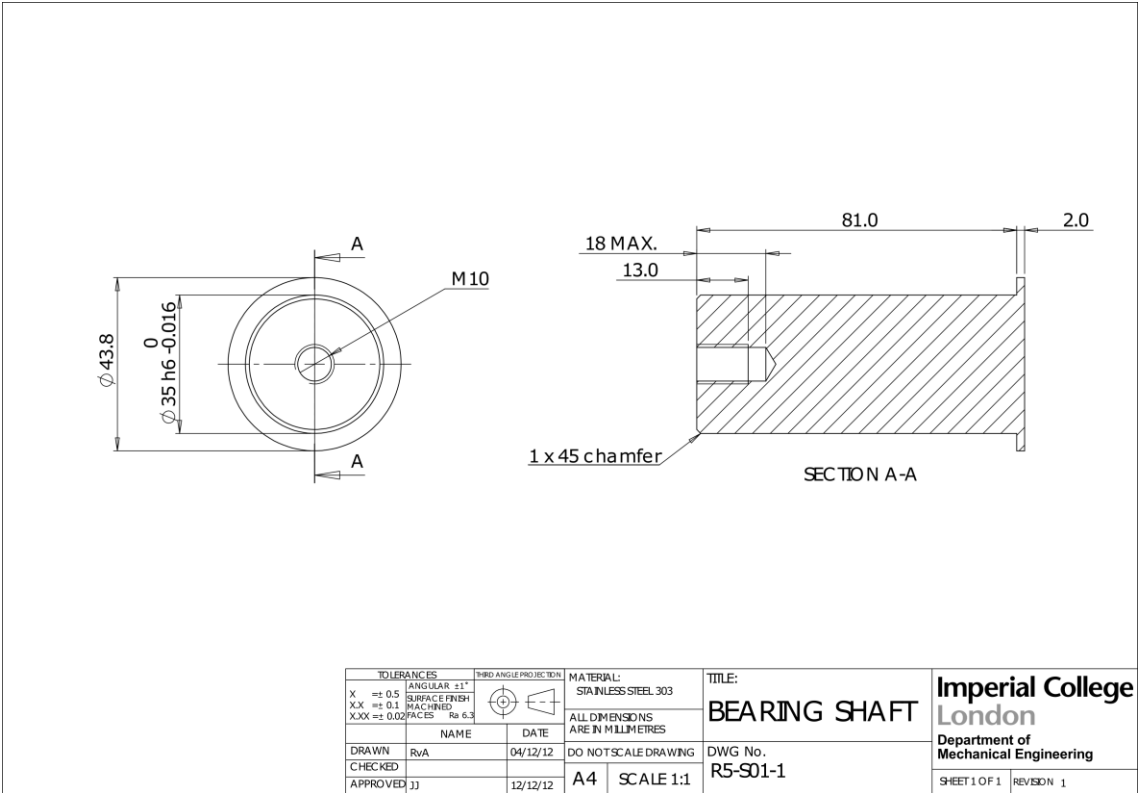
TOLERANCES		THIRD ANGLE PROJECTION		MATERIAL: STAINLESS STEEL ALUMINIUM ALLOY  ALL DIMENSIONS ARE IN MILLIMETRES	TITLE:  <b>CONSTRAINING WASHER</b>	<b>Imperial College London</b>  Department of Mechanical Engineering
X	± 0.5	ANGULAR ±1°				
XX	± 0.1	SURFACE FINISH MACHINED				
XXX	± 0.02	FACES Ra 6.3				
NAME		DATE	DO NOT SCALE DRAWING		DWG No.	
DRAWN	RvA	05/12/12			R5-F06-1	
CHECKED			A4 SCALE 1:1			
APPROVED	JJ	12/12/12				SHEET 1 OF 1 REVISION 1

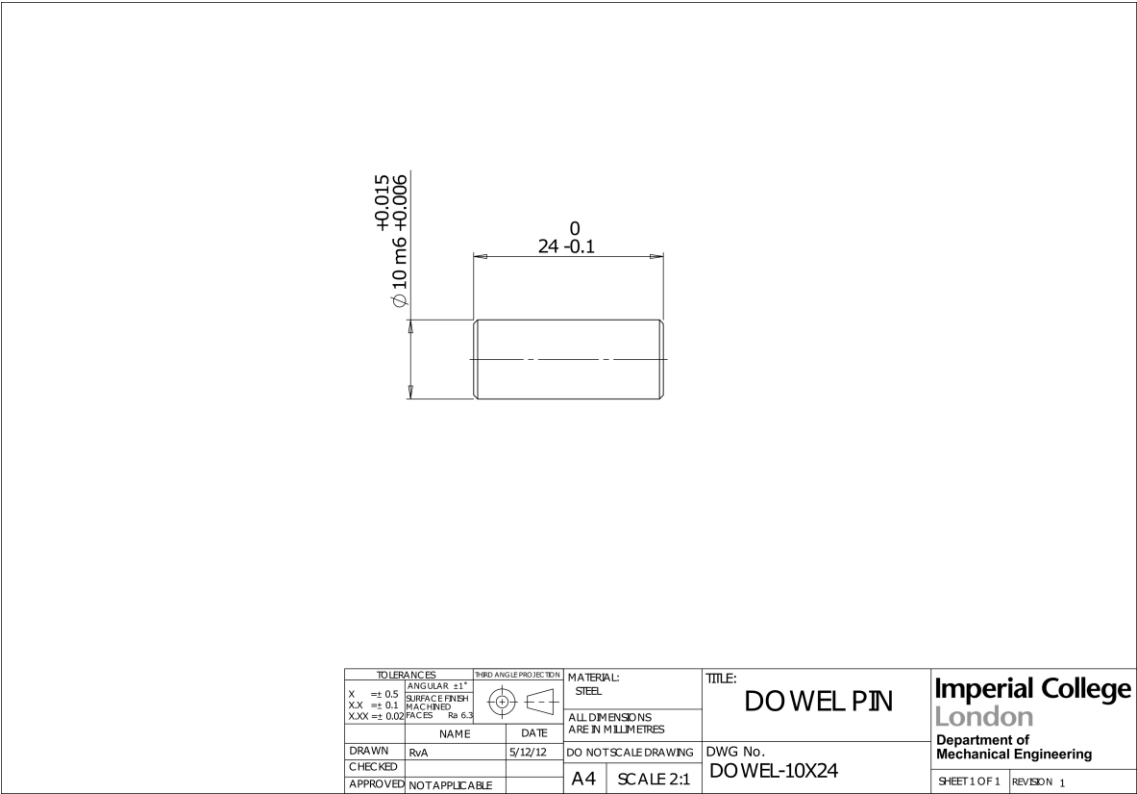
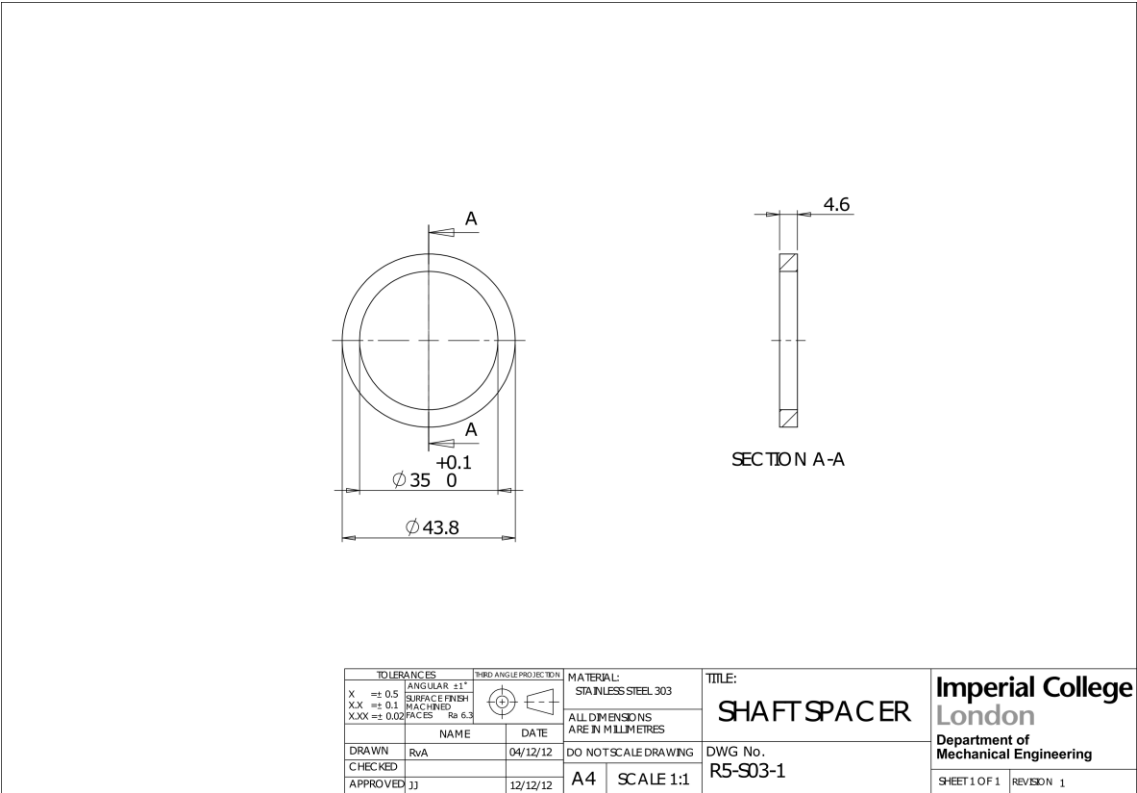


TOLERANCES		THIRD ANGLE PROJECTION	MATERIAL: ALUMINIUM ALLOY 6082 T6	TITLE: <b>SPACER</b>	<b>Imperial College</b> <i>London</i> <b>Department of</b> <b>Mechanical Engineering</b>			
X	± 0.5	ANGULAR ±1°						
XX	± 0.1	SURFACE FINISH MACHINED				ALL DIMENSIONS ARE IN MILLIMETRES		
XXX	± 0.02	FACES Ra 6.3						
NAME		DATE	DO NOT SCALE DRAWING	DWG No.				
DRAWN	RvA	30/05/13		R5-F07-1				
CHECKED			A4	SCALE 1:1				
APPROVED	JJ	30/05/13			SHEET 1 OF 1 REVISION 1			

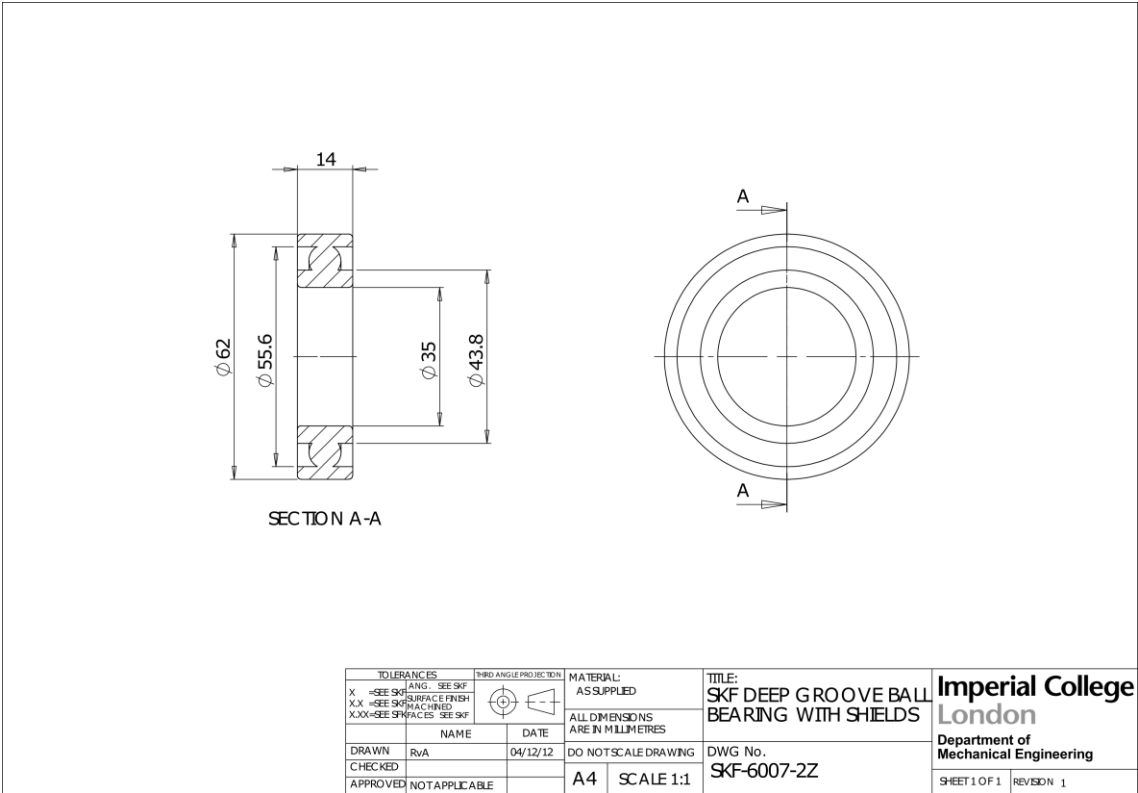








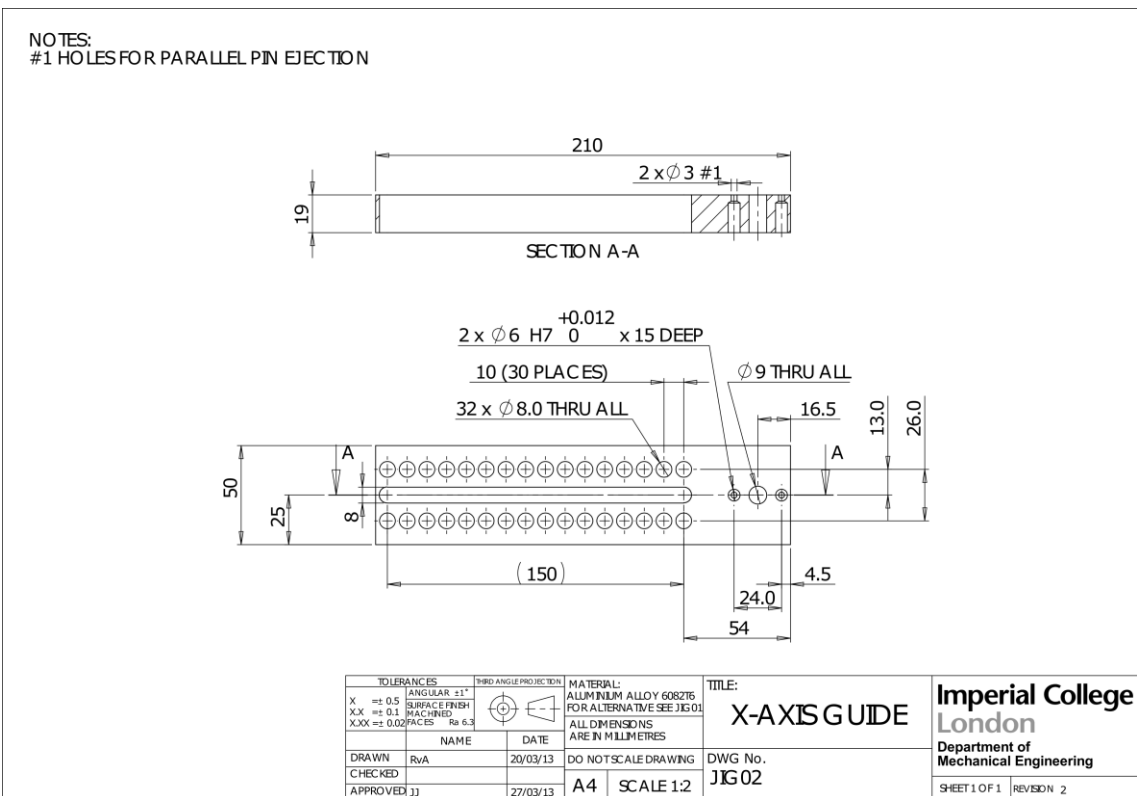
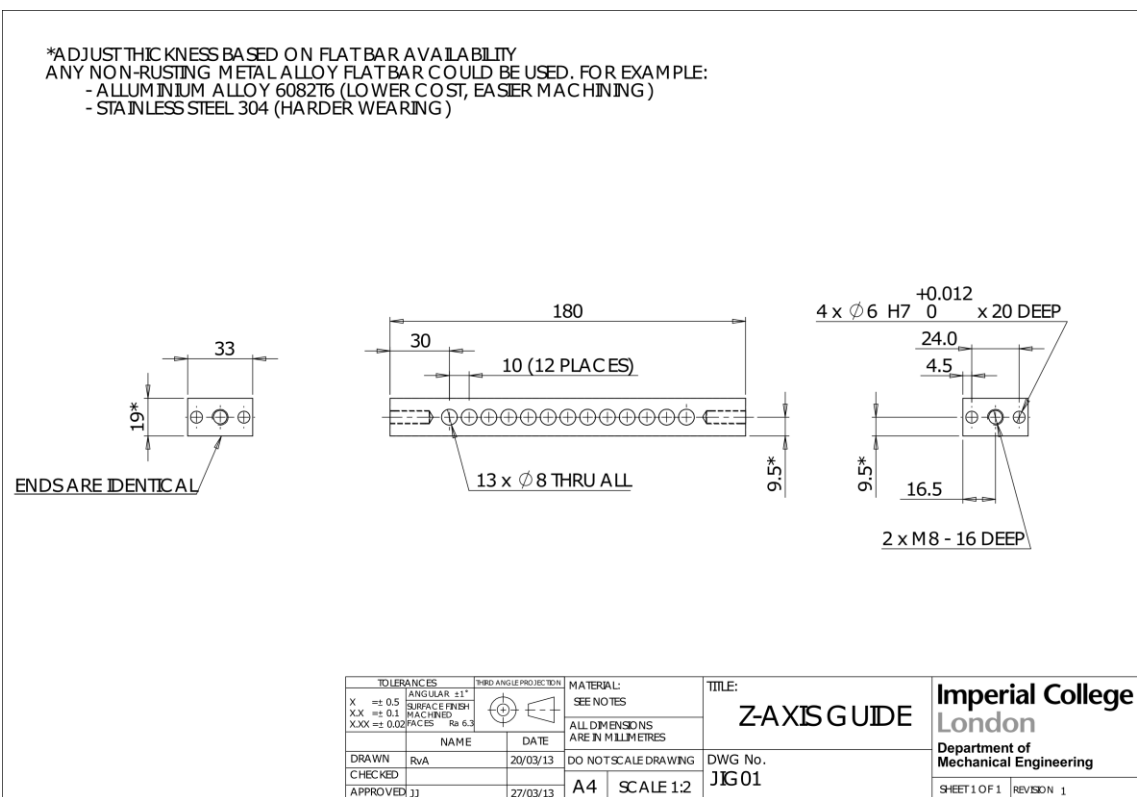


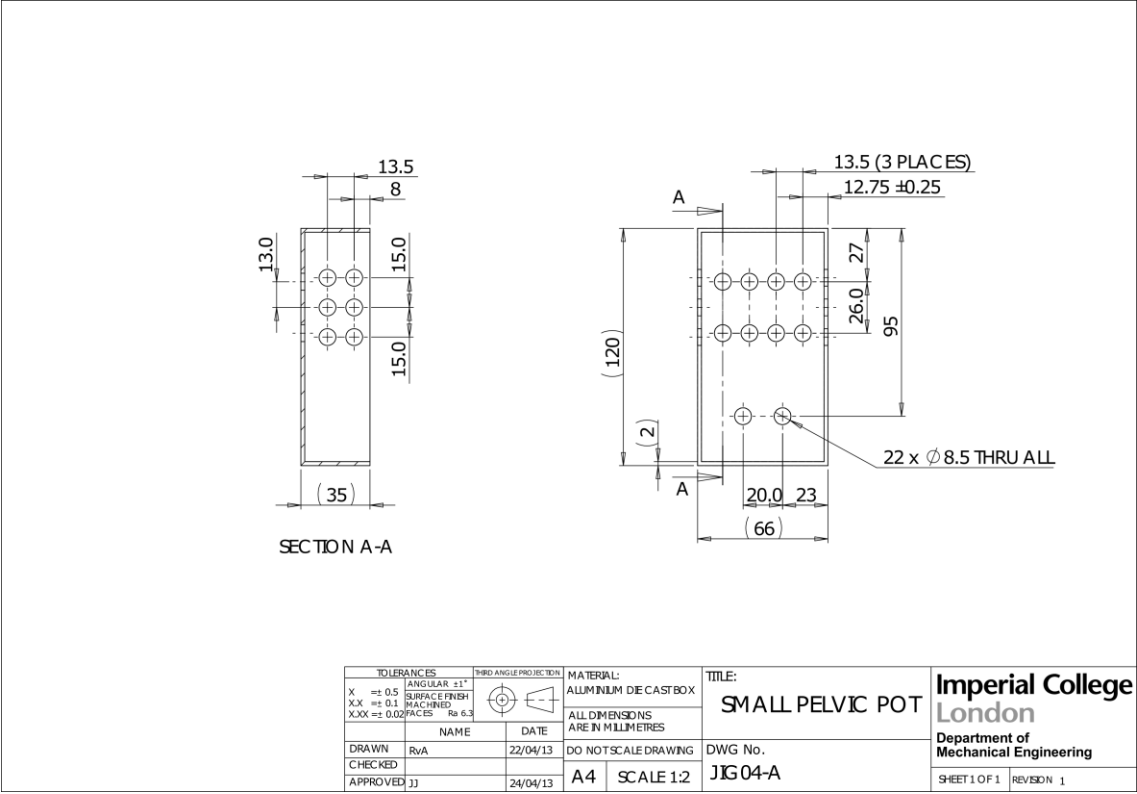
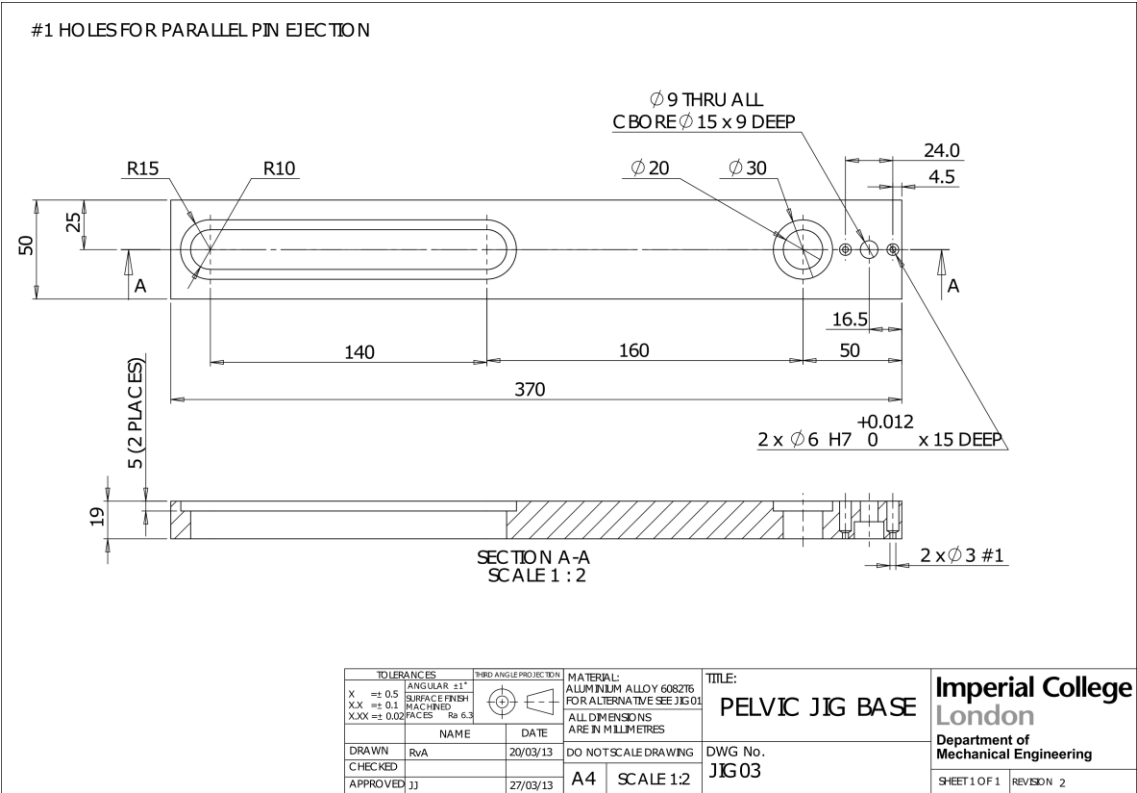


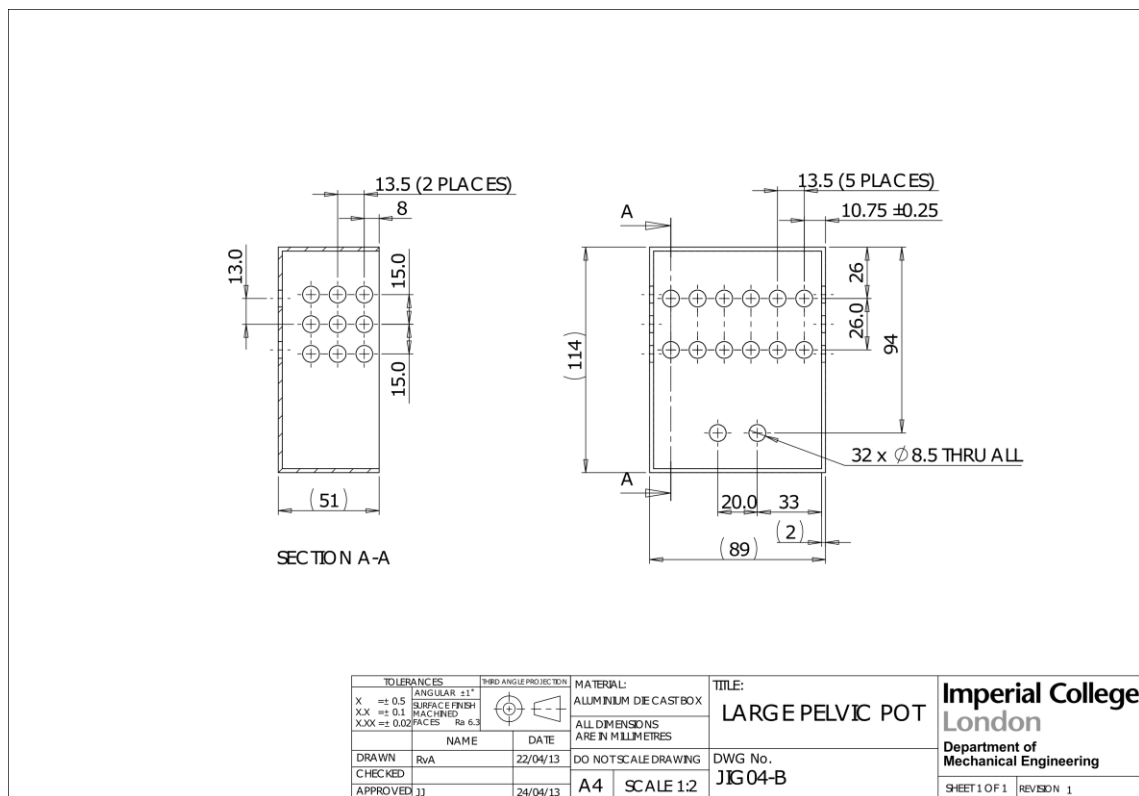


# A5 Repeatable in-vitro alignment jigs appendices

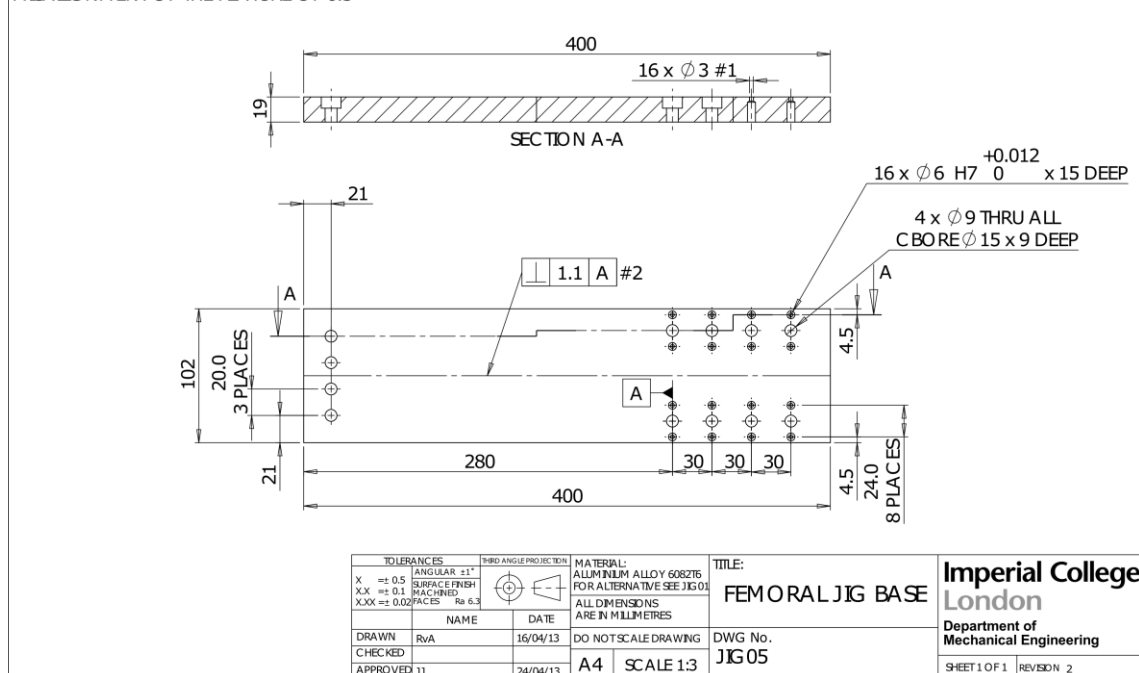
## A5.1 Component Drawings

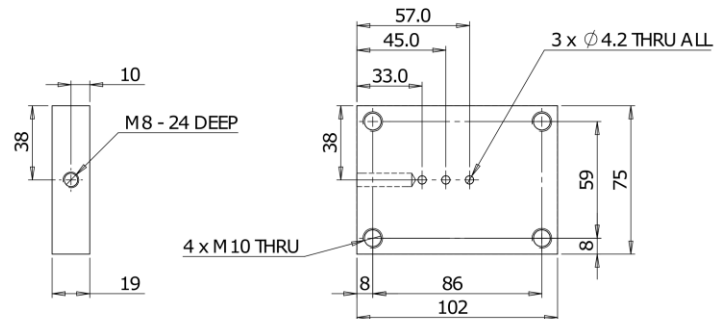






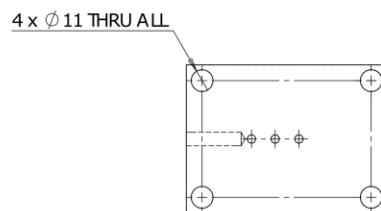
#1 HOLES FOR PARALLEL PIN EJECTION  
#2 MACHINE CENTRE LINE (DEPTH 1MM) WITH SPOT DRILL, 90° END MILL, OR EQUIVALENT, SUCH THAT IT IS PERPENDICULAR TO THE LINES CONNECTING THE CENTRE MARKS OF EACH PARALLEL PIN HOLE-PAIR (FOR EXAMPLE DATUM A). THE MECHANICAL AXIS OF THE FEMUR IS ALIGNED AGAINST THIS LINE WHEN USING THE JIG AND HENCE ANY DEVIATIONS FROM PERPENDICULAR WILL BIAS FEMORAL ORIENTATION TO EITHER AB/ADDUCTION. THE GEOMETRIC TOLERANCE GIVEN EQUATES TO A MAXIMUM MISALIGNMENT OF THE FEATURE OF 0.5°



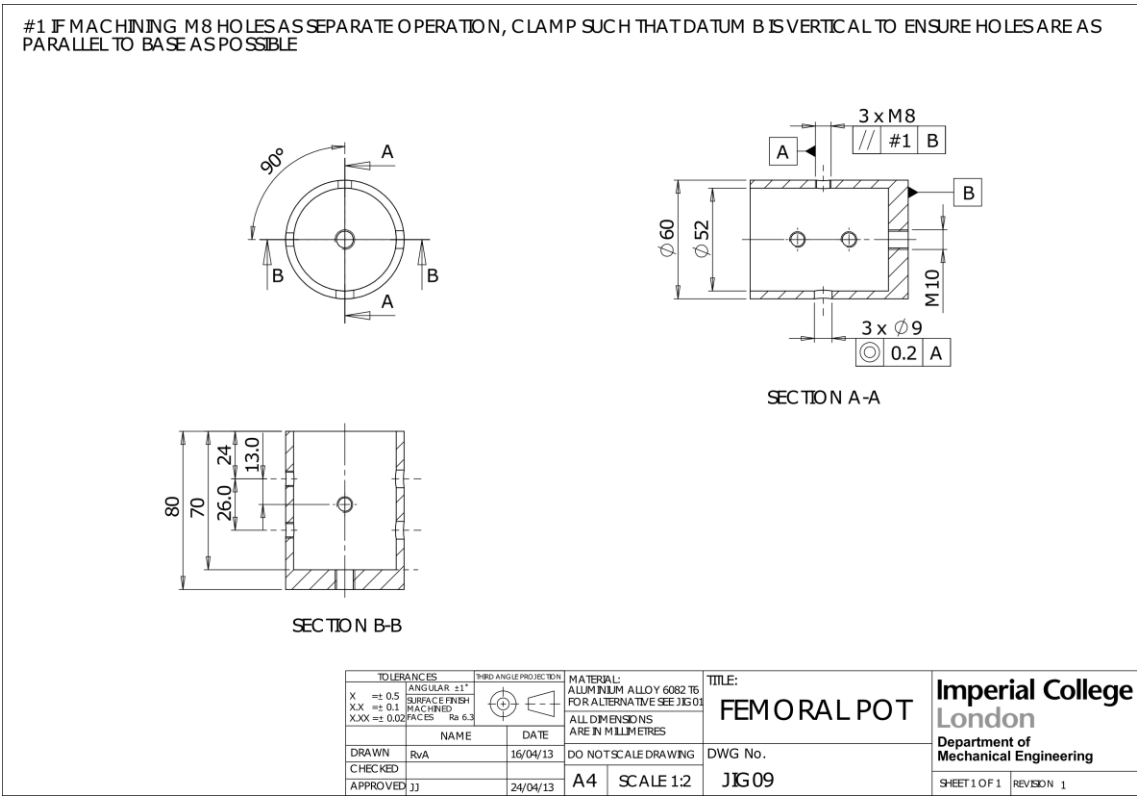
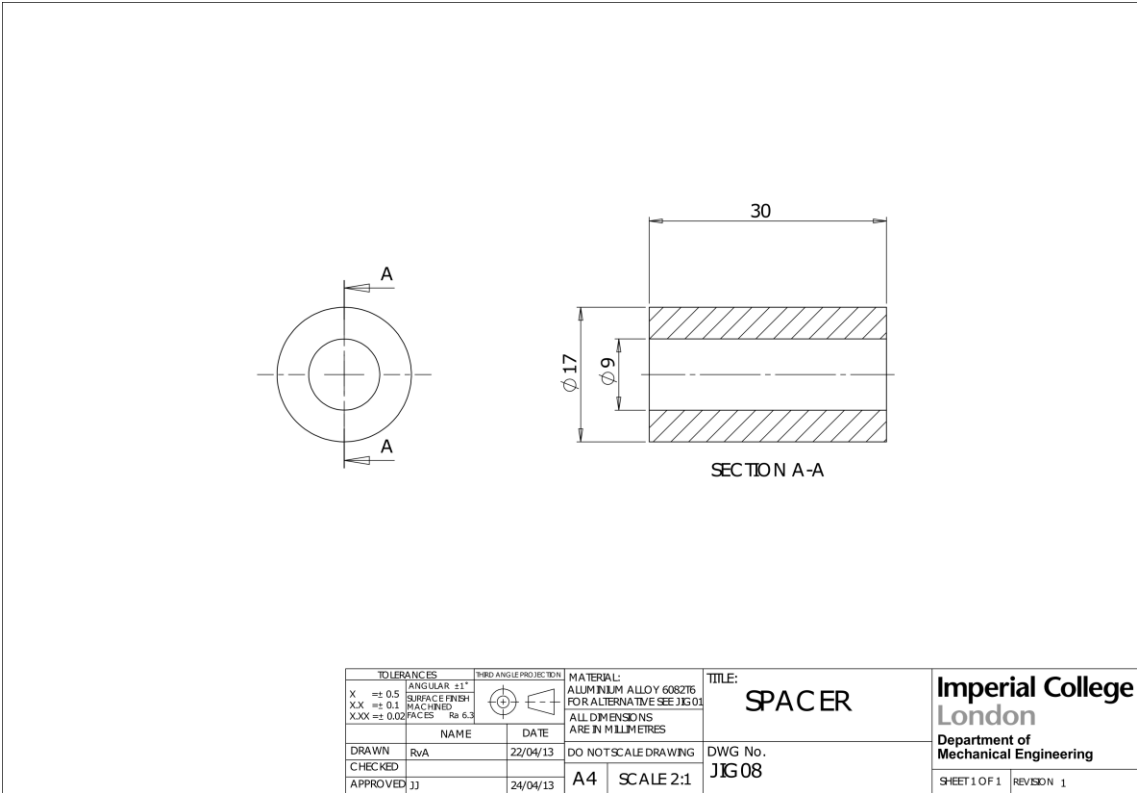


TOLERANCES		THIRD ANGLE PROJECTION		MATERIAL:		TITLE:	
X	± 0.5	ANGULAR	± 1°	ALUMINIUM ALLOY 6082T6 FOR ALTERNATIVE SEE JIG 01		EPICONDYLE CLAMP 1	
XX	± 0.1	SURFACE FINISH					
XXX	± 0.02	MACHINED FACES	Ra 6.3				
NAME		DATE		ALL DIMENSIONS ARE IN MILLIMETRES		DWG No.	
DRAWN		16/04/13		DO NOT SCALE DRAWING		JIG 06	
CHECKED				A4		SCALE 1:2	
APPROVED JJ		24/04/13				SHEET 1 OF 1	
						REVISION 1	

IDENTICAL TO JIG 06 BUT WITH  $\phi 11$  THRU HOLES INSTEAD OF TAPPED HOLES



TOLERANCES		THIRD ANGLE PROJECTION		MATERIAL:		TITLE:	
X	± 0.5	ANGULAR	± 1°	ALUMINIUM ALLOY 6082T6 FOR ALTERNATIVE SEE JIG 01		EPICONDYLE CLAMP 2	
XX	± 0.1	SURFACE FINISH					
XXX	± 0.02	MACHINED FACES	Ra 6.3				
NAME		DATE		ALL DIMENSIONS ARE IN MILLIMETRES		DWG No.	
DRAWN		16/04/13		DO NOT SCALE DRAWING		JIG 07	
CHECKED				A4		SCALE 1:2	
APPROVED JJ		24/04/13				SHEET 1 OF 1	
						REVISION 1	



## A5.2 Calculating directions of the axes of the ISB and Pot reference frames

### A5.2.1 ISB Pelvic Reference Frame Axes

After digitising the anterior superior iliac spines (Figure 11.13), the direction of the Z-axis, is described by the normalised vector found from subtracting the point defining the positions of the left anterior superior iliac spine,  $ASIS_L$ , from the right,  $ASIS_R$ . I.e. a unit vector pointing to the right:

$$\mathbf{Z} = \mathbf{ASIS}_R - \mathbf{ASIS}_L \quad (11.21)$$

$$\hat{\mathbf{Z}} = \frac{\mathbf{Z}}{|\mathbf{Z}|}$$

The Y-axis is found as a vector perpendicular to a plane defined by the left and right anterior superior iliac spine and the mid-point of the posterior superior iliac spines,  $PSIS$ . This can be calculated as the cross product between the Z-axis, and a vector pointing anteriorly in the plane:

$$\mathbf{Y} = \hat{\mathbf{Z}} \times \left[ \left( \frac{\mathbf{ASIS}_R + \mathbf{ASIS}_L}{2} \right) - \left( \frac{\mathbf{PSIS}_R + \mathbf{PSIS}_L}{2} \right) \right] \quad (11.22)$$

$$\hat{\mathbf{Y}} = \frac{\mathbf{Y}}{|\mathbf{Y}|}$$

Finally, the X-axis is mutually perpendicular to the Y and Z-axes and points anteriorly. It can also be calculated via the cross product:

$$\hat{\mathbf{X}} = \hat{\mathbf{Y}} \times \hat{\mathbf{Z}} \quad (11.23)$$

### A5.2.2 ISB Femoral Reference Frame Axes

For a right (or left) femur, the direction of the y-axis is the unit vector that points superiorly from the mid-point of the medial and lateral femoral epicondyles ( $EC_M$  and  $EC_L$  respectively), to the femoral head centre,  $FHC$ . Note the distinction between the pelvic and femoral body reference frames, the pelvic frames uses uppercase letters, the femoral frame lowercase letters for the axes:

$$\mathbf{y} = \mathbf{FHC} - \left( \frac{\mathbf{EC}_M + \mathbf{EC}_L}{2} \right) \quad (11.24)$$

$$\hat{\mathbf{y}} = \frac{\mathbf{y}}{|\mathbf{y}|}$$



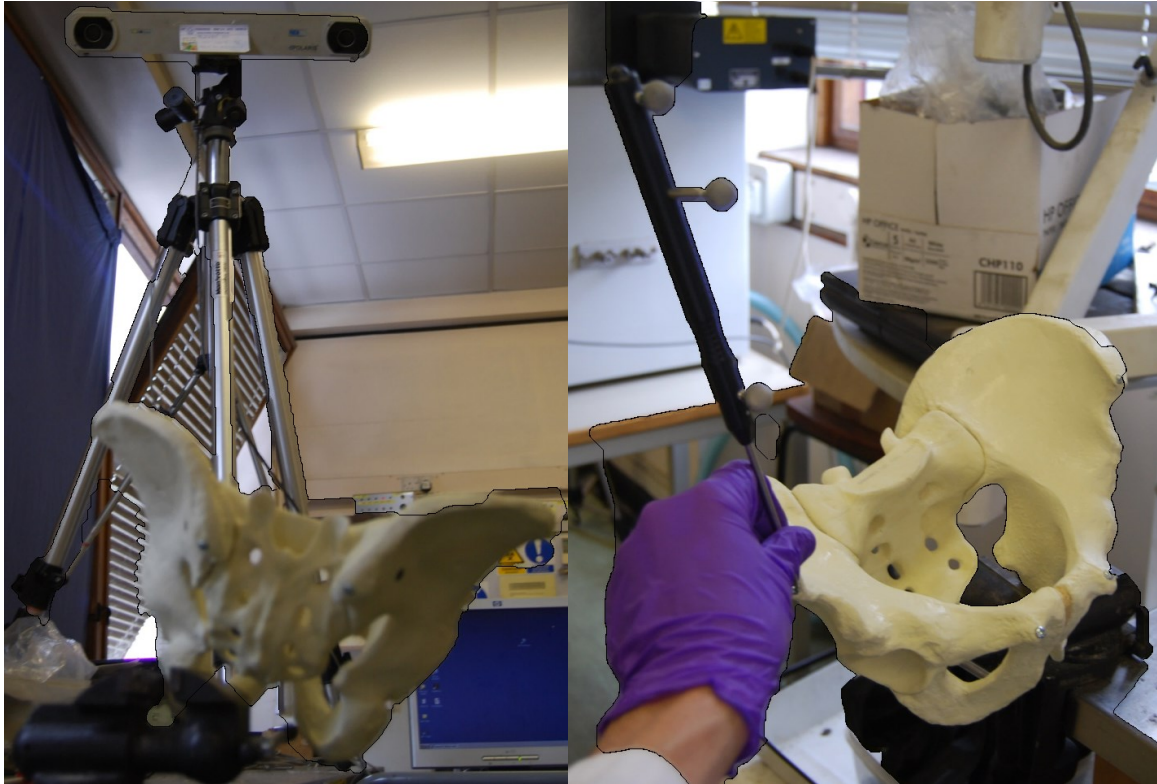


Figure 11.13 Left) a posterior view of a pelvis and the optical tracker. Right) anterior view of a pelvis with the right anterior superior iliac spine being digitised with the optical tracking probe.

Then the x-axis is found as the normal vector to a plane containing the femoral head centre and the femoral epicondyles. Therefore it can be calculated as the cross-product between the y-axis and a vector pointing approximately to the right in this plane:

$$\text{Right Femur:} \quad \mathbf{x} = \hat{\mathbf{y}} \times (\mathbf{EP}_L - \mathbf{EP}_M) \quad (11.25)$$

$$\text{Left Femur:} \quad \mathbf{x} = \hat{\mathbf{y}} \times (\mathbf{EP}_M - \mathbf{EP}_L)$$

$$\hat{\mathbf{x}} = \frac{\mathbf{x}}{|\mathbf{x}|}$$

Finally, the z-axis is mutually perpendicular to the x and y-axis and pointing to the right (laterally for a right femur, medially for a left femur) and is thus calculated:

$$\hat{\mathbf{z}} = \hat{\mathbf{x}} \times \hat{\mathbf{y}} \quad (11.26)$$

#### A5.2.3 Pelvic Pot's and Rig's Reference Frame Axes

The pelvic pot and the pelvis testing rig have rectangular features which equate to the coronal and sagittal planes. In a neutral position, the ISB X-axis is normal to the coronal plane and the Z-axis normal to the sagittal plane and so >100 points were digitised on surfaces and a least-squares fit was used to calculate the direction of a unit

normal vector thus giving accurate estimates of unit vector X and Z-axes (Figure 11.14).

$$\hat{\mathbf{X}}_{approx} = \text{lsplane}([\mathbf{p}_C]) \quad (11.27)$$

$$\hat{\mathbf{Z}} = \text{lsplane}([\mathbf{p}_S]) \quad (11.28)$$

Where:  $\mathbf{p}_C$  and  $\mathbf{p}_S$  are matrices of the digitised points on the coronal and sagittal plane respectively and lsplane is a MatLab function (Smith, 2002) that uses a singular value decomposition (see A5.4) to find the normal vector. The cross product of these axes was then used to calculate the unit vector Y-axis:

$$\hat{\mathbf{Y}} = \hat{\mathbf{Z}} \times \hat{\mathbf{X}}_{approx} \quad (11.29)$$

Whilst the Y-axis is mutually perpendicular to the X and Z-axes, the X and Z-axes were calculated from experimental data and hence were not exactly perpendicular (ranging between 87-93°). So that subsequent calculations could be performed with an orthogonal reference frame, the X axis was recalculated as the cross product between the Y and Z-axes thus correcting this small deviation from perpendicular:

$$\hat{\mathbf{X}} = \hat{\mathbf{Y}} \times \hat{\mathbf{Z}} \quad (11.30)$$

Whilst the least-squares normal vector method provided an excellent way to calculate the pot/rig's coordinate axes based on >100 points, pilot data showed that the direction of least-squares normal vectors (pointing anteriorly/posteriorly, or medially/laterally) varied between repeats as the pot/rig was rotated in the field of view of the optical tracking system; for example sometimes the X-axis pointed anteriorly, and sometimes posteriorly. Thus additional single points were digitised at extreme locations of medial/lateral, anterior/posterior, superior/inferior when collecting the data. These points were used to calculate three unit vectors that were known to point laterally (medially for a left pelvis), anteriorly, and superiorly; i.e. with a known  $\pm$  sign convention. These direction reference vectors (based on only two points) were paired with the appropriate higher accuracy X/Y/Z axis (based on >100 points) and the angle between them was calculated using the vector dot product (equation (11.15), page 194). This angle was used to determine if the X/Y/Z axis was pointing in the correct direction: it was close to 0° in cases where the axis pointed in the correct direction, and approximated to 180° in cases where the X/Y/Z axis needed to be inverted:

$$\theta_1 = \cos^{-1}(\hat{\mathbf{X}} \cdot \hat{\mathbf{AP}}); \theta_2 = \cos^{-1}(\hat{\mathbf{Y}} \cdot \hat{\mathbf{SI}}); \theta_3 = \cos^{-1}(\hat{\mathbf{X}} \cdot \hat{\mathbf{ML}}) \quad (11.31)$$

$$\text{if } \theta_1 \approx 180^\circ \text{ then } \hat{\mathbf{X}} = -\hat{\mathbf{X}}; \text{ if } \theta_2 \approx 180^\circ \text{ then } \hat{\mathbf{Y}} = -\hat{\mathbf{Y}}; \text{ if } \theta_3 \approx 180^\circ \text{ then } \hat{\mathbf{Z}} = -\hat{\mathbf{Z}}$$

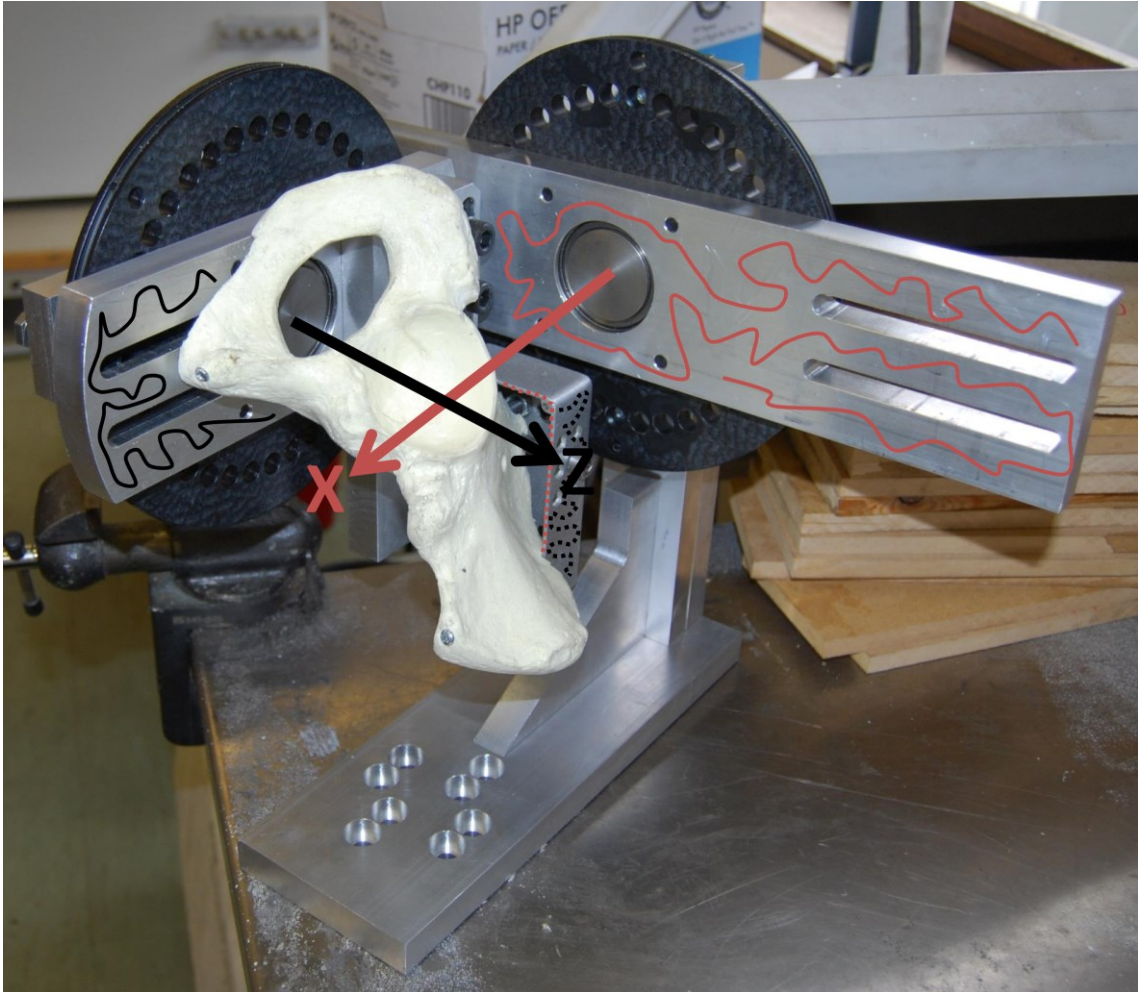


Figure 11.14 Calculating the pelvic rig's frame of reference.

The optical tracker was used to collect more than 100 points on the coronal plane (red wavy line) and the sagittal plane (black wavy line) to calculate the X and Z axes respectively (the normal vectors to these planes). The Y axis was calculated to be mutually perpendicular to these measured axes. The dotted red and black lines on the pelvic pot highlight the equivalent features on the pot that were used to digitise these axes when not mounted in the rig (the red dots highlight the pot face, but for some measurements were also taken on the back of the pot depending on the orientation in the optical tracker's field of view).

Where  $\widehat{AP}$  is a unit vector pointing approximately anteriorly,  $\widehat{SI}$  is a unit vector pointing approximately superiorly and  $\widehat{ML}$  is a unit vector pointing approximately laterally to the right (medially to the right for a left hip).

#### A5.2.4 Femoral Pot's Reference Frame Axes

The y-axis for the femoral pot was calculated as the least-squares fitted normal to >100 digitised points on the pot's transverse (top/bottom) plane (Figure 11.15):

$$\hat{y} = \text{lsplane}([p_T]) \quad (11.32)$$

Where  $[p_T]$  is a matrix of points on the transverse plane. The x-axis was calculated as a unit vector between two digitised points recorded at the anterior and posterior centres of a bolt which mounts the femur into the pot:

$$\hat{x}_{approx} = B_A - B_P \quad (11.33)$$

Where  $B_A$  is the anterior bolt centre and  $B_P$  is the posterior bolt centre. The z-axis is calculated as the cross product of the y and x-axis:

$$\hat{z} = \hat{x}_{approx} \times \hat{y} \quad (11.34)$$

As for the pelvic pot, the x-axis was then recalculated with the cross product to ensure all axes were perpendicular to each other.

$$\hat{x} = \hat{y} \times \hat{z} \quad (11.35)$$

Similarly extreme points in an anterior/posterior, medial/lateral and superior/inferior directions were used to confirm that the calculated axes had the correct sign convention using equation (11.31) with the femoral pot axes.

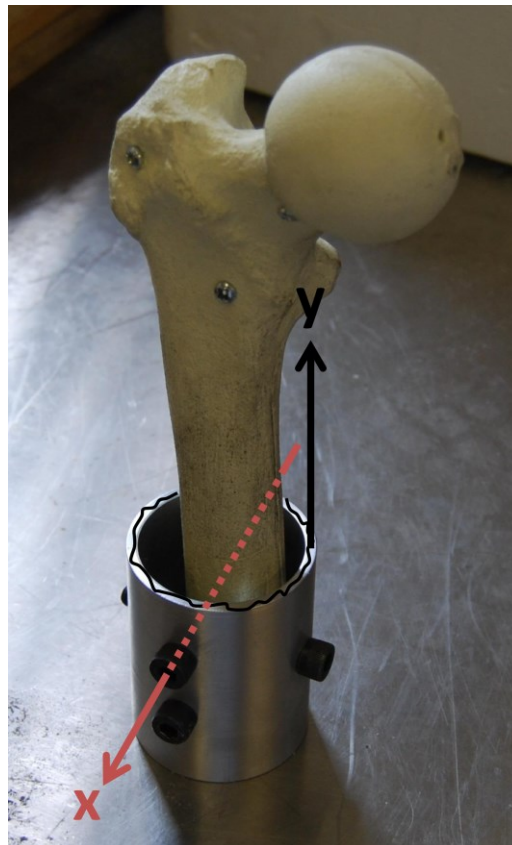


Figure 11.15 Calculating the femoral pot's frame of reference.

More than 100 points taken on the top plane of the pot (black wavy line) were used to calculate the y-axis (the normal vector to these points). Digitised points on an x-axis bolt were used to calculate the x-axis. The z-axis was calculated to be mutually perpendicular to these measured axes.

### A5.3 Transforming points into the ISB/Pot reference frame

The twelve unit vectors calculated with equations (11.21)-(11.26), (11.28)-(11.30), (11.32), (11.34) and (11.35) and represent the axes of the ISB pelvic/femoral reference frame for the intact/potted case in the global (optical tracker) frame of reference. These axes can be used to transform between the global and local (pot/ISB) reference frames.

Using the notation for an intact pelvis as an example, expressing these axes as a matrix:

$$[{}^G\mathbf{T}_{ISB}] = [\hat{X} \quad \hat{Y} \quad \hat{Z}] = \begin{bmatrix} X_{Gx} & Y_{Gx} & Z_{Gx} \\ X_{Gy} & Y_{Gy} & Z_{Gy} \\ X_{Gz} & Y_{Gz} & Z_{Gz} \end{bmatrix} \quad (11.36)$$

Where  $X_{Gx}$  is the x-component of the ISB X-axis unit vector in the global reference frame,  $X_{Gy}$  is the y-component of the ISB X-axis unit vector in the global reference frame and so on. The matrix  ${}^G\mathbf{T}_{ISB}$  is effectively a transformation matrix from the ISB system, to the global (optical tracker) system.

The seven repeatable anatomical landmarks are digitised in the global frame of reference, hence:

$$[{}^G\mathbf{p}] = \begin{bmatrix} p_{1Gx} & p_{2Gx} & p_{3Gx} & p_{4Gx} & p_{5Gx} & p_{6Gx} & p_{7Gx} \\ p_{1Gy} & p_{2Gy} & p_{3Gy} & p_{4Gy} & p_{5Gy} & p_{6Gy} & p_{7Gy} \\ p_{1Gz} & p_{2Gz} & p_{3Gz} & p_{4Gz} & p_{5Gz} & p_{6Gz} & p_{7Gz} \end{bmatrix} \quad (11.37)$$

Where  ${}^G\mathbf{p}$  is a matrix of all seven anatomical landmarks and  $p_{1Gx}$  is the x-component of point 1 in the global reference frame,  $p_{1Gy}$  is the y-component of point 1 in the global reference frame and so on.

The points can be converted into the ISB reference frame for the pelvis by multiplying by the inverse of the transformation matrix detailed in equation (11.36) (which is equal to its transverse as the transformation matrix is orthogonal by definition):

$$[{}^{ISB}\mathbf{p}] = [{}^G\mathbf{T}_{ISB}]^{-1} [{}^G\mathbf{p}] = [{}^{ISB}\mathbf{T}_G] [{}^G\mathbf{p}] = \begin{bmatrix} X_{Gx} & X_{Gy} & X_{Gz} \\ Y_{Gx} & Y_{Gy} & Y_{Gz} \\ Z_{Gx} & Z_{Gy} & Z_{Gz} \end{bmatrix} \begin{bmatrix} p_{1Gx} \\ p_{1Gy} \\ p_{1Gz} \end{bmatrix} \quad (11.38)$$

The same strategy can be used to convert to the ISB femoral frame or the pots' reference frames. The sawbones alignment tests are principally concerned with the rotary orientation of the bones within the pots, however if translation were also important, the transformation matrix could be modified to a 4x4 matrix and include a reference to the coordinate system origin (Kwon, 1998). Also, the inverted transformation matrix detailed above,  ${}^{ISB}\mathbf{T}_G$ , from the global (optical tracker) to the local

(Pelvic) frame of reference is the same as the definition published elsewhere excluding translation terms (Kwon, 1998; Shabana, 2013):

$$[T_{L/G}] = \begin{bmatrix} \mathbf{i} \cdot \mathbf{i}' & \mathbf{j} \cdot \mathbf{i}' & \mathbf{k} \cdot \mathbf{i}' \\ \mathbf{i} \cdot \mathbf{j}' & \mathbf{j} \cdot \mathbf{j}' & \mathbf{k} \cdot \mathbf{j}' \\ \mathbf{i} \cdot \mathbf{k}' & \mathbf{j} \cdot \mathbf{k}' & \mathbf{k} \cdot \mathbf{k}' \end{bmatrix} \quad (11.39)$$

Where:  $T_{L/G}$  is a transformation matrix from the global to a local frame of reference.  $\mathbf{i}$  is the unit vector of the x-axis of the global reference frame (i.e.  $[1 \ 0 \ 0]^T$  for the optical tracker),  $\mathbf{j}$  is the unit vector of the y-axis of the global reference frame (i.e.  $[0 \ 1 \ 0]^T$  for the optical tracker) and  $\mathbf{k}$  is the unit vector of the z-axis of the global reference frame (i.e.  $[0 \ 0 \ 1]^T$  for the optical tracker);  $\mathbf{i}'$  is the unit vector of the X-axis of the body reference frame (i.e.  $[X_{Gx} \ X_{Gy} \ X_{Gz}]^T$  for the pelvic body frame),  $\mathbf{j}'$  is the unit vector of the Y-axis of the body reference frame (i.e.  $[Y_{Gx} \ Y_{Gy} \ Y_{Gz}]^T$  for the pelvic body frame) and  $\mathbf{k}'$  is the unit vector of the Z-axis of the body reference frame (i.e.  $[Z_{Gx} \ Z_{Gy} \ Z_{Gz}]^T$  for the pelvic body frame). Therefore, calculating the dot products of these vectors gives:  $\mathbf{i} \cdot \mathbf{i}' = [1 \ 0 \ 0]^T \cdot [X_{Gx} \ X_{Gy} \ X_{Gz}]^T = X_{Gx}$  and so on. These unit vector dot products are the direction cosines of the body frame of reference with respect to the global axes. For example if  $\alpha_1$  is the angle between the body (ISB) X-axis and the global (optical tracker) x-axis,  $\alpha_2$  is the angle between the body X-axis and the global y-axis, and  $\alpha_3$  the angle between the body X-axis and the global z-axis then  $\mathbf{i} \cdot \mathbf{i}' = \cos \alpha_1$ ,  $\mathbf{j} \cdot \mathbf{i}' = \cos \alpha_2$  and  $\mathbf{k} \cdot \mathbf{i}' = \cos \alpha_3$ .

## A5.4 Calculating misalignment

### A5.4.1 Defining a relevant measure of misalignment

In an ideal case, a bone could be orientated in a pot such that the pot's mechanical features could be used to replicate the axes of the ISB reference frame. Then, if these pots were used to mount the femur/pelvis into a testing rig, then the rig's neutral position and relative movements would be equivalent to those in the ISB coordinate system.

In reality, the orientation of the bones would not be perfectly preserved during by the drilling jig method so if the points were transformed into the pot's frame of reference, they would not be identical to those in ISB frame of reference. This means that if the specimens were subsequently mounted into a test rig, their relative pose in the rig's neutral position would not be equivalent to the ISB neutral position, and the relative movements would be about axes that would not exactly align with those defined by the ISB.



Assuming that the bone specimens are rigid bodies, the relative spacing of the seven repeatable landmarks (Table 5.1, page 95) would be unchanged by the drilling jig method and hence the misalignment would be equivalent to a change in the body's reference frame. Therefore, the degree of misalignment could be quantified as the equivalent hip joint rotation away from the ideal ISB neutral position that would result in the same relative pose of the pelvis and femur that was achieved using the drilling jig method.

Potting a hemipelvis and femur using the drilling jigs are two separate procedures and hence independently cause misalignment and so it is necessary to quantify the misalignment of the femoral and pelvic reference frames separately. Therefore, for femoral reference frame misalignment calculations, the pelvic reference frame is assumed to be perfectly preserved (a stationary pelvis), and vice-versa. Calculating of the rotation matrix that defines the misalignment is known as an attitude determination problem and the solution derived in the following sections.

#### *A5.4.2 The history of the attitude determination problem*

The attitude determination problem to calculate the rotation matrix that describes the transformation between two reference frame was first posed in 1965 in order to estimate the rotational position of a satellite based on measurements taken in a known (global) frame of reference (Wahba, 1965). Wahba posed the problem of calculating the proper orthogonal matrix  $[R]$  that minimises the least-squares loss function:

$$\sum_{i=1}^n \|\hat{\mathbf{v}}_i^* - [R]\hat{\mathbf{v}}_i\|^2 \quad (11.40)$$

Where  $\hat{\mathbf{v}}_i^*$  represented direction cosines of objects observed in the satellite's frame of reference, and  $\hat{\mathbf{v}}_i$  are direction cosines of the same objects in a known reference frame. Various solutions were presented however an elegant theoretical analysis and computationally robust solution was proposed by Markley (Markley, 1988) using singular value decomposition (Golub and Reinsch, 1970).

In the following years, singular value decomposition was also adopted in biomechanics studies for determining joint rotation matrices (Söderkvist and Wedin, 1993; Challis, 1995). When considering joint kinematics, it is also often relevant to track the joint translations and hence an additional translation term appears in the least squares problems:

$$\sum_{i=1}^n \|\mathbf{q}_i - [R]\mathbf{p}_i - \mathbf{d}\|^2 \quad (11.41)$$

Where  $q_i$  represents the  $i^{\text{th}}$  point measured in the reference frame 2 (e.g. the pot's reference frame),  $p_i$  represents the  $i^{\text{th}}$  point in the reference frame 1 (e.g. the ISB frame for intact specimens),  $[R]$  is the joint rotation matrix and  $d$  the translation vector that maps points from reference frame 1, to those in reference frame 2 (Söderkvist and Wedin, 1993; Challis, 1995).

#### A5.4.3 Solving for the joint rotation matrix

Numerous authors have presented the solution to this attitude determination problem (Arun et al., 1987; Markley, 1988; Söderkvist and Wedin, 1993; Challis, 1995). The approach taken is summarised below.

The translation vector and rotation vector have the same centroid and this centroid equals the mean of the points (Arun et al., 1987). Hence the translation vector is equivalent to the distance travelled by the mean of the points rotated into reference frame 2:

$$d = \bar{q} - [R]\bar{p} \quad (11.42)$$

Therefore, the number of unknowns can be reduced from twelve to nine by re-expressing the loss term:

$$\sum_{i=1}^n \|q'_i - [R]p'_i\|^2 \quad (11.43)$$

Where  $p'_i$  and  $q'_i$  are the  $i^{\text{th}}$  points centred about their means in reference frames 1 and 2 respectively:

$$q'_i = q_i - \bar{q} \quad (11.44)$$

$$p'_i = p_i - \bar{p} \quad (11.45)$$

Expanding the lost term in (11.43) gives:

$$\sum_{i=1}^n \|q'_i - [R]p'_i\|^2 = \sum_{i=1}^n (q'_i - [R]p'_i)^T (q'_i - [R]p'_i) = \sum_{i=1}^n (q'^T_i q'_i + x'^T_i x'_i - 2q'^T_i [R]p'_i)$$

Where superscript  $T$  represents the transpose. Hence minimising the loss term is equivalent to maximising:

$$\sum_{i=1}^n (q'^T_i [R]p'_i) = \text{trace}([R]^T [C]) \quad (11.46)$$

Where  $[C]$  is the cross-dispersion matrix:



$$[C] = \sum_{i=1}^n q'_i p'^T_i = [q'] [p']^T \quad (11.47)$$

Finding the singular value decomposition of  $[C]$  (which can be computed with an inbuilt MatLab command):

$$[U][S][V]^T = [C] \quad (11.48)$$

Where  $[U]$  and  $[V]$  are orthogonal matrices consisting of the orthonormal eigenvectors of  $[C][C]^T$  and  $[C]^T[C]$  respectively and  $[S]$  is a matrix of the positive square roots of the eigenvalues of  $[C]^T[C]$ , which are known as the singular values. Substituting (11.48) into (11.46) and noting that a trace is invariant under cyclic permutations, the loss term is minimised if the following expression is maximised:

$$\text{trace}([R]^T[U][S][V]^T) = \text{trace}([V]^T[R]^T[U][S]) \quad (11.49)$$

However, since  $[S]$  is diagonal, only the diagonal components of the product  $[V]^T[R]^T[U]$  can influence the calculation result and hence the diagonal components of  $[V]^T[R]^T[U]$  need to be maximised. Now since  $[V]$ ,  $[R]$  and  $[U]$  (and their transposes) are all orthogonal matrices (with unit vector rows/columns) then their product must also be orthogonal (with unit vector rows/columns). Therefore each of the diagonal terms of their product must be less than or equal 1 (otherwise the rows/columns could not be unit vectors and hence the product would not be orthogonal). Hence, the trace is a maximum when:

$$[V]^T[R]^T[U] = [I] \quad (11.50)$$

Pre-multiplying (11.50) by  $[V]$ , and post-multiplying by  $[U]^T$  (for an orthogonal matrix its transpose is its inverse) and then taking the transpose gives  $[R]$ :

$$[R] = [U][V]^T \quad (11.51)$$

However, when  $\det([R]) = -1$ , the resulting matrix is a reflection and not a rotation (Arun et al., 1987; Markley, 1988; Söderkvist and Wedin, 1993; Challis, 1995) hence, this equation is modified to the following to account for this rare exception:

$$[R] = [U] \begin{bmatrix} 1 & 0 & 0 \\ 0 & 1 & 0 \\ 0 & 0 & \det([U][V]^T) \end{bmatrix} [V]^T \quad (11.52)$$

#### A5.4.4 Decomposing the joint rotation matrix into Euler angles

Rotation matrices about one of the orthogonal x, y and z-axis can be defined as follows:

$$[R_x] = \begin{bmatrix} 1 & 0 & 0 \\ 0 & \cos \alpha & -\sin \alpha \\ 0 & \sin \alpha & \cos \alpha \end{bmatrix} \quad (11.53)$$

$$[R_y] = \begin{bmatrix} \cos \beta & 0 & \sin \beta \\ 0 & 1 & 0 \\ -\sin \beta & 0 & \cos \beta \end{bmatrix} \quad (11.54)$$

$$[R_z] = \begin{bmatrix} \cos \gamma & -\sin \gamma & 0 \\ \sin \gamma & \cos \gamma & 0 \\ 0 & 0 & 1 \end{bmatrix} \quad (11.55)$$

For a hip, flexion,  $\gamma$ , is an anti-clockwise rotation about the pelvic Z-axis; adduction,  $\alpha$ , is a clockwise/anti-clockwise rotation (for left/right hips respectively) rotation about the floating axis that is orthogonal to the femoral y-axis and pelvic Z-axis; and internal rotation,  $\beta$ , is a clockwise/anti-clockwise rotation (for left/right hips respectively) about the femoral y-axis (Wu et al., 2002; Cappozzo et al., 2005). Note that whilst the reference frames and joint rotation matrices are orthogonal, the axes of rotation are only orthogonal in the neutral position. Indeed, at 90° hip ab/adduction, Gimbal lock occurs as the flexion/rotation axes are parallel.

Since matrix multiplication is not commutative, the rotation matrix that describes a transformation about all three axes is dependent on the order of rotation. For the hip, the order of rotation is: first, the hip is flexed/extended about the pelvic Z-axis, then the hip is ad/abducted about the floating axis and then internally/externally rotated about the femoral y-axis (Cappozzo et al., 2005; Turley et al., 2011). This corresponds with a clinical understanding of the joint movements. Note that when the second rotation occurs, the floating axis is equivalent to the femoral x-axis.

The following rules are then applied to determine the joint rotation matrix: in the neutral starting position, it is assumed that the proximal and distal body reference frames align and hence the transformation matrix is simply the identity matrix. Then, for any subsequent rotation of the proximal/distal reference frame, it is necessary to pre-/post-multiply respectively by the relevant rotation matrix (Cappozzo et al., 2005). Hence, using these rules and using the order flexion-adduction-rotation the hip joint rotation matrix becomes:

$$[{}^P R_f] = \{([R_z][I])R_x\}R_y = R_z R_x R_y \quad (11.56)$$

Substituting in (11.53)-(11.55) give the following rotation matrix (Cappozzo et al., 2005; Turley et al., 2011):

$$\begin{aligned} {}^P\mathbf{R}_f &= \begin{bmatrix} r_{11} & r_{12} & r_{13} \\ r_{21} & r_{22} & r_{23} \\ r_{31} & r_{32} & r_{33} \end{bmatrix} \\ &= \begin{bmatrix} \cos \gamma \cos \beta - \sin \gamma \sin \alpha \sin \beta & -\sin \gamma \cos \alpha & \cos \gamma \sin \beta + \sin \gamma \sin \alpha \cos \beta \\ \sin \gamma \cos \beta + \cos \gamma \sin \alpha \sin \beta & \cos \gamma \cos \alpha & \sin \gamma \sin \beta - \cos \gamma \sin \alpha \cos \beta \\ -\cos \alpha \sin \beta & \sin \alpha & \cos \alpha \cos \beta \end{bmatrix} \end{aligned} \quad (11.57)$$

This matrix can then be used to decompose the rotation matrix calculated in (11.52) into angles of flexion, adduction and rotation (Cappozzo et al., 2005):

$$\alpha = \sin^{-1} r_{32} \quad (11.58)$$

$$\beta = \tan^{-1} \left( \frac{-r_{31}}{r_{33}} \right); \text{ or } \beta = \sin^{-1} \left( \frac{-r_{31}}{\cos \alpha} \right) \quad (11.59)$$

$$\gamma = \tan^{-1} \left( \frac{-r_{12}}{r_{22}} \right); \text{ or } \gamma = \sin^{-1} \left( \frac{-r_{12}}{\cos \alpha} \right) \quad (11.60)$$

If using the tangent formula, it is necessary to note the sign of the numerator and denominator (i.e. opposite/adjacent) to determine which quadrant the angle is in and hence the exact solution including the correct sign convention. For a right hip, positive angles represent adduction, internal rotation and flexion, for a left hip the positive angles represent abduction, external rotation and flexion and hence ab/adduction and internal/external rotation angles for a left hip need to be multiplied by minus one to maintain the sign convention used in this thesis.

#### A5.4.5 Practical implementation of the solution for the misalignment calculations

Recalling that in a neutral position, the femoral reference frame is equal to the pelvic reference frame and that. Making the following assumptions:

- Bone specimens are rigid bodies.
- Femoral and pelvic misalignment calculations are independent and hence can be calculated separately: femoral misalignment is calculated assuming that the ISB pelvic system has been perfectly preserved, and vice-versa
- The pots can be perfectly mounted into a testing rig such that the rotation axes of the rig align with the hip joint centre and thus any translational misalignments are eliminated; only the rotational misalignment is important.
- The pots can be perfectly mounted into a testing rig based on their mechanical features such that in the rig's neutral position the pelvic and femoral reference frames align. This means that in a neutral position, the femoral pot's reference frame perfectly

aligns with the pelvis reference frame and vice-versa (as is the case for the ISB system).

The following steps can be used to quantify the femoral/pelvis misalignment from the neutral ISB position when mounted in a testing rig in a neutral position using the bone pots:

- i. Using equations (11.21)-(11.23) and (11.27)-(11.31) for pelvic specimens, or equations (11.24)-(11.26) and (11.31)-(11.35) for femoral specimens, convert the digitised axes points into unit vectors describing the ISB and pot's reference frames. From here, the words body and specimen can refer to either the pelvis or the femur depending on which dataset is being analysed.
- ii. Transform intact specimen's points,  $\mathbf{p}$ , from the global (optical tracker) reference frame into the ISB reference frame using equation (11.38).
- iii. Transform potted specimen points,  $\mathbf{q}$ , from the global (optical tracker) reference frame into the potted reference frame using equation (11.38).
- iv. Centre the transformed points about their mean using equations (11.44) and (11.45) to find  $\mathbf{p}'$  and  $\mathbf{q}'$ .
- v. Calculate the cross-dispersion matrix  $[\mathbf{C}]$  using equation (11.47).
- vi. Calculate the  $[\mathbf{U}]$  and  $[\mathbf{V}]^T$  from the singular value decomposition of  $[\mathbf{C}]$ , equation (11.48).
- vii. Calculate  $[\mathbf{R}]$ , the rotation of the body reference frame from equation (11.52).
- viii. For femoral misalignment calculations: the femur is misaligned relative to its pot and the pot's reference frame is perfectly aligned to the pelvic pot's reference frame (see assumptions); hence  $[\mathbf{R}]$  describes the rotation of the femoral body, relative to the pelvic reference frame and so  $[\mathbf{}^P\mathbf{R}_f] = [\mathbf{R}]$ . However, for the pelvic misalignment calculations: the pelvis is misaligned relative to its pot which is perfectly aligned to the femoral reference frame; hence  $[\mathbf{R}]$  describes the rotation of the pelvic body, relative to the femoral frame of reference (the inverse of the normal hip rotation matrix definition) and so  $[\mathbf{}^P\mathbf{R}_f] = [\mathbf{R}]^{-1}$ .
- ix. Finally, decompose the joint rotation matrix,  $[\mathbf{}^P\mathbf{R}_f]$ , into angles of flexion/adduction/rotation using (11.57)-(11.60).

### A5.5 Quantification of optical tracking errors

The repeatable landmarks were recorded a minimum of three times rotating the specimen in the field of view of the optical tracker each time. Theoretically, once transformed into the ISB/pot's/rig's reference frame the repeats should be identical, however, this is not the case and so the error of the measurement system can be quantified by calculating the misalignment between these repeats. This was done for each of the ISB/potted pelvic/femoral datasets using the same method detailed in A5.4, comparing each repeat against each repeat within a specimen.

The ranges of the errors are plotted in Figure 11.16 and Figure 11.17 for the pelvic and femoral datasets respectively. As expected, the errors occur symmetrically, being equally likely to occur in flexion/extension, in adduction/abduction or in internal/external rotation. However, it can be seen that in some cases the errors between repeats within a specimen can be more than  $6^\circ$ . Given that the average misalignments recorded in

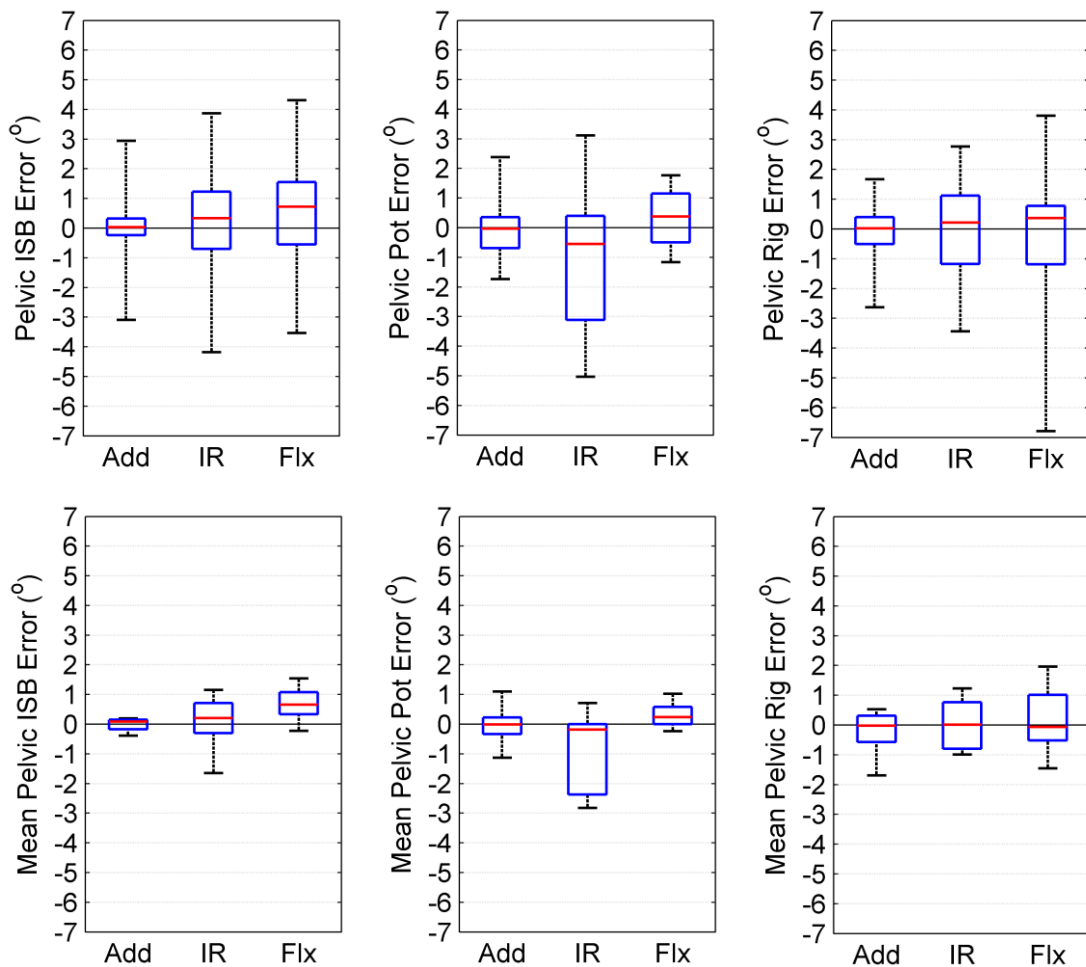


Figure 11.16 Box plots of error estimates for the optical tracking digitising methodology in terms of adduction, internal rotation and flexion (all positive) for the pelvic ISB, pot and rig datasets.

Top) all possible comparisons within a specimen ( $n \geq 8 \times 3$ ). Bottom) the same errors as top, however this time plotted as an average error for each specimen ( $n = 8$ ).

the main experiment was less than  $1.5^\circ$  in all rotation directions (Figure 5.2 and Figure 5.5), this means that using just a single repeat would be unreliable. However, by averaging data within a specimen, the errors are effectively reduced as the error distribution is symmetrical. For nearly all datasets in all rotation directions, when repeats were averaged within a specimen, the error was reduced to: a median of less than  $0.5^\circ$ , an interquartile range (50 % of the data) within  $\pm 1^\circ$  and all data within  $\pm 3^\circ$ . Therefore it can be concluded that taking three or more repeats when digitising points is essential when using the optical tracking system.

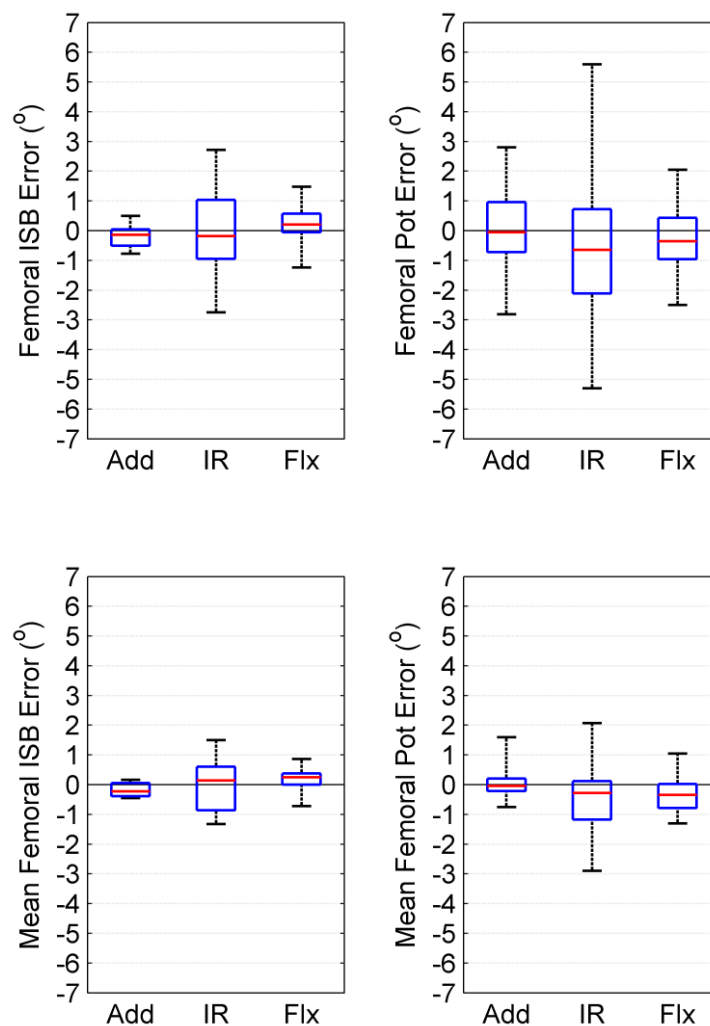





Figure 11.17 Error estimates for the optical tracking digitising methodology in terms of adduction, internal rotation and flexion (all positive) for the femoral ISB and pot datasets.

Top) all possible comparisons within a specimen ( $n \geq 8 \times 3$ ). Bottom) the same errors as top, however this time plotted as an average error for each specimen ( $n=8$ ).

# A6 Envelope of passive hip motion appendices

## A6.1 Ethical Approval Letter

	 Research Ethics Service	
<hr/>		
<b>East of Scotland Research Ethics Service (EoSRES) REC 2</b> (formerly Tayside Fife & Forth Valley REC) Tayside Medical Sciences Centre (TASC) Residency Block C, Level 3 Ninewells Hospital & Medical School George Pirie Way Dundee DD19SY		
Mr Richard J. van Arkel Research Postgraduate Imperial College London Imperial College London 362 Mechanical Engineering Building Exhibition Road, London SW7 2AZ	Date: Your Ref: Our Ref: Enquiries to: Direct Line: Email:	30 April 2013  LR/13/ES/0052 Mrs Lorraine Reilly 01382 383878 <a href="mailto:eosres.tayside@nhs.net">eosres.tayside@nhs.net</a>
 Dear Mr van Arkel		
<b>Study title:</b>	<b>The role of the capsule, labrum and ligament teres in stability of a hip in deep flexion</b>	
<b>REC reference:</b>	<b>13/ES/0052</b>	
<b>Protocol number:</b>	<b>P003</b>	
<b>IRAS project ID:</b>	<b>116482</b>	
 The Proportionate Review Sub-committee of the East of Scotland Research Ethics Service REC 2 reviewed the above application on 30 April 2013.		
<p>We plan to publish your research summary wording for the above study on the NRES website, together with your contact details, unless you expressly withhold permission to do so. Publication will be no earlier than three months from the date of this favourable opinion letter. Should you wish to provide a substitute contact point, require further information, or wish to withhold permission to publish, please contact the Co-ordinator Mrs Lorraine Reilly, <a href="mailto:lorraine.reilly@nhs.net">lorraine.reilly@nhs.net</a>.</p>		
<b>Ethical opinion</b>		
<p>There were no ethical issues noted.</p>		
<p>On behalf of the Committee, the sub-committee gave a favourable ethical opinion of the above research on the basis described in the application form, protocol and supporting documentation, subject to the conditions specified below.</p>		
<b>Ethical review of research sites</b>		
<p>The favourable opinion applies to all NHS sites taking part in the study, subject to management permission being obtained from the NHS/HSC R&amp;D office prior to the start of the study (see "Conditions of the favourable opinion" below).</p>		
<b>Conditions of the favourable opinion</b>		
<p>The favourable opinion is subject to the following conditions being met prior to the start of the study.</p>		
		



Management permission or approval must be obtained from each host organisation prior to the start of the study at the site concerned.

Management permission ("R&D approval") should be sought from all NHS organisations involved in the study in accordance with NHS research governance arrangements.

Guidance on applying for NHS permission for research is available in the Integrated Research Application System or at <http://www.rdforum.nhs.uk>.

Where a NHS organisation's role in the study is limited to identifying and referring potential participants to research sites ("participant identification centre"), guidance should be sought from the R&D office on the information it requires to give permission for this activity.

For non-NHS sites, site management permission should be obtained in accordance with the procedures of the relevant host organisation.

**Sponsors are not required to notify the Committee of approvals from host organisations.**

It is the responsibility of the sponsor to ensure that all the conditions are complied with before the start of the study or its initiation at a particular site (as applicable).

**You should notify the REC in writing once all conditions have been met (except for site approvals from host organisations) and provide copies of any revised documentation with updated version numbers. The REC will acknowledge receipt and provide a final list of the approved documentation for the study, which can be made available to host organisations to facilitate their permission for the study. Failure to provide the final versions to the REC may cause delay in obtaining permissions.**

#### Approved documents

The documents reviewed and approved were:

Document	Version	Date
Evidence of insurance or indemnity		01 August 2012
Investigator CV		22 April 2013
Investigator CV		22 April 2013
Protocol	P003	30 January 2013
REC application		15 April 2013

#### Membership of the Proportionate Review Sub-Committee

The members of the Sub-Committee who took part in the review are listed on the attached sheet.

#### Statement of compliance

The Committee is constituted in accordance with the Governance Arrangements for Research Ethics Committees and complies fully with the Standard Operating Procedures for Research Ethics Committees in the UK.

#### After ethical review

##### Reporting requirements

The attached document "After ethical review – guidance for researchers" gives detailed guidance on reporting requirements for studies with a favourable opinion, including:





- ☐ Notifying substantial amendments
- ☐ Adding new sites and investigators
- ☐ Notification of serious breaches of the protocol
- ☐ Progress and safety reports
- ☐ Notifying the end of the study

The NRES website also provides guidance on these topics, which is updated in the light of changes in reporting requirements or procedures.

#### Feedback

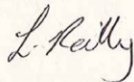
You are invited to give your view of the service that you have received from the National Research Ethics Service and the application procedure. If you wish to make your views known please use the feedback form available on the website. Information is available at National Research Ethics Service website > After Review

**13/ES/0052:**

***Please quote this number on all correspondence***

We are pleased to welcome researchers and R & D staff at our NRES committee members' training days – see details at <http://www.hra.nhs.uk/hra-training/>

Yours sincerely



*hs* **Dr Anthony Davis**  
Alternate Vice-chair

[eosres.tayside@nhs.net](mailto:eosres.tayside@nhs.net)

Enclosures:

List of names and professions of members who took part in the review  
"After ethical review – guidance for researchers"

Copy to:

Christine Buicke, Imperial College London  
Imperial College London R&D office



**A6.2 Analysis of HIP98 joint reaction force directions**

The HIP98 database (Bergmann et al., 2001) includes joint reaction force data relative to the femur for a variety of daily activities including: walking (slow, normal and fast), stair climbing and descending, rising from a chair and sitting down, knee bending and standing on one leg. All available data from these activities (4 patients, with typically 4 trials per activity) was imported into MatLab and the direction of the joint reaction force was calculated and plotted (Figure 11.18).

It can be seen that the average force in the sagittal plane aligns with the superior-inferior femoral axis, resulting in a near zero superior-anterior angle for the joint reaction force for the majority of most daily activities. However, the interquartile-range for the force direction in the coronal plane was angled approximately 10-20° medially from the superior-inferior femoral axis.

For the experiment, the force was angled superiorly in the sagittal plane and at the top end of interquartile range in the coronal plane (angled 20° medially from the superior-inferior axis). The top end of this range was used for two reasons: firstly, the gluteus medius, plays a large role in medialising the joint reaction force and so is included in many in-vitro models to improve their fidelity (Cristofolini, 1997; Konrath et al., 1998). However, gluteus medius weakness is common in hip replacement patients (Perron et al., 2000; Masonis and Bourne, 2002; Foucher et al., 2007; Toms et al., 2008); therefore, it is likely that the superior-medial angle is underestimated in the instrumented total hip replacement patients. Secondly, having a more medialised force has a benefit of stabilising the hip during the experiment; when the hip in deep flexion and adduction, a more medial force directs the femoral head more into the acetabulum reducing the risk of edge loading (chapter 3), subluxation or even dislocation (Bartz et al., 2000).

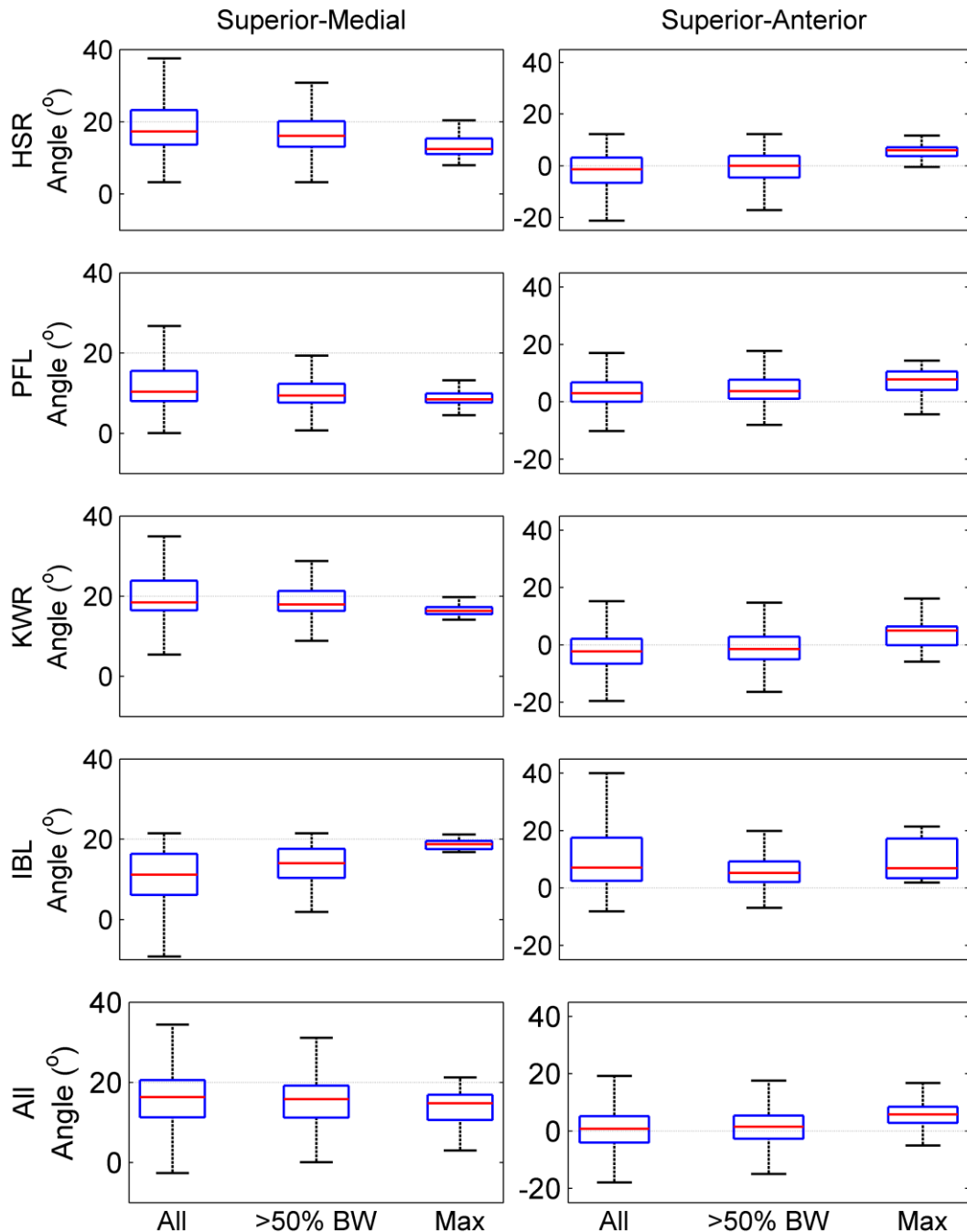


Figure 11.18 Box plots of the angle the hip joint reaction force makes in the coronal plane (left) and sagittal plane (right) for different patients (different rows).

The different boxes represent all force data from HIP98 (Bergmann et al., 2001), force data with non-negligible loads (more than 50 % BW, this excludes forces such as those before seat-off when rising from a chair) and for the peak force during the activity. The dashed lines at 20° and 0° highlight the force direction used during testing.

### A6.3 Servo-hydraulic control protocol

Pilot testing showed the servo-hydraulic machine was capable of running in load-control (its vertical axis) or torque-control (about its vertical axis) however it was unreliable when the machine was run in simultaneous load/torque control on both axes; it frequently crashed/overloaded the specimens. For physiologically representative

loading, it was necessary to operate the machine in load control to maintain a constant 100 N vertical load in the event that the hip translates even slightly proximally/distally. However, running the rotation axis in position control could also be problematic as the angular positions of 5 Nm internal/external restraint need to be known to do this yet they are outcome measures of the experiment. To counter this dilemma, the testing protocol was run as follows:

- i. In neutral flexion/abduction, the servo-hydraulic machine's vertical axis was set to operate in load control at 100 N.
- ii. The servo-hydraulic machine was manually operated until the hip provided 6 Nm of external rotation torque, and then internally rotated to 6 Nm passive restraint recording the angular positions at these limits.
- iii. A angular position sinusoid with a 10 s period was defined based on the angular positions recorded in step ii: the angular rotation cycle started at the mid-point ( $t = 0$  s), rotated to maximum external rotation ( $t = 2.5$  s), then rotated back through the mid-point ( $t = 5$  s) to the position of maximum internal rotation ( $t = 7.5$  s), and then back to the mid-point ( $t = 10$  s).
- iv. Steps ii and iii were repeated for all hip positions to establish up to 30 sinusoid unique waveforms for each cadaveric specimen.
- v. A preconditioning cycle (A6.3) was performed using the sinusoidal waveform for the neutral flexion/abduction position operating the rotating axis of the servo-hydraulic machine in position control.
- vi. Testing with the rotation axis in position control was performed using the established sinusoidal waveforms in all hip positions and the data presented in the results (sections 6.3.1-6.3.3) was recorded.

This protocol enabled the tests to be conducted without the servo-hydraulic machine overloading the specimens, thus protecting them from inadvertent damage. Aside from enabling testing, this protocol had an additional advantage: it meant that the servo-hydraulic machine was not changing rotation direction at exactly the point of interest for 5 Nm rotational angular positions and torsional stiffness measurements preventing the change of direction from affecting the results and ensuring that the machine made a reading a 5 Nm restraint for all hips. Moreover, establishing the sinusoidal waveforms also meant the specimens were preconditioned at least once in all hip positions by rotating them past the point of interest for measurements (5 Nm restraint); this is additional to the preconditioning protocol detailed in chapters 6 and 7.

#### A6.4 Significant two-way interactions involving hip rotation for slack-to-taut and torsional stiffness

No three-way interaction was detected for either the range of rotation to transition from slack to 5 Nm restraint ( $p=0.056$ ) or for the torsional stiffness at the point of 5 Nm of passive restraint ( $p=0.140$ ). However, as stated in results section 6.3.3, there two-way interactions between flexion and ab/adduction across both directions of rotation (both  $p<0.036$ ). Whilst outside the scope of the hypothesis for the study, additional two-way interactions were detected: for slack-to-taut between rotation direction and flexion when across all ab/adduction, and for torsional stiffness between rotation direction and ab/adduction across all flexion/extension (Figure 11.19, both  $p<0.024$ ). Subsequent pairwise analysis showed only three differences (all  $p<0.049$ ). The greatest mean significant difference for slack-to-taut was  $5 \pm 4^\circ$ , and for torsional stiffness was  $0.15 \pm 0.18 \text{ Nm/}^\circ$ . These differences were smaller than the variation across both directions of rotation with hip position (up to  $15 \pm 6^\circ$  and  $0.45 \pm 0.19 \text{ Nm/}^\circ$  for slack-to-taut and torsional stiffness respectively, Figure 6.7).

From these results it can be concluded whilst there were small specific differences between internal and external rotation restraint in some hip positions, rotation restraint can be considered symmetrical in most hip positions once the ligaments have tautened. This can be seen in Figure 6.4 where at each hip position the distance between the taut/slack transition and 5 Nm restraint varies little.

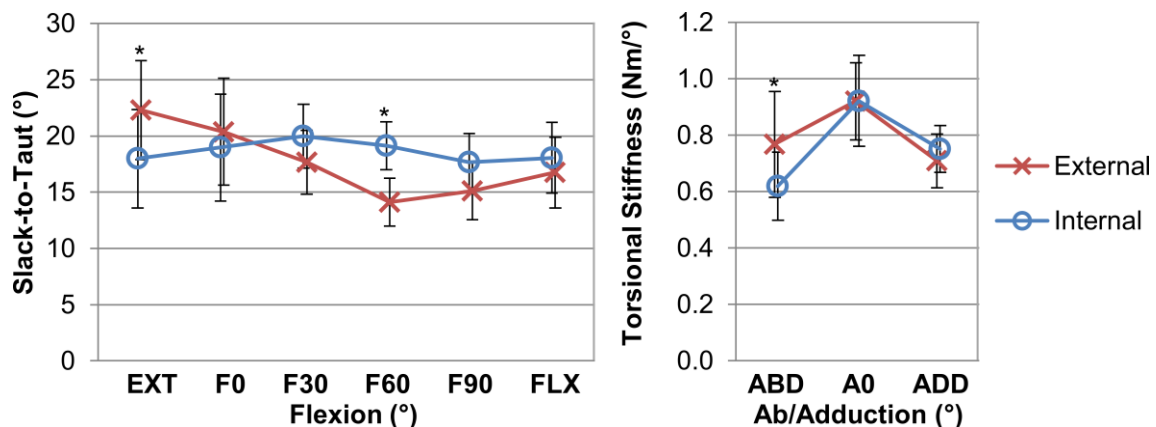


Figure 11.19 Mean angular change between the transition point and 5 Nm of rotational restraint (left) and torsional stiffness (right) with 95 % confidence intervals for internal and external rotation. It can be seen that the magnitude of restraint is largely symmetrical for hip rotation.

The only significant differences (\*) were in extension and 60° flexion for taut-to-slack (both  $p<0.012$ ) and in high abduction ( $p=0.049$ ) for torsional stiffness.

### **A6.5 A comparison between angular positions of labral impingement and capsular restraint**

#### *A6.5.1 Method*

Following the testing outlined in chapter 6, the capsule and ligamentum teres were resected and the 30 hip internal/external rotations movements were repeated, and the passive resistance re-measured, taking note of any visually detectable labral impingements. In the absence of the hip ligaments, any passive resistance must come from labral impingements and thus the position where the labrum started to impinge could be quantified by using the same algorithm that previously detected the slack/stiff transition point. If no labral impingements were detected (i.e. the joint rotated between the 5 Nm limits without any passive restraint) then for the purposes of the statistical analysis, the labrum impingement boundaries were set to the maximum value of hip rotation (i.e. the 5 Nm restraint limits).

After resecting the hip ligaments, it was found that the hip could dislocate in deep hip flexion combined with adduction, preventing any labral impingements that may have occurred from being measured. So that all specimens could be included in the data analysis (a requirement of a repeated measures design), missing values were substituted as follows: for external rotation, where the femoral neck was never close to impinging on the labrum in deep flexion, it was assumed that the labrum did not impinge. For internal rotation, the angular position where the labrum started to impinge was assumed to be the same as the angle where the intact hip transitioned from slack to stiff, thus overemphasizing any unmeasured labral impingements and biasing the results against a conclusion that the capsule protects against impingement in these positions. In total, dislocation affected 5/8 specimens but only 3.1 % (26/848) of measurements made.

#### *A6.5.2 Statistical Analysis*

Data were analysed in SPSS (version 22, SPSS Inc., Chicago, Illinois) with three-way repeated measures analysis of variance with post-hoc t-test with a Bonferroni correction. The independent factors were flexion (EXT, F0, F30, F60, F90, and FLX), ab/adduction (ABD, A0, and ADD) and ligament state (intact and resected). The dependent variable was the slack/stiff transition points with separate analyses performed for internal and external rotation.

### A6.5.3 Results

External rotation data for one female specimen was lost due to the capsule rupturing from the bone when 5 Nm torque was applied in external rotation meaning that subsequent hip rotation results are presented for only eight specimens. The slack/stiff transition point occurred before the points of labral impingement in nearly all hip positions (Figure 11.20). Moreover, in most hip positions the labrum did not impinge at all (Figure 11.21)

For internal rotation, there was a significant three-way interactions between the flexion/adduction hip position and the ligament state ( $p=0.009$ ). Post-hoc analyses showed that the slack/stiff transition point was significantly less than the position of labral impingement in all but four hip positions (all  $p<0.036$ ); however in positions of high flexion and neutral or high abduction there were no significant differences. Specifically, there were no differences at: 60 flexion and high abduction ( $p=0.334$ ), 90 flexion and neutral or high abduction (both  $p>0.153$ ), and deep flexion (FLX) and neutral ab/adduction ( $p=0.063$ ).

For external rotation, there was no significant three-way interaction ( $p=0.372$ ) however there was a significant two-way interaction between ligament state and ab/adduction across all flexion angles ( $p=0.001$ ). Post-hoc analyses showed that the slack/stiff transition point was significantly less than the position of labral impingement at all levels of ab/adduction (all  $p<0.001$ ). However, the significant differences were smaller in low flexion (EXT, F0 and F30) and high abduction (Figure 11.20).

### A6.5.4 Discussion

The most important finding in this appendix is that in all but a few hip positions, the positions where the hip ligaments started to restraint rotation were significantly less than the positions where the labrum started to impinge (Figure 11.20) and for most hip positions, the capsule developed 5 Nm of passive restraint before the labrum impingement at all (Figure 11.21). This suggests that the capsular ligaments could help prevent labral impingements in the native hip.

The translations of the femoral head were not controlled but were allowed to occur freely in response to the applied load and any differences in femoral head translations could change the point at which the labrum started to impinge. Therefore, this appendix is limited in that it assumes any differences in the translation of the femoral head were small in comparison the movement of the femoral neck caused by the hip rotation movement. This is a reasonable assumption given that the hip approximates to a spherical ball and socket joint (Cereatti et al., 2010) with the applied load forcing it to

be concentric in most hip positions. In positions where this was not the case and the hip dislocated, the data analysis was biased against the most important finding that the capsule helps prevent labral impingement in the native hip by assuming the positions of labral impingement and slack/stiff transition point for capsular rotational restraint were identical in these cases.

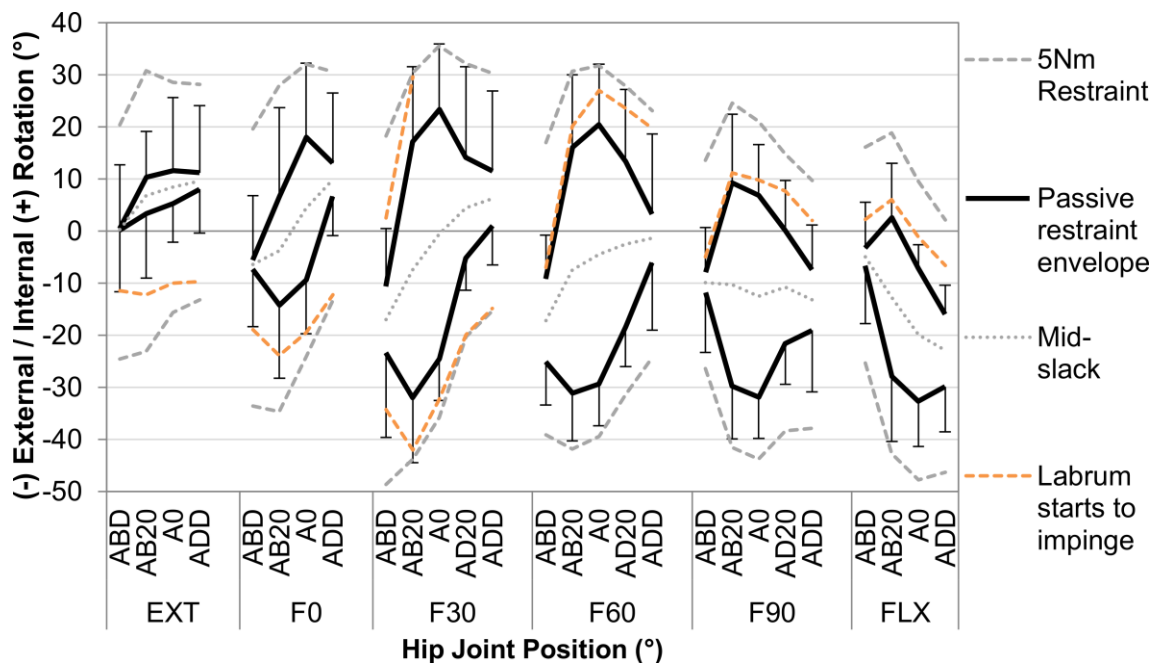


Figure 11.20 A comparison between the passive restraint envelope and the positions of labral impingement.

It can be seen that in the majority of hip positions, the capsule begins to tauten (black lines) before the labrum starts to impinge (dashed orange lines) though in positions of high abduction, the labrum started to impingement at the same angular position where passive resistance was measured in the intact hip suggesting that in these positions, labral impingement occurs in the same position/before the point where the capsular ligaments start to tauten.

This study found that the difference between the positions of labral impingement and the passive restraint envelope were smallest in hip high abduction and either low flexion/extension and external rotation, or high/deep flexion and internal rotation, suggesting that the native hip is at risk of labral impingements in these positions. This agrees with the result presented in chapter 7. Moreover, visual observation suggested that in these full abduction positions the labral impingements occurred most commonly in the posterosuperior region acetabulum which agrees well with clinical observations in ballet dancers with normal hip anatomy who have high range of motion requirement and have been found to impinge in this hip position (Charbonnier et al., 2011).

#### A6.6 Transition point sensitivity study

In the data analysis, a gradient value of  $0.03 \text{ Nm/}^\circ$  was chosen based on pilot data for automatically detecting the slack/stiff transition point for the passive restraint envelope.



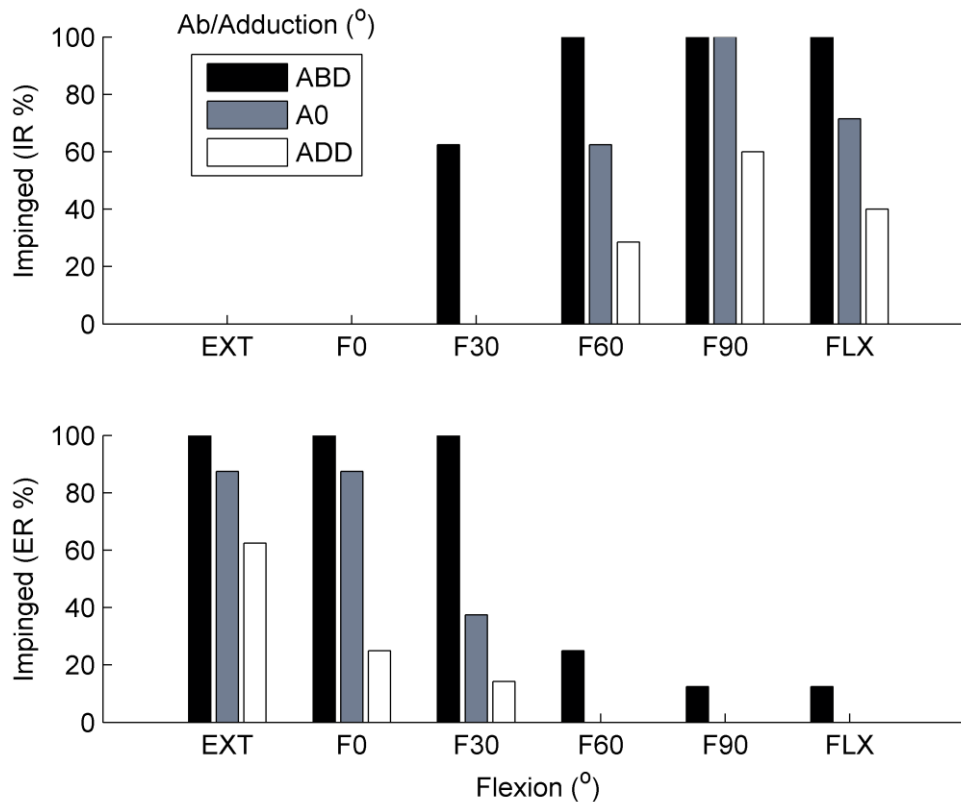


Figure 11.21 The proportion of specimens for which a labral impingement was recorded before the 5 Nm restraint limit for internal rotation (top) and external rotation (bottom) in all hip positions.

The sensitivity of the results to this value was tested by repeating the data analysis with values of 0.01 Nm/° and 0.05 Nm/° and the change in slack region was measured (Figure 11.22).

It was found that reducing the slack-to-taut cut-off gradient to 0.01 Nm/° decreased the slack/stiff transition angles for internal and external rotation across all angles of hip flexion and ab/adduction by a mean ( $\pm$  S.D.) change of  $2.7 \pm 1.6^\circ$  and  $2.4 \pm 1.1^\circ$  respectively. Increasing the gradient to 0.05 Nm/° increased the mean transition angle of internal and external rotation by  $1.5 \pm 0.6$  Nm/° and  $1.3 \pm 0.6$  Nm/° respectively. These changes are small in comparison to the variation in slack region across different hip positions (up to  $44 \pm 15^\circ$ , Figure 6.5, page 115) and importantly the shape of the slack region does not vary with changes to the cut-off gradient (Figure 11.23). A similar small variation in the position of the mid-slack point was also observed; reducing the cut-off gradient to 0.01 Nm/°, or increasing it to 0.05 Nm/° resulted in a mean absolute change in the mid-slack point of only  $0.7 \pm 0.5^\circ$  and  $0.3 \pm 0.2^\circ$  respectively. Again, this is small compared to the variation in mid-slack with hip position (up to  $33 \pm 8^\circ$ , Figure 6.6, page 117). It should be noted that changing the cut-off gradient does not affect the points of 5 Nm restraint (which were direct experimental readings) and so the changes in of slack-to-taut are the inverse of the changes in the

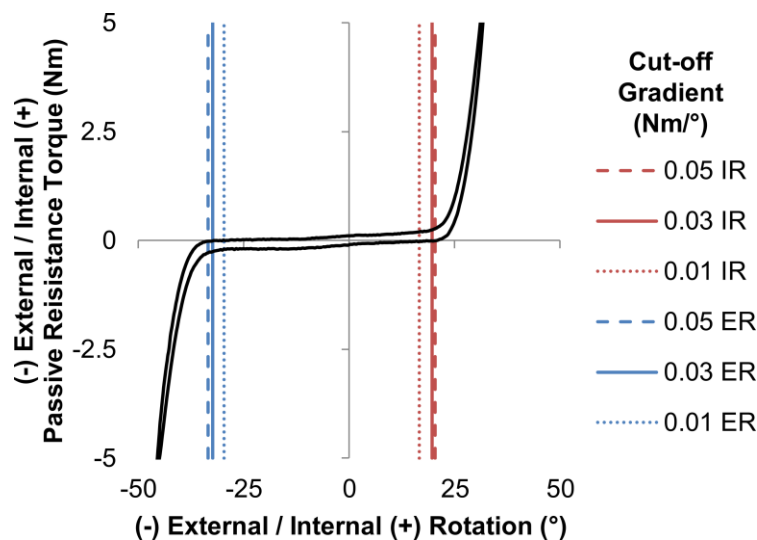


Figure 11.22 A torque-rotation plot for one hip specimen in 60° flexion and neutral ab/adduction. Reducing the cut-off value effectively reduces the slack region as a smaller gradient is required to be considered taut. The opposite is true when increasing the cut-off gradient.

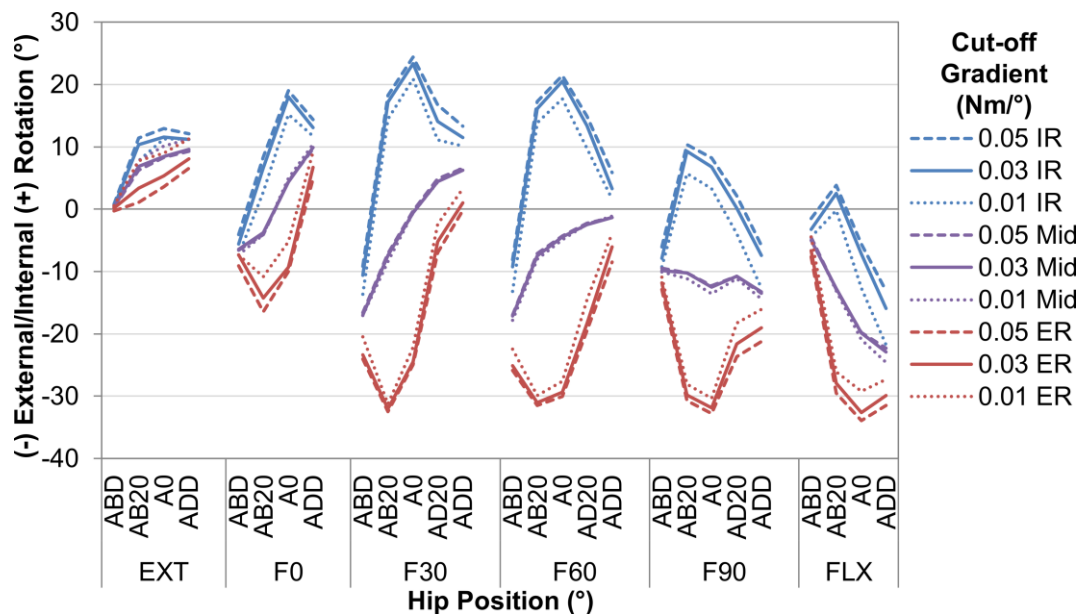


Figure 11.23 Sensitivity of the passive restraint envelope and slack region to variation in the cut-off gradient for automatic detection of the slack region.

It can be seen that whilst increasing/decreasing the cut-off gradient does increase/decrease the range of slack, the variation of the slack region across hip range of motion is much greater that caused by changes to the cut-off value, and that internal and external rotation is affected evenly, resulting in little change to the shape of the curves or location of the mid-slack point.

slack region; as the amount of internal or external rotation slack increases, the slack-to-taut decreases by the same amount. The torsional stiffness, a measure taken from the gradient, is also not affected by changes in the cut-off value.

In conclusion, whilst changing the slack/stiff transition gradient does result in small changes to the slack region, mid-slack and slack-to-taut results, these changes are small in comparison to the measured statistical differences and so do not affect the outcome of the experiment.

### A6.7 Extended comparison of the results with the literature

In Figure 11.24, the results of this study are compared against published values in the literature for ab/adduction and internal/external rotation in a neutral hip position. The passive restraint envelope from the hip capsule is less than clinical measurement, and less than hard bone-bone impingement limits to hip ROM indicating that the capsule likely plays an important role in restraining hip motion. This adds further support to the discussion in section 6.4.3.

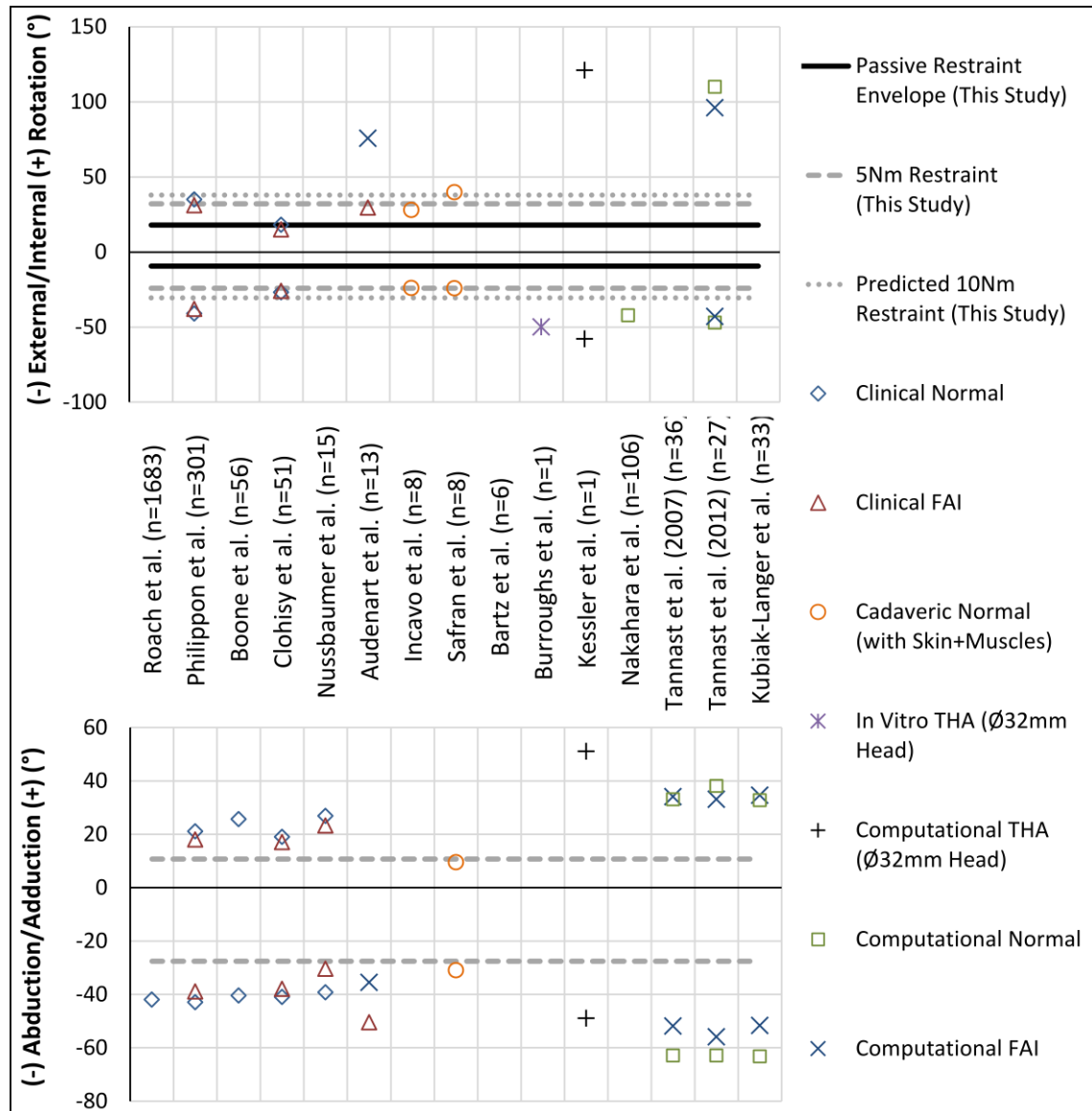


Figure 11.24 A comparison between clinical, experimental and computational range of motion measurements and the results from the present study for internal and external rotation at neutral ab/adduction and neutral flexion/extension (top), and for flexion/extension with neutral ab/adduction and internal/external rotation (bottom).

It can be seen that the passive restraint envelope (for un-resisted rotation) measured in this study are within clinical measurements for normal subjects, compare well to previous cadaveric work and are always less than results from studies which only consider bony impingement as a limit to hip rotation (computational studies). The predicted 10 Nm restraint values are calculated using the mean torsional stiffness measured at 5 Nm restraint.

### **A6.8 A comparison between the passive restraint envelope and kinematics from activities of daily living**

The data were compared against kinematics from normal daily activities by interpolating the discrete values measured to match exact flexion/extension and ab/adduction kinematics recorded during daily activities (Bergmann et al., 2001; Nadzadi et al., 2003). The ab/adduction 5 Nm passive restraint ROM limits were linearly interpolated for a given flexion/extension angle, and the internal/external 5 Nm passive restraint ROM limits and taut/slack boundaries were bilinearly interpolated for a given flexion/extension and ab/adduction angle. For the few data points where the hip position exceeded the 5 Nm ROM limit for flexion/extension or ab/adduction, a small extrapolation was used.

Activities of daily living that require a low range of motion (Bergmann et al., 2001) are unlikely to recruit the ligaments in a stabilising/restraining role as the hip kinematics are typically less than that required to tauten the ligaments to 5 Nm; for most of the activity, the kinematics are entirely within the slack-region showing the hip is moving freely under the action of muscles (Figure 11.25). Conversely, other activities of daily living, that are known to challenge hip range of motion and are at risk of dislocation for hip replacements (Nadzadi et al., 2003) would recruit the capsule in a stabilising/restraining role as the kinematics exceed that required to tauten the ligaments (Figure 11.26).

This comparison is limited in that it compares mean optically-tracked patient data against mean in-vitro cadaveric data and is not a subject specific comparison. Also, whilst the data from this study and Nadzadi et al. is presented in the ISB co-ordinate system, that from Bergmann et al. is not (although the co-ordinate system are similar).

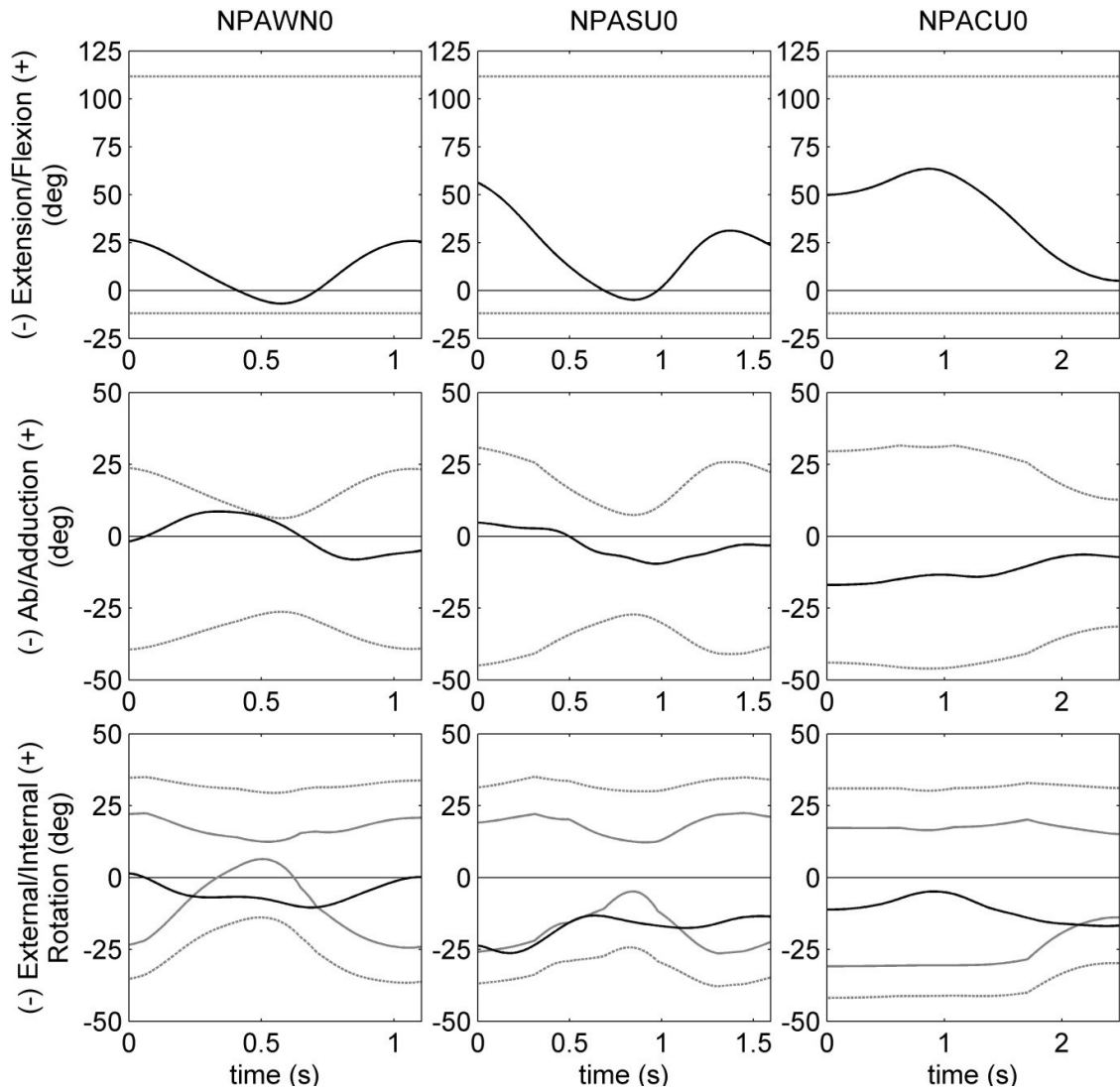


Figure 11.25 A comparison between average kinematics (solid black curves) of a hip replacement patient (Bergmann et al., 2001) for gait (left), stair climbing (middle) and rising from a high (50 cm) chair (right), with the range of motion required to develop 5 Nm of passive restraint from the hip ligaments (dashed grey curves).

Also shown is the slack-range of hip rotation (solid grey curves, bottom only). It can be seen that these activities of daily living would not develop significant tension in the hip ligaments.

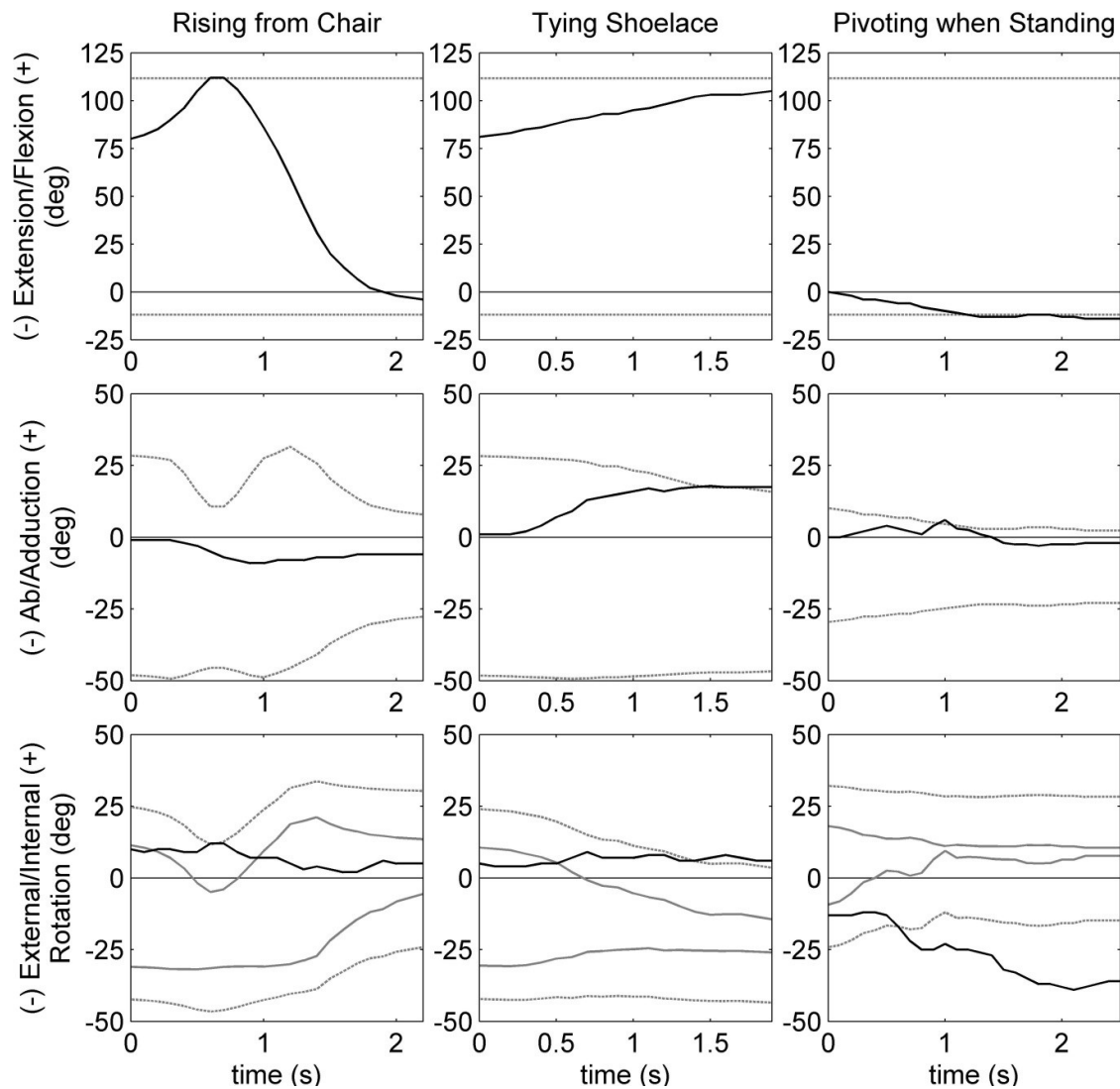


Figure 11.26 A comparison between average kinematics (solid black curves) for high-dislocation-risk activities of daily living (Nadzadi et al., 2003) including a deep flexion sit-to-stand (left), tying a shoe-lace whilst sitting (middle) and pivoting whilst standing (right), with range of motion required to develop 5 Nm of passive restraint from the hip ligaments (dashed grey curves).

Also shown is the slack-range of hip rotation (solid grey curves, bottom only). It can be seen that these activities of daily living would recruit the capsular ligaments in a stabilising/restraining role as they would become taut during the movement.

## **A7 Primary restraints for hip rotation appendices**

### **A7.1 Identification and resection of the hip ligaments**

Ligaments were identified using a mixture of anatomical drawings and definitions (Fuss and Bacher, 1991; Gray, 2008; Martin et al., 2008; Telleria et al., 2011) (Figure 11.27) and palpation. The lateral iliofemoral, ischiofemoral and pubofemoral capsular ligaments could be cut without risking inadvertent damage to adjacent ligaments by targeting these ligaments at either their unique acetabular origin (pubofemoral, ischiofemoral) or femoral insertion (lateral iliofemoral). However, the medial iliofemoral ligament shares its acetabular origin with the lateral iliofemoral ligament and its femoral insertion with the pubofemoral ligament and hence extra care had to be taken when cutting this ligament, especially when it had to be resected first as part of the randomised cutting order. Figure 11.27 shows the medial iliofemoral ligament taut in the intact hip capsule and Figure 11.28 shows how the ligament was safely cut by identifying and marking the pubofemoral and lateral iliofemoral ligament fibres in their functional positions.

### **A7.2 Root mean squared error**

An increase in passive resistance torque after cutting a ligament would imply that a pushing/pulling force, which provided a positive torque that actively aided joint rotation, was removed by cutting the ligament. However, ligaments can only passively restrain hip rotation and not actively push or pull; in this experiment, only the servo-hydraulic machine was capable of actively rotating the hip. Therefore, any positive increases in passive resistance torque recorded after cutting a ligament must have been measurement errors and hence can be used to estimate the root mean squared error (RMSE) for the experiment.

In total, there were small increases measured in 21 % (382/1836) of readings. Based on these known errors, the RMSE was calculated to be 0.27 Nm, or 5 % contribution to rotational restraint. In nearly all hip positions, the primary restraint contributed more than 50 % of the total passive resistance and hence is an order of magnitude greater than this RMSE and hence the most important findings are unlikely to be affected by measurement errors. Also, ligaments were only considered to be secondary restraints if their contributions were greater than 10 %, twice the estimated RMSE.

With over one fifth of the measurements having known errors (positive torque changes) these errors could be cause for concern despite their low RSME (5 %). However, this



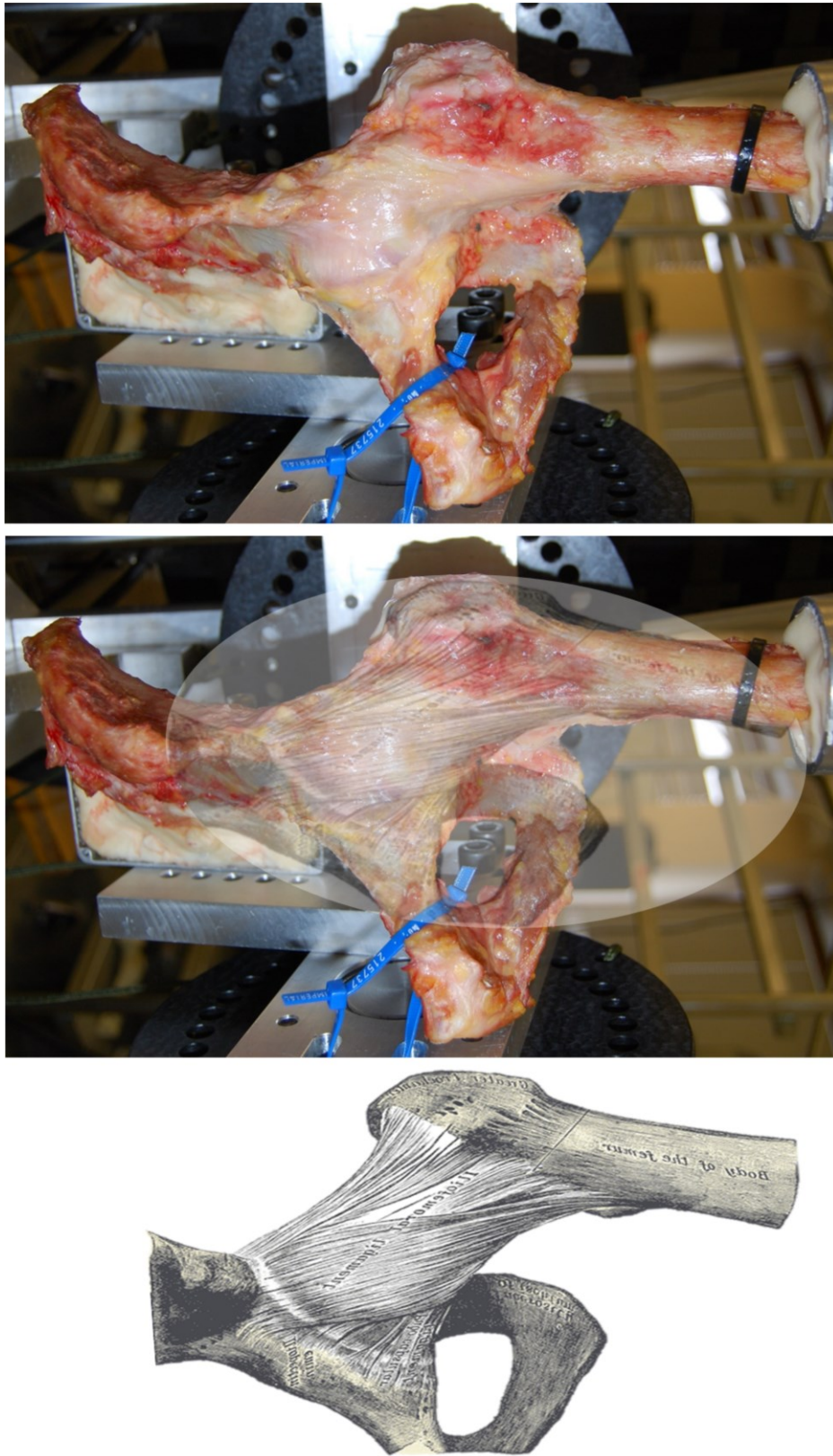


Figure 11.27 Anatomical drawing of the medial and lateral arms of the iliofemoral ligament (left) (Gray, 1918) and corresponding photo of a hip specimen (right) in a neutral hip position. The medial iliofemoral ligament is taut and is identified through palpation and comparison with the published anatomical drawing, which is emphasised by overlapping images (middle). Anatomical drawing reproduced from 20th U.S. edition of Gray's anatomy (copyright expired, available in the public domain).



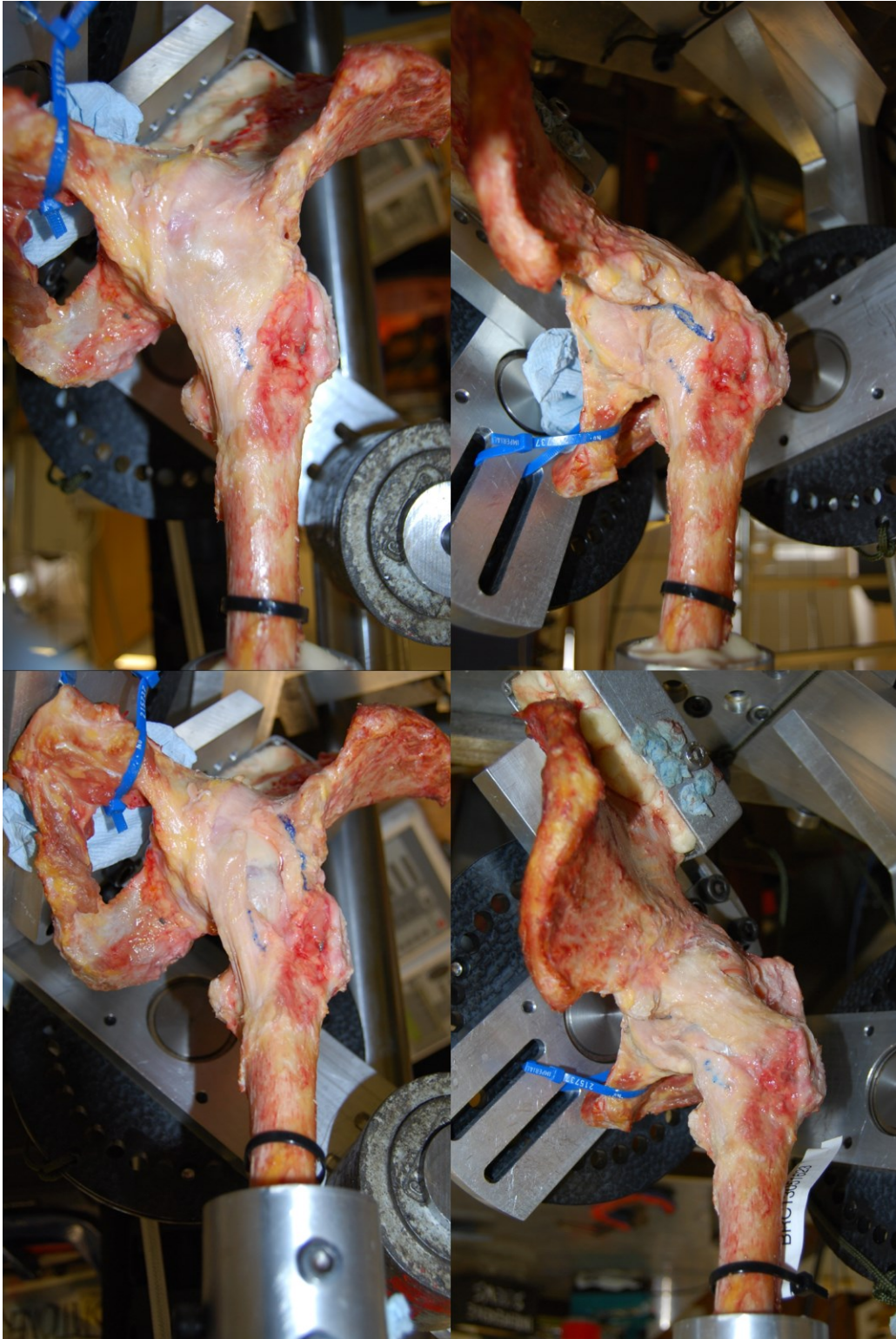


Figure 11.28 Cutting the medial iliofemoral ligament example

The pubofemoral ligament is identified in extension, abduction and external rotation and its lateral boundary is marked at its shared femoral insertion with the medial iliofemoral ligament (top left). The lateral arm of the iliofemoral ligament is identified in hip flexion and external rotation and its inferior fibres marked to distinguish it at its shared acetabular origin with the medial iliofemoral ligament (top right). By cutting lateral of the marked pubofemoral fibres at the femur and inferior to the lateral iliofemoral fibres at the acetabulum, the medial iliofemoral ligament is cut transversely across all its fibres whilst keeping the pubofemoral (bottom left) and lateral iliofemoral (bottom right) ligaments intact.

concern is diminished when considering the RMSE alongside the number of measurements where cutting a ligament had a negligible effect: the changes in passive resistance torque were less than 0.25 Nm (5 % contribution) for nearly half the ligaments cuts (876/1836), and were less than 0.05 Nm (1 % contribution) for more than a quarter of the data (476/1836). For these cases, where cutting the ligament effectively had no effect, even a small measurement error in either the before or after cut measurement could feasibly give a positive increase in passive resistance torque which helps explain the known error rate.

### A7.3 Post-hoc analyses comparing capsular, labral and ligamentum teres contributions to rotational restraint

Table 11.1 The mean  $\pm$  standard deviation percentage contributions of the capsular ligaments (C), the ligamentum teres (LT) and the labrum (L) to internal rotation restraint in all hip positions.

Significant differences between these contributions detected by the post-hoc paired t-tests with a Bonferroni correction are indicated with an \*

Hip position (°)		Capsular Ligaments (%)	Ligamentum Teres (%)	Labrum (%)	C vs LT (p-value)	C vs L (p-value)	LT vs L (p-value)
Extended	Add	98 $\pm$ 2	0 $\pm$ 1	1 $\pm$ 1	<0.001*	<0.001*	0.195
	0	97 $\pm$ 4	1 $\pm$ 1	2 $\pm$ 3	<0.001*	<0.001*	0.337
	Abd	97 $\pm$ 4	0 $\pm$ 1	2 $\pm$ 4	<0.001*	<0.001*	0.201
0	Add	98 $\pm$ 2	1 $\pm$ 1	1 $\pm$ 1	<0.001*	<0.001*	1.000
	0	96 $\pm$ 8	0 $\pm$ 1	3 $\pm$ 6	<0.001*	<0.001*	0.391
	Abd	96 $\pm$ 8	0 $\pm$ 1	4 $\pm$ 8	<0.001*	<0.001*	0.467
30	Add	93 $\pm$ 6	4 $\pm$ 4	3 $\pm$ 5	<0.001*	<0.001*	1.000
	0	93 $\pm$ 16	1 $\pm$ 3	6 $\pm$ 13	<0.001*	<0.001*	0.510
	Abd	87 $\pm$ 17	1 $\pm$ 2	12 $\pm$ 15	<0.001*	<0.001*	0.115
60	Add	94 $\pm$ 9	1 $\pm$ 2	5 $\pm$ 7	<0.001*	<0.001*	0.371
	0	83 $\pm$ 19	3 $\pm$ 6	13 $\pm$ 14	<0.001*	0.001*	0.084
	Abd	66 $\pm$ 24	7 $\pm$ 12	28 $\pm$ 14	0.003*	0.046*	0.003*
90	Add	97 $\pm$ 6	0 $\pm$ 1	3 $\pm$ 5	<0.001*	<0.001*	0.254
	0	74 $\pm$ 16	5 $\pm$ 9	21 $\pm$ 17	<0.001*	0.003*	0.169
	Abd	71 $\pm$ 13	1 $\pm$ 2	27 $\pm$ 13	<0.001*	0.003*	0.001*
Flexed	Add	95 $\pm$ 6	1 $\pm$ 1	4 $\pm$ 5	<0.001*	<0.001*	0.185
	0	90 $\pm$ 8	1 $\pm$ 1	9 $\pm$ 8	<0.001*	<0.001*	0.022*
	Abd	74 $\pm$ 15	2 $\pm$ 2	24 $\pm$ 15	<0.001*	0.003*	0.006*

Table 11.2 The mean  $\pm$  standard deviation percentage contributions of the capsular ligaments (C), the ligamentum teres (LT) and the labrum (L) to external rotation restraint in all hip positions.

Significant differences between these contributions detected by the post-hoc paired t-tests with a Bonferroni correction are indicated with an \*

Hip position (°)		Capsular Ligaments (%)	Ligamentum Teres (%)	Labrum (%)	C vs LT (p-value)	C vs L (p-value)	LT vs L (p-value)
Extended	Add	85 $\pm$ 10	0 $\pm$ 1	14 $\pm$ 10	<0.001*	<0.001*	0.012*
	0	82 $\pm$ 14	1 $\pm$ 1	17 $\pm$ 13	<0.001*	0.001*	0.017*
	Abd	74 $\pm$ 17	2 $\pm$ 1	25 $\pm$ 16	<0.001*	0.012*	0.018*
0	Add	95 $\pm$ 3	1 $\pm$ 1	4 $\pm$ 3	<0.001*	<0.001*	0.055
	0	82 $\pm$ 17	0 $\pm$ 1	18 $\pm$ 17	<0.001*	0.003*	0.056
	Abd	74 $\pm$ 15	2 $\pm$ 3	24 $\pm$ 16	<0.001*	0.009*	0.028*
30	Add	88 $\pm$ 9	9 $\pm$ 8	3 $\pm$ 2	<0.001*	<0.001*	0.164
	0	88 $\pm$ 10	6 $\pm$ 7	6 $\pm$ 4	<0.001*	<0.001*	1.000
	Abd	76 $\pm$ 11	7 $\pm$ 8	17 $\pm$ 8	<0.001*	<0.001*	0.129
60	Add	87 $\pm$ 8	11 $\pm$ 7	2 $\pm$ 1	<0.001*	<0.001*	0.014*
	0	83 $\pm$ 16	13 $\pm$ 17	4 $\pm$ 3	0.002*	<0.001*	0.493
	Abd	88 $\pm$ 7	5 $\pm$ 4	7 $\pm$ 7	<0.001*	<0.001*	1.000
90	Add	87 $\pm$ 9	12 $\pm$ 8	1 $\pm$ 1	<0.001*	<0.001*	0.008*
	0	83 $\pm$ 20	16 $\pm$ 20	2 $\pm$ 2	0.006*	<0.001*	0.279
	Abd	94 $\pm$ 4	2 $\pm$ 3	4 $\pm$ 3	<0.001*	<0.001*	0.595
Flexed	Add	86 $\pm$ 9	13 $\pm$ 9	1 $\pm$ 1	<0.001*	<0.001*	0.011*
	0	86 $\pm$ 7	12 $\pm$ 7	2 $\pm$ 2	<0.001*	<0.001*	0.013*
	Abd	92 $\pm$ 6	3 $\pm$ 6	5 $\pm$ 4	<0.001*	<0.001*	1.000

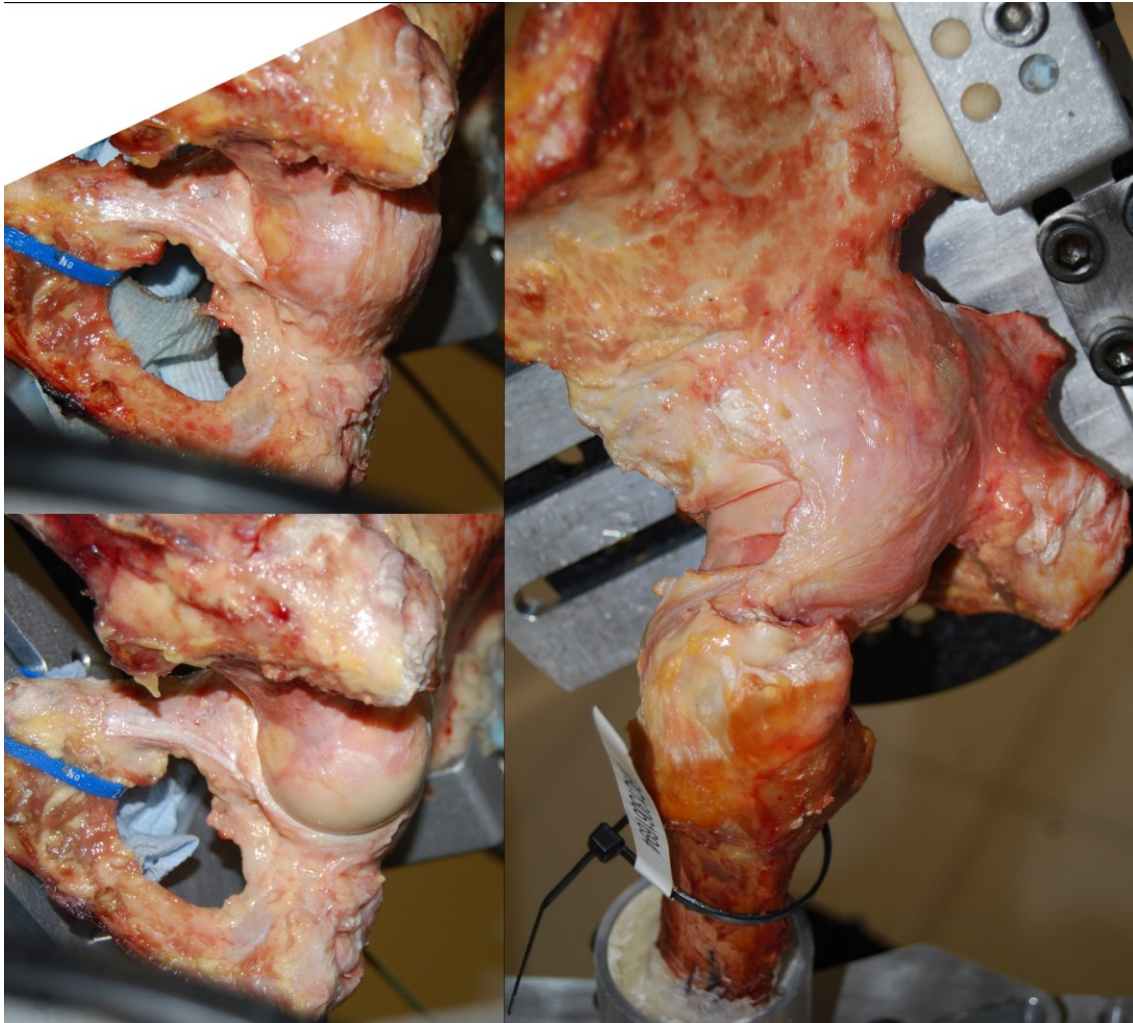
**A7.4 Photos of the periarticular passive soft-tissues of the hip**

Figure 11.29 Photos of the ischiofemoral ligament.

Lateral-inferior view of a hip in deep flexion, adduction and internal rotation (left) with the only the ischiofemoral ligament intact (top) and with all capsular ligaments resected (bottom). Posterior lateral view of a different hip with the ischiofemoral ligament taut in mid-flexion and internal rotation; the lateral iliofemoral ligament has been resected whilst preserving the superior femoral insertion of the ischiofemoral ligament. When the ischiofemoral ligament is intact it cradles the femoral head in a supportive string, however when resected the femoral head is exposed and at risk of subluxation and dislocation. Additional views of the ischiofemoral ligament are available in Figure 7.5, page 133.



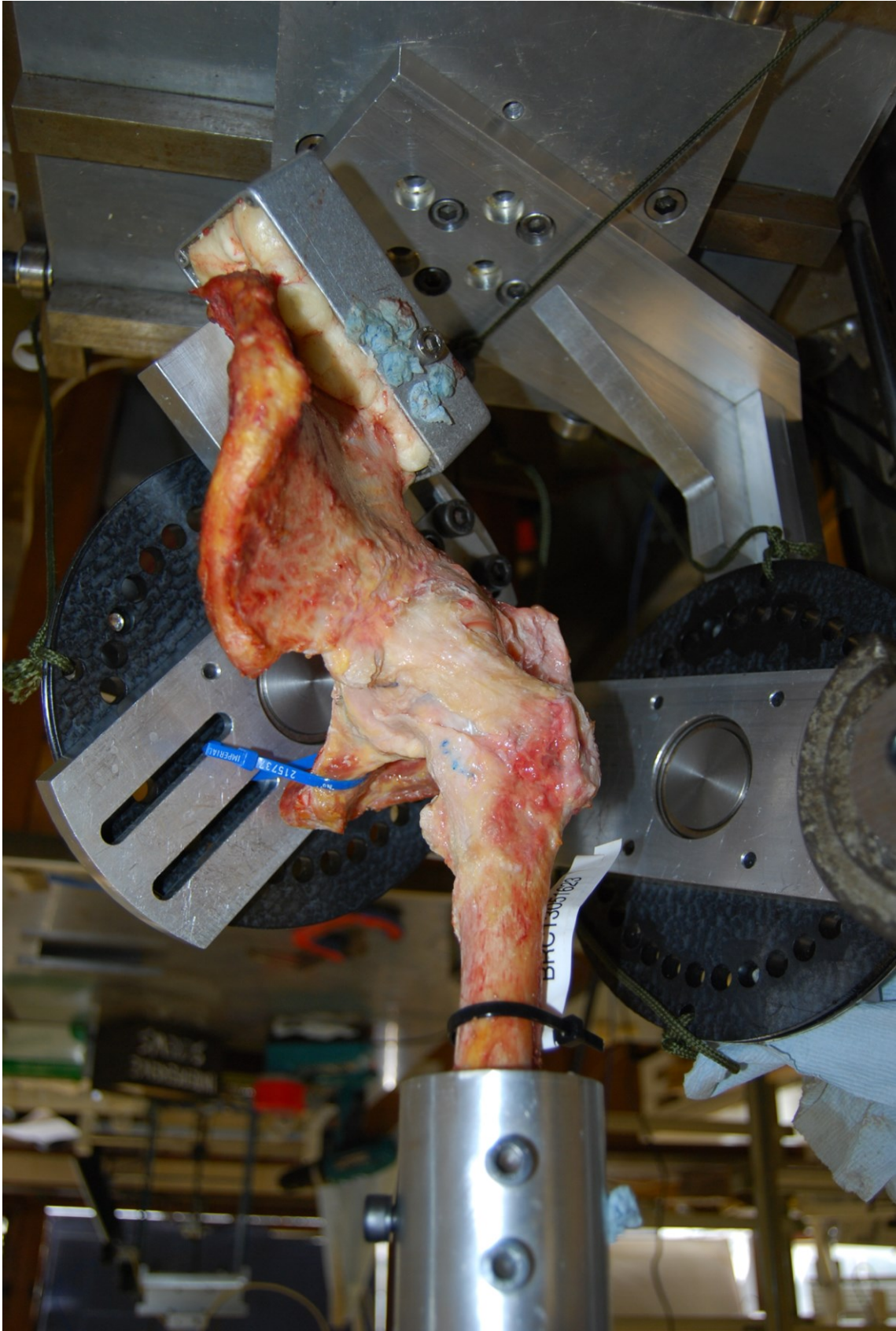


Figure 11.30 Anterolateral view of the lateral iliofemoral ligament taut in mid-flexion, abduction and external rotation.

The medial iliofemoral and ischiofemoral ligaments have been resected. Figure 6.1, page 109 also shows a photo of the lateral iliofemoral ligament.



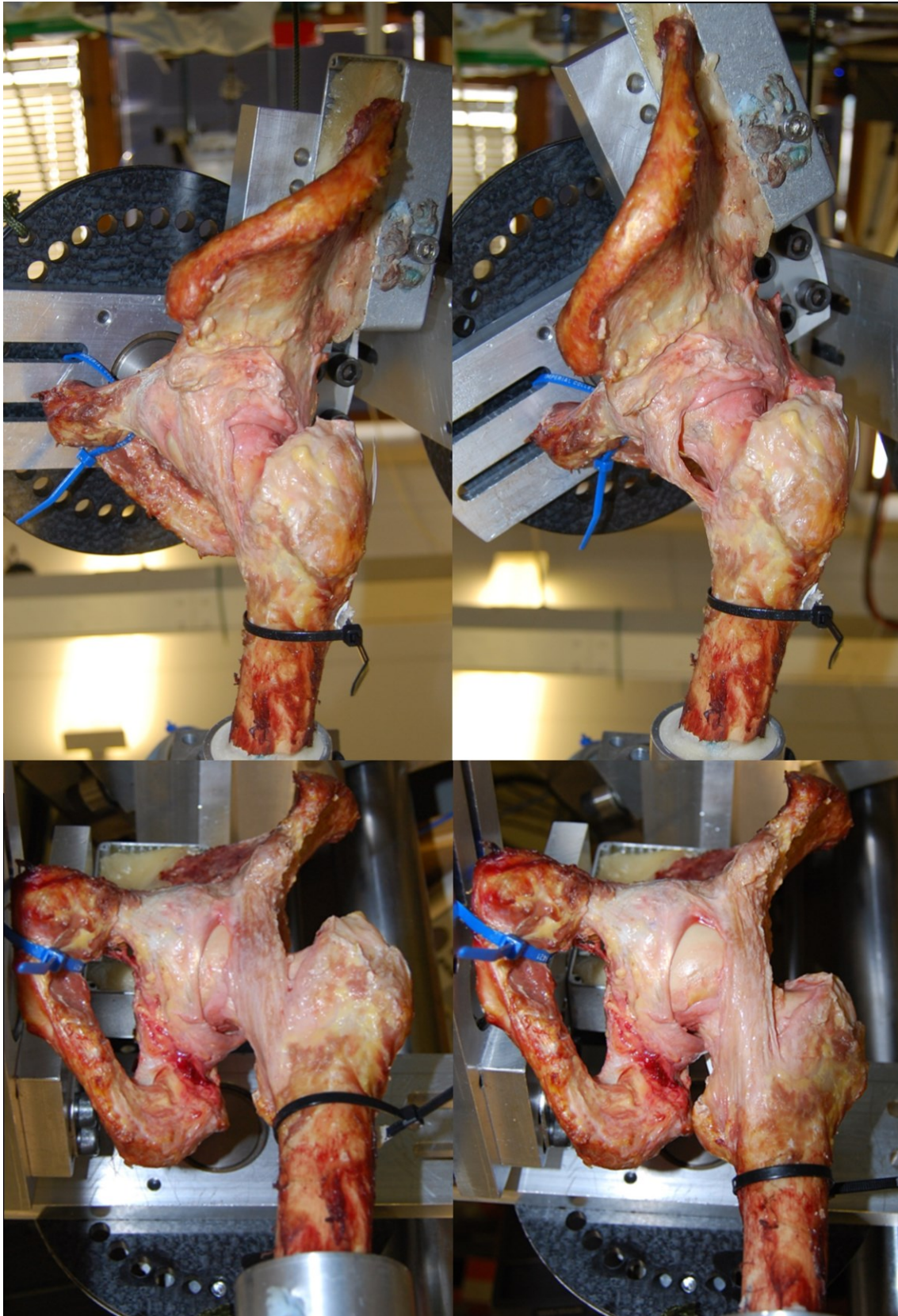


Figure 11.31 Lateral views of the medial iliofemoral ligament taut in extension (top left) and slack in flexion (top right) and anterior inferior views of it taut in internal and external rotation in hip extension (bottom left and right respectively). All other ligaments have been resected.



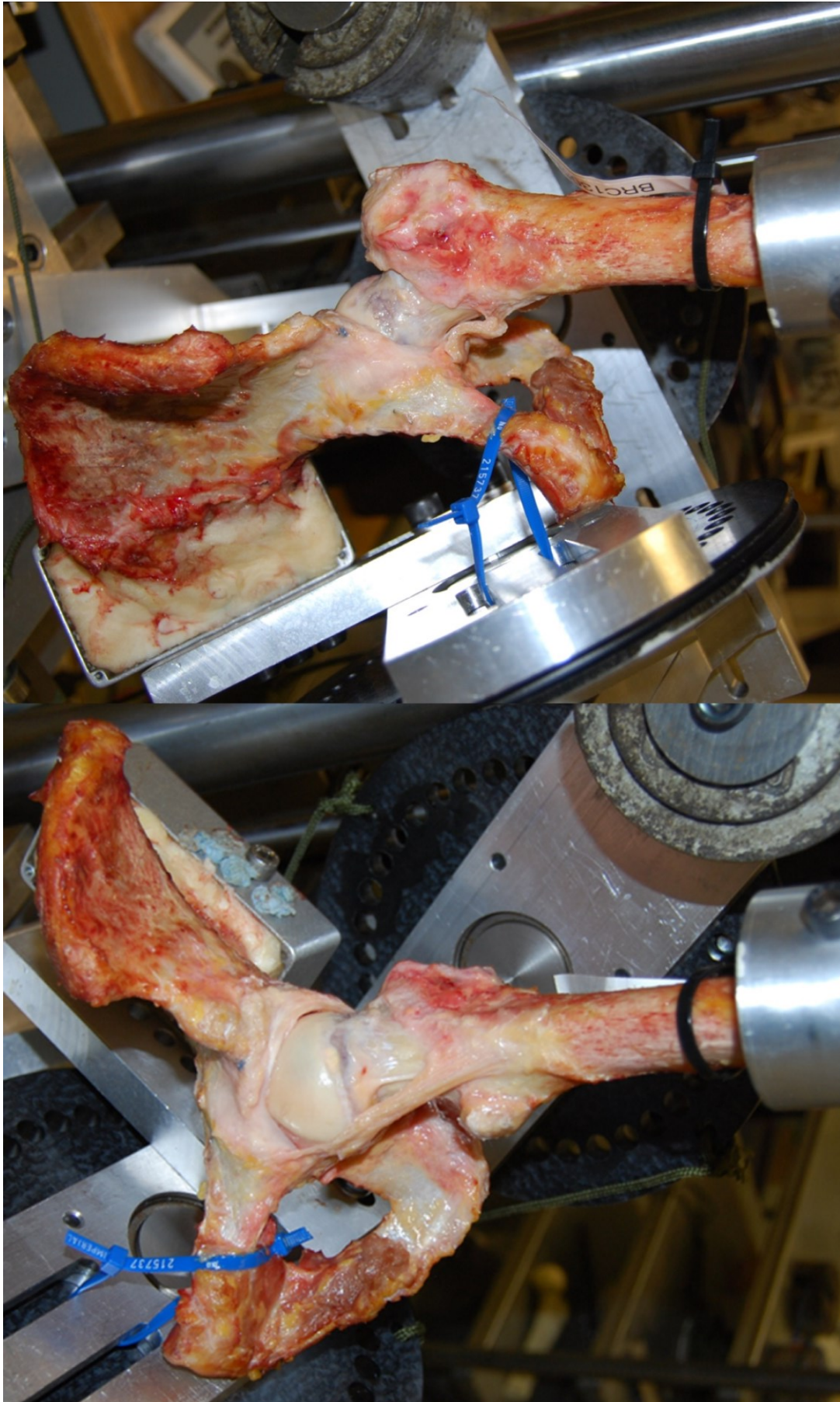


Figure 11.32 Anterior views a hip in neutral flexion. The pubofemoral ligament taut in abduction (left), and slack in adduction (right).



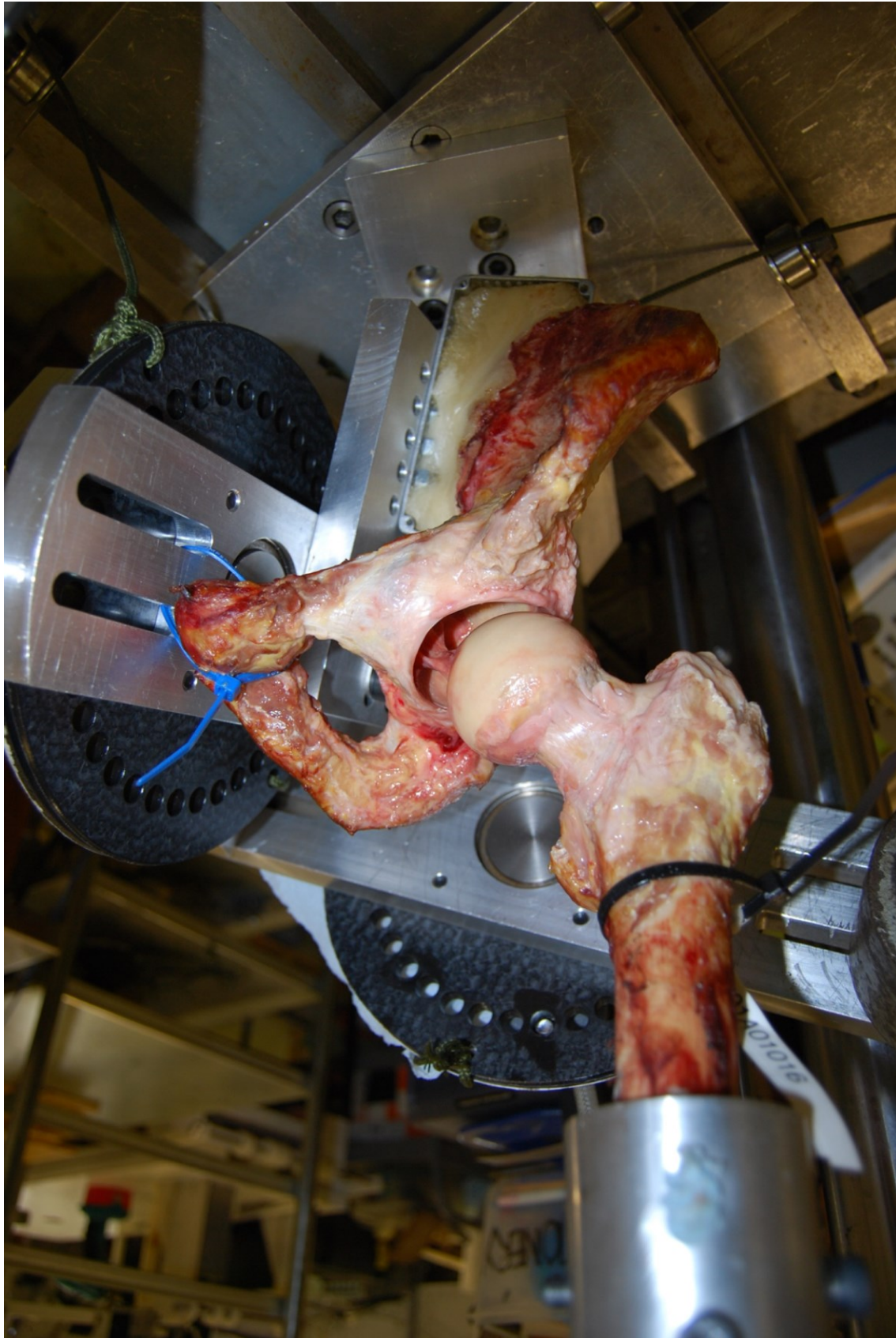


Figure 11.33 Anteroinferior view a hip in mid-flexion, abduction and distraction so that the intra-articular ligamentum teres can be seen (not its functional position).



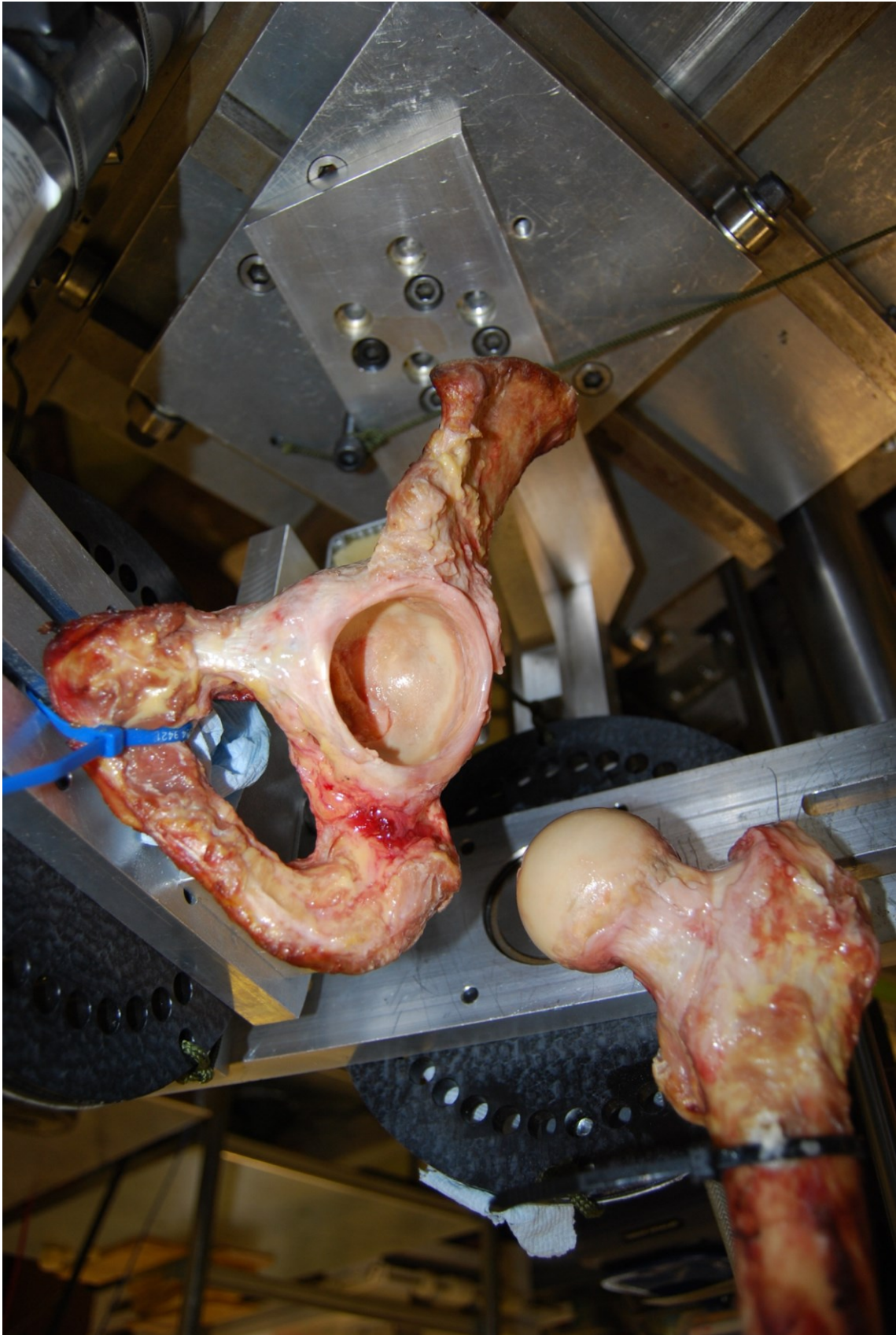


Figure 11.34 Lateral-inferior view of a distracted hip with all ligaments resected showing the labrum at the rim of the acetabulum. The intra-articular portions of the posterior and superior portions of the labrum can be seen.

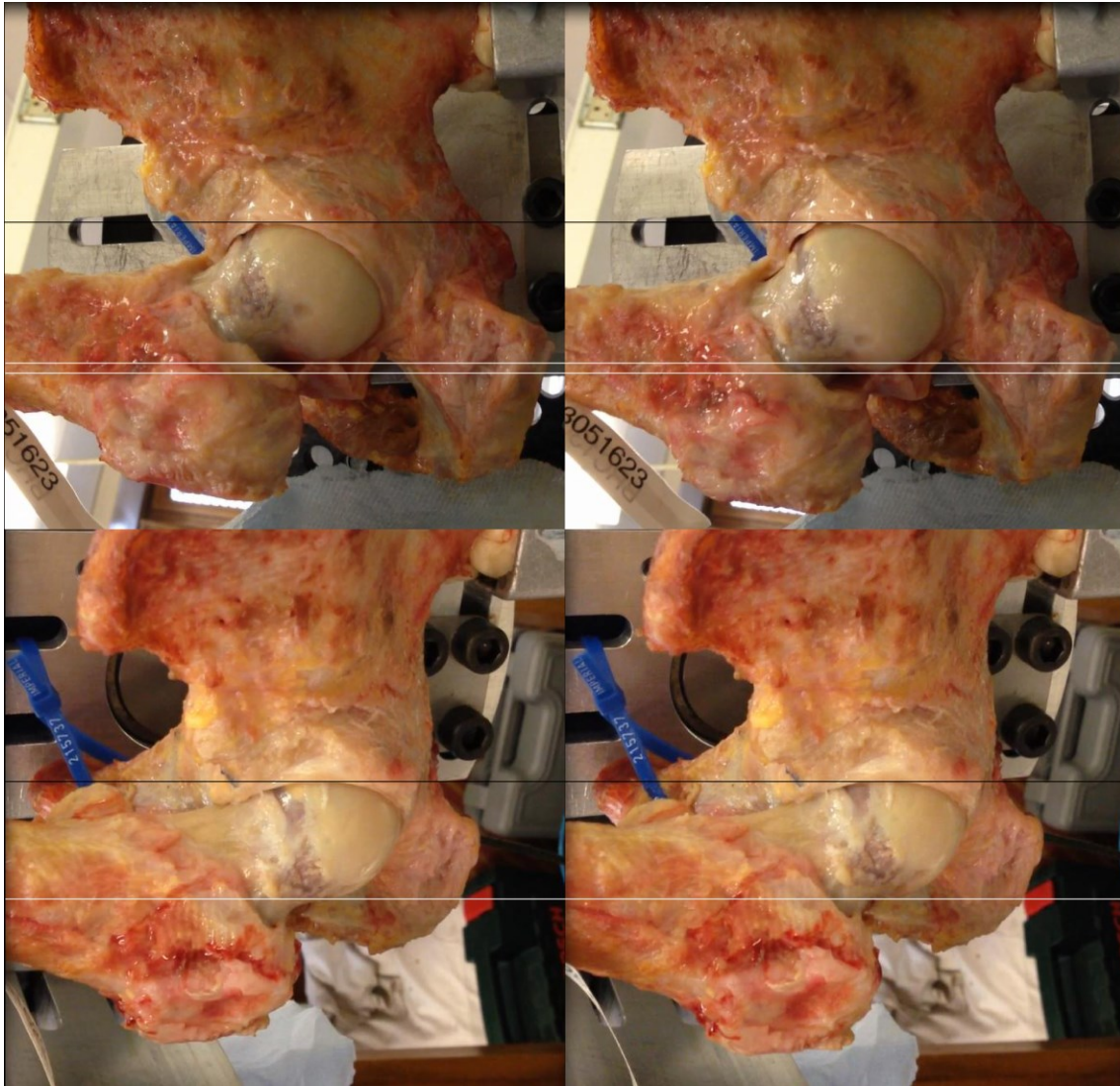
**A7.5 Subluxation caused by the ligamentum teres**

Figure 11.35 Small subluxation of the femoral head caused by the ligamentum teres.

Lateral views of the same hip specimen taken from two videos in identical hip positions (adducted in 90° flexion) are shown. In the image pair from the first video the ligamentum teres is intact (top), and in the second image pair it is resected (bottom). The white lines are tangent to the most lateral (relative to the femur) or inferior (relative to the pelvis) part of the femoral head. The black lines help show that the photos are aligned. It can be seen that there is a small lateral/inferior subluxation when the ligamentum teres is intact as the hip moves from partial external rotation (left) to maximum external rotation (right). However, this subluxation is not present after resection of the ligamentum teres.



### A7.6 Male versus female contributions

Figure 11.36 and Figure 11.37 show the ligament contribution results from chapter 7 with male and female specimens plotted separately. It can be seen that there was no observable differences between the two genders in terms of the primary restrains to rotation. However with only two female specimens included for external rotation results, and three for internal rotation results, more data is needed to draw firm conclusions.

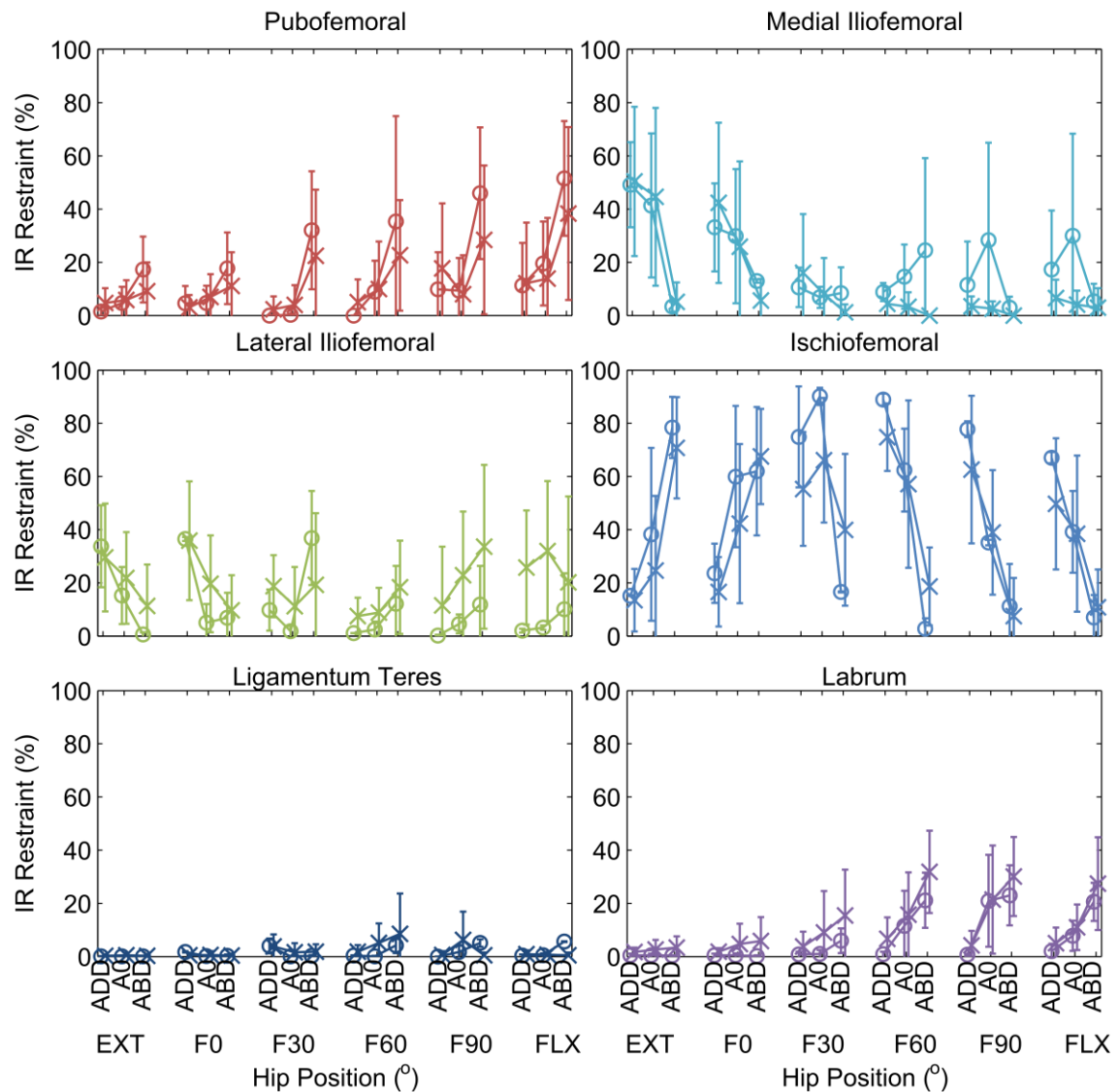


Figure 11.36 Male (X) versus female (O) contributions to internal rotational restraint with standard deviation for all six periarticular soft-tissues in all hip positions tested. It can be seen there is little difference between the genders.

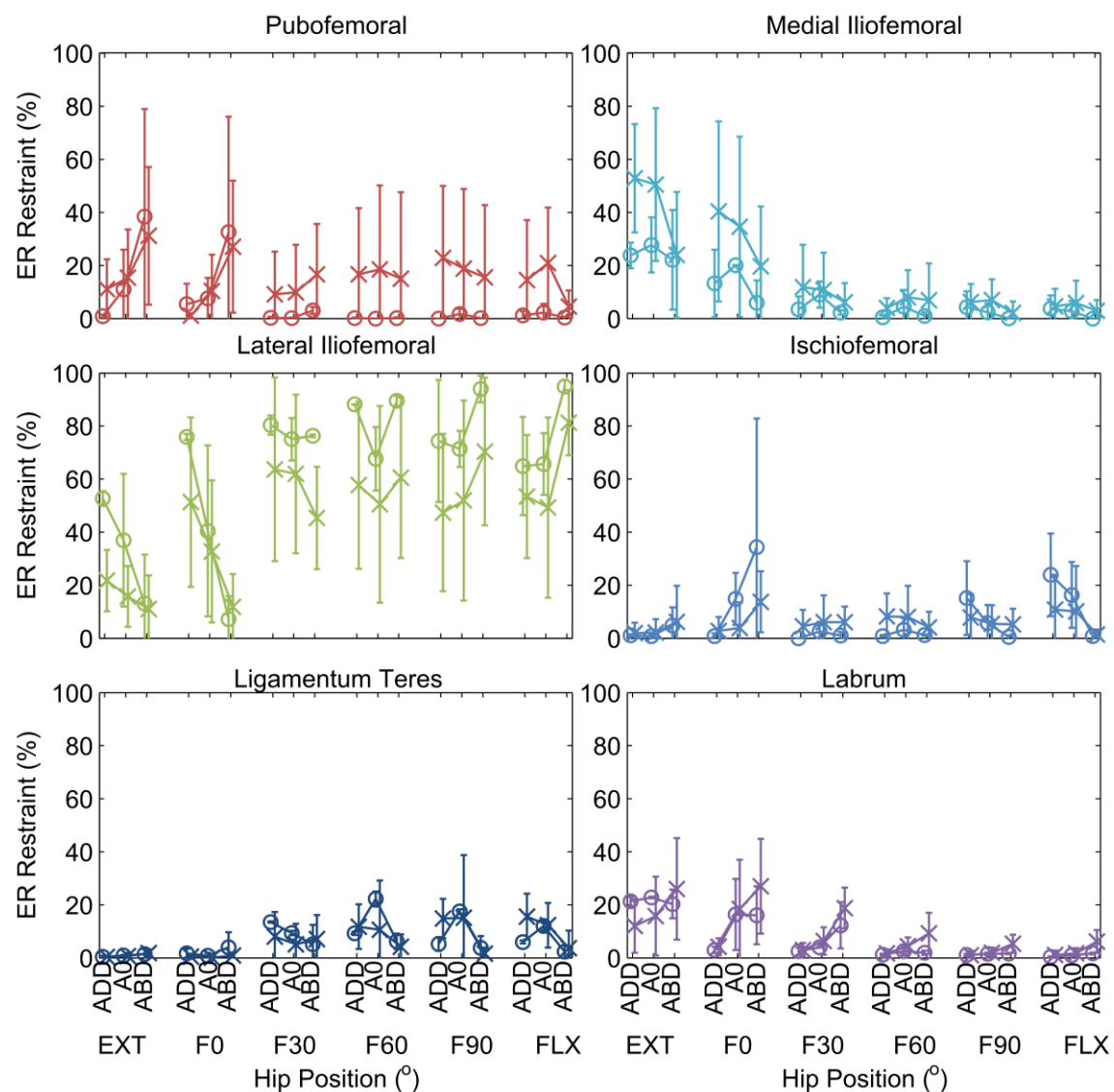


Figure 11.37 Male (X) versus female (O) contributions to external rotational restraint with standard deviation for all six periarthritic soft-tissues in all hip positions tested. It can be seen there is little difference between the genders.